



## City Research Online

### City, University of London Institutional Repository

---

**Citation:** Stimpson, M. J. (1993). The effect of electromagnetic fields and impurities on crystal growth mechanisms. (Unpublished Doctoral thesis, City, University of London)

This is the accepted version of the paper.

This version of the publication may differ from the final published version.

---

**Permanent repository link:** <https://openaccess.city.ac.uk/id/eprint/29607/>

**Link to published version:**

**Copyright:** City Research Online aims to make research outputs of City, University of London available to a wider audience. Copyright and Moral Rights remain with the author(s) and/or copyright holders. URLs from City Research Online may be freely distributed and linked to.

**Reuse:** Copies of full items can be used for personal research or study, educational, or not-for-profit purposes without prior permission or charge. Provided that the authors, title and full bibliographic details are credited, a hyperlink and/or URL is given for the original metadata page and the content is not changed in any way.

THE EFFECT OF ELECTROMAGNETIC FIELDS AND IMPURITIES

ON

CRYSTAL GROWTH MECHANISMS

---

A THESIS SUBMITTED FOR THE DEGREE OF

DOCTOR OF PHILOSOPHY

BY

MARTIN JAMES STIMPSON

Department of Chemistry

City University

London

April 1993

**THE EFFECT OF ELECTROMAGNETIC FIELDS AND IMPURITIES**  
**ON**  
**CRYSTAL GROWTH MECHANISMS**

**CONTENTS**

	Page
Table of Contents	2
Acknowledgements	3
Declaration	4
Abstract	5
CHAPTER ONE      INTRODUCTION	6
CHAPTER TWO      EXPERIMENTAL TECHNIQUES	20
CHAPTER THREE    THE EFFECT OF ELECTROMAGNETIC FIELDS ON CALCIUM CARBONATE PRECIPITATION	44
CHAPTER FOUR     PRECIPITATION STUDIES OF FORMATION WATER AND SEA WATER AS ENCOUNTERED IN THE PETROLEUM INDUSTRY	158
CHAPTER FIVE     CONCLUSIONS	297
APPENDICES       APPENDIX A	301
APPENDIX B	302

## ACKNOWLEDGEMENTS

I would like to thank Prof.J.D.Donaldson for his guidance and support throughout the course of this work. I am also indebted to Dr.S.M.Grimes, Dr.S.J.Clark, Dr.M.Kashanipour and Miss.Z.Khan for their cooperation and advice. Thanks to Dr.K.C.Bass and Sara Childe for proof reading this thesis.

I am grateful for the help of Mr.A.Smith and Dr.R.Keatch of S.B.Systems for their collaboration and use of their scaling prediction model. Thanks to David Engelfield and Mike Darvill for their assistance on the Hydromag system.

I would like to thank the technical staff at City University, in particular Mr.R.Hazeley-Jones for his help. In addition, I would like to thank my friends, especially Dr.A.P.A.Thomas for his constant motivation in combination with many interesting discussions.

In addition I would like to thank my parents and family for their encouragement and support throughout my studies.

Special thanks to Carolyn Tilly whose sustained patience and encouragement during the whole of my studies have enabled me to complete this thesis.

Additional thanks are extended to SERC and Hydromag who provided the CASE award for this study.

DECLARATION

I grant powers of discretion to the University Librarian to allow this thesis to be copied, in whole or in parts, without further reference to me. This permission covers single copies made for study purposes, subject to the normal conditions of acknowledgement.

A handwritten signature in cursive script, appearing to read 'M. Stimpson'.

Martin Stimpson

## ABSTRACT

The precipitation, crystallisation and aggregation processes in  $\text{CaCO}_3$ ,  $\text{BaSO}_4$ - $\text{SrSO}_4$ - $\text{CaCO}_3$  and  $\text{CaSO}_4$ - $\text{CaCO}_3$  systems have been studied. For the  $\text{CaCO}_3$  system the effects of applied magnetic fields on the formation of calcium carbonate scale were the subject of a detailed investigation. The study of the  $\text{BaSO}_4$ - $\text{SrSO}_4$ - $\text{CaCO}_3$  and  $\text{CaSO}_4$ - $\text{CaCO}_3$  systems was designed to determine (1) the effects of varying the ion concentrations in simulated offshore oilfield formation and sea waters and (2) the effect of the ratio of mixing the simulated waters on the rate of deposition of scale.

The scale-forming properties of  $\text{CaCO}_3$  are shown to be affected by applied magnetic fields. Propensity to scale data obtained by measuring the back pressure as scale builds up in a microbore tube show that the passage of calcium-containing solutions through a magnetic field prior to  $\text{CaCO}_3$  precipitation delays deposition. The effects of (1) flow rate of both calcium and hydrogen carbonate ion solutions through an electromagnetic field, (2) sodium hydrogen carbonate concentration and (3) temperature on  $\text{CaCO}_3$  deposition are also reported. Heat exchanger experiments show that applied magnetic field treatment causes major differences in the crystal and aggregate sizes of the precipitates and significantly reduces the quantity of scale formed. The results are interpreted in terms of the direct interaction of applied fields on charged species in fluids. The data from the present work taken with the results from previous work show that these field interactions are part of a general phenomenon.

The precipitation and aggregation properties of the solids formed in the  $\text{BaSO}_4$ - $\text{SrSO}_4$ - $\text{CaCO}_3$  and  $\text{CaSO}_4$ - $\text{CaCO}_3$  systems from mixed simulated formation and sea waters are reported. Precipitation tests and scale prediction model data for the  $\text{BaSO}_4$ - $\text{SrSO}_4$ - $\text{CaCO}_3$  system provide information on the amount of each solid formed and explain changes in the propensity to scale. Data for both systems on the changes arising from increasing each significant ion concentration in the simulated offshore oilfield waters are also reported. All the changes in the propensity to scale measurements are related to solubility effects, ion-pair effects and kinetic effects.

## CHAPTER 1

### INTRODUCTION

	Page
1.1 BACKGROUND TO THE PRESENT WORK	7
1.2 SCALE DEPOSITION MECHANISMS	9
1.2.1 Introduction	9
1.2.2 Key Requirements for Scale Deposition	9
1.2.3 Solubility	11
1.2.4 Supersaturation	12
1.2.5 Nucleation	13
1.2.6 Scale Formation	16
1.3 OBJECTIVES	17
1.4 SCOPE OF THE WORK IN THIS THESIS	17
REFERENCES	19

## CHAPTER 1

### INTRODUCTION

#### 1.1 BACKGROUND TO THE PRESENT WORK

The tendency of water to deposit certain of its dissolved constituents as scale on heated surfaces has enormous economic and environmental consequences. Scale formation in industrial applications can cause reduction in pipe-carrying capacity, reduction in the thermal conductivity of heat transfer surfaces, localisation of corrosion attack, increase in operating costs due to inefficiencies, down time and maintenance. British industry spends approximately £1000 million each year to clean, repair and replace equipment damaged by these scales.

Calcium carbonate is probably the most common compound found in scale in systems such as steam boilers, heat exchangers, evaporators and calorifiers. It is found in combination with other deposits, such as calcium sulphate, magnesium hydroxide, calcium phosphate, complex silicates and iron compounds. During off-shore oil production scale formation occurs with the most common types of scale being barium sulphate, strontium sulphate, calcium sulphate and calcium carbonate. They are rarely found in their pure form but, more often than not, in combination with each other depending on the chemical constituents found in the waters.

Scale control can be achieved either by preventing it from forming by using chemical inhibitors or by removal; once it has formed by using chemical and/or mechanical methods. The use of chemical treatments to prevent and remove scale is being restricted by tougher environmental laws, especially in the U.S.A. The prevention of scale in industrial applications needs to be met by newer, more environmentally acceptable methods.

The water treatment industry has used many physical devices to

alleviate and remove scale in hard water areas. The majority of these devices used permanent or electromagnetic fields. The reported positive effects from these devices include one or both of the following: decreased precipitation and growth of hard mineral scales; and/or partial dissolution (and/or removal) and change in the consistency of previously deposited scale.

The magnetic field effect phenomena have been reported over many years and occur as a result of the interaction of a fluid with an applied magnetic field. The technique generally consists of passing water through a magnetic field of specific magnitude and orientation which is usually installed either within or around a feed pipeline and is sometimes referred to as magnetic water treatment.

Several different mechanisms have been postulated to provide explanations as to how the treatment of fluids through magnetic fields prevents scale formation. However, none of these mechanisms has been wholly accepted, due largely to the absence of sufficient scientific backup.

Since 1984, the research group at City University, London [1], have investigated the effect of magnetic fields on fluids. The experimental work has shown that the effect of magnetic fields on several types of fluid precipitate systems can result in changes in crystal morphology, crystal phase, crystallinity, particle size and levels of supersaturation of fluids. These results indicate that the main effect of the field is to prevent and/or reduce scale formation through the modification of crystal growth mechanisms. Such modification, in part, has been explained in terms of the significant field-charge interactions of the applied field and the ions and nucleating species in the fluid.

Indeed, the direct field-charge interaction between particular charged species in treated fluids and the applied magnetic field has been recognised, principally by researchers at City University, as being possibly the most significant factor in

explaining the observed magnetic field effect phenomena in fluids.

A review of the magnetic treatment of fluids is given in Section 3.2, and includes the magnetic treatment of water, the effect of magnetic fields on chemical reactions and the magnetic field effects on calcium carbonate precipitation. The aim of the following section is to describe the key requirements for scale deposition.

## 1.2 SCALE DEPOSITION MECHANISMS

### 1.2.1 Introduction

Scale deposition, unlike other types of deposition is a complex crystallisation process. In any crystallisation or precipitation process there is a competition between growth of material on the crystals or precipitates and growth on the walls of the vessel in which the operation is being carried out. Scale results from the unwanted deposition of solid materials on surfaces and particularly on pipework, heat exchangers, and the walls of reactors and storage vessels. The rate of formation of the initial scale layer and its subsequent rate of growth are determined by the interaction of several rate processes: nucleation, diffusion, chemical reaction, and ordering of the scale crystal lattices. Figure 1.1 is a general schematic diagram of scale deposition mechanisms. The more important controlling parameters of each stage of scale deposition are indicated.

### 1.2.2 Key Requirements for Scale Deposition

All crystallisation and precipitation processes including the formation of scale depend upon two main factors, *viz.* (i) the solubility of the solid being deposited in the fluid in which it is dissolved, and (ii) the nucleation process which produces precipitation and crystallisation. For scale formation to be controlled or prevented, the treatments must involve the

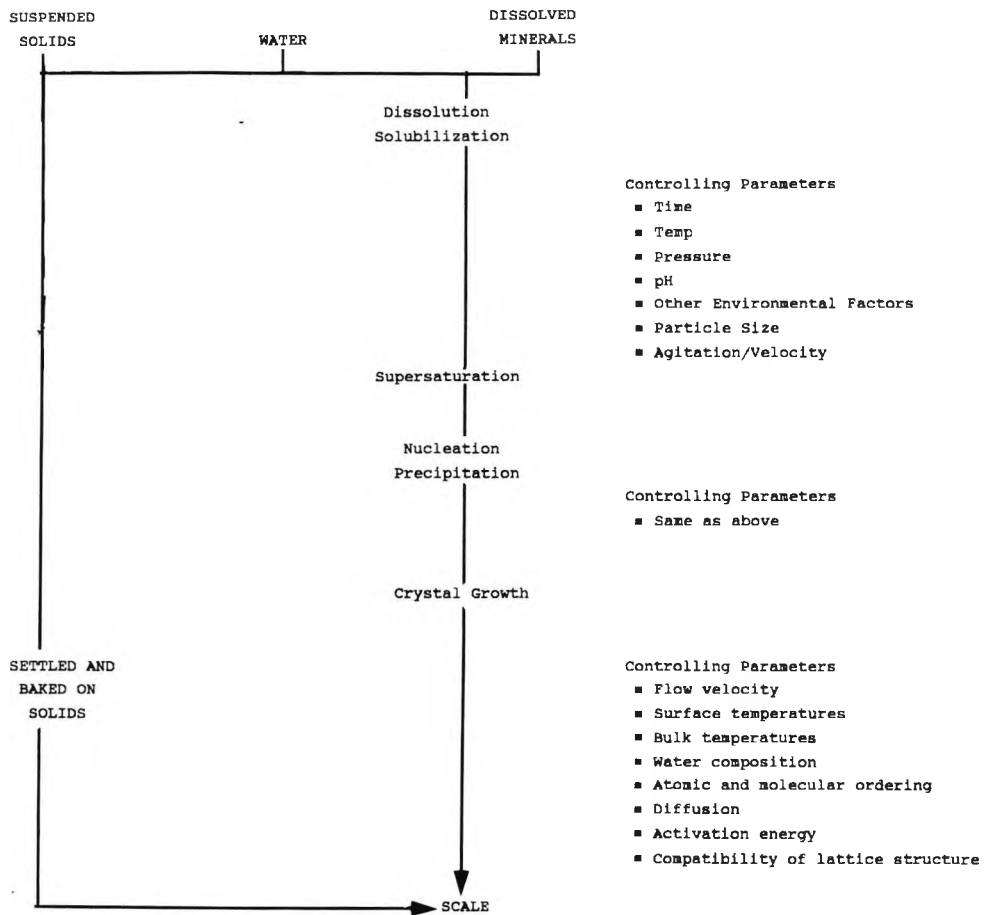


Figure 1.1 General schematic diagram of water formed scale deposit mechanisms.

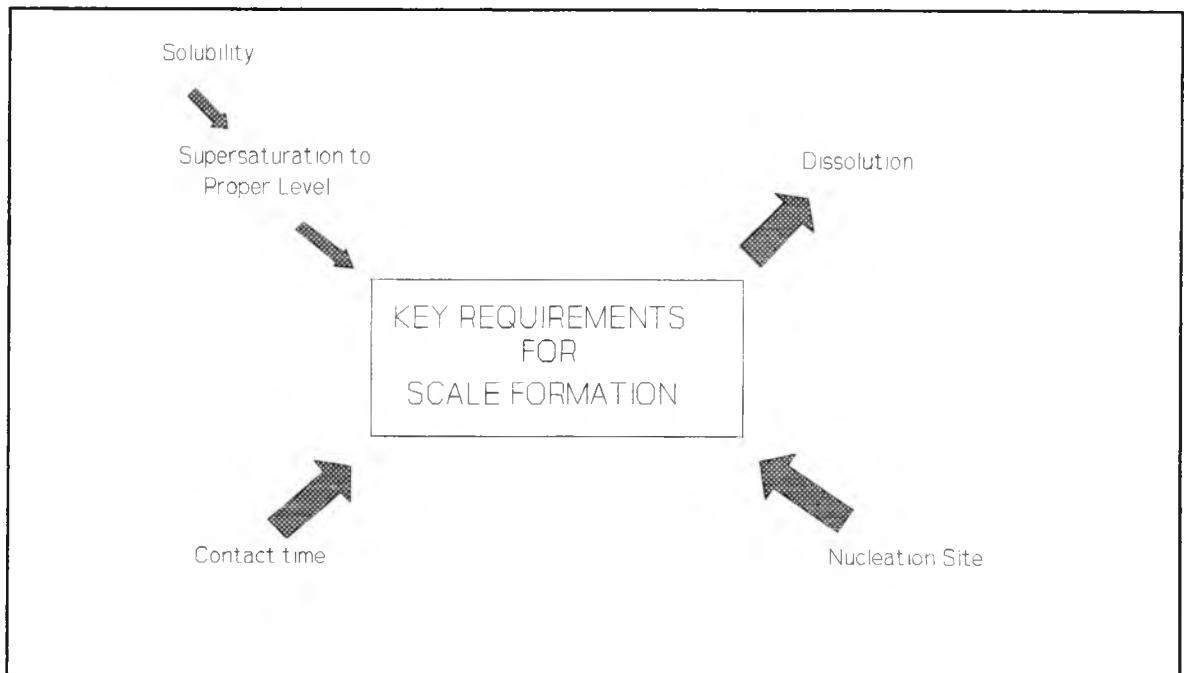


Figure 1.2 Key requirements for scale deposition.

following factors: either changing the levels of potential scale-forming materials in the fluid and/or altering the mechanism of the growth of solid materials from fluids. Some methods of scale prevention, such as acid dosing and ion-exchange are designed to control solubility by preventing the formation of supersaturated solutions.

Yorke and Schorle [2] state that crystallisation from solutions of a material directly on the site of scale formation requires three simultaneous factors: (a) supersaturation, (b) nucleation, and (c) adequate contact time. Figure 1.2 is a schematic diagram of the key scale-forming requirements, showing the relationship of the steps necessary for scale formation.

### 1.2.3 Solubility

The most common scale-forming compounds have low solubilities in the fluid in which they are dispersed. Most, though not all of these scale-forming constituents are inversely soluble, i.e. their solubilities tend to decrease with increasing temperatures. Therefore, when these supersaturated solutions are in contact with heat transfer surfaces they precipitate solids due to their lower equilibrium solubility. The solubilities (g/100g) of some of the most common scale-forming compounds in water at 25°C are:

Barium sulphate	0.0002
Magnesium hydroxide	0.0009
Calcium carbonate	0.0014
Calcium phosphate	0.0020
Strontium sulphate	0.0113
Calcium sulphate dihydrate	0.2410

The solubilities of the solid materials produced in each scaling system investigated in this thesis are discussed in the relevant chapters.

#### 1.2.4 Supersaturation

The primary cause of scale deposition is supersaturation. When the solubility product of a deposit-forming material is exceeded, it precipitates and forms scale under the required conditions, which may be called secondary causes: pressure changes, changes in pH values, increase or decrease in temperature, change in flow rate, surface geometry and chemistry.

A saturated solution is one in which the solid phase (solute) is in equilibrium with the material dissolved in the solution. Supersaturated solutions are solutions that contain higher concentrations of dissolved solute than their equilibrium concentration. If the supersaturation level is low, slow crystal growth rate will result, while at high supersaturation levels, the rate of precipitation can exceed the rate at which ions can be incorporated into the crystal lattice, leading to the breakdown of single crystal interfaces and the onset of non-uniform or dendritic crystal growth. The supersaturation level clearly affects the rate of crystal growth and hence the particle size of the solid product. This is illustrated in Figure 1.3, which is derived from data for supersaturated solutions of barium sulphate obtained by mixing solutions of barium ions with solutions of sulphate ions. At very low barium sulphate concentrations ( $10^{-4}$ - $10^{-3}$  moles  $\text{dm}^{-3}$ ), crystal growth is limited by the availability of the material and a sol is formed. At very high concentrations (2-3 moles  $\text{dm}^{-3}$ ) high viscosity of the fluid retards the rate of crystal growth to form a gel. At intermediate concentrations precipitation of crystalline barium sulphate occurs. Effects such as these are significant in understanding scale formation and its control.

Supersaturated solutions can arise for a number of reasons including: (i) mixing of incompatible streams, (ii) concentration of the solution, (iii) temperature changes, (iv) pressure changes, and (v) pH changes.

Particle size also has an effect on supersaturation. When solids of very fine particle size are suspended in a fluid, concentrations greater than those appropriate to the equilibrium solubility can be achieved. A 20% increase in concentration above the equilibrium solubility value was found for 0.4 micron particles of calcium sulphate dihydrate in water, while an increase of about 80% was found for 0.1 micron particles of barium sulphate in water.

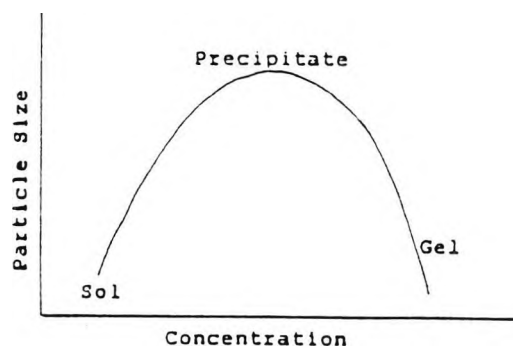


Figure 1.3 Nature of solid deposit from supersaturated barium sulphate at different concentrations (Moles  $\text{dm}^{-3}$ ).

#### 1.2.5 Nucleation

The nucleation process is the initial step in the deposition of solids from supersaturated solutions. Two basic nucleation mechanisms have been recognised: homogeneous, on nuclei formed spontaneously from the mother phase, and heterogeneous, on foreign particles or substrates, such as dust, corrosion products, rough surfaces on container walls and pipework. Of the two mechanisms, heterogeneous nucleation is the dominant mechanism during scale formation as it requires less energy (lower activation energy). It occurs at lower supersaturations, delaying homogeneous nucleation until all the available heterogeneous nuclei are used up. Natural variations in water

cause heterogeneous nucleation, thus making impurities a significant cause of scaling problems.

Nucleation can occur within two different states of supersaturation, viz. (i) the metastable state, and (ii) the labile state. These states are represented by the areas shown in the schematic temperature-concentration diagram in Figure 1.4. The solid line represents the normal solubility curve for a solute in a solvent. The upper broken line represents the supersolubility curve that delineates the point at which spontaneous nucleation can occur (above that line). This line is poorly defined and varies significantly depending on factors, such as seeding, agitation, temperature, pH, pressure and the presence of anti-nucleating additives. Three zones are represented in the diagram: stable, metastable and labile. In the stable region (undersaturated), nucleation does not occur; in the metastable region which exists above the equilibrium solubility curve, nucleation is usually limited because submicroscopic crystals have a higher solubility than the equilibrium solubility; and in the labile region, spontaneous nucleation is probable.

Solutions may stay supersaturated for long periods without scale being formed. In a pure system, the width of the metastable region is given thermodynamically by the free energy of the formation of a nucleus (activation energy). The presence of metal surfaces and impurities usually promotes the nucleation because of the lower activation energy. Therefore, in most cases the presence of different dissolved impurities determines the width of the metastable region, so that heterogeneous nucleation is the dominant mechanism during scale formation. In these systems the nucleation occurs either on the impurities suspended in water or directly on metal surfaces. When formed, the nuclei will develop into visible crystals (scale).

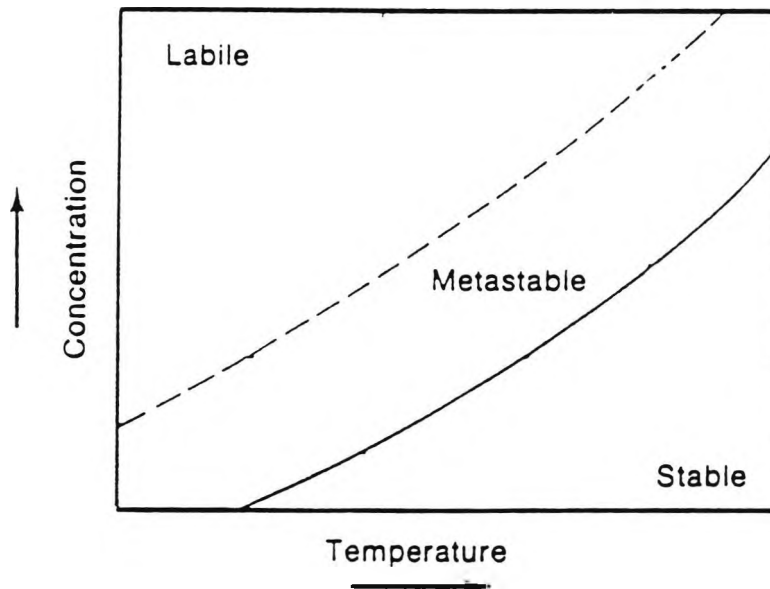


**Figure 1.4 Solubility-supersolubility diagram.**

Nucleation and subsequent crystal growth from a supersaturated solution can be described as a series of steps, *viz.* (a) a starting point, (b) a requisite number of ions/molecules agglomerating, (c) diffusion of ions/molecules to the solution crystal face, (d) adsorption of ions/molecules from the interface onto the crystal surface, (e) surface diffusion to energetically favourable positions on the crystal surface, (f) orientation of the ions/molecules into a fixed lattice, (g) formation of stable nuclei, and (h) growth of larger crystals at the expense of smaller crystallites. All the phenomena described are simultaneously involved when scale is formed and collectively determine the texture of the scale. Should any one mechanism be inhibited, another will dominate. This is particularly important because any factor that can affect any stage of the nucleation-growth process could alter the scale-forming characteristics of the precipitates obtained from supersaturated solutions.

In some descriptions of crystallisation, it has been suggested

that the control of crystal growth can only be achieved when stable nuclei are formed and which are not destroyed by equilibrium redissolution. More recently, however, the importance of clusters of material in solution prior to the formation of stable nuclei has been realised.

#### 1.2.6 Scale Formation

For scale to form after a solution has become supersaturated and nucleation has occurred, there must be sufficient contact time between the solution and the nucleating sites on the surface. Generally, the longer the contact time of a surface with a scale-forming solution the more likely scale formation becomes. This time can vary from seconds to years depending entirely on the degree of supersaturation, the type of scale-forming material, the type and number of nucleating sites, temperature, pressure and agitation.

The amount of scale formed is a function of the number of the initial crystal sites and the growth of the crystal material on those nuclei. Once the scale forms, the deposition rate, for the same degree of supersaturation and the same contact time, is generally greater than it is during nucleation. Hasson *et al* [3] have shown that this is true for calcium sulphate, but no appreciable difference in the rate of calcium carbonate deposition was observed whether on a clean, scaled or unscaled surface.

When scale deposits on a fresh metal heat transfer surface, the first layer of scale is deposited directly onto the metal surface and is influenced to some degree by the characteristics of the metal surface. Subsequent layers of scale, however, form on the scale surface rather than the metal surface. In certain cases the rates of scale growth between the two types of surface are quite different. In other cases, the surface does not appear to influence the rate of deposition. The scale layer contributes nuclei for further scale deposition.

### 1.3 OBJECTIVES

The main objectives of the research in this thesis are twofold: firstly, to investigate the direct field-charge interactions of the charged species present in the calcium carbonate scaling system with applied electromagnetic fields, and to show that the effect of the magnetic treatment of fluids is a general phenomenon. Secondly, a detailed study into scale formation in the off-shore oil industry, looking at the two major scaling systems present, these being the  $\text{BaSO}_4$ - $\text{SrSO}_4$ - $\text{CaCO}_3$  and the  $\text{CaSO}_4$ - $\text{CaCO}_3$  systems in the absence of applied electromagnetic fields.

### 1.4 SCOPE OF THE WORK IN THIS THESIS

The purpose and objectives of the work described in this thesis have been outlined in this introductory chapter. In Chapter 2 the analytical techniques used throughout the work are described.

Chapter 3 describes the effect of electromagnetic treatment of unsaturated aqueous solutions of calcium ions. The first section of the work describes the rate of deposition of calcium carbonate as determined by the propensity to scale measurements. The effects of varying the following: (i) flow rates on the calcium ion solutions through the electromagnetic field; (ii) temperature and (iii) hydrogen carbonate ion concentrations on the rate of deposition of scale were also studied. The second section describes the magnetic treatment of water under industrial and laboratory conditions as heat exchanger experiments, focusing on the deposits formed.

Chapter 4 is a detailed study of unsaturated simulated solutions of formation water and sea water, as encountered in the off-shore oil industry. This chapter is divided into six sections, with the first four investigating the  $\text{BaSO}_4$ - $\text{SrSO}_4$ - $\text{CaCO}_3$  scaling system, and the final two sections investigating the  $\text{CaSO}_4$ - $\text{CaCO}_3$  scaling system, with the rate of deposition of scale being determined by propensity to scale measurements. Precipitation studies were

carried out when unexplained but significant differences were found in the propensity to scale. Sections 1 and 2 describe the effect of varying each constituent ion concentration in simulated formation water and sea water on the rate of deposition of scale for the  $\text{BaSO}_4$ - $\text{SrSO}_4$ - $\text{CaCO}_3$  system. The third section describes the effect of mixing the most and least scale-forming formation water and sea water as determined by the first two sections on the rate of deposition of scale. The fourth section describes the effect of ratio mixing of formation water and sea water on the rate of deposition of scale. Sections 5 and 6 describe the effect of varying each constituent ion concentration in simulated formation water and sea water on the rate of deposition of scale for the  $\text{CaSO}_4$ - $\text{CaCO}_3$  scaling system.

Chapter 5 summarises the main inferences from each of the experimental chapters and gives an overview of the present work.

## REFERENCES

1. Donaldson, J.D., New Scientist, Feb. 1988, 43-46.
2. Yorke, J.L. and Schorle, B.J., "Scale Formation and Prevention," Salt Water Purification, ed. Spiegler, K.S., New York: John Wiley and Sons, Inc., 1962.
3. Hasson, D., Mordercai, A., William, R., Rozenman, T. and Windreich, S., I and EC Fundamentals, 1968, 7 (1), 59-65.

## CHAPTER 2

### EXPERIMENTAL TECHNIQUES

	Page
2.1 PROPENSITY TO SCALE MEASUREMENTS	21
2.2 ATOMIC ABSORPTION SPECTROPHOTOMETRY	27
2.3 CHROMATOGRAPHY	32
2.4 X-RAY POWDER DIFFRACTION	36
2.5 MICROSCOPY	40
REFERENCES	43

## CHAPTER 2

### EXPERIMENTAL TECHNIQUES

The main experimental techniques used throughout the work described in this thesis were:

- (1) Propensity to Scale Measurements (P.M.A.C.)
- (2) Atomic Absorption Spectrophotometry (A.A.S.)
- (3) Ion-exchange Chromatography
- (4) X-ray Diffraction
- (5) Microscopy

#### 2.1 PROPENSITY TO SCALE MEASUREMENTS

The propensity to scale measurements in this study were carried out using the P.M.A.C. Pressure Measurement and Control system. It is designed to monitor the changes in pressure that occur across a microbore tube, at fixed temperatures as scale builds up. The P.M.A.C. system is comprised of four component units, *viz.*: (i) an accurate flow pumping unit, consisting of two peristaltic pumps, (ii) a heating apparatus (oven) for the microbore tube, (iii) a pressure sensor and measurement unit and (iv) a chart recorder.

Two different P.M.A.C. units were used in this study. The first was used for the  $\text{CaCO}_3$  scaling system (Chapter 3) and the  $\text{CaCO}_3$ - $\text{CaSO}_4$  scaling system (Chapter 4). The second was used for the  $\text{BaSO}_4$ - $\text{SrSO}_4$ - $\text{CaCO}_3$  scaling system (Chapter 4). These units differ in their oven designs for mixing the scaling solutions. Figure 2.1 is a schematic layout for the first unit, with Figure 2.2 showing the preheating and microbore tubes. The schematic layout for the second P.M.A.C. unit is shown in Figure 2.3. Figure 2.4 shows the preheating and microbore tubes.

The two units are similar except for their method of mixing points in the oven. The first P.M.A.C. unit mixes the two solutions at a 4 piece junction, where the other two connections

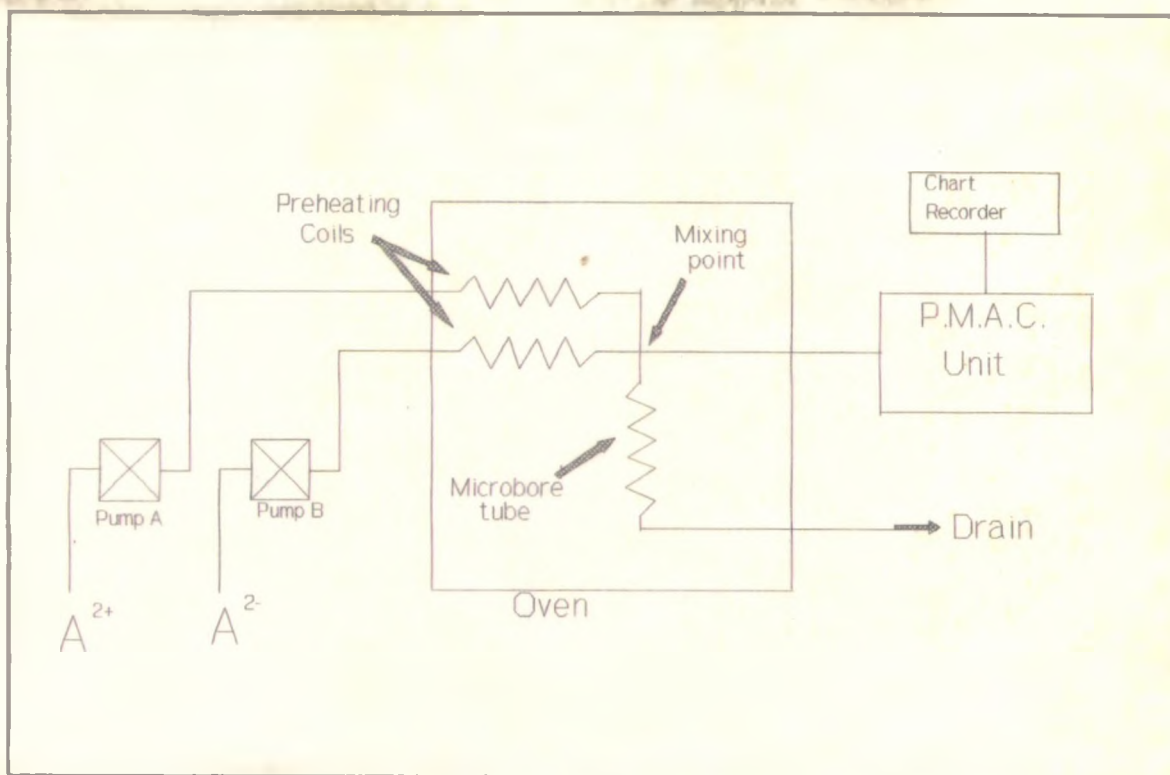


Figure 2.1 Schematic diagram of the P.M.A.C. system used for the  $\text{CaCO}_3$  and  $\text{CaSO}_4\text{-CaCO}_3$  scaling systems.

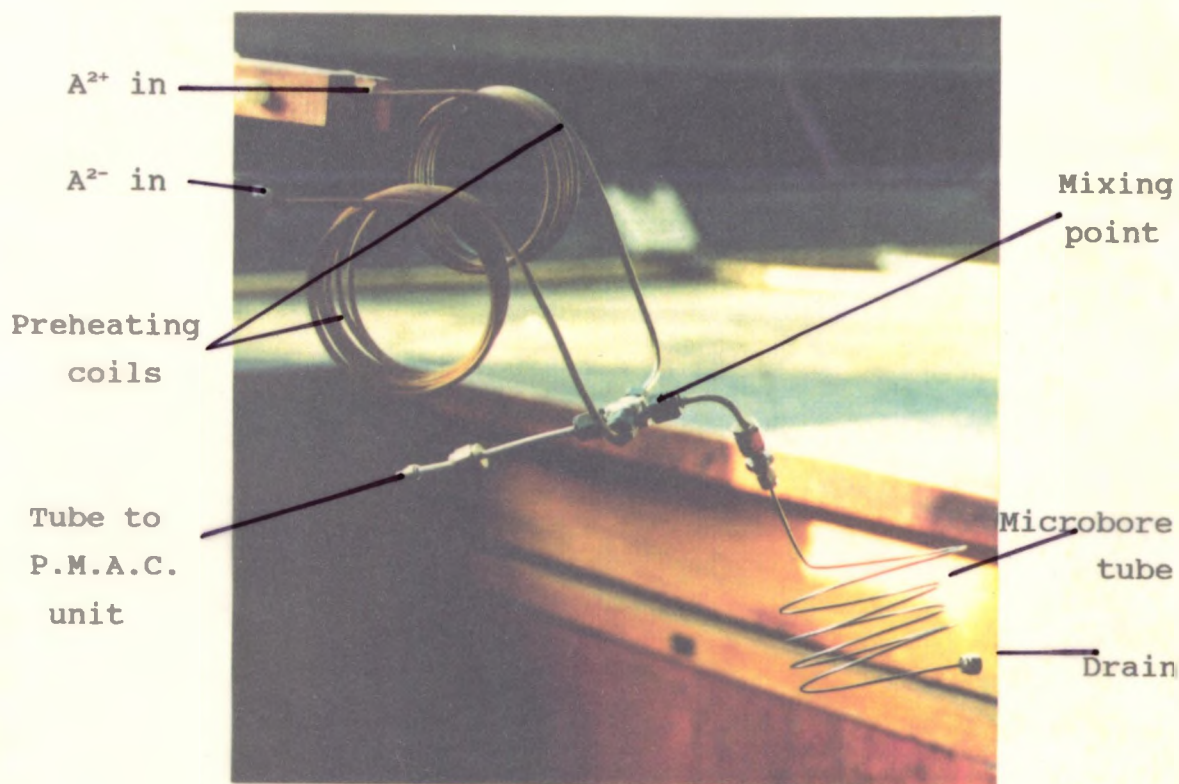
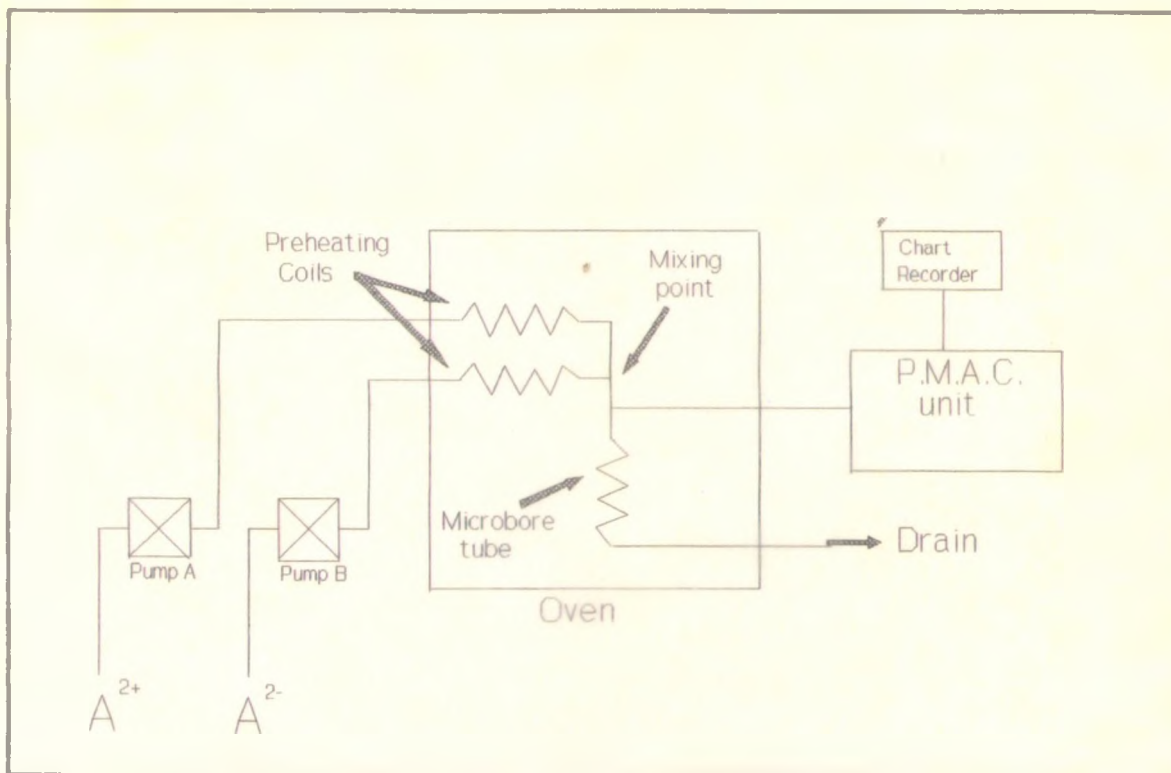
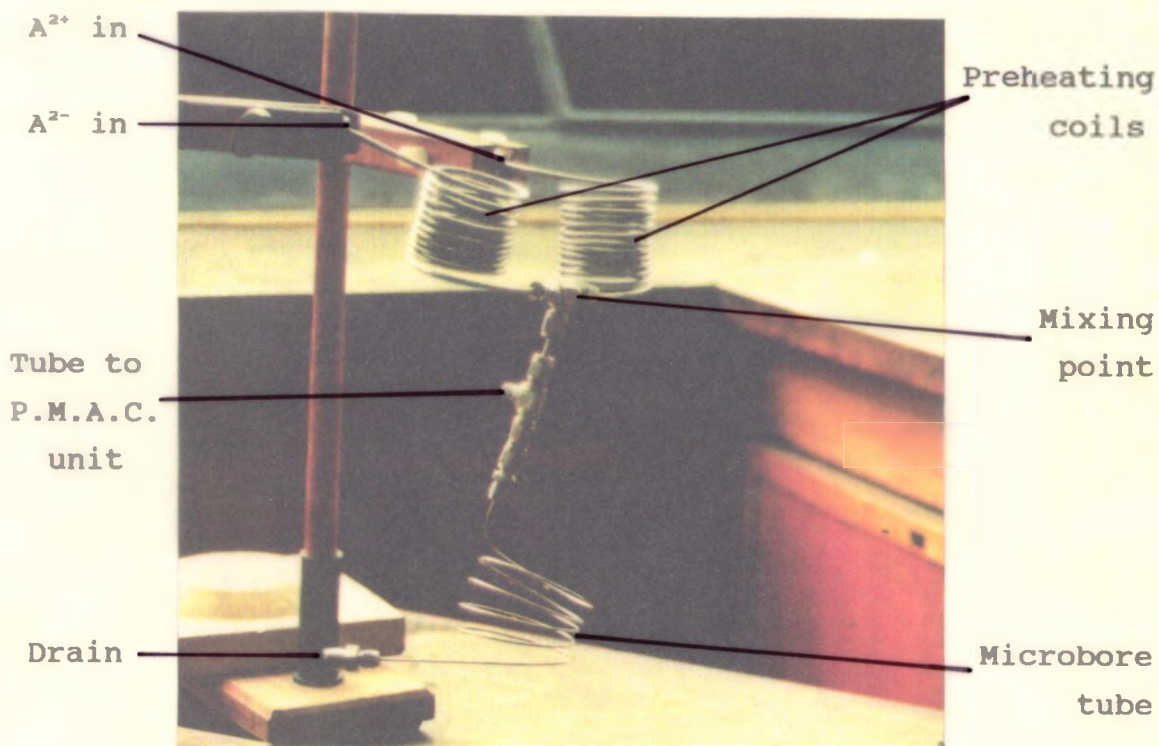


Figure 2.2 Layout of the preheating and microbore tubes.



**Figure 2.3 Schematic diagram of the P.M.A.C. used for the  $BaSO_4$ - $SrSO_4$ - $CaCO_3$  scaling system.**



**Figure 2.4 Layout of the preheating and microbore tubes.**

go to the pressure sensor and the microbore tube. The second unit has the two solutions mixing at a T-piece, and the mixed solution is then pushed down to another T-piece connecting the pressure sensor to the microbore tube. A complete P.M.A.C. unit is shown in Figure 2.5.

Both P.M.A.C. units operate in the same manner as described in the following sections.

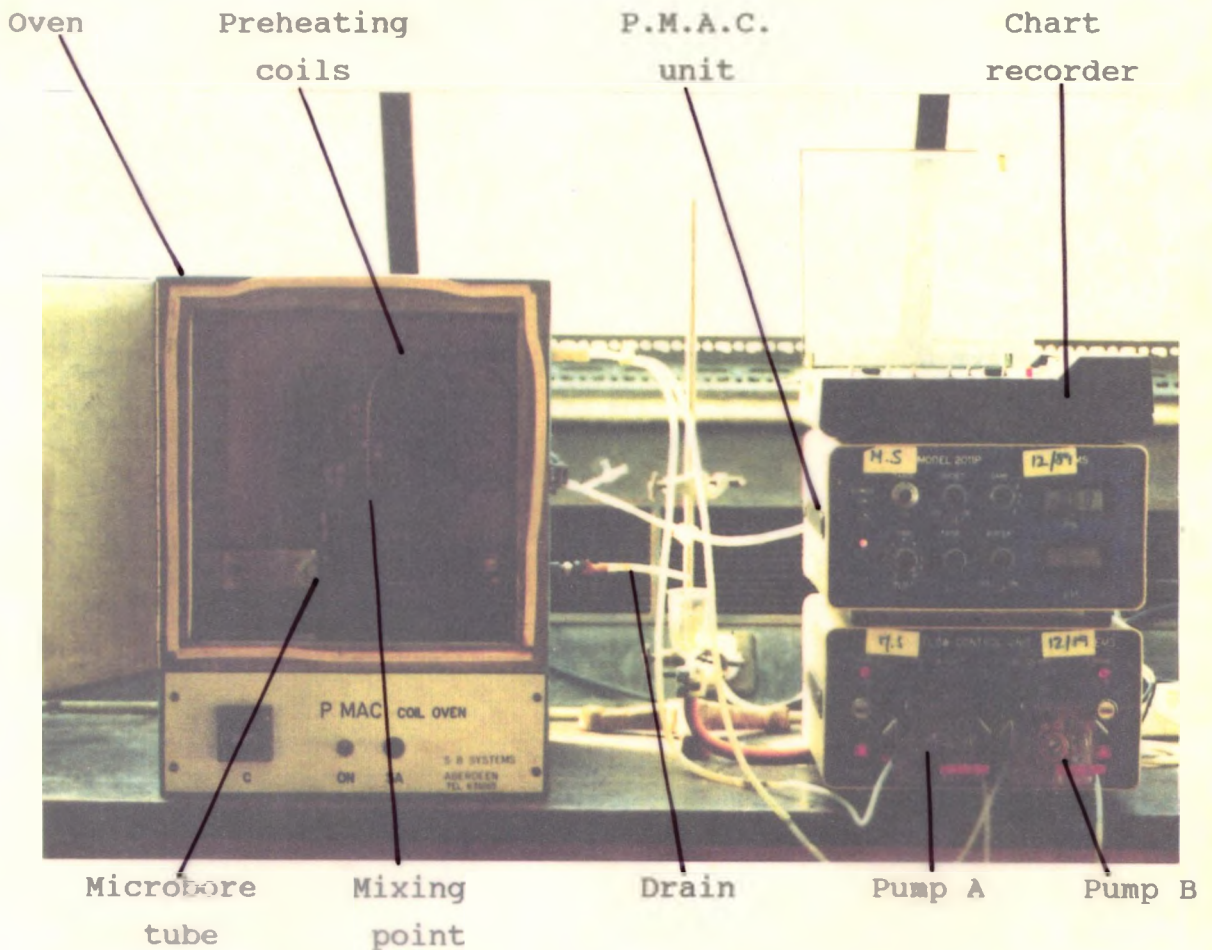


Figure 2.5 P.M.A.C. scaling system.

P.M.A.C. system operation

The P.M.A.C. system operates by encouraging the precipitation of solids from solutions to form scale at controlled temperatures on the wall of a microbore tube. The buildup of scale in the

microbore tube over time is monitored by the change in back pressure as the solutions are pumped through the microbore tube. The accurate pressure measurement of scale buildup over a period of time can directly indicate changes in the rate of deposition of scale as either the temperature or concentration of the solutions are altered.

The two scaling solutions, containing cation(s) and anion(s) respectively are pumped using two peristaltic pumps into the oven preheating coils at fixed flow rates. The two solutions are mixed by the methods already described and are passed into the microbore tube.

The constant pumping of the solution at constant temperature causes the chemical interaction between the cation(s) and anion(s), resulting in a buildup of scale, which reduces the diameter of the microbore tube. This reduction in diameter increases the fluid velocity and pressure drop across the coil. The pressure drop is monitored by a ceramic pressure sensor inside the P.M.A.C. unit and the resultant signal is conditioned and amplified to produce a buffered output. This smoothed output is then externally recorded in the form of a scaling curve, showing the change in Pressure (P) across the coil against time. Figure 2.6 is an example of a scaling curve obtained for the  $\text{CaSO}_4$ - $\text{CaCO}_3$  scaling system.

#### P.M.A.C. components

##### (i) Microbore tube

The coiled microbore tube used in this work had a bore size of 1.1 mm (i.d.) and a total length of one metre (uncoiled). Both the inlet (attached to both peristaltic pump lines via the preheating coils) and outlet (connected to the drain) were mounted in the oven (accuracy  $\pm 1^\circ\text{C}$ ) as shown in Figures 2.1 and 2.3. The coil was made from stainless steel to resist attack from potentially corrosive solutions that can cause pitting in the tube, which in turn can severely interfere with the accurate

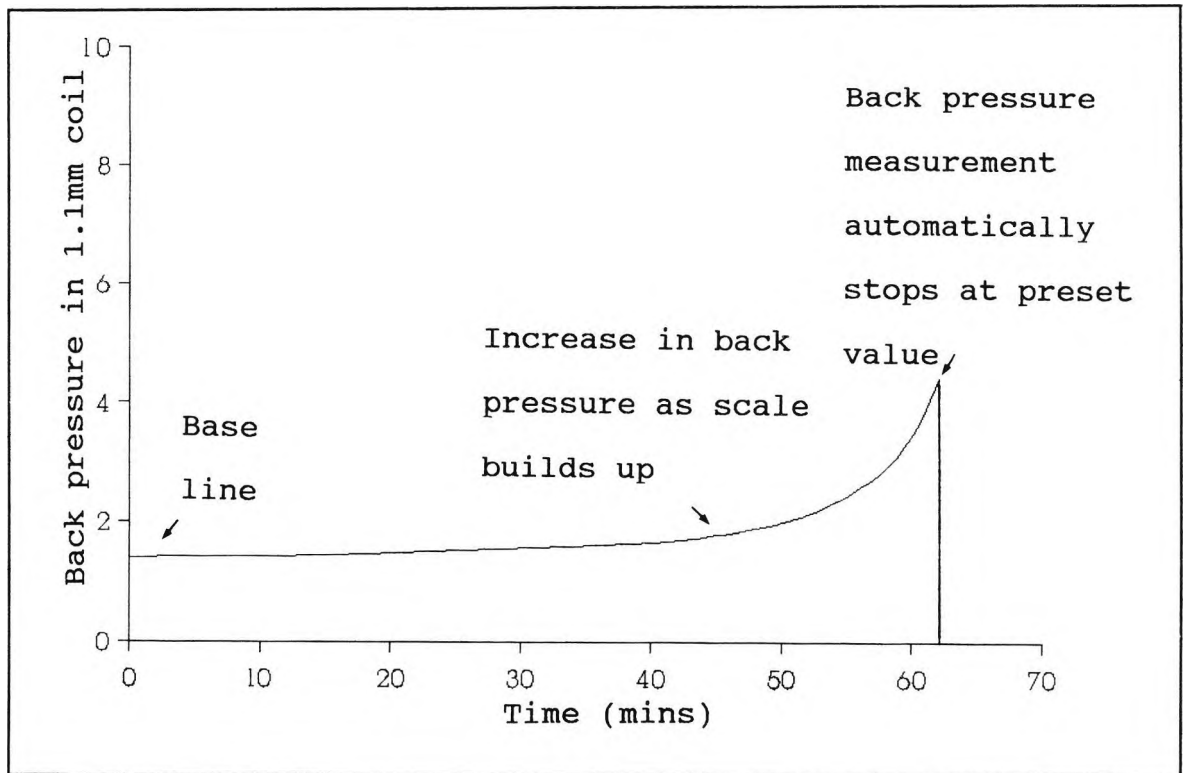


Figure 2.6 Example of the back pressure measurement for the  $\text{CaSO}_4$ - $\text{CaCO}_3$  scaling system.

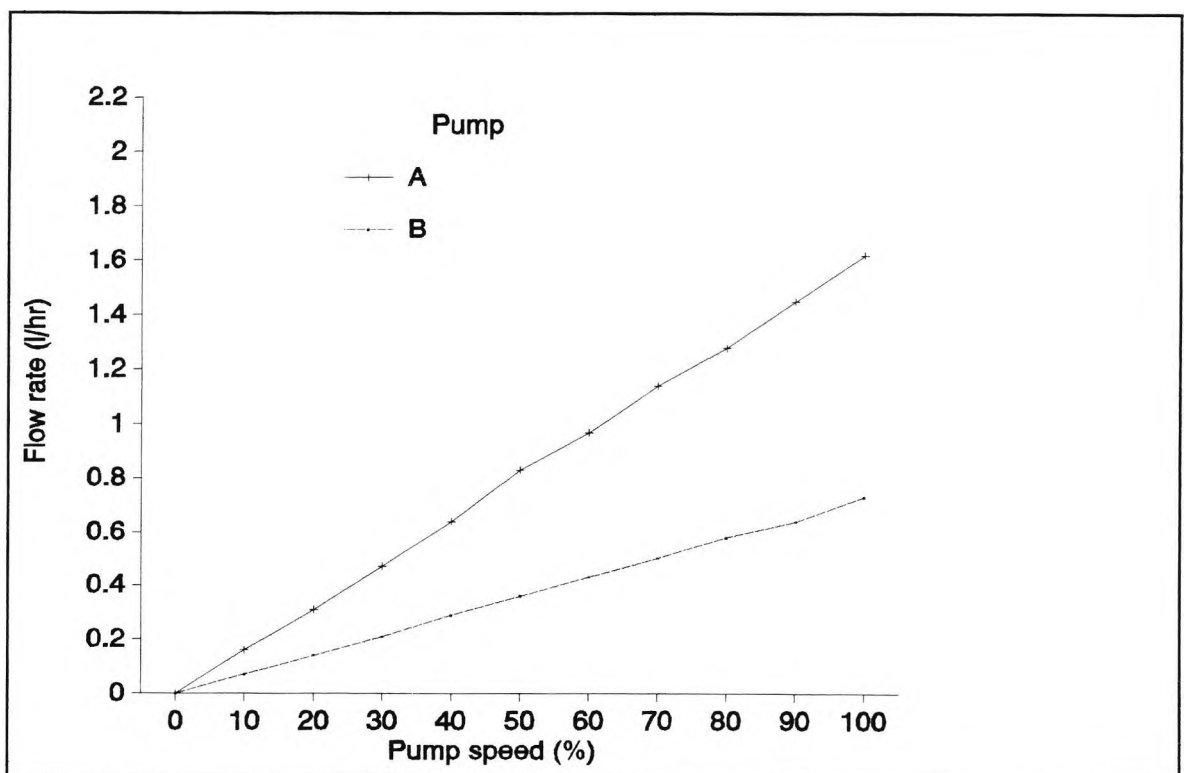


Figure 2.7 Flow rates for the P.M.A.C. pumps in Figure 2.1.

measurement of the pressure drop in the coil. In all the experiments, the cleaning of the microbore tube is very important as any foreign particles in the tube may cause not only a partial blockage but also the pre-nucleation of scale. This will give inaccurate and unrepresentative measurements of the rate of deposition of scale.

#### (ii) Peristaltic pumps

The peristaltic pumps used in this work were of an advanced modified design (Watson Marlow Model 2011) and used optical tachometer feedback to give precise repeatable pump speeds under varying load conditions. Both pump heads used 1.6 mm i.d. silicone tubing connecting the scaling solutions to the preheating and microbore tubes. The flow rates for each solution were frequently calibrated in order to monitor any fluctuations. The flow rates for Pump A and Pump B for the P.M.A.C. unit used for the  $\text{CaCO}_3$  and  $\text{CaSO}_4$ - $\text{CaCO}_3$  scaling systems are shown in Figure 2.7.

### 2.2 ATOMIC ABSORPTION SPECTROPHOTOMETRY

Atomic Absorption Spectrophotometry (A.A.S.) can be used to determine most elements. In this method, a solution containing low concentrations of metallic elements is atomised into a vapour containing free atoms of the elements. A hollow cathode lamp (light source) emits radiation, which is characteristic of the element to be determined and this radiation is directed through the vapour. The analyte atoms dispersed throughout the vapour absorb a proportion of the radiation, resulting in a decrease in the radiation emerging from the vapour and it is the decrease in radiation which is measured by a detector. A monochromator is included in the system so that energy of the desired wavelength can be isolated from that of neighbouring wavelengths emitted from the light source [1]. Sensitivity is defined as that concentration of an element in ppm (or  $\mu\text{g/ml}$  or  $\text{mg/l}$ ) in aqueous solution which gives a 1% absorption signal.

### Hollow-cathode lamps

Hollow-cathode lamps are the most common sources for A.A.S. The lamps comprise a hollow cup cathode made from the element to be determined and a tungsten anode housed in a glass envelope containing an inert gas at low pressure (Figure 2.8) [1]. Ionization of the inert gas occurs when a potential is applied across the electrodes, and a current of about 5 to 10 mA is generated as ions and electrons migrate to the electrodes. If the potential is sufficiently large, the gaseous cations acquire enough kinetic energy to dislodge some of the metal atoms from the cathode surface and produce an atomic cloud; this process is called sputtering. A portion of the sputtered metal atoms are in excited states and thus emit their characteristic radiation as they return to the ground state. Eventually, the metal atoms diffuse back to the cathode surface or to the glass walls of the tube and are redeposited. The cylindrical configuration of the cathode tends to concentrate the radiation in a limited region of the tube; this design also enhances the probability that redeposition will occur at the cathode rather than on the glass walls. The total light obtained is subsequently passed on to a monochromator, usually a grating or prism, to separate the resonance line from other nearby spectral lines.

### Atomization systems

The gas combination most often used to produce atomization of the vapours in A.A.S. is air-acetylene or nitrous oxide-acetylene. Air-acetylene is the preferred flame for the determination by A.A.S. Its temperature is approximately 2300°C and it may be used as an oxidising lean blue flame. Nitrous oxide-acetylene has a maximum temperature of about 2900°C and it is used for the determination of elements which form refractory oxides. Light emission from the  $N_2O/C_2H_2$  flame is very strong at certain wavelengths, causing fluctuations in the analytical result at those wavelengths. However, it is unlikely to be a problem when using primary wavelengths of the elements but occurs when using the secondary wavelength.

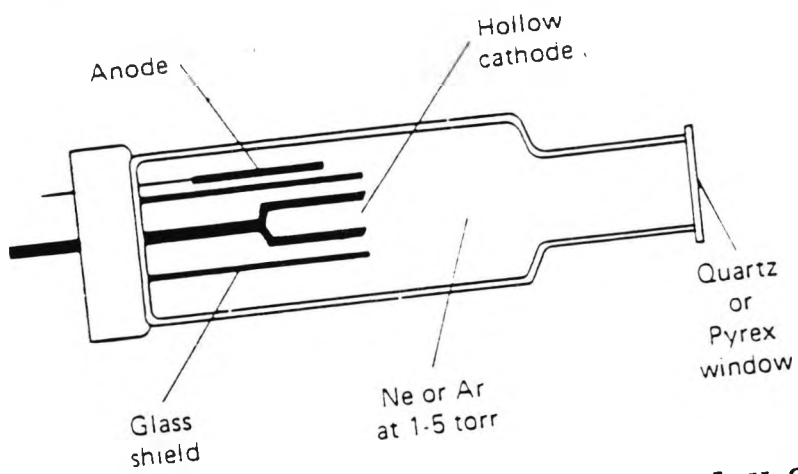


Figure 2.8 Schematic cross-section of a hollow cathode lamp.

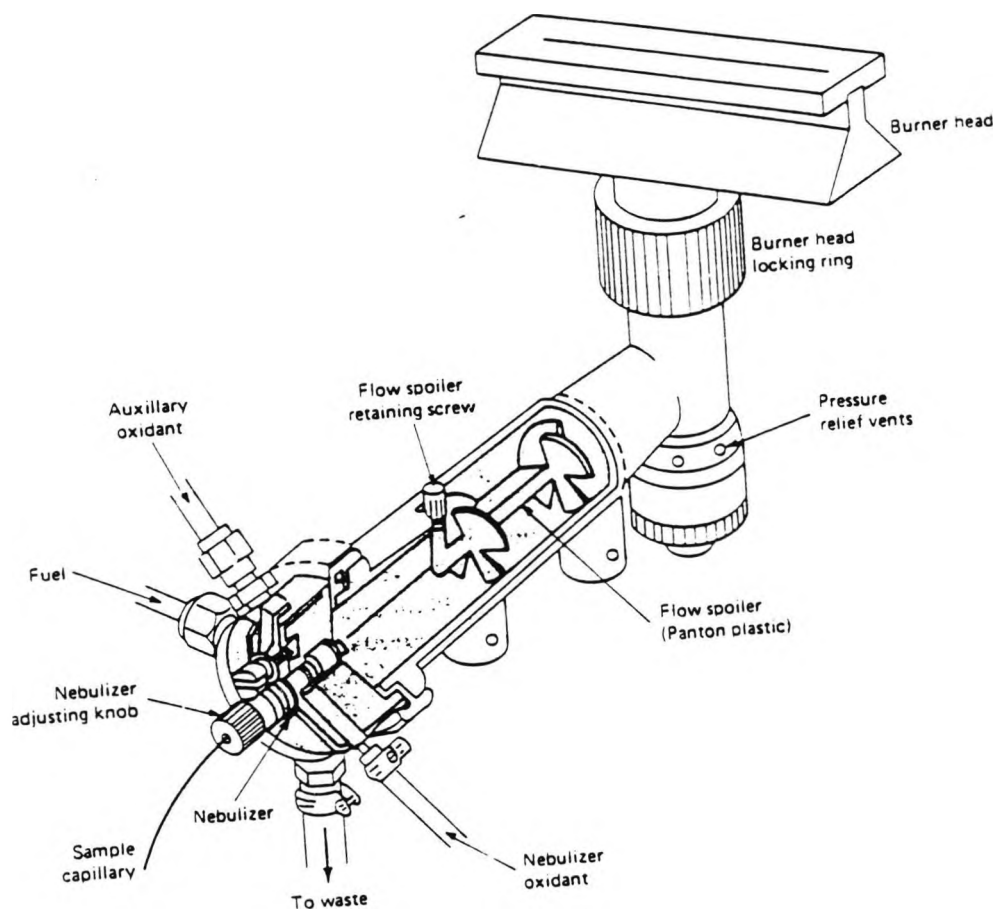


Figure 2.9 A laminar flow burner.

### Burner nebulizer system

The laminar flow premix system is the only type of burner in general use for A.A.S. The liquid sample is introduced into the burner through a nebulizer by venturi-action of the nebulizer oxidant. Figure 2.9 shows a cross-section of a nebulizer premix burner assembly. In passing through the nebulizer the liquid sample is broken into a droplet spray. The premix burner contains, in addition to the nebulizer, a premix chamber and burner head. The premix chamber is designed to mix the fuel, oxidant and sample. Not all the liquid entering the premix burner passes into the flame because the premix chamber allows the larger droplets to condense (aided by the flow spoiler system) and pass out of the chamber to the liquid drain tube. Rejection of these larger droplets helps to minimise light scattering effects in the flame.

### Optical system

In A.A.S. the monochromator is placed after the atom reservoir to help diminish light flux onto the phototube. Figure 2.10 is a schematic diagram of a typical single and double-beam instrument. The instruments used in the present work were the Perkin-Elmer 370 and Perkin-Elmer 2380 Atomic Absorption Spectrophotometers. They are both double beam models, where the beam from the hollow cathode source is split by a mirrored chopper, with one half passing through the flame and the other around it. The two beams are then recombined by a half-silvered mirror and passed into a grating monochromator. A photomultiplier tube acts as a transducer from which the output is fed into a lock-in amplifier which is synchronized with the chopper drive. The ratio between the reference and sample signal is then amplified and fed to the readout which may be a meter, digital device or recorder. Double beam instruments lose a factor of 2 in signal, as a result of this process. The main purpose of this system is to cancel the instabilities in the source by correcting for fluctuations in the lamp output.

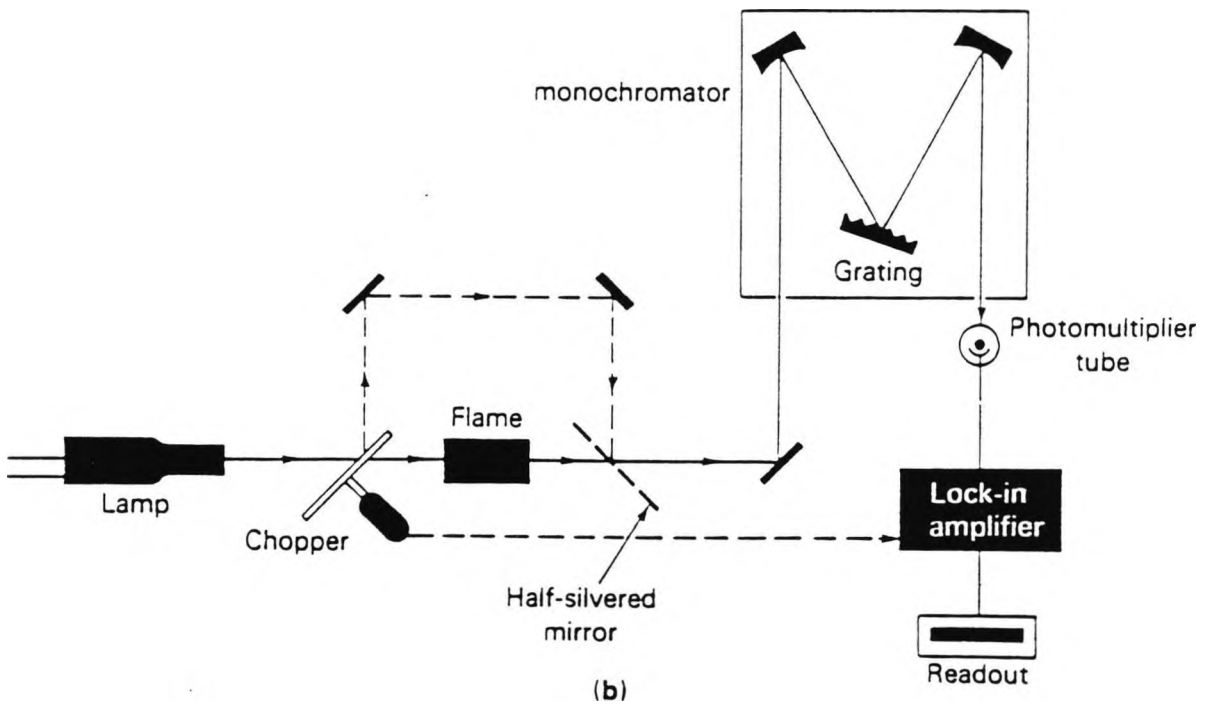
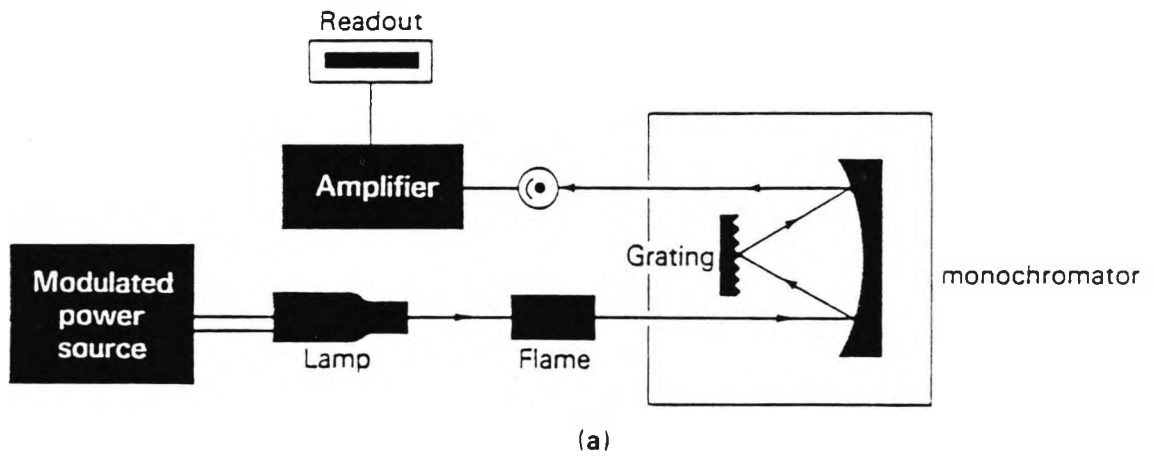


Figure 2.10 Typical flame spectrophotometers: (a) single-beam design; (b) double-beam design.

### 2.3 CHROMATOGRAPHY

Chromatographic techniques depend principally on the variation in the rate at which different components of a mixture migrate through a stationary phase under the influence of a mobile phase. During a chromatographic separation, solute molecules are continually moving back and forth between the stationary and mobile phases. While they are in the mobile phase, they are carried forward with it but remain virtually stationary during the time spent in the stationary phase. The rate of migration of each solute is therefore determined by the proportion of time it spends in the mobile phase, or in other words, by its distribution ratio. The process whereby a solute is transferred from a mobile to a stationary phase is known as "sorption".

#### Ion-exchange chromatography

Ion-exchange separations are limited to samples containing ionized or partially ionized solutes; ion-exchange chromatography is used in the separation of anionic and cationic species. The process involves an interchange of ions of like sign between the solution and an essentially insoluble solid in contact with the solution. The stationary phase consists of a polystyrene-based resin, crosslinked with divinylbenzene (DVB) and contains fixed charged groups and mobile counter-ions, which can be reversibly exchanged for those of a solute carrying a like charge, as the mobile phase travels through the system. The proportion of DVB is between 2 and 20% and results in a three dimensional crosslinked structure that is rigid, porous and highly insoluble [2]. The extent of crosslinking, expressed as the weight percent of DVB, affects the rigidity of the structure and the pore size. A low degree of crosslinking produces beads which swell appreciably when in contact with a polar solvent and have large pores enabling ions to diffuse into the structure and exchange rapidly. This phenomenon of swelling results from the osmotic pressure set up when a resin bead, which can be considered to be a concentrated electrolyte solution, is surrounded by a more

dilute polar solution. Solvent flows into the bead and distends the structure in an attempt to reduce the osmotic pressure by dilution. Resins with a high degree of crosslinking have smaller pores and are more rigid. The degree of crosslinking and thus pore size is controlled by the polymerization process.

For the exchange of cations, the exchange function is usually a sulphonate group, whereas for the analysis of anions, a quaternary ammonium group is commonly employed, as shown in Figure 2.11. The different rates of migration result from variations in the affinity of the stationary phase for different ionic species. The mobile phase contains an ion of low resin

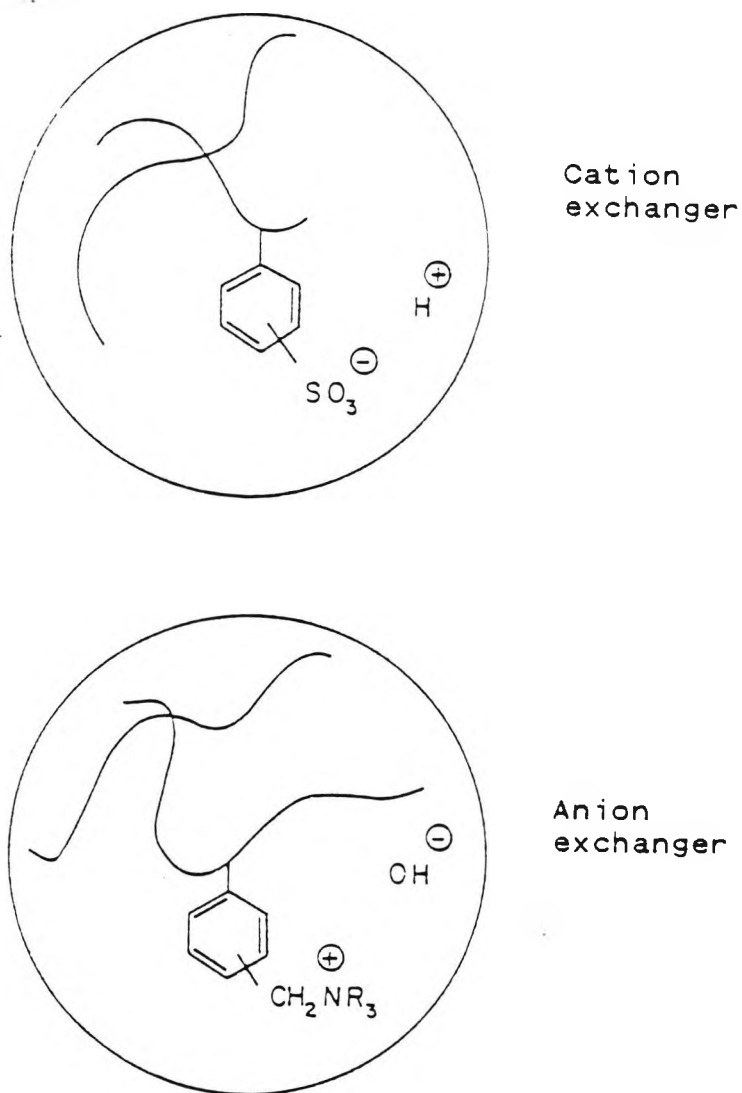


Figure 2.11 Representation of common forms of ion-exchanger.

affinity, and the separated components collected at the bottom of the column are thus accompanied by a relatively high concentration of this ion. Procedures often adopted in ion-exchange chromatography are "gradient elution", involving continuous variation in the composition of the eluting agent, "stepwise elution", in which the composition is altered at specific points during the separation, and "complexing elution", where a reagent which forms complexes of varying stability with the sample components is included in the solution. Acids, bases and buffers are most widely used as eluting agents.

### Instrumentation

The major components of a modern chromatographic instrument, as used in this work and developed by Dionex, are illustrated in Figure 2.12.

The mobile phase is pumped through the chromatographic system by a double reciprocating pump [3]. A pulse-free flow, necessary for both UV/Vis and amperometric detectors, is ensured by a complex electronic control of the pump.

The samples are introduced into the system via a loop injector shown schematically in Figure 2.13. The two outlets of the sample loop which is loaded at atmospheric pressure, are joined by a three-way valve. After the valve is switched the sample is transported onto the column by the mobile phase.

The two ion-exchange columns are coupled in series and form the most important part of the chromatograph. The selection of a suitable stationary phase as well as of the appropriate chromatographic parameters, determines the quality of the analysis. The column bodies are fabricated with inert materials and are generally operated at room temperature. In some instances, such as in the analysis of carbohydrates and amino-acids, it is necessary to thermostat the columns at elevated temperature.

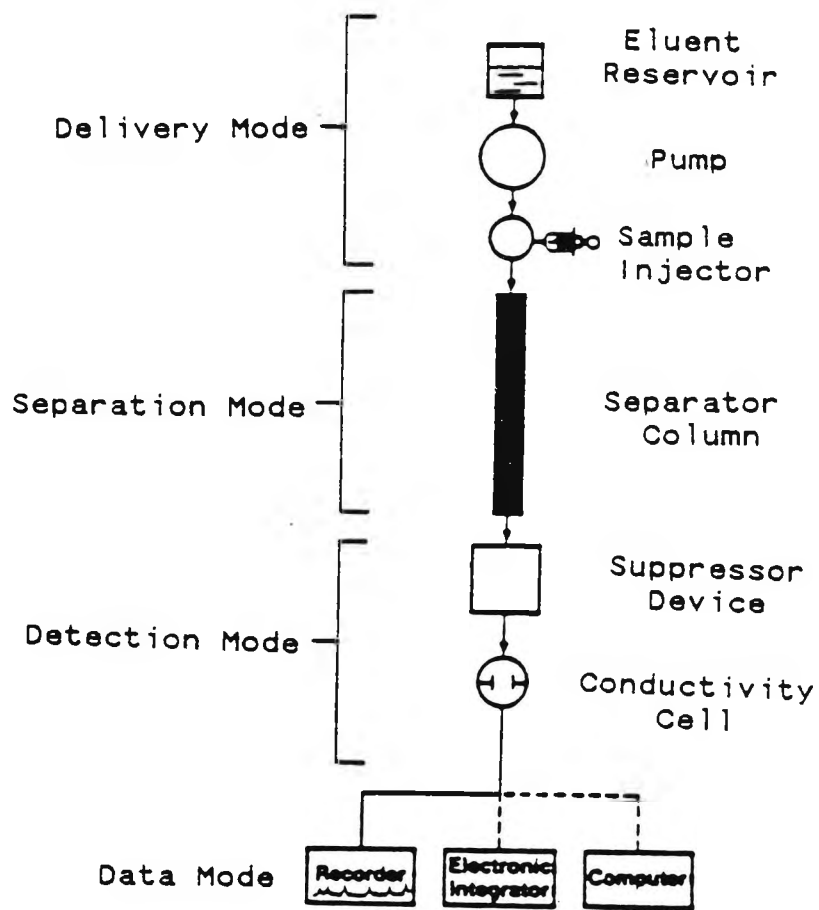


Figure 2.12 A typical Dionex ion-exchange chromatograph configuration.

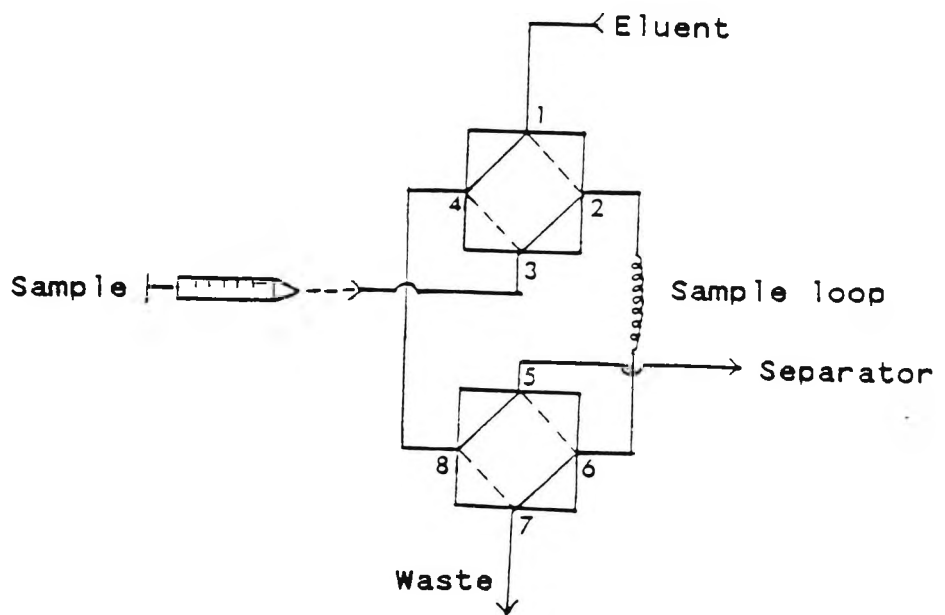


Figure 2.13 The loop injector.

The performance of a detector (which serves to identify and quantify the species being analyzed) depends upon (a) linearity, (b) resolution, and (c) noise.

The most widely used detector in ion-exchange chromatography is the conductivity detector. This detection system usually incorporates a suppressor device that serves to chemically reduce the background conductivity of the eluent, which simultaneously converts the species of interest into a more conductive form [4]. UV/Vis., amperometric, and fluorescence detectors are sometimes used in addition to the conductivity detector.

The chromatogram is obtained via a recorder or computer. Quantitative results are derived from the calculation of peak areas or peak heights that are proportional to the concentration of the species being determined.

The ion chromatography traces for the standard sample containing  $\text{Cl}^-$  5 ppm,  $\text{NO}_3^-$  5 ppm and  $\text{SO}_4^{2-}$  5 ppm and for a sample are shown in Figure 2.14.

#### 2.4 X-RAY POWDER DIFFRACTION

X-ray powder diffraction is a physical technique used in the characterisation of solids. It has been in use since the early part of this century for the "fingerprint" identification of crystalline materials and for the determination of crystal structures [5].

The principles of X-ray powder diffraction are illustrated in Figure 2.15. A monochromatic beam of X-rays strikes a finely powdered sample which, ideally consists of randomly orientated crystals. In such a sample, the various lattice planes are also randomly orientated. Thus, for each set of planes at least some crystals must be orientated at the Bragg angle, theta ( $\theta$ ), to the incident beam and so diffraction occurs for these crystals and planes. The diffracted beam may be detected either by surrounding

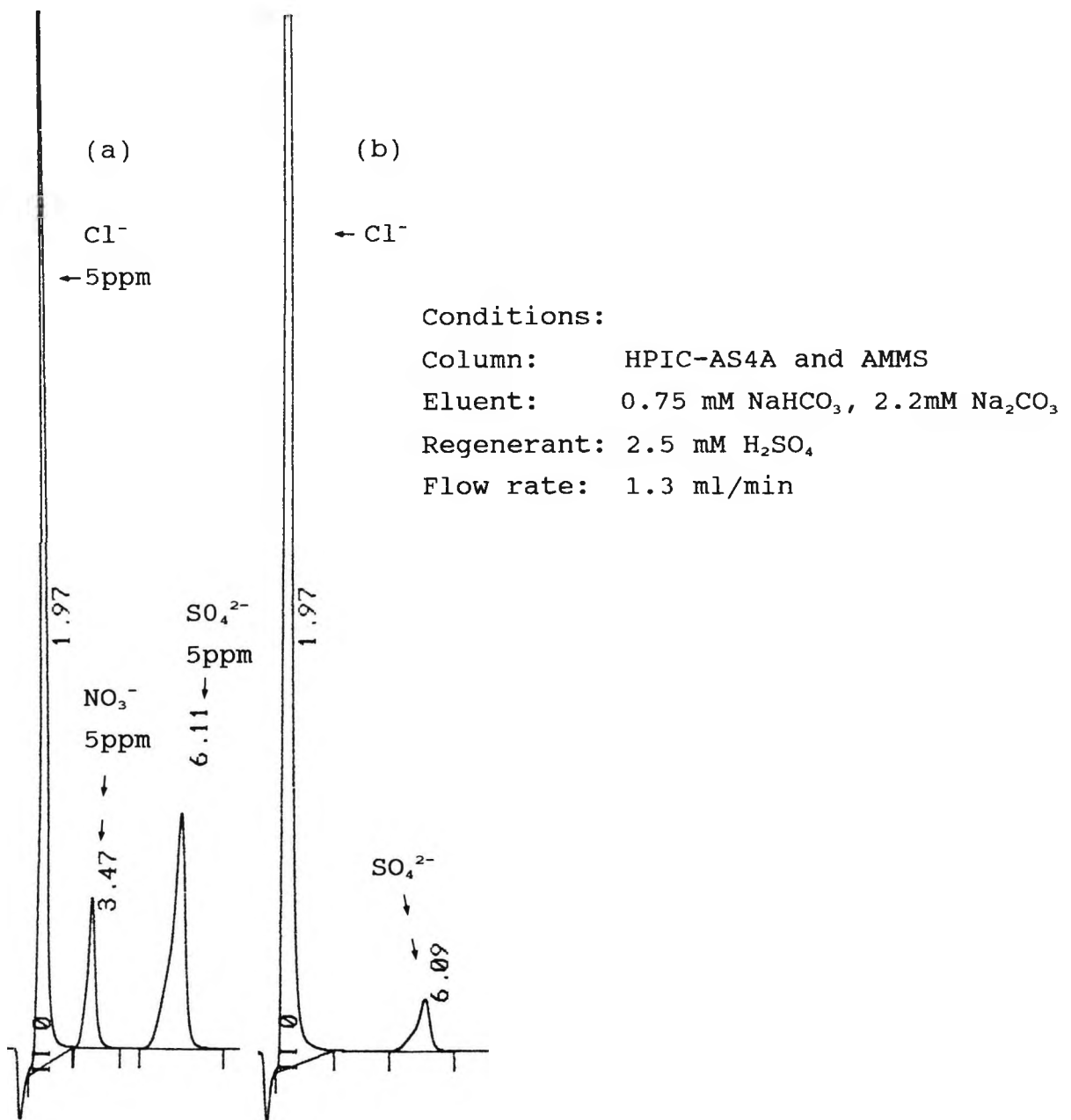


Figure 2.14 Chromatographic traces of: (a) standard sample (Cl<sup>-</sup>, NO<sub>3</sub><sup>-</sup>, and SO<sub>4</sub><sup>2-</sup>); and (b) a sulphate sample.

the sample with a strip of photographic film (Debye-Scherrer and Guinier focusing methods) or by using a movable detector, such as a Geiger counter connected to a chart recorder (diffractometer).

The original powder method, (Debye-Scherrer method) is used little nowadays, although its mode of operation is instructive. For a given set of lattice points, the diffracted radiation forms the surface of a cone. The only requirement for diffraction is that the planes be at an angle, theta ( $\theta$ ), to the incident beam.

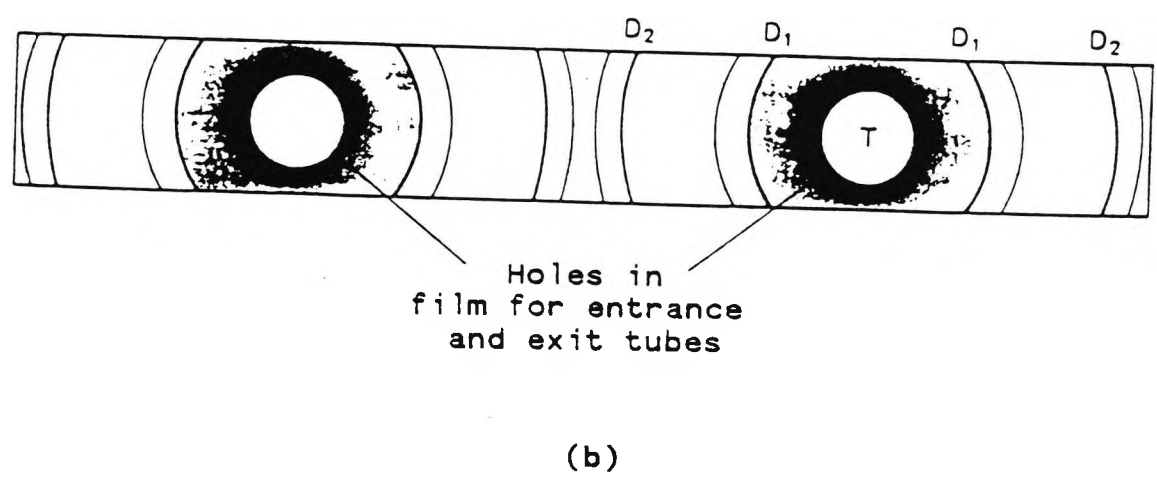
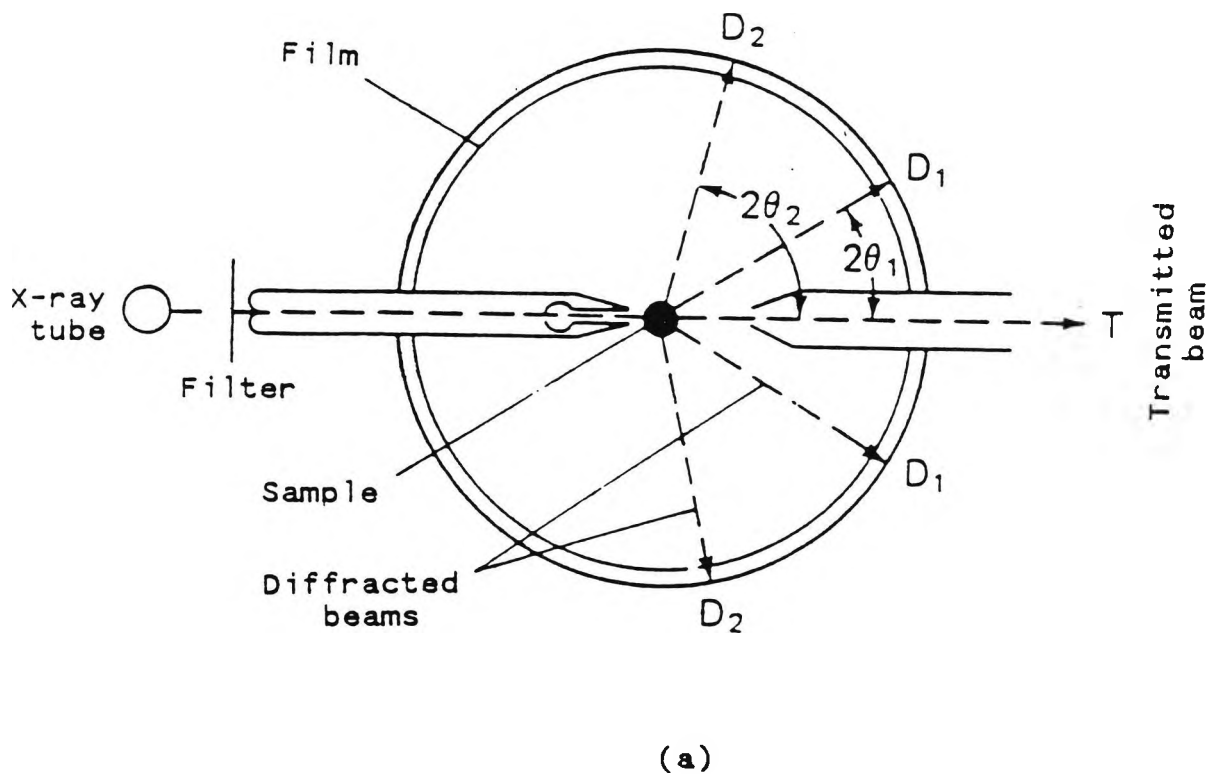


Figure 2.15 Schematic diagram of: (a) a powder camera, and (b) the film strip after development.

In finely powdered samples, crystals are positioned randomly about the incident beam and the resulting diffracted beams appear to be emitted from the sample as cones of radiation. Since the Bragg angle is  $\theta$ , the angle between diffracted and undiffracted beams is  $2\theta$  and the angle of the cone is  $4\theta$ . Each cone of radiation is produced by a different set of planes. A thin strip of film wrapped around the sample detects the cones which appear as arcs, symmetrical about the two orifices in the film (these allow entry and exit of the incident and undiffracted beams). Finely ground samples produce a continuous line; in coarser samples, relatively few particles are present and so do not satisfy the assumption that they lie in all possible orientations, which may result in the arcs being "spotty".

To obtain the d-spacing, the separation  $S$ , between pairs of corresponding arcs is measured, and by knowing the radius  $R$ , the following expression is applied:

$$\frac{S}{2\pi R} = \frac{4\theta}{360}$$

From this  $2\theta$  and  $d$  may be obtained for each pair of arcs.

Modern film methods, such as Guinier focusing methods, make use of a convergent intense incident beam. A single crystal of quartz or graphite is placed between the X-ray source and the sample to obtain a convergent beam. The orientation of the crystal is adjusted so that it diffracts the incident beam and converts it from a divergent to a convergent beam. The beam then strikes the sample and the diffracted beams are arranged to focus at the surface of the film.

Another modern powder technique as used in this work is diffractometry. Again, a convergent beam is used and the resolution is fairly good. An advantage of this method is the reduction in exposure time (typically 10 minutes to 1 hour). The instrument has a proportional scintillation or Geiger counter as

the detector, which is connected to a chart recorder. The counter is usually set to scan over a range of  $2\theta$  values at a constant velocity. Generally the range 10 to  $80^\circ$ ,  $2\theta$  is sufficient to cover the most useful part of the powder pattern. The output to chart paper consists of a plot of peaks against values of  $2\theta$ .

### Interpretation

The principal features of a powder pattern are the d-spacings and intensities. The d-spacings (positions) of the lines in a powder pattern are governed by the values of the unit cell parameters ( $a$ ,  $b$ ,  $c$ ,  $\alpha$ ,  $\beta$ , and  $\gamma$ ). The intensities provide information on the types of atoms present in the sample. Intensities are recorded relative to the intensity of the strongest line of the pattern which is arbitrarily assigned as 100. For a particular substance the line positions are essentially fixed and are characteristic of that substance. Intensities may vary somewhat from sample to sample, depending on the method of sample preparation and instrumental conditions.

An important use of the powder method is the qualitative analysis of crystalline phases. For the identification of unknown materials, an invaluable reference source is "The Powder Diffraction File" (Joint Committee on Powder Diffraction Standards, U.S.A.); supplementary data are issued annually.

### 2.5 MICROSCOPY

Observation of materials, such as minerals, ceramics and biological material is difficult owing to their small particle size and lack of contrast. These complications are overcome with the aid of specially designed microscopes. Various types of microscope are available and can be divided into two groups: optical and electron. With both techniques the sample can be viewed in transmission (the beam of light or electrons passes through the sample) or in reflection (the beam of light or electrons is reflected off the sample surface).

## Optical microscopy

The polarising or petrographic microscope is a transmission instrument. Samples usually take the form of fine powders or thin slices severed from a solid piece. It is widely used in geology and mineralogy and can be used profitably in solid state chemistry. The metallurgical or reflected light microscope is suitable for examining the surfaces of materials, especially opaque ones.

Specimens viewed under the polarising microscope are often fine particles ranging from 10 to 100  $\mu\text{m}$ . Substances of these dimensions are frequently transparent whereas they would be opaque in bulk form. The sample is immersed in a liquid whose refractive index is in close proximity with that of the sample. In this case the liquid medium was water. If the solid is examined in air, much of the light is reflected off the surface of the sample rather than transmitted through it. Difficulties are then encountered in measuring the various optical properties of the solid.

The principal components of a polarising microscope are indicated in Figure 2.16. The source may emit either white or monochromatic light. Only light rays whose vibrational direction is parallel to the polariser are permitted to pass through. The resulting plane polarised light passes through lenses and apertures onto the sample which is mounted on the microscope stage.

Light transmitted by the sample and immersion liquid is detected by the objective lens. The instrument usually has several of these of different magnification, which are readily interchangeable. The analyser may be placed in or out of the path of light. It is similar to the polariser but it is orientated so that its vibrational direction is at  $90^\circ$  to that of the polariser. When the analyser is "in", only light vibrating in the correct direction is permitted to pass through and onto the eyepiece. When the analyser is "out", the microscope behaves as

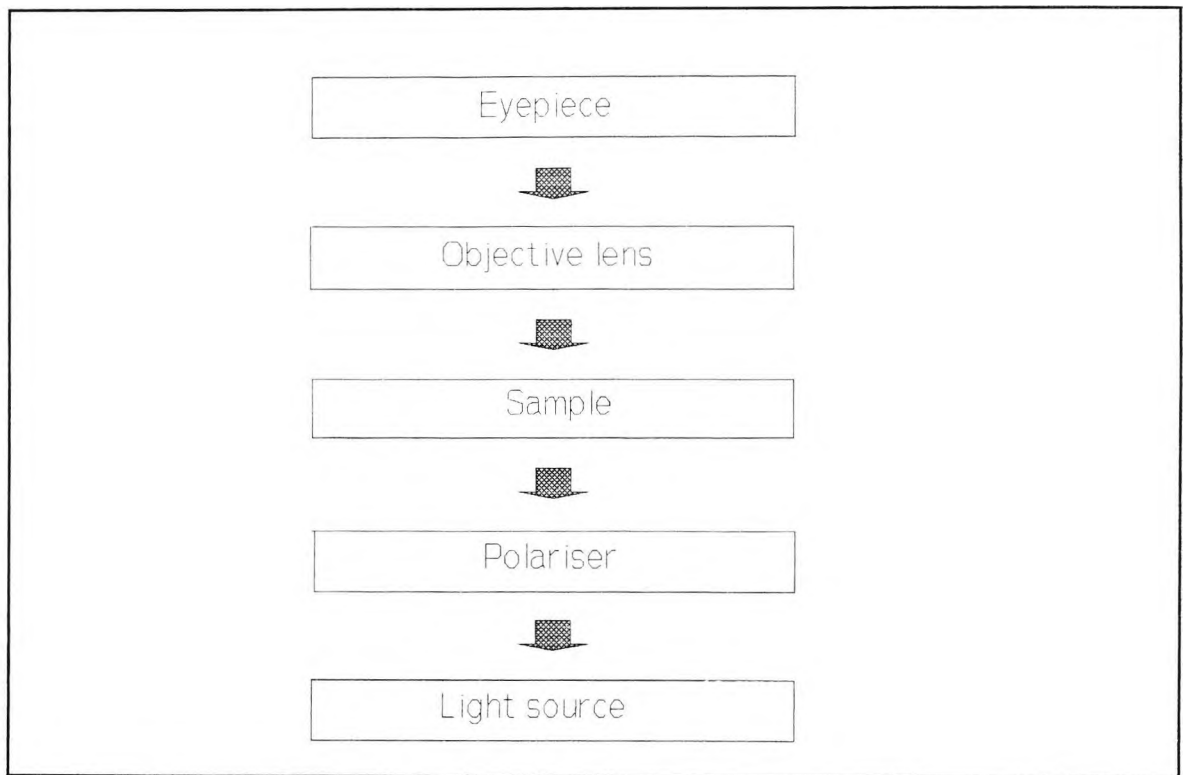


**Figure 2.16 Basic components of a polarising microscope.**

a simple magnifying microscope.

The reflected light microscope is similar to the transmission instrument with the exception that the source and objective lens are on the same side of the sample. It is used to examine solid aggregates of opaque material, such as metals, minerals and ceramics. The information derived from this technique primarily concerns the texture of the solid, i.e. the phases present and their identification and the number, size and distribution of particles.

## REFERENCES

1. Salvin, W., "Atomic absorption Spectroscopy", 2nd ed., Interscience, New York, 1978.
2. Fifield, F.W. and Kealey, D., "Analytical Chemistry", International Textbook Co. Ltd., London, 1983.
3. Weiss, J., "Handbook of Ion Chromatography", Calif., 1986.
4. Small, H., Stevens, T.S. and Bauman, W.C., Anal. Chem., 1975, 47, 1801.
5. Ekaireb, S.E., Ph.D. Thesis, The City University, London, 1990.

## CHAPTER 3

### THE EFFECT OF ELECTROMAGNETIC FIELDS ON CALCIUM CARBONATE PRECIPITATION

	Page
3.1 INTRODUCTION	46
3.2 MAGNETIC TREATMENT OF FLUIDS	47
3.2.1 Magnetic Treatment of Water	47
3.2.2 The Effect of Magnetic Fields on Chemical Reactions	50
3.2.3 Magnetic Field Effects on Calcium Carbonate Precipitation	53
3.3 THE CHEMISTRY AND STRUCTURE OF CALCIUM CARBONATE	56
3.4 HYDROMAG ELECTROMAGNETIC UNITS	65
3.4.1 Hydromag Industrial Case Histories	66
3.5 OBJECTIVES	70
3.6 EXPERIMENTAL TECHNIQUES	70
3.6.1 Propensity to Scale Measurements	70
3.6.2 Electromagnetic Treatment of Aqueous Solutions: Circulating Apparatus	72
3.6.3 Heat Exchanger Experiments	75
3.7 PROPENSITY TO SCALE EXPERIMENTS	77
3.7.1 The Effect of Magnetic Treatment of Calcium Solutions on the Propensity to Scale using Polypropylene and Copper Piping	79
3.7.2 The Effect of Flow Rate for the Hydromag DN15 unit on the Propensity to Scale using Polypropylene and Copper Piping	80
3.7.3 The Effect of Flow Rate for the Hydromag DN15 unit on the Propensity to Scale	85

3.7.4	The Effect of Sodium Hydrogen Carbonate Concentration on the Propensity to Scale	95
3.7.5	The Effect of Temperature on the Propensity to Scale	116
3.7.6	The Effect of Magnetic Treatment of Both Calcium and Sodium Hydrogen Carbonate Solutions on the Propensity to Scale	124
3.7.7	The Effect of Passing the Calcium Solutions and London Tap Water through the Magnetic field Once Only on the Propensity to Scale	128
3.7.8	Summary of the Propensity to Scale Results	132
3.8	HEAT EXCHANGER EXPERIMENTS	134
3.8.1	Heat Exchanger Experiments Under Laboratory Conditions	134
3.8.2	Heat Exchanger Experiments Under Industrial Conditions	138
3.8.3	Summary of the Results	143
3.9	DISCUSSION	143
3.9.1	Interpretation of the Observed Magnetic Phenomena	144
3.10	CONCLUSIONS	153
	REFERENCES	155

## CHAPTER 3

### THE EFFECT OF ELECTROMAGNETIC FIELDS ON CALCIUM CARBONATE PRECIPITATION

#### 3.1 INTRODUCTION

The formation of scale in industry can cause economic and environmental problems. Calcium carbonate is by far the most common scale (occurring naturally as limestone, marble and chalk), so that most natural waters contain some soluble calcium and simple contact with air or decaying organic matter will expose this calcium to varying concentrations of carbon dioxide. The result of this combination is a potential precipitate ( $\text{CaCO}_3$ ) that can adhere and form scale at some point in the water-use cycle, with these deposits increasing as water is heated. A water containing 145 ppm calcite, flowing at 5000 litres per day, will produce 4.8 kg of scale each year at 60°C and 29.9 kg at 80°C [1]. Several other deposits are known to form scale, e.g. calcium, strontium and barium sulphates (see Chapter 4) and calcium phosphate. British industry spends approximately £1000 million each year to clean, repair and replace equipment damaged by these scales. In addition to the obvious flow restrictions which can be caused by the deposits, the presence of even small amounts of scale can drastically reduce the thermal conductivity of heat transfer surfaces. Although calcium carbonate is the most abundant scale, it is the easiest type of scale deposit to control, being prevented or removed by pH or acid treatment. However, such chemical treatment of scale removal is being restricted by tougher environmental laws, especially in the U.S.A. The prevention and removal of scale in industry, therefore, needs to meet these guidelines with more acceptable methods.

In the water treatment industry, many devices have been invented, patented and marketed for decades to alleviate and remove scale in hard water areas. These devices generally involve the use of

electrical circuits (external to the device), galvanic cells, magnetic fields (permanent and electromagnetic) or variations and combinations of these. The reported effects of these devices include one or both of the following: decreased precipitation and growth of hard mineral scales; and/or partial dissolution (and/or removal) and change in the consistency of previously deposited scale.

The aim of the following sections is twofold: firstly, to review the magnetic field phenomena resulting from the interaction of fluids with applied magnetic fields; and secondly, to describe the chemistry of calcium carbonate and determine which parameters lead to its deposition as a scale.

### 3.2 MAGNETIC TREATMENT OF FLUIDS

#### 3.2.1 Magnetic Treatment of Water

The first magnetic field devices for scale control were patented and registered by Hay [2] in 1873 (U.S.A.). Research into magnetic treatment of fluids started in the 1930s, coinciding with the worldwide marketing of newer magnetic field devices.

Magnetic water treatment (MWT) is a technique still shrouded in controversy. The unsubstantiated marketing claims of some suppliers for their devices, has led to them promising "magic" results with no scientific reasoning, resulting in many engineers being very sceptical as to whether MWT actually works. This controversy is not helped by the lack of scientific literature on the effects of MWT in reducing scale build-up and descaling, because most of the literature that is available describes badly designed experiments. Hence there is no generally accepted scientific explanation of how the magnetic treatment of fluids such as water works to reduce scale formation.

The mechanisms postulated fall broadly into two categories: the first assumes that the magnetic field alters the physical

properties or the structure of water itself and the second assumes that it can act on the suspension or the solution.

Joshi and Kamat [3] have reported changes in the pH, surface tension and dielectric constants of magnetically treated water. They claim that both pH and surface tension changed by increasing the magnetic field over the range of 1.9 to 5.7 kGauss. The dielectric constant change was identical with changing field strength.

Klassen [4] studied the changes in the I.R. spectra of magnetically treated water. He claimed that the magnetic field is responsible for the structural changes in water. These claims have been studied further but no theoretical or experimental work has been able to substantiate them [5,6]. There is reason to believe that Klassen's measurements were incorrect due to the inclusion of impurities in the dissolved water.

Drost-Hansen and Kavjic [7] also support the view that water is structurally modified as a result of magnetic treatment, basing their theory on structurally modified interfacial water, referred to as "vicinal water". Eliassen *et al* [8] do not agree with this theory because it is thermodynamically implausible.

Minenko and Petrov [9] have published a theory for magnetic treatment, presuming the efficiency of the treatment to be proportional to the Lorentz Force acting on the particle moving in a magnetic field. They claim that the most important factor affecting precipitation in this period is nucleation and that the change in the growth part of precipitation is evident after 5 minutes.

Proponents of mechanisms that relate to the field affecting particulates in solution include Ellingsen and Fjeldsend [10] who suggest that magnetic treatment changes the properties of either the surface or the double layer surrounding the colloidal particles. Their theory is based on precipitation studies where

the rate of precipitation is dependent upon the magnetic field strength. Further work showed that the formation of calcite was promoted by magnetic treatment. Ellingsen and Kristiansen [11] have reported that the rate of precipitation of calcium carbonate was changed by 10 minutes after passing ground water through an electromagnetic field. They claim that the influence of magnetic fields on aqueous solutions may last for several hours after passing through the field and unscientifically attribute this phenomenon to a "Memory Effect".

Several authors have suggested that MWT devices may be effective only because they act as sacrificial anodes, increasing the concentration of certain ions in water which, in turn, inhibits the rate of precipitation and subsequent scale buildup. Duffy [5,12] conducted experiments to determine the effect of magnetic fields on water and aqueous solutions on the corrosion of steel, to determine the effect of iron compounds on the precipitation of calcium carbonate. His results showed that magnetisation did not alter the physical properties of water, but increased the corrosion rate of 1018 steel by 18.6%. He showed that iron impurities retard the rate of calcium carbonate precipitation and hinder the crystallisation of calcite. He surmised that magnetic treatment stems from an increase in  $\text{Fe}(\text{OH})_3$  concentration in solution generated by magnetically induced corrosion, which inhibits the nucleation and/or growth of crystalline scale.

Herzog *et al* [13] also investigated the effect of magnetic fields on calcium carbonate nucleation and growth with calcium solutions containing several synthetic ferric hydroxide species. These ferric hydroxide species were thought to act as key intermediates by inducing the heterogeneous nucleation of calcium carbonate. They found that this mechanism was unlikely, but showed instead that trace concentrations of  $\text{Fe}^{2+}$  firstly inhibit calcite, but not aragonite growth, and secondly inhibit the transformation of aragonite into calcite. Similar effects were observed with  $\text{Fe}^{3+}$  but to a lesser degree.

Speranskiy et al [14] have proposed that "magnetic coagulation" occurs in water passing through a magnetic field. According to this mechanism, "raw" water contains coarsely dispersed and colloiddally dispersed iron oxides which are magnetised in the field and then adhere to each other by "magnetic coagulation".

### 3.2.2 The Effect of Magnetic Fields on Chemical Reactions

Thomas [15] has shown that the rate of polymerisation of acrylonitrile can be increased by magnetic treatment. The polymerisation of acrylonitrile to polyacrylonitrile is an exothermic reaction and the rate of reaction was observed by thermometric measurement. The active catalyst species used was propan-2-ol in potassium hydroxide solution. He surmised that the increase in the rate of polymerisation measured by heat output on magnetic treatment was caused by the breaking or weakening of the ion-pair interaction between potassium and propan-2-oxide ions ( $RO^- \dots K^+$ ). The weakening of the ion pairs thus releases the active catalytic species ( $OR^-$ ) and favours the polymerisation reaction.

Many dyestuffs consist of charged organic molecules and in a large number of cases the solution of dyestuff contains ion pairs between the dye molecule and an appropriate counter ion. Thomas [15] has investigated methylene blue, and has found that magnetic fields do not alter the nature of the chromophore in the dye solution but can significantly reduce its intensity. It is possible that the magnetic field is acting on specific energy levels but it seems more likely that the effect arises from magnetic field interactions with the counter ion-dye ion pair.

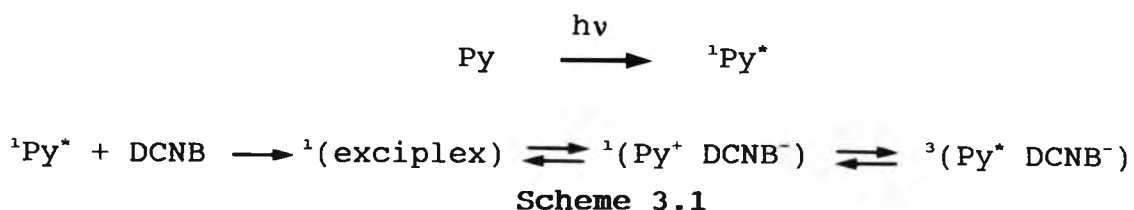
In the work at City University, magnetic treatment of the dispersal of clays in water has resulted in changes in their settling rates. Similar results have been reported for emulsions as well as dispersions, for example, the enhancement of de-emulsification of light oil and tars in wastewater [16].

There have been a number of reports of the use of magnetic fields to increase the adhesion of cured polyepoxides to various substrates including steel, aluminium and copper. Evidence has been found for changes in the crystallinity, ordering and packing of the molecules due to orientation effects in the magnetic field. It seems likely that the increases in adhesive strength reported also arise because of direct interactions between the field and the weak electrostatic bonds providing the adhesion [17,18].

Nematic liquid crystals, such as disodium chromoglycate in water, orientate in a magnetic field, and addition of amino-acids or other chiral molecules causes the liquid crystal to become cholesteric, with the helix axis aligned parallel to the magnetic field [19].

There have been reports of magnetic fields affecting the rates of some reactions by direct field charge interaction, including (a) the reduction of tolyldiazonium tetrafluoroborates by  $\text{Fe}^{2+}$  [20], and (b) the Harcourt-Essen reaction [21].

The effects of magnetic fields on the kinetics of chemical and biological reactions can arise from the modification of energy levels in the reacting species by interaction with the field [22]. This type of reaction is well illustrated by reactions involving radical pairs. In the photochemical reaction between pyrene and dicyanobenzene, irradiation of pyrene at 340nm produces pyrene singlet radicals. These then react with dicyanobenzene via an exciplex to give ion radical pairs [23]. These ion radical pairs consist of positively charged pyrene radicals ( $\text{Py}^*$ ) and negatively charged dicyanobenzene ( $\text{DCNB}^-$ ) as shown in Scheme 3.1.



An alternative method of increasing the geminate period in a free radical reaction is to contain the reaction in a microemulsion or micelle. Large increases in reaction yield have been observed for such reactions on application of fields of about 20mT. In the photolysis of dibenzylketone trapped in the micelle [24], irradiation leads eventually to the triplet radical pair.



This ion pair eliminates CO to give the triplet biradical



which is also trapped in the middle. The geminate recombination of the  $\text{PhCH}_2\cdot$  radical pairs to give biphenyl  $\text{Ph}(\text{CH}_2)_2\text{Ph}$  is then in competition with the formation of escape products resulting from the escape of free  $\text{PhCH}_2\cdot$  radicals from the micelle. The geminate reaction is favoured by application of small applied magnetic fields which permit easier triplet-singlet interconversions. A second example involves the investigation of the photochemistry of 2,4-diphenylpentan-3-one in fields of 3T, in which increased yields of 40% of the photoisomerism products were reported over the values observed in zero field situations [25].

Photosynthetic primary processes occur at special membrane-fixed reaction centres in the chloroplasts of green plants, algae and some types of bacteria. The process involves the formation of radical ion pairs with the positive ion being a chlorophyll-type moiety and the negative ion, a primary acceptor species. Magnetic fields can affect these radical ion pairs in the same way as they do non-biological systems.

The effects of external magnetic fields of 2T on the photogenerated geminate and escape radical ion pairs of the chlorophyll radical cation and a para-benzoquinone radical anion have been studied and clear evidence has been found for magnetic field effects [26].

Magnetic fields have also been shown to have profound effects on other processes, such as crystallisation, for example:

- on the crystallisation pattern of 4-n-octylbiphenyl grown from a saturated benzene solution [27].
- on changes in morphology of DL-valine [28].
- on the improvement in crystallisation of basic tin (II) sulphate [29].
- on the precipitation of aluminium hydroxide [30].
- on deposition of polymers from acrylic-based leather dye formulations [31].

### 3.2.3 Magnetic Field Effects on Calcium Carbonate Precipitation

This section is not intended to reflect all known magnetic field effects on calcium carbonate precipitation, but to describe studies that are of particular interest and relevance to the work carried out in this chapter. Many authors have concentrated their findings on magnetic fields in two areas: either removing existing hard scale ( $\text{CaCO}_3$ ), or treating hard water to prevent scale deposition. Very few studies have been conducted which quantitatively determine the buildup of precipitate with time.

Ellingsen and Kristiansen [11] measured rates of calcium carbonate precipitation from samples of Norwegian ground water which had first been exposed to a magnetic field and deliberately made supersaturated with respect to calcium carbonate by subsequent addition of calcium hydroxide. They observed that calcium carbonate precipitated more readily in the samples which were exposed to progressively stronger magnetic fields. They claimed the precipitation rate was surface controlled. They established a "turning point" for the rate of precipitation in magnetic fields and found it was pH dependent. Below a given pH, the rate increased, while at a higher pH, the rate decreased. They attributed this "turning point" to the point where the zeta potential of colloid particles crosses zero in solution.

Ellingsen and Fjeldsend [10] investigated crystal growth and solubility. The crystal growth experiments used water which was slightly supersaturated with calcium carbonate and circulated it through a crystal growth cell after being magnetically treated. The crystal growth of calcium carbonate was observed on a bottom plate in the growth cell. Crystal growth occurred by either heterogeneous nucleation onto the plate or by nuclei "dropping" out of solution. Their results showed that magnetically treated water produced less crystals, which were predominantly calcite. The untreated water produced crystals that had a more complex crystal habit, a mixture of calcite and aragonite. The solubility experiments focused on the effect of impurities on the rate of solubility of calcium carbonate. The rate of solubility was greater in untreated water than treated water. They interpreted their findings in terms of the magnetic field changing the properties of either the surface or the double layer surrounding colloid particles (zeta potential). Both the rate of precipitation and solubility are, among other factors, dependent upon available surface between the growing crystals and the solvent.

Kronenberg [32] carried out crystal growth experiments and found that upon evaporation, magnetically treated water samples gave rise to crystals which were reduced in size by 67% from an untreated sample. He assumed that since the crystals were a source of scale formation, magnetic treatment was 67% effective.

The magnetic field effects described so far have been associated with the field influencing the crystal growth characteristics of scale formation. However, the investigators have provided very little evidence to substantiate this interpretation. The research group at City University, [1], have been investigating the effect of magnetic fields on several crystallisation and precipitation systems since 1984. Their findings show that the main effect of the field is to prevent or reduce scale formation through the modification of crystal growth mechanism. Such modification has, in part, been explained in terms of the significant field charge

interactions of the applied field and the ions on nucleating species in the fluid. The work has shown that treating several types of fluid precipitate systems magnetically has produced significant changes in the following: particle size (for  $\text{CaCO}_3$ ); crystallinity (for  $\text{CaSO}_4 \cdot 2\text{H}_2\text{O}$  and  $\text{Sn}_3\text{O}(\text{OH})_2\text{SO}_4$ ); crystal morphology (for  $\text{CaSO}_4 \cdot 2\text{H}_2\text{O}$ ); crystal phase (for  $\text{CaCO}_3$ ); solubility (for several precipitates) and rate of precipitation.

Particle size changes have been shown for calcium carbonate precipitation [33], with the magnetic field causing an increase in particle size. This increase in particle size resulted in a reduction in surface area and surface charges and, therefore, in the ability of the calcite crystals to adhere together to form scale. The magnetic field appears to act as a crystal growth modifier, and hence prevents scale formation. Descaling is a secondary downstream effect because the water is no longer supersaturated with calcite due to the crystallisation of larger particles. Other precipitates which have shown changes in particle size include calcium sulphate dihydrate and calcium phosphate, both of which showed a decrease in particle size [33], and barium sulphate, which showed an increase in particle size [33].

Changes in the crystallinity of precipitates have been observed in systems subjected to magnetic treatment. These changes in crystal size show up in microscopic examination and distinguish between single crystal and aggregated particles in the precipitates. The crystal morphology of  $\text{CaSO}_4 \cdot 2\text{H}_2\text{O}$  crystals has been shown to change when grown in magnetic fields. This change arises because of interaction between the fluid and the nucleating and growing crystals.

The crystal phase changes were found in evaporation experiments with hard water. It was found that before treatment, the calcium carbonate precipitated contained calcite and aragonite in the ratio 4:1, but after treatment, the ratio of these phases was 1:4. Changes in solubility have been shown for several

precipitates. Barium sulphate and calcium phosphate [29] both showed an increase in solubility and similar data has been obtained for aluminium hydroxide and zinc phosphate [34].

The data from the City University group demonstrates that magnetic fields act to change (a) the solubility of precipitates in fluids, including the dissolution of existing scale and (b) the nucleation and crystal growth process of precipitating systems. Three components of the precipitating solution could be influenced by a magnetic field: (i) the highly charged surface of the growth nuclei, (ii) the anions and (iii) the cations, which are involved in the crystal growth process. The work described in this chapter focuses predominantly on the role ions play on the crystal growth process. This is demonstrated by treating pure water solutions of either cations ( $\text{Ca}^{2+}$ ) or anions ( $\text{HCO}_3^-$ ) in an electromagnetic field (using the Hydromag electromagnetic system). To evaluate whether electromagnetic fields can influence the precipitation rate and therefore the crystal growth process of calcium carbonate. London tap water was treated in the Hydromag unit and heated to form a scale deposit on heat exchangers to see if changes in the crystal structure occurred.

### 3.3 THE CHEMISTRY AND STRUCTURE OF CALCIUM CARBONATE

Ubiquitous calcium carbonate: we are in awe of its beauty (pearl); we build our world with it (cement); it shapes our education (chalk); and eventually we use it to build a final monument to ourselves (gravestones). In short, the uses and problems of calcium carbonate are as abundant as the deposits in which it occurs.

Calcium carbonate exists in three different crystalline forms: calcite, aragonite and vaterite. When it precipitates out of solution onto the surface of a heat exchanger or boiler, it is usually as a mixture of calcite and aragonite. The predominance of one crystalline phase over the other depends on conditions,

such as pH, temperature, the nature of the metal substrate and the ions present [35]. Calcite is thermodynamically stable relative to aragonite, but aragonite is often the first phase to precipitate out of solution, particularly at elevated temperatures, such as those encountered in boilers and heat exchangers. Aragonite may recrystallise into calcite naturally over a given period of time [36]. This recrystallisation, in addition to the natural ripening and growth of existing calcite crystals, makes scale deposits cement together to form hard, compact and crystalline encrustations.

The habit and crystal shape of calcium carbonate has been found to alter when other substances are present in solution. It is claimed that below 30°C, calcium carbonate precipitated from a hydrogen carbonate solution crystallises as calcite and as aragonite above this temperature. In the presence of sodium and potassium chlorides larger crystals are found to precipitate [37]. Bivalent magnesium and strontium salts below 30°C modify the shape of calcite crystals, although such crystal forms are considered unstable. Habit and crystal size may be intentionally modified by the use of chemical additives. It has been claimed that addition of chemicals can also affect a phase change from aragonite to calcite [38].

Wray and Daniels [39] have studied the influence of temperature and ageing on crystal forms of precipitated calcium carbonate to determine the conditions necessary to precipitate calcite, pure aragonite or specific mixtures of the two. They observed that the temperature range is small and critical. At 40°C, the precipitate is nearly pure calcite; at 45°C it is 30% calcite and 70% aragonite initially, but changes during two hours of digestion to more than 90% calcite. At 50°C, the precipitate is mostly aragonite. They also found that the formation of aragonite was induced by adding impurity ions larger than those of calcium to the precipitating solution. The addition of strontium, barium or lead ions under pH conditions high enough to favour co-precipitation produced aragonite.

Meigen [40] studied the differences in the reaction velocities of precipitated calcium salts in the presence of different metal ions. The results showed that the formation of aragonite was favoured when trace amounts of zinc, manganese, cobalt and iron ions were present in a precipitating calcium carbonate solution. The formation of calcite was promoted when trace amounts of copper, lead and silver ions were present.

Faivre [41] in his studies of calcium carbonate, produced all three crystalline forms, calcite, aragonite and vaterite. Calcium carbonate was precipitated by mixing solutions of calcium chloride and sodium carbonate. He found that below 35°C the only precipitate formed was calcite, but between 35 and 60°C a mixture of calcite, aragonite and vaterite was formed.

Calcite is the most stable form of calcium carbonate and its unit cell structure is shown in Figure 3.1. There are wide variations in calcite crystal habits; they range from the perfect double refracting type of Iceland Spar to single crystals which weigh 30 tons or more [42]. Green, red or blue varieties of calcium carbonate exist, but most forms are colourless or white.

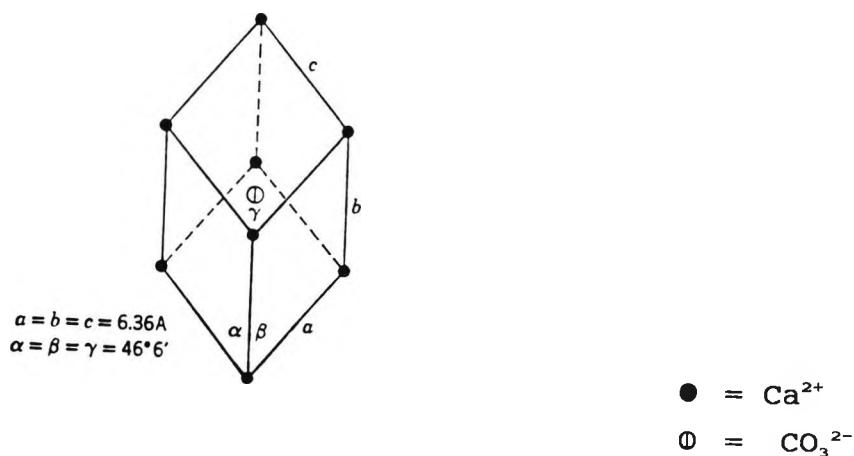


Figure 3.1 The unit cell of calcite,  $\text{CaCO}_3$

Green calcium carbonate may be due to copper, red can be due to appreciable quantities of manganese, and blue calcium carbonate is caused by the presence of  $\text{Fe}^{2+}$  or  $\text{Fe}^{3+}$  ions. Calcite may be recognised by its perfect (1011) rhombohedral cleavage and is differentiated from dolomite  $(\text{Ca},\text{Mg})\text{CO}_3$  and aragonite by the use of organic dyes. Calcite is stained in acid solutions, whereas dolomite is stained in basic solutions. Calcite is the principal constituent of limestone. It also occurs in many calcareous metamorphic rocks, such as marble. It is not surprising, therefore, to find calcium carbonate in solution in almost all surface and ground waters. Divalent cations may partially replace calcium in calcite; these substitutions have been found in scale samples. A common substitution for calcium is magnesium, which forms magnesium calcites. Natural manganese-bearing calcites may contain from 0 to 42%  $\text{MnCO}_3$  [43]. The substitution of  $\text{Fe}^{2+}$  for some calcium in calcite is fairly common; small amounts of strontium commonly substitute for calcium in calcite, although calcite generally contains less strontium than aragonite. Finally barium can replace calcium in calcite.

Aragonite was named after the Spanish province Aragon, in which it was first located. Aragonite is less common and less stable than calcite. Its crystalline orthorhombic structure was initially investigated by Huggins [44]. It is unlike calcite in that it shows poor cleavage characteristics. Aragonite is the form of calcium carbonate commonly found in pearls, but aragonite found in mother of pearl is structurally different from aragonite occurring in a pearl formed by the same mollusc [45,46]. It also forms stalactites in caves in limestone districts. Aragonite has a higher specific gravity (2.94) than calcite (2.71), so that in bromoform it sinks and is readily distinguishable from calcite, which floats.

Metastable vaterite is comparatively rare and crystallises at ordinary temperatures and pressures. It readily converts to aragonite, calcite or both; the transformation can be influenced by many factors. Vaterite has a spheroidal crystal structure

which can qualitatively resemble aragonite. However, it is not a common constituent of boiler scale or other deposits and is thought to exist for very short periods, if at all, in hot moist environments. Where vaterite is formed, its formation has been attributed to the presence of crystal modifying additives.

The solubility of calcium carbonate in distilled water is very low, but it can be greatly increased by CO<sub>2</sub> partial pressure, by changes in temperature and by the concentration of other salts in solution. Miller [47] investigated the solubility of calcium carbonate at various temperatures and CO<sub>2</sub> pressures and the data are shown in Table 3.1.

Table 3.1 shows that at any CO<sub>2</sub> partial pressure between 1 and 100 bars the solubility of calcite decreases with temperature, even though the solubility increases with pressure.

**Table 3.1 Solubility of calcite at various temperatures and CO<sub>2</sub> pressures.**

Grams CaCO <sub>3</sub> per litre - partial pressure CO <sub>2</sub> in bars-					
Temp. °C	1	10	20	50	100
0	1.34	2.46	-	-	-
10	1.11	2.15	-	-	-
30	0.72	1.63	2.01	2.62	-
50	0.43	1.17	1.46	1.86	2.15
70	0.30	0.79	0.99	1.30	1.49
90	0.23	0.58	0.70	0.90	1.04
100	0.20	0.52	0.61	0.77	0.88
105	0.19	0.49	0.53	0.71	0.81

Ellis [48] determined the solubility of calcite in water from 100 to 300°C and at partial pressures of 1 to 62 atmospheres. Table 3.2 shows the solubility decrease with temperature between 100 and 300°C, regardless of the CO<sub>2</sub> pressure.

**Table 3.2 Calcite solubility as a function of temperature and CO<sub>2</sub> pressure.**

Solubility grams/1000g water					
pCO <sub>2</sub> atm.	Temperature °C				
	100	150	200	250	300
1	0.216	0.094	0.040	0.015	0.006
4	0.360	0.158	0.063	0.024	0.009
12	0.555	0.221	0.091	0.036	0.012
62	-	0.405	0.152	0.051	0.014

Pytkowicz and Connors [49] showed the effects of pressure on the solubility of calcium carbonate in sea water. When calcium carbonate was subjected to 1000 atmospheres of pressure its saturation concentration increased to approximately 2.7 times that at 1 atmosphere pressure.

Kitano [50], in a series of laboratory and field investigations, studied some of the factors which help to explain the occurrence of calcium carbonate in thermal spring locations. He found that below 25°C and in the absence of CO<sub>2</sub>, only calcite was formed in a Ca(HCO<sub>3</sub>)<sub>2</sub> solution. Above 25°C, aragonite was formed. At temperatures over 40°C and less than 60°C a large amount of vaterite was formed. The overall effect was that when the mother liquor increased in temperature the proportion of calcite decreased. In addition, unstable vaterite readily formed at high temperatures from a Ca(HCO<sub>3</sub>)<sub>2</sub> solution containing sodium chloride as shown in Table 3.3.

Table 3.3 Crystal forms of calcium carbonate formed from  $\text{Ca}(\text{HCO}_3)_2$  solutions containing sodium chloride.

Mother solution		Crystal forms of $\text{CaCO}_3$ , %		
Temp°C	NaCl in $\text{Ca}(\text{HCO}_3)_2$ soln. g/l	Vaterite	Calcite	Aragonite
30	1.5	0	100	0
50	1.5	12	14	74
60	1.5	40	10	50
70	1.5	35	5	60
80	1.5	40	8	52
100	1.5	63	10	27
80	0.3	14	8	78
80	3.0	52	10	38
80	15.0	49	9	42
100	1.5	78	9	13
100	3.0	91	6	3
100	25.0	91	8	1

In another case, where the effect of magnesium chloride was studied at various temperatures, it was found that the proportion of aragonite increased, but that of calcite decreased (see Table 3.4). It was concluded that the presence of magnesium chloride in the mother liquor hindered the formation of vaterite.

When calcium carbonate was precipitated from a  $\text{Ca}(\text{HCO}_3)_2$  solution containing sodium chloride and magnesium chloride at high temperatures, and through which carbon dioxide was bubbled continuously during calcium carbonate formation, only calcite was formed as shown in Table 3.5.

**Table 3.4 The effect of magnesium chloride on crystal forms of calcium carbonate formed from  $\text{Ca}(\text{HCO}_3)_2$  solutions.**

Mother solution		Crystal forms of $\text{CaCO}_3$ %		
Temp°C	$\text{MgCl}_2$ in $\text{Ca}(\text{HCO}_3)_2$ soln. g/l	Vaterite	Calcite	Aragonite
10	0.6	0	88	12
10	4.5	0	0	100
30	0.5	0	30	70
30	1.5	0	0	100
50	0.15	0	7	93
50	4.5	0	0	100
70	0.15	0	5	95
70	4.5	0	0	100
100	0.15	0	0	100
100	4.5	0	0	100

**Table 3.5 The effect of aeration with  $\text{CO}_2$  on the crystal forms of  $\text{CaCO}_3$ .**

Mother solution		Crystal forms of $\text{CaCO}_3$ %		
Temp°C	Salt in $\text{Ca}(\text{HCO}_3)_2$ soln. g/l	Vaterite	Calcite	Aragonite
70	3 (NaCl)	0	100	0
80	3 (NaCl)	0	100	0
80	3 ( $\text{MgCl}_2$ )	0	100	0
80	10 ( $\text{MgCl}_2$ )	0	100	0
80	15 ( $\text{MgCl}_2$ )	0	100	0

The solubility of a solid material varies with the nature of the solution as illustrated by the data in Tables 3.6 and 3.7, for the solubility of calcium carbonate in aqueous solutions of sodium chloride at 25°C and magnesium chloride at 5°C. The data show that at constant carbon dioxide pressure the solubility of calcite increases with increasing sodium chloride concentration.

**Table 3.6 Solubility of CaCO<sub>3</sub> (calcite) in aqueous solutions of sodium chloride at 25°C.**

Partial pressure of CO <sub>2</sub> in Atm.	Millimoles per 1000g. water	
	Ca(HCO <sub>3</sub> ) <sub>2</sub>	NaCl
0.965	8.96	3.79
0.965	9.37	14.8
0.965	9.67	34.8
0.962	10.70	82.8
0.958	12.41	236.0

**Table 3.7 Solubility of CaCO<sub>3</sub> in aqueous solutions of MgCl<sub>2</sub>.6H<sub>2</sub>O at 5°C.**

Grams MgCl <sub>2</sub> .6H <sub>2</sub> O per 1000g water	Grams CaCO <sub>3</sub> per 1000cc solvent
0	2.337
50	3.404
86.9	4.083
350	3.301
1150	2.205
2300 (sat'd)	1.406

For magnesium chloride solutions a maximum solubility is reached at approximately 4% of saturation. At saturation the solubility is decreased below that of distilled water.

### 3.4 HYDROMAG ELECTROMAGNETIC UNITS

The electromagnetic units used in this work were supplied by Hydromag U.K. Ltd. The Hydromag unit was invented by Frau Schulze in the late 1970s. Initial trials were conducted and the final prototypes were tested for 2 years before they were finally manufactured and marketed in 1985. Hydromag units were initially sold in Germany but are now sold throughout Europe.

The internal design of the Hydromag unit is shown in Figure 3.2. Water is passed through the Hydromag in a controlled and precise direction, through steps of  $90^\circ \pm 30'$ . Experimentation of the initial units found that the most efficient conditioning effect was to produce lines of force or power lines of 2500 gauss. The internal construction ensures that the lines of force produced by the magnetic coil are concentrated in the correct direction, and that water crosses these power lines at the correct angle ( $90^\circ$ ). The magnetic field is controlled by a voltage supplied to an external control box, which also reverses the polarity of the magnetic field for 10 seconds every minute. This reversal of polarity removes particles which are adhering to the Hydromag unit, producing a self-cleaning device.

The outer casings are made by a process which produces grey steel by melting the raw materials in a furnace at  $1550^\circ\text{C}$ . The molten grey steel is poured into castings and "fast cooled" at ambient temperature. They are magnetised by heating them slowly in an oven to  $870^\circ\text{C}$  over a period of 3 days and cooled slowly for 2 days to  $350^\circ\text{C}$ , when they are removed and cooled rapidly at ambient conditions. The casings are machined to an accuracy of 0.1mm by computerised lathes, to ensure that the internal design specifications are achieved. The machined casings are then either electroplated with  $25\mu\text{m}$  copper,  $25\mu\text{m}$  nickel and  $5\mu\text{m}$  chromium (for normal water usage applications) or PTFE-coated to resist chemical attack by more aggressive fluids. The Hydromag units are assembled in Hydrotec's factory, where the wound copper wires which generate the electromagnetic field and the electronic

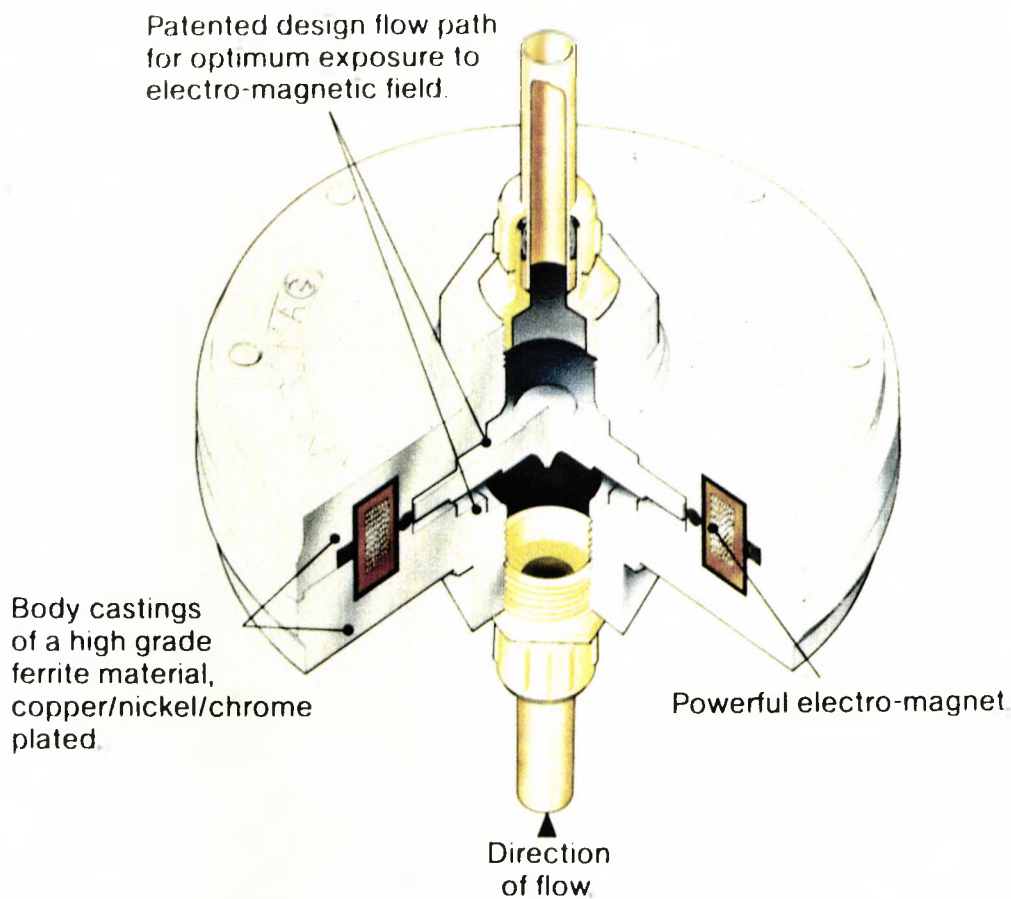


**Figure 3.2 Internal design of the Hydromag unit.**

control boxes which reverse the polarity are fitted and tested. Figure 3.3 shows the two different protective coatings of the Hydromag units.

### **3.4.1 Hydromag Industrial Case Histories**

Hydromag units have been installed in many different industrial applications. When scale formation occurs from untreated hard water the equipment life is shortened significantly. Equipment which is prone to scale formation includes the following: evaporative condensers, cooling towers, calorifiers, heat exchangers, humidifiers, pumps, jets and cooling circuits. Hydromag units have been used in all these types of equipment and have either significantly reduced or completely removed scale formation.

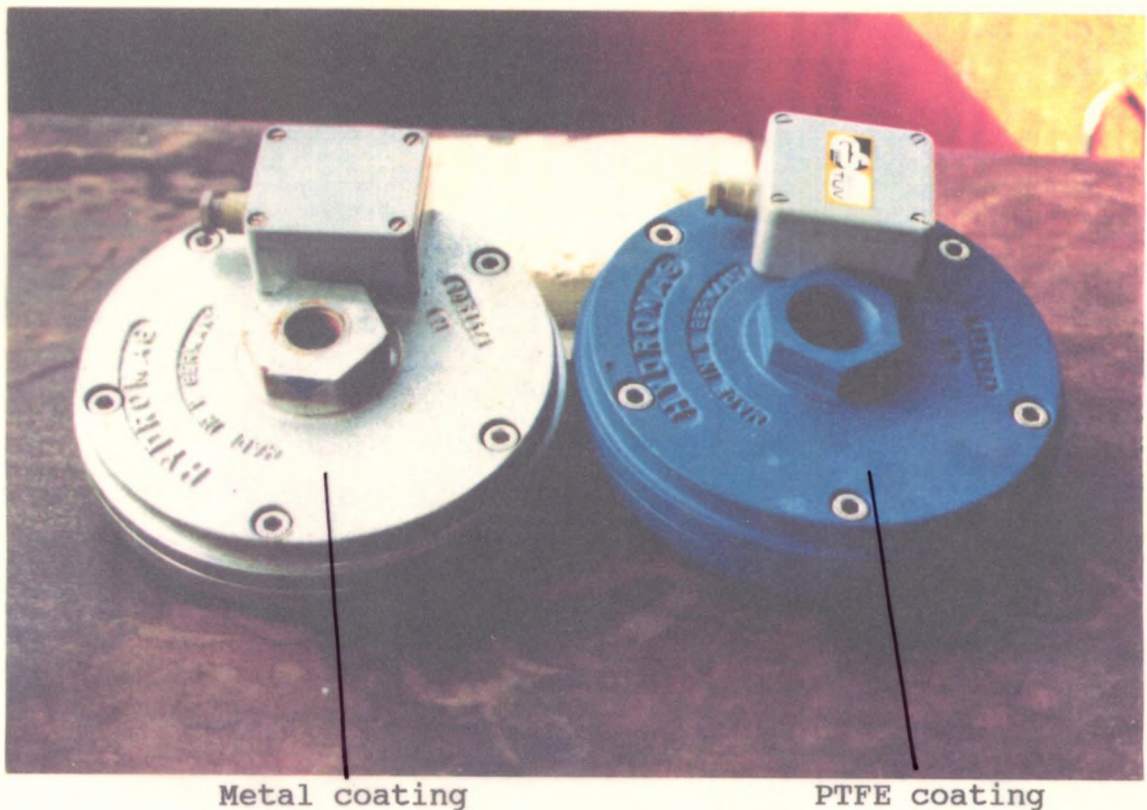


Figure 3.3 Protective coatings of the Hydromag units.

The effectiveness of scale prevention was shown at Raychem, Swindon in the process cooling coil system. Prior to Hydromag installation, the cooling coils blocked after 5000 hours, necessitating descaling and refitting expensive reconditioned coils. In addition, scaling affected routine servicing, because of the increased time for the system to cool. The Hydromag unit has prevented scale formation, so that routine maintenance time is reduced and descaling of the cooling system is not necessary. Also, computer monitored tests have shown that the reconditioned coils supplied with the Hydromag treated water give a cooling performance close to a new coil.

Prior to the installation of a Hydromag unit, the buildup of calcium carbonate scale in humidifiers at Epson Computers, Telford required the costly replacement of the humidifier elements every six weeks. Trials showed that humidifiers fitted with a Hydromag unit had virtually no scale, whereas the humidifiers with untreated water were solid with scale, as shown in Figure 3.4.



**Figure 3.4 Humidifiers after a six week trial.**

In another water usage study at the National Power's, Fawley site, installation of a Hydromag unit in their calorifier system was shown to result firstly in the removal of existing calcium carbonate scale, and secondly to change the deposit from being thick and hard to being an easily removable sludge.

Two boarding schools have benefitted from the introduction of Hydromag units, they are the Bryanston and the Royal Russell Schools. The problem at Bryanston's boarding house caused the water heater to scale up every 4 months. Four years after installation the main benefits are: no blocked shower heads, significant savings of time and money for maintenance and more efficient burning of expensive fuel. At the Royal Russell school, Hydromag units were installed together with a new calorifier and plate heat exchanger to supply hot water to the school and its boarding houses. Six months after installation no trace of scale was found on opening the two heating systems.

The food manufacturing and processing industries are also affected by scale formation, because of the large quantities of hot and cooled water used. Milking parlours, such as T.W.Clothier, use water heaters to clean pipework after milking and these will scale up in months. Water treated in the Hydromag unit eliminated this scale and led to more efficient milk production. In the manufacture of cheese, scaling problems occur from cleaning the equipment in factories with hot water, required by the strict hygiene regulations. The installation of Hydromag units at the T.W.Clothier and the Barber Ltd. cheese plants has stopped their hot water pumps from rocking-up, saving the companies time and money in maintenance costs and replacement pumps. Hydromag units have also been used in the Family Loaf Bakery. The baking process involves passing water through fine jets to form a mist, which covers the baked loaves, controlling the weight loss during cooling. Prior to installation the jets were replaced every 3 months because the required humidity was not being achieved, and to compensate for this weight loss in the finished loaf the company was adding 2-3 grams of dough per loaf prior to baking. At 1 million loaves a week, this increase in costs because of scale was substantial. The Hydromag units have stopped the jets blocking and have improved their baked loaf production efficiency.

Hotels are renowned for their water usage: in their kitchens, bars, showers, laundries and leisure areas. All these places are prone to severe scale formation in hard water areas, with shower heads blocking in the rooms, heating equipment in the kitchens leaving rock solid deposits and blockages in pipework which reduce the efficiency of ice making and glass-washing equipment. The installation of Hydromag units at several major hotels in the U.K. has seen the removal of all the above problems, reducing maintenance costs significantly.

### 3.5 OBJECTIVES

The primary objectives of the work described in this chapter was to investigate the effects of electromagnetic fields on the rate of precipitation of calcium carbonate when unsaturated aqueous solutions of either calcium or hydrogen carbonate ions were continuously circulated through the Hydromag unit. The investigations highlighted the field-charge interaction of either univalent ( $\text{HCO}_3^-$ ) or divalent ( $\text{Ca}^{2+}$ ) charged species in pure aqueous solution with the electromagnetic field and the resulting effect of this interaction on the rate of calcium carbonate precipitation. The investigation included a study of the effect of flow rate for aqueous solutions passing through the Hydromag unit on calcium carbonate precipitation, as determined by their propensity to scale. The effects of hydrogen carbonate concentration and temperature on calcium carbonate precipitation as determined by the propensity to scale of magnetically treated solutions were also studied.

Heat exchanger experiments were carried out on treated and untreated London tap water to evaluate the effects of the Hydromag units on the scale formation process in the laboratory. The experiments measured the differences in the crystal structures of the scale and the weight of scale deposited after a set period of time at a certain temperature. Industrial trials were also carried out to evaluate the effectiveness of Hydromag units in higher water usage environments. These trials also investigated the differences in crystal structure and the quantity of scale deposited.

### 3.6 EXPERIMENTAL TECHNIQUES

#### 3.6.1 Propensity to Scale Measurements

The propensity to scale measurements were carried out using the P.M.A.C. Pressure Measurement And Control equipment described in Chapter 2 (Section 2.1). The formation of calcium carbonate scale

was induced by dissolving sources of calcium and hydrogen carbonate ions in pure aqueous solutions to give the precipitation reaction shown in Equation 3.1.



Equation 3.1

The precipitation process in Equation 3.1 was carried out using volumetric solutions of the following compounds: calcium nitrate tetrahydrate ( $\text{Ca}(\text{NO}_3)_2 \cdot 4\text{H}_2\text{O}$  A.R. Grade) as the source of calcium ions; and sodium hydrogen carbonate ( $\text{NaHCO}_3$  A.R. Grade) as the source of hydrogen carbonate ions. These solutions were made up in distilled water and in the quantities of 2.5 litres for hydrogen carbonate and 10 litres for calcium with varying concentrations.

The propensity to scale measurements were based on the time taken for the scale formed from the mixing of aqueous solutions of calcium and hydrogen carbonate ions to build up a back pressure of 5.0 psi in the microbore tube above the distilled water base line. The changes in back pressure measurements were recorded on a chart recorder set at a chart speed of  $6 \text{ cm hr}^{-1}$ . The solutions were pumped into the microbore tube at a fixed temperature and at set flow rates, using single channel pumps for both solutions.

The microbore tube was cleaned by (i) injecting 10ml of dilute nitric acid to dissolve the calcium carbonate, returning the base line to its base value and (ii) flushing the tube with distilled water to remove any traces of nitric acid together with dissolved salts. This cleaning process was used for all the propensity to scale experiments described in this chapter.

### 3.6.2 Electromagnetic Treatment of Aqueous Solutions: Circulating Apparatus

The treatment of electromagnetic and replicate non-electromagnetic (dummy) scaling solutions was carried out by the circulating apparatus shown schematically in Figure 3.5 and pictorially in Figure 3.6. The apparatus was comprised of two 15 litre glass vessels (one for each of the electromagnetic and dummy treated solutions); polypropylene and PVC tubing of 0.5 inch internal diameter (i.d.); copper piping of 0.5 inch i.d.; brass valves to adjust the flow rate of the scaling solution through the electromagnet or dummy unit; Totton motorised magnetic centrifugal pumps and a Hydromag electromagnetic and non-electromagnetic (dummy) unit. The Hydromag DN15 units had a 1 metre piece of 0.5 inch copper piping between the Totton pump and the unit with a shorter piece of copper piping on the exit from the unit. After each set of experiments, the PVC tubing and glass vessels of the treated solutions were cleaned thoroughly with dilute hydrochloric acid and with several washes of distilled water to remove any traces of acid.

In each set of experiments, electromagnetic and dummy treatments were carried out simultaneously and consisted of continuously circulating, in the majority of cases, the calcium solution through the Hydromag electromagnetic unit and a replicate non-electromagnetic (dummy) unit, which had the same geometry as the permanent electromagnetic unit and zero field.

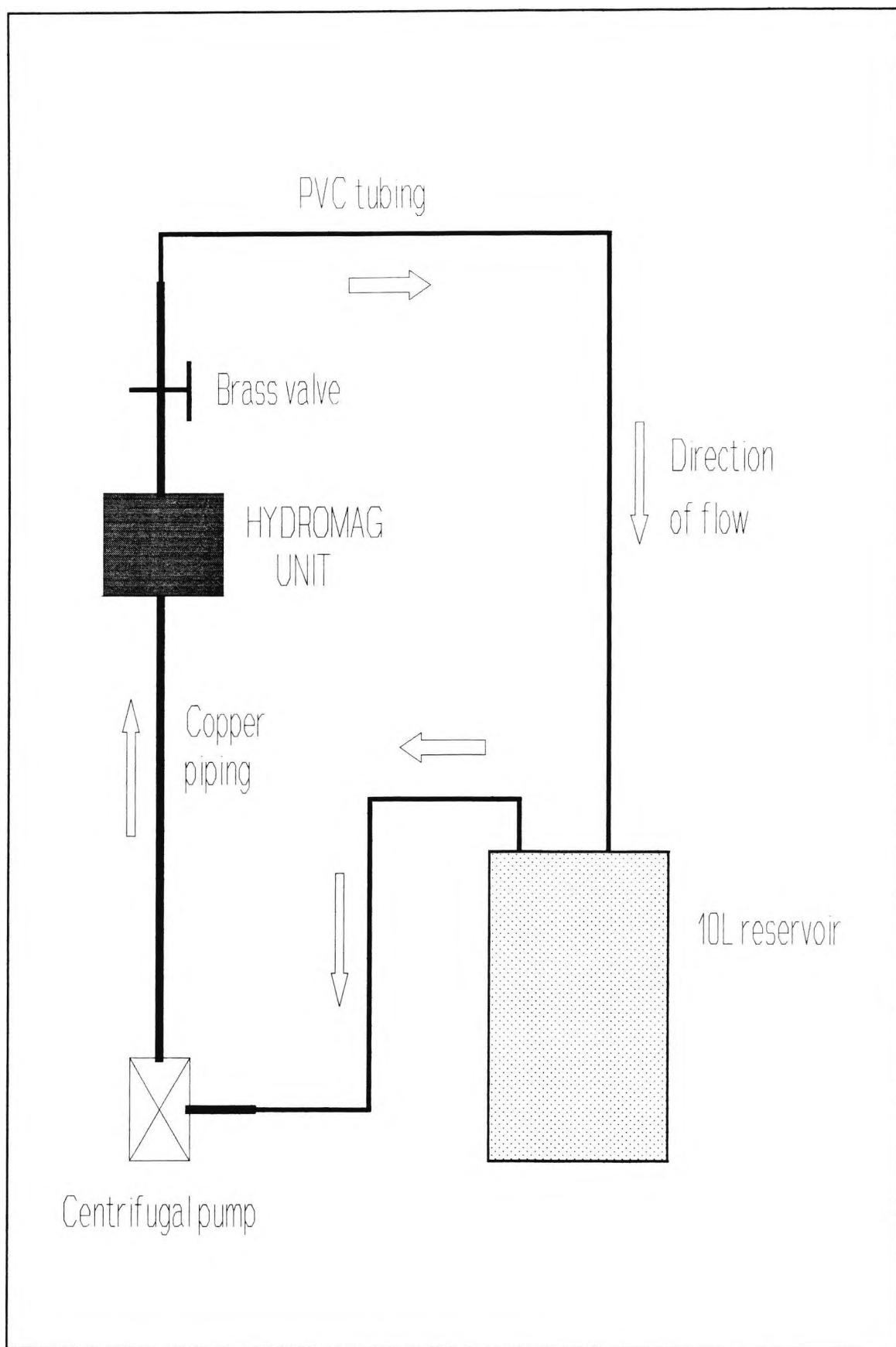


**Figure 3.5 Schematic diagram of the circulating apparatus.**

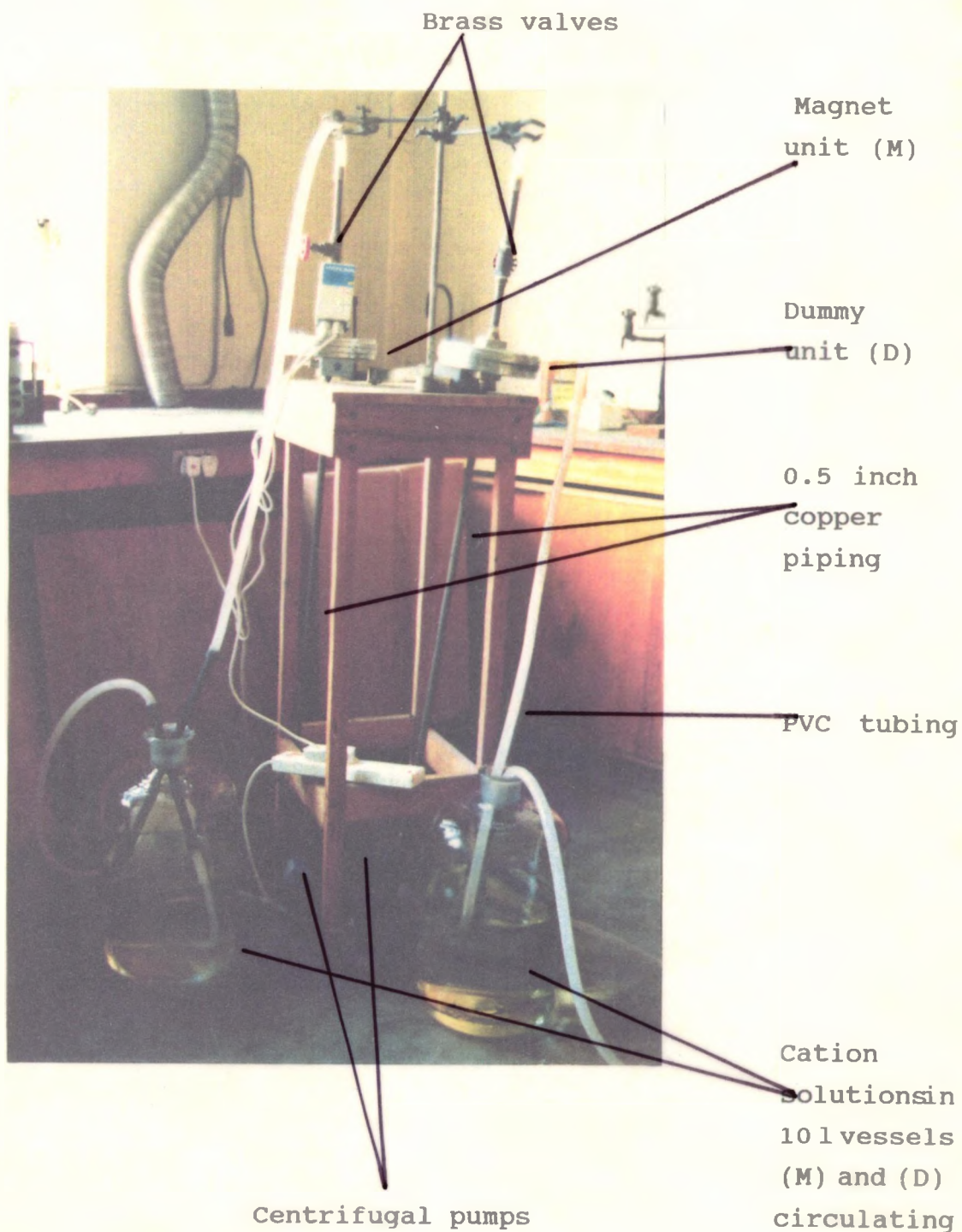


Figure 3.6 Magnetic treatment circulation apparatus.

### 3.6.3 Heat Exchanger Experiments

The heat exchanger experiments were carried out in the equipment shown in Figure 3.7. London tap water was used as the fluid to be treated by the Hydromag electromagnetic unit. The apparatus was comprised of PVC tubing and copper piping of 0.5 inch i.d.; Hydromag electromagnetic and non-electromagnetic (dummy) units; glass connectors; burette taps to regulate the water flow into the glass beakers; two 1 litre Pyrex glass beakers with an overflow pipe fitted at the top to act as a drain; Lyvia immersion heaters connected to a rheostat to regulate the heat exchanger and a thermometer to check the water temperature.

The water was passed from a dual tap source at a rate of 6 litres per minute into the two Hydromag DN15 units, whereupon it was split by a glass connector which drip fed some of the water continuously into the two beakers, leaving the majority of the treated and untreated water to go to waste. The pre-weighed beakers were allowed to fill with the waters before the cleaned immersion heaters were turned on. The immersion heaters were connected through a rheostat to regulate the voltage at which they operated, thereby allowing the water temperature to be controlled accurately by measurement with a thermometer. Hot water was removed by an overflow pipe at the top of the beaker. The experiments were carried out over a set time and temperature. After each experiment the beakers were decanted carefully to remove the water and then placed in an oven at 120°C, until constant weight was achieved. The scale was removed for further analysis and the beakers and immersion heaters were cleaned in very dilute hydrochloric acid and washed thoroughly in water to remove all the existing deposits before the next experiment.

Heat exchanger experiments were carried out over set periods of time and at set temperatures to evaluate the effectiveness of the Hydromag electromagnetic units under laboratory conditions, in reducing or eliminating scale formation. The experiments measured the quantity of scale deposited on the beaker, comparing

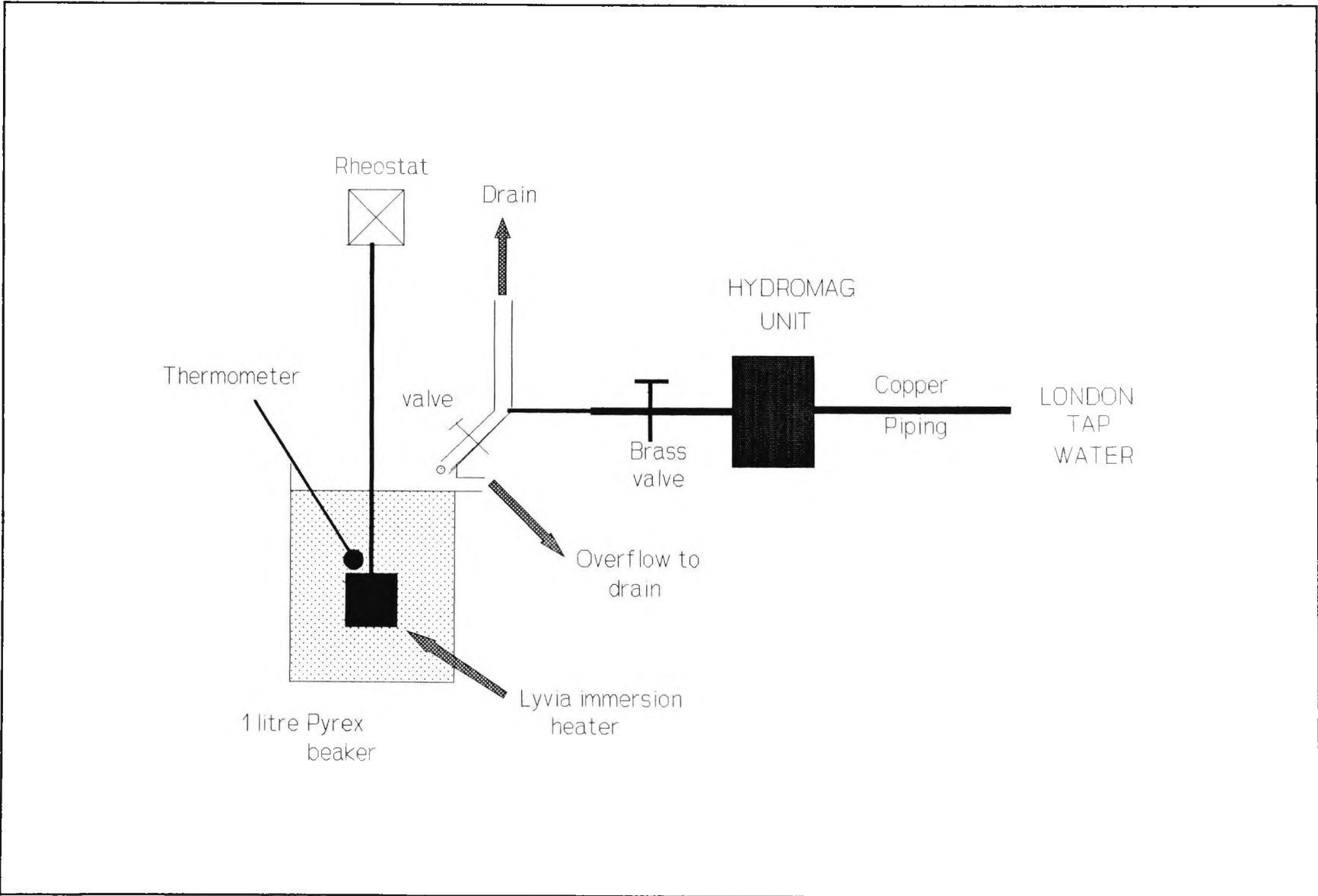


Figure 3.7 Schematic diagram of the heat exchanger apparatus.

differences between treated and untreated water. The dried scale samples were removed from the beaker and microscopic and x-ray diffraction analyses were carried out.

### 3.7 PROPENSITY TO SCALE EXPERIMENTS

In this work, the propensity to scale experiments consisted of mixing treated calcium solutions with sodium hydrogen carbonate solutions in the microbore tube at a fixed temperature and concentration. The resultant build-up of calcium carbonate scale was measured by the P.M.A.C. unit as described in Section 3.6.1.

The propensity to scale measurements were carried out after the electromagnetic and non-electromagnetic (dummy) solutions had undergone a circulation period of 16 hours through the Hydromag DN15 unit, whereupon circulation was stopped. This was to ensure that the electromagnetic effect reached a maximum before back pressure measurements were recorded. For each set of experiments carried out, three different types of treatment were used, with the treated solutions being either control, dummy or electromagnetic (or magnetic). The details of these solutions are:

- (i) Control scaling tendency measurements were obtained by mixing a calcium solution, which did not undergo any type of treatment or turbulent flow, with a sodium hydrogen carbonate solution.
- (ii) Replicate non-electromagnetic or dummy tendency scaling measurements were obtained by mixing a calcium solution with a sodium hydrogen carbonate solution after the calcium solution had been circulated through the Hydromag DN15 unit with no electric power.
- (iii) Magnetic tendency scaling measurements were obtained by mixing a calcium solution with a sodium hydrogen carbonate solution after the calcium solution had been circulated through the Hydromag DN15 unit with the electric power on.

Sufficient replicate propensity to scale experiments (runs) were carried out to obtain statistically significant results, taken as being situations in which the standard deviation was less than 10% of the mean (the detailed standard deviation figures are given in Appendix A). These results are given as % in all the tables.

For some of the results in this section, the percentage reduction in the propensity to scale for an electromagnetically treated solution over a control is given. This was calculated from Equation 3.2 given by:

Let C= Control, E= Electromagnetic, D= Dummy all average values

If  $D - C = B$  (Turbulence and aeration factors)

and  $E - B = E'$  (Electromagnetic value omitting turbulence and aeration factors)

$$\frac{E' - C}{C} \times 100 = \% P.R.$$

**Equation 3.2 Percentage Reduction in the Propensity to Scale**

% P.R. = Percentage Propensity Reduction

The calculation shows the reduction in the tendency of an electromagnetically treated solution to precipitate as compared to an untreated (control) solution, which is taken to have a propensity to scale value of 100%. Also taken into account in the calculation are the turbulence and aeration factors, caused by circulation, which tangibly influence the scaling times (precipitation rate) for the electromagnetic and dummy solutions, when compared to an uncirculated control solution.

The first two sets of experiments described in this section were carried out with the aim of optimising the electromagnetic treatment conditions for the precipitation of calcium carbonate.

### 3.7.1 The Effect of Magnetic Treatment of Calcium Solutions on the Propensity to Scale using Polypropylene and Copper Piping

The aim of this set of experiments was to determine if the magnetic treatment of a calcium solution, when passed through different types of piping connected to the Hydromag DN15 unit, would have any effect on the precipitation rate of calcium carbonate. The calcium solutions were circulated through both polypropylene and copper pipework systems using the circulating system described in Section 3.6.2. In these experiments no dummy runs were carried out, only magnetic and control experiments.

A 250 ppm calcium solution was continuously circulated through the Hydromag DN15 units, fitted with copper or polypropylene at a flow rate of 7.5 litres per minute. The circulation period was 16 hours before the first propensity to scale measurements were recorded. The sodium hydrogen carbonate concentration used was 0.05 Molar. The flow rates into the P.M.A.C. microbore tube for this experiment were 1.5 litres per hour for the calcium solution and 0.4 litres per hour ( $1 \text{ hr}^{-1}$ ) for the hydrogen carbonate solution, with the two solutions being mixed at a temperature of  $70^{\circ}\text{C}$ . The results for these experiments are given in Table 3.8.

**Table 3.8 Effect of different piping on the propensity to scale**

Treatment	Av. Time (mins)	%	S.D.	Time Range (mins)	No. of Runs
Control	24.2	8.31	2.00	21.0-26.8	8
Copper	41.8	6.41	2.68	37.5-45.5	6
Polypropylene	25.1	4.82	1.21	23.5-26.5	6

Where % =  $\frac{\text{Standard Deviation}}{\text{Av. Time}} \times 100$

Av. Time

The results indicate that the magnetic treatment of the calcium solution, when passing through copper pipework, affects the scaling time of calcium carbonate precipitation. The magnetically treated calcium solution, passing through copper pipework, was shown to significantly increase the precipitation time of calcium carbonate, when compared to the magnetically treated calcium solution in polypropylene pipework and the control solution. The results show that the Hydromag units have no significant effect on the propensity to scale in polypropylene pipework system at the flow rate of 7.5 l/min, when compared to the control experiments.

### 3.7.2 The Effect of Flow Rate for the Hydromag DN15 unit on the Propensity to Scale using Polypropylene and Copper Piping

The aim of this set of experiments was to determine the optimum flow rate for circulating calcium solutions through the Hydromag DN15 unit when connected to the polypropylene or copper pipework systems. The optimum flow rate was found when the biggest significant reduction in the precipitation of calcium carbonate was observed in the propensity to scale measurements.

The Hydromag DN15 unit used in this work (field strength 2.5 kGauss) is widely used in industrial and domestic situations (Section 3.4). The DN15 units are purported to operate most effectively, i.e. at an optimum in preventing the buildup of scale deposits, at an optimum flow rate which differs for each unit (0.5-4.0 inch diameter piping) [51]. The optimum flow rates are based on calculations for the maximum Lorentz Force (see Section 3.9.1, for the ions present in solution), taking into account the pressure drop across each unit. No experimental studies have been previously carried out to assess the effect of flow rate on the rate of precipitation of calcium carbonate for any of the Hydromag units. Therefore these experiments determined for both pipework systems, the optimum flow rate required to give the biggest reductions in the propensity to scale for the calcium carbonate scaling system.

A 250 ppm calcium solution was continuously circulated through the Hydromag DN15 unit, connected to the polypropylene or copper pipework system, using the apparatus described in Section 3.6.2. The flow rates of the two systems through the DN15 units were adjusted by using the brass or polypropylene valves. The calibration of the valves for each flow rate investigated was carried out manually, using a graduated 5 litre jug and a digital stopwatch. This calibration was accurate to within 5%. In these experiments the calcium solutions were circulated through the Hydromag DN15 unit at 3, 6, 9, 12 and 15 litres per minute, for each pipework system. The propensity to scale measurements were carried out at 70°C, mixing the calcium solutions with a 0.05 Molar sodium hydrogen carbonate solution. The flow rates into the P.M.A.C. microbore tube for these experiments were 1.5 lhr<sup>-1</sup> for the calcium solution and 0.4 lhr<sup>-1</sup> for the hydrogen carbonate solution.

The results for the average scaling times for the flow rate experiments for an increase in back pressure of 5 psi are given in Table 3.9, and shown graphically in Figure 3.8. The details of replicate runs for each flow rate experiment are given in Appendix Tables A.1 to A.5. In the tables the following terms are abbreviated: Hydromag unit with copper pipework- Mag Cu and Hydromag unit with polypropylene pipework- Mag PP.

**Table 3.9 Effect of different flow rates on the propensity to scale: Average scaling times (mins).**

Treatment	Flow Rate Litres /minute				
	3	6	9	12	15
Control	26.8	26.4	27.6	27.0	27.3
Mag PP	27.9	25.0	31.5	28.8	27.4
Mag Cu	53.1	45.3	43.6	40.2	40.1

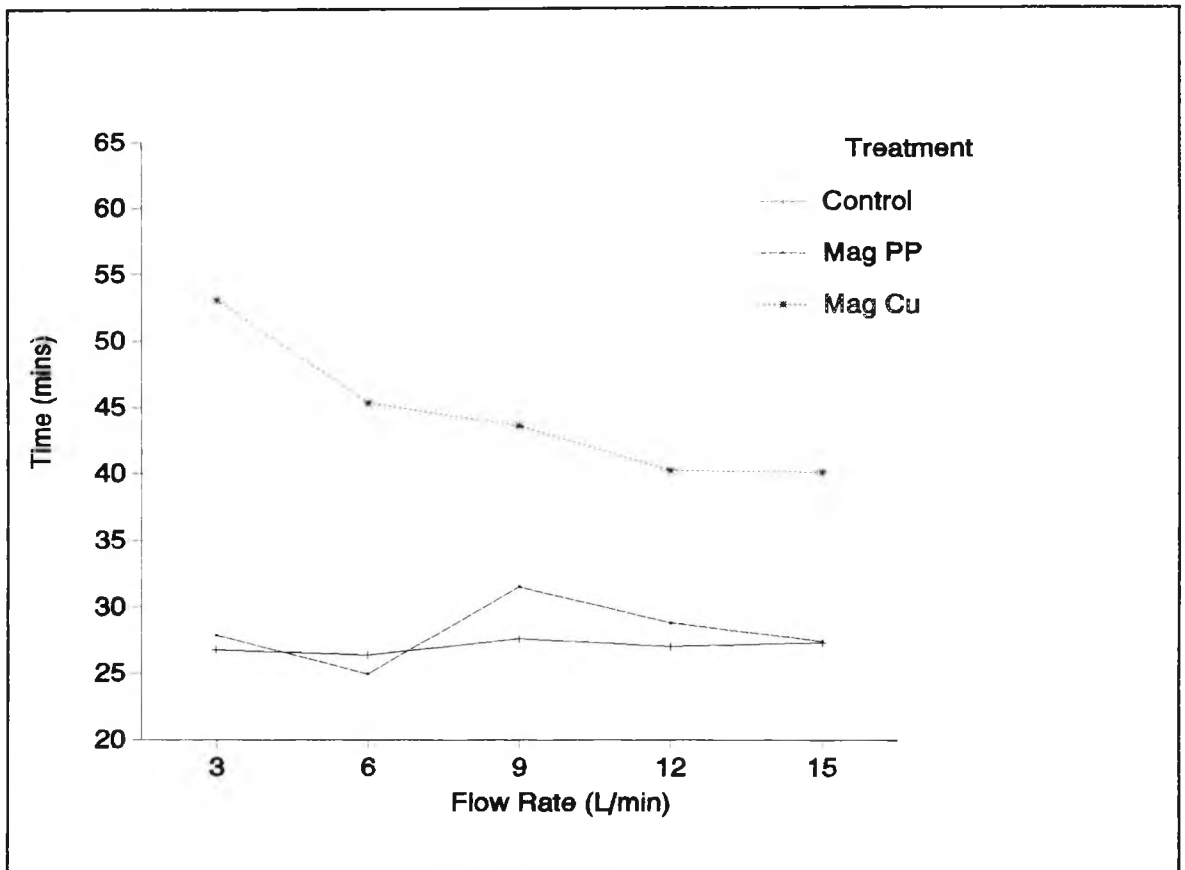


Figure 3.8 Effect of flow rate on the propensity to scale: Average scaling times (mins).

The results indicate that varying the flow rate of the 250 ppm calcium solution in each experiment through the Hydromag DN15 unit connected with copper pipework, caused a significant decrease in the rate of deposition of scale, when compared to the Hydromag DN15 unit connected with polypropylene piping and the control. The decrease in the rate of scale deposition was found to vary slightly at flow rates greater than 6 l/min, but at lower flow rates a significant decrease was found as shown in Figure 3.8. This indicates that the most effective flow rate for the circulating calcium solution was 3 l/min in this experiment. At this flow rate the magnetic treatment of the calcium solution gave an average scaling time of 53.1 minutes, with a standard deviation of 4.3. The results for the calcium solution circulated at different flow rates through the Hydromag DN15 unit connected with polypropylene piping and the control are very similar. This confirms that there is no effect on the propensity to scale if

the calcium solutions are passed through polypropylene piping connected to the Hydromag DN15 unit, as found in Section 3.7.1.

The consistency of the measurements is shown in Figure 3.9, for 6 repeat runs of propensity to scale measurement for the flow rate experiment of 12 l/min, for the three calcium solution treatments. Figure 3.10 shows the scaling profiles for the three treatments in this experiment.

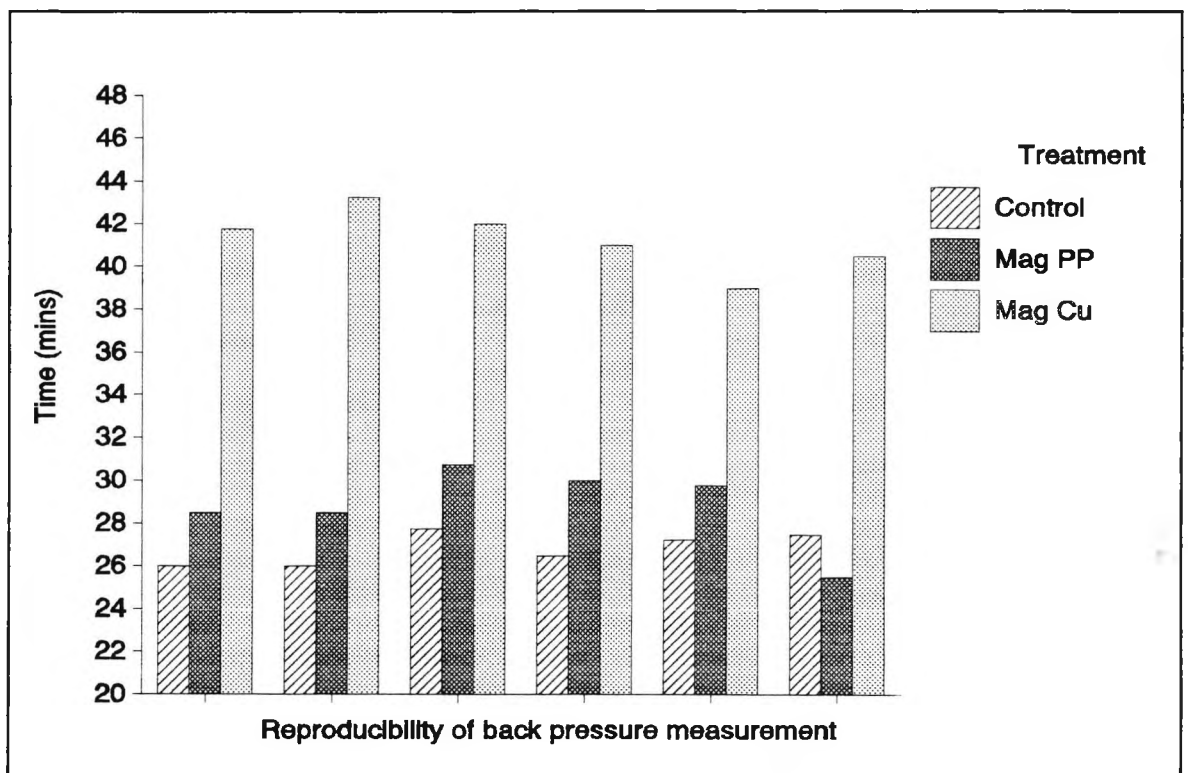
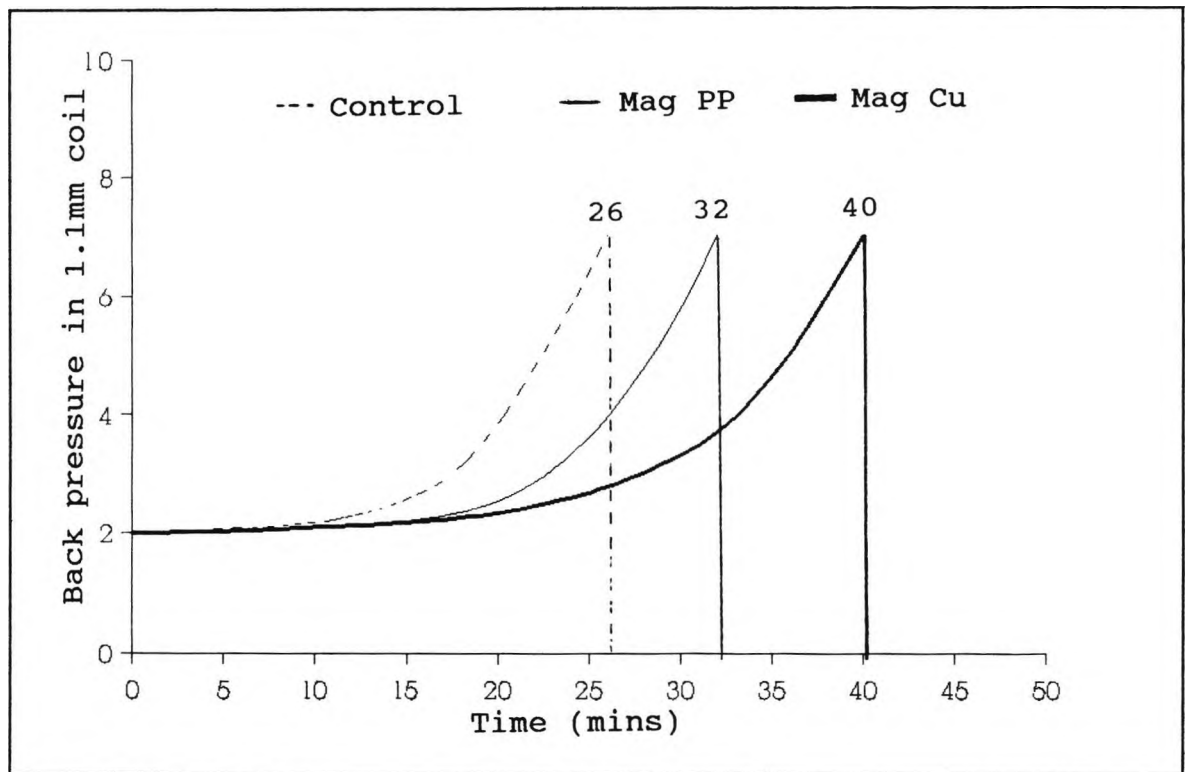


Figure 3.9 Reproducibility of propensity to scale measurements for the treatment of calcium solutions at 12 l/min.

During these experiments, it was found that prolonged circulation through the Hydromag DN15 unit connected with copper pipework caused a yellow/brown discolouration in the calcium solution. These solutions were tested for their copper and iron contents and were found to contain trace amounts (<0.1 ppm) of iron, and 1.9 ppm of copper, which was caused by the calcium solution being circulated through the copper pipework system. The results showed that a significant reduction in the propensity to scale occurred after a minimal circulation period of 16 hours. Therefore all



**Figure 3.10 Scaling profiles in the propensity to scale measurements for the treatment of calcium solutions at 12 l/min.**

subsequent experiments were circulated for 16 hours, whereupon magnetic treatment was ceased and propensity to scale measurements were carried out. The Hydromag DN15 unit connected with polypropylene pipework had no such contamination problems. The contamination of ions, such as copper, zinc [52] and iron [13] can affect the nucleation processes and hence the crystal growth of calcium carbonate. Due to the contamination after each set of circulating periods, the PVC tubing and glass vessels of the copper pipework systems were cleaned successively with dilute hydrochloric acid, tap water and distilled water to remove any traces of acid, and ensure minimal contamination from the pipework.

These results clearly demonstrate that the Hydromag DN15 unit connected with the polypropylene piping does not affect the propensity to scale measurements for the calcium carbonate scaling system at the flow rates investigated. The Hydromag DN15 unit connected with the copper pipework caused a significant

reduction in the propensity to scale, at all the flow rates investigated, with the optimum being 3 l/min. The results, however, are affected by the presence of a relatively high level of copper ions in the calcium solution, due to contamination, which may affect the propensity to scale.

### 3.7.3 The Effect of Flow Rate for the Hydromag DN15 unit on the Propensity to Scale

The aim of this set of experiments was to determine the optimum flow rate for circulating calcium solutions through the Hydromag DN15 unit, when connected to cleaned PVC tubing and contained in clean glass vessels. The optimum flow rate was found when the biggest significant reduction in the rate of precipitation of calcium carbonate was observed in the propensity to scale measurements. Two different circulating systems were used: (i) passing the calcium solution through the Hydromag unit with the power on (Magnet) and (ii) passing the calcium solution through the Hydromag unit with the power off (dummy). The dummy unit had the same geometry as the magnetic unit but with a zero field. Both of these circulating systems were connected to the Hydromag units with copper piping to investigate the effect of passing the calcium solution through copper pipework when the magnetic field was either on or off.

The flow rate measurements were carried out for three different calcium concentrations, to evaluate the change in the optimum flow rate at different calcium concentrations. Table 3.10 shows the experimental conditions used in the flow rate experiments.

In all three flow rate experiments the calcium solutions were circulated for 16 hours through the Hydromag units using the apparatus described in Section 3.6.2. The flow rates for both systems were adjusted by using the brass valve. The calibration of the brass valves for each flow rate investigated was carried out manually, using a graduated 5 litre jug and a digital stopwatch. This calibration was accurate to within 5%. After each

**Table 3.10 Experimental conditions in the flow rate experiments.**

Experiment	Ca <sup>2+</sup> conc. ppm	NaHCO <sub>3</sub> conc. (M)	Flow rates used (l/min)	Temp°C
A	250	0.05000	3,6,9,12	70
B	500	0.03125	3,6,9,12	70
C	750	0.03125	3,6,9,12	70

flow rate experiment the PVC tubing and the glass vessels were cleaned as described in Section 3.7.2. Measurements of the copper and iron concentrations for the magnetic and dummy calcium solutions were recorded for each experiment.

#### **A. Flow rate experiments using a 250 ppm calcium solution**

The concentrations of the calcium and sodium hydrogen carbonate solutions and the flow rates investigated at 70°C are given in Table 3.10. The flow rates into the P.M.A.C. microbore tube for this set of experiments were 1.3 lhr<sup>-1</sup> for the calcium solutions and 0.4 lhr<sup>-1</sup> for the sodium hydrogen carbonate solution.

The results for the average scaling times for the flow rate experiments are given in Table 3.11, and shown graphically in Figure 3.11. The details of replicate runs for each flow rate experiment are given in Appendix Tables A.6 to A.9.

**Table 3.11 Effect of flow rate on the propensity to scale for a 250 ppm calcium solution: Average scaling time (mins).**

Treatment	Flow rate l/min			
	3	6	9	12
Control	30.1	29.2	31.0	30.0
Dummy	44.1	38.1	45.0	57.6
Magnet	65.3	73.1	61.7	62.1

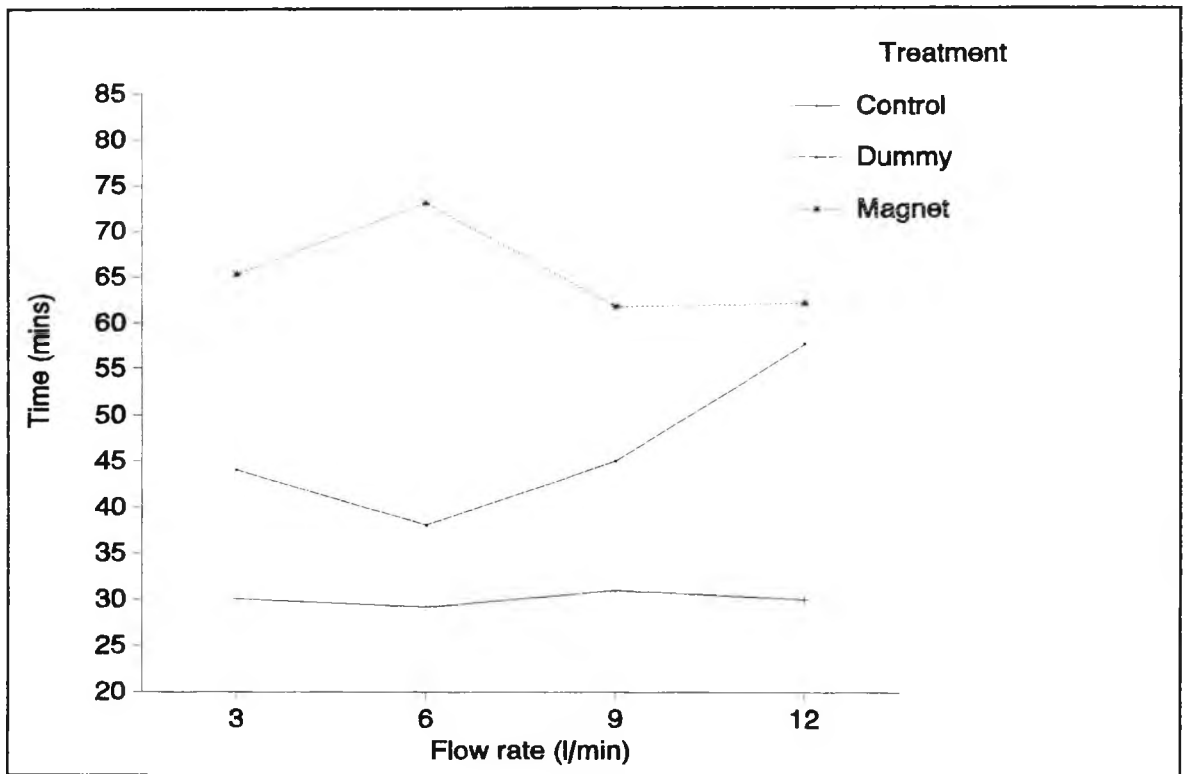


Figure 3.11 Effect of flow rate on the propensity to scale for a 250 ppm calcium solution: Average scaling time (mins).

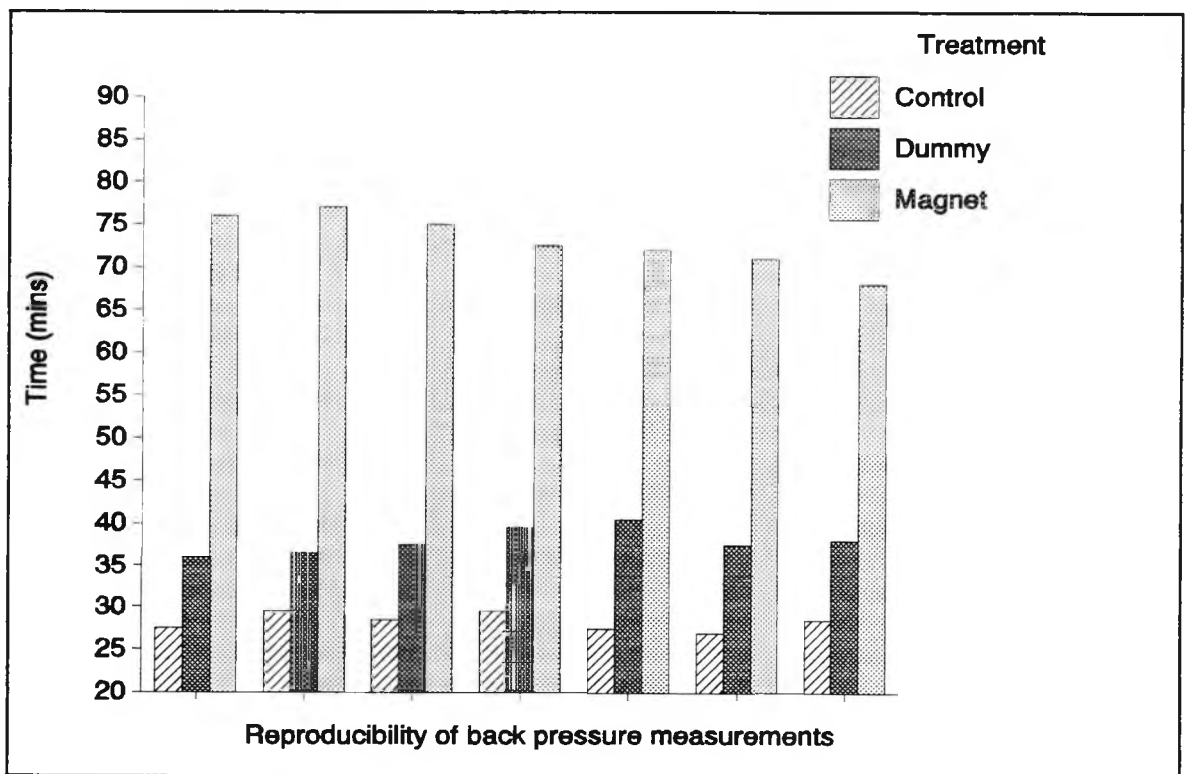


Figure 3.12 Reproducibility of propensity to scale measurements for the treatment of calcium solutions at 6 l/min.

The consistency of the measurements is shown in Figure 3.12, for 7 repeat runs of propensity to scale measurement for the flow rate experiments of 6 l/min, for the three calcium solution treatments. Figure 3.13 shows the scaling profiles for the three treatments in this experiment.

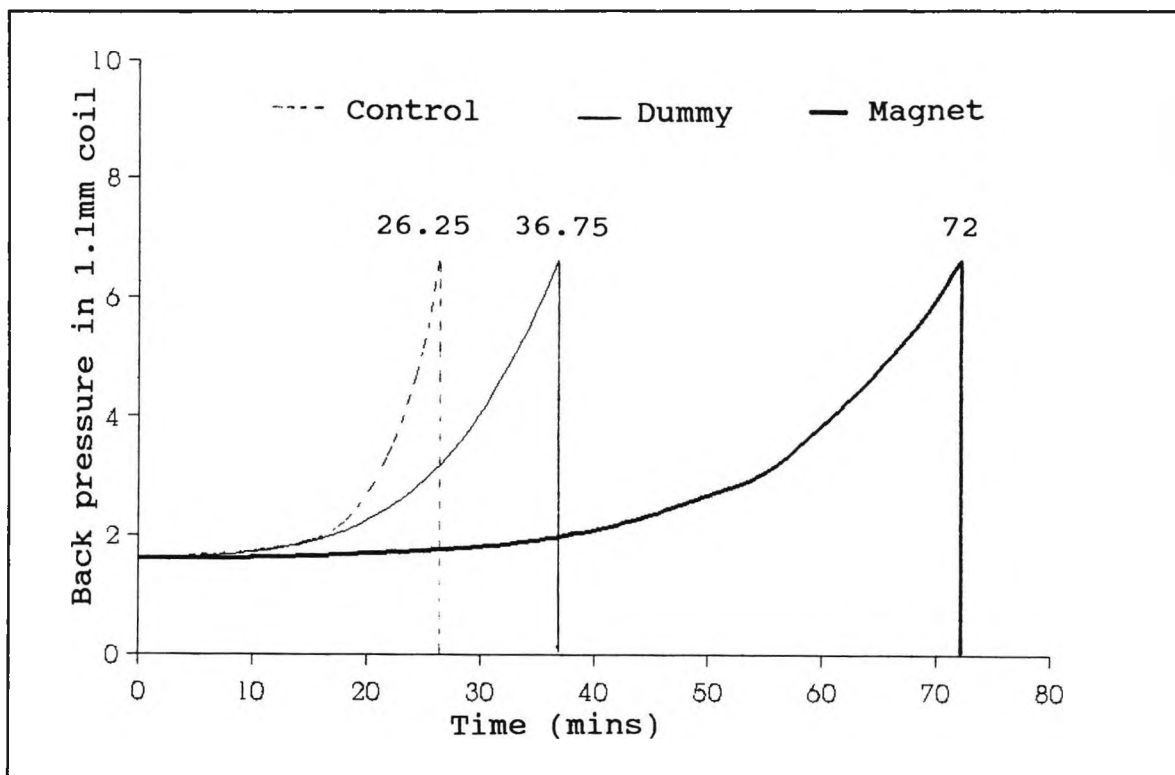


Figure 3.13 Scaling profiles for the propensity to scale measurements for the treatment of calcium solutions at 6 l/min.

The iron content for both magnetic and dummy solutions was  $<0.1$  ppm. The copper content for the dummy solution was found to be greater than that for the magnetic samples in all the cases tested, averaging 0.5 and 0.3 ppm, respectively.

#### B. Flow rate experiments using a 500 ppm calcium solution

The concentrations of the calcium and sodium hydrogen carbonate solutions and the flow rates investigated at  $70^{\circ}\text{C}$  are given in Table 3.10. The flow rates into the P.M.A.C. microbore tube for this set of experiments were  $1.3 \text{ lhr}^{-1}$  for the calcium solution and  $0.4 \text{ lhr}^{-1}$  for the sodium hydrogen carbonate solution.

The results for the average scaling times for the flow rate experiments are given in Table 3.12 and shown graphically in Figure 3.14. The details of replicate runs for each flow rate experiment are given in Appendix Tables A.10 to A.13.

**Table 3.12 Effect of flow rate on the propensity to scale for a 500 ppm calcium solution: Average scaling time (mins).**

Treatment	Flow rate l/min			
	3	6	9	12
Control	29.4	29.5	31.3	30.2
Dummy	37.1	39.2	46.4	51.7
Magnet	63.3	72.3	64.8	63.1

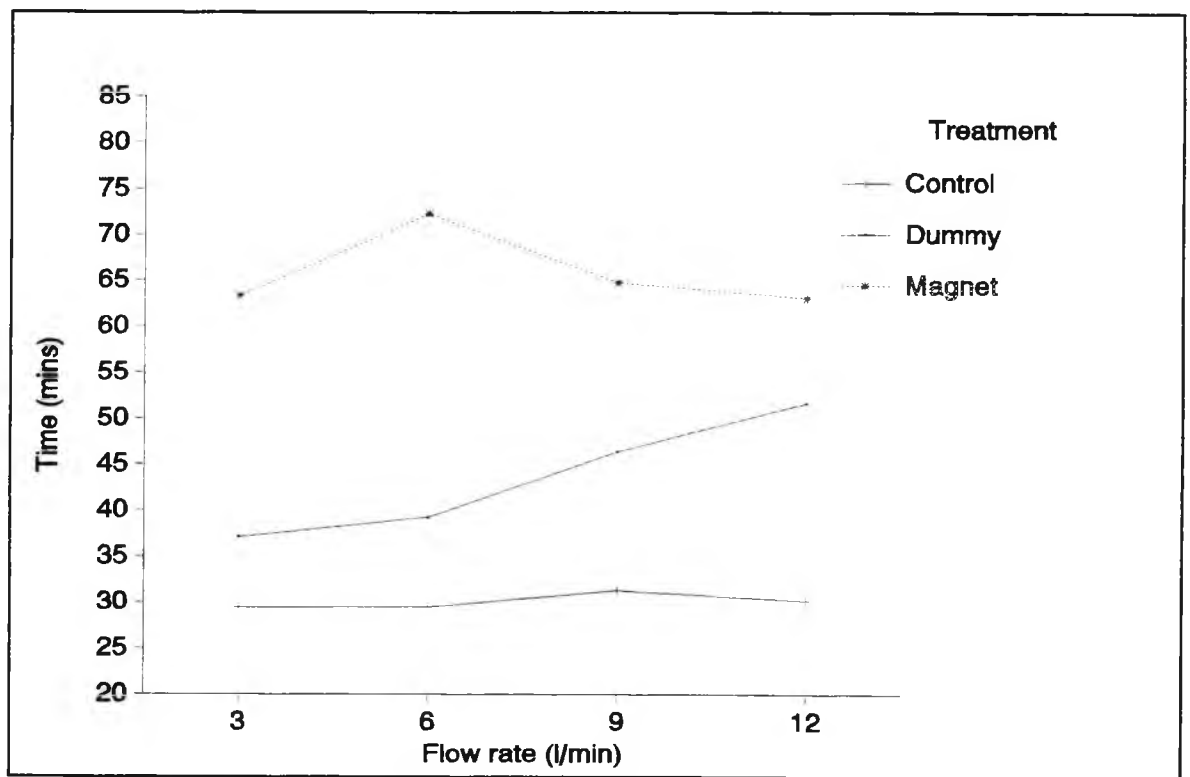


**Figure 3.14 Effect of flow rate on the propensity to scale for a 500 ppm calcium solution: Average scaling time (mins).**

The consistency of the measurements is shown in Figure 3.15, for seven repeat runs of propensity to scale measurement for the flow rate experiments of 9 l/min, for the three calcium solution treatments. Figure 3.16 shows the scaling profiles for the three treatments in this experiment.

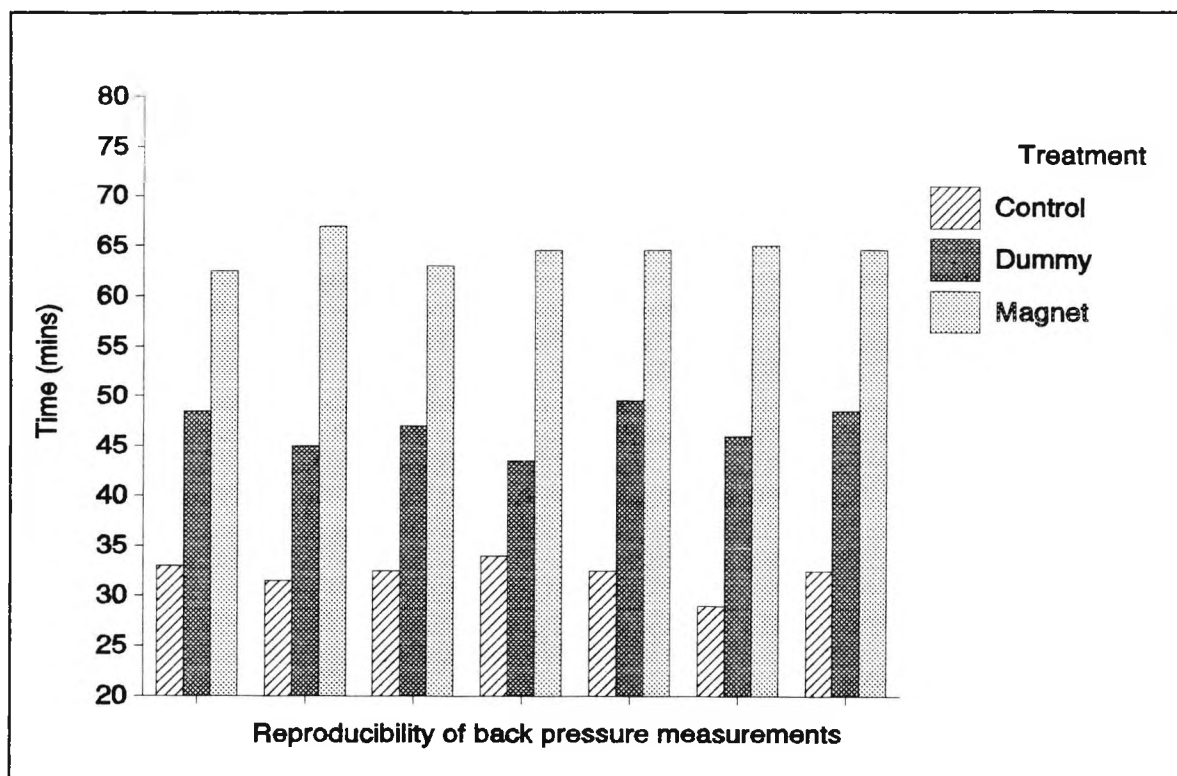


Figure 3.15 Reproducibility of propensity to scale measurements for the treatment of calcium solutions at 9 l/min.

The iron content for both magnetic and dummy solutions was <0.1 ppm. The copper content for the dummy solution was greater than that for the magnetic samples in all the cases tested, averaging 0.6 and 0.25 ppm, respectively.

### C. Flow rate experiments using a 750 ppm calcium solution

The concentrations of the calcium, sodium hydrogen carbonate solutions and the flow rates investigated at 70°C are given in Table 3.10. The flow rates into the P.M.A.C. microbore tube for this set of experiments were 1.3 lhr<sup>-1</sup> for the calcium solution and 0.4 lhr<sup>-1</sup> for the sodium hydrogen carbonate solution.

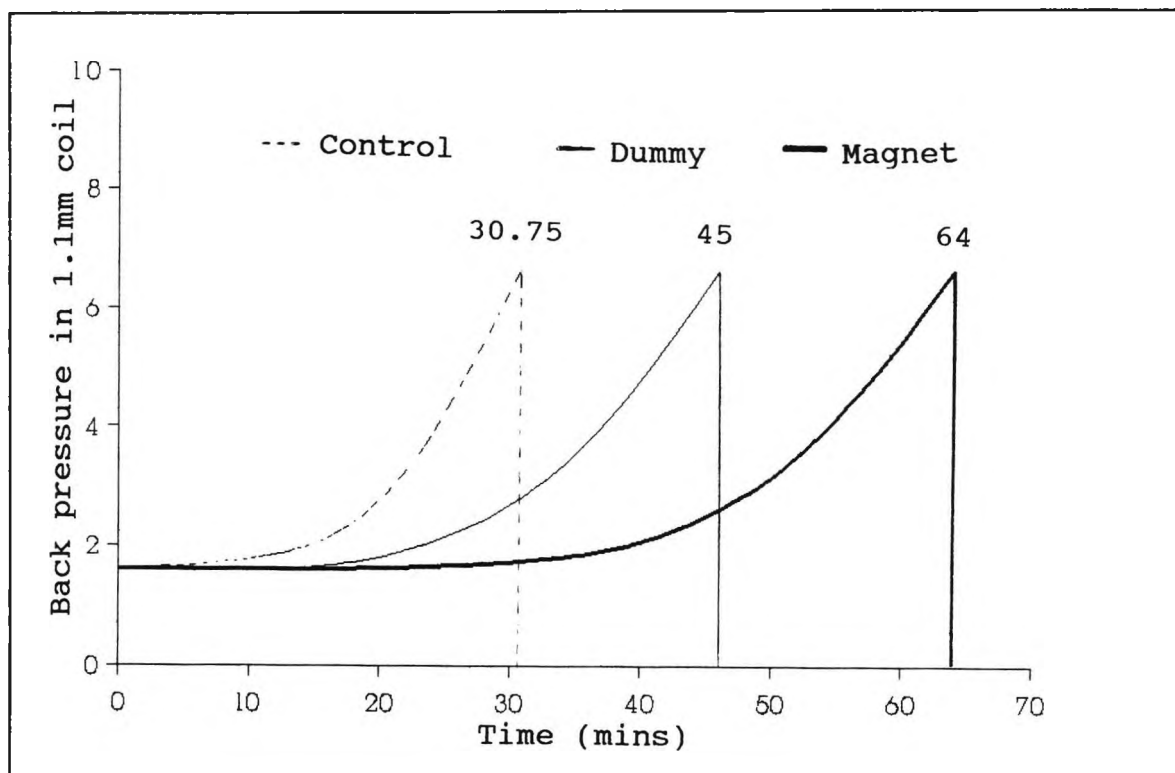


Figure 3.16 Scaling profiles in the propensity to scale measurements for the treatment of calcium solutions at 9 l/min.

The results for the average scaling times for the flow rate experiments are given in Table 3.13 and shown graphically in Figure 3.17. The details of replicate runs for each flow rate experiment are given in Appendix Tables A.14 to A.17.

Table 3.13 Effect of flow rate on the propensity to scale for a 750 ppm calcium solution: Average scaling time (mins).

Treatment	Flow rate l/min			
	3	6	9	12
Control	32.8	30.8	29.5	28.9
Dummy	45.6	44.9	48.6	49.5
Magnet	59.3	67.2	61.3	56.9

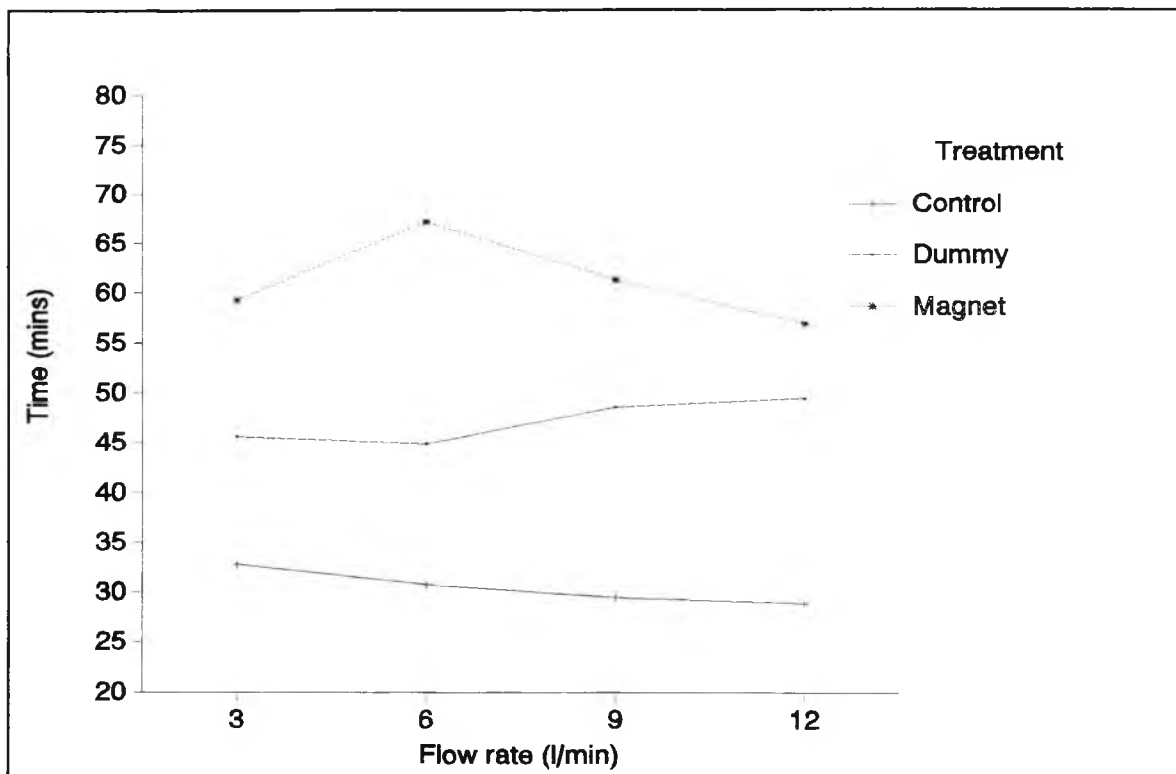


Figure 3.17 Effect of flow rate on the propensity to scale for a 750 ppm calcium solution: Average scaling time (mins).

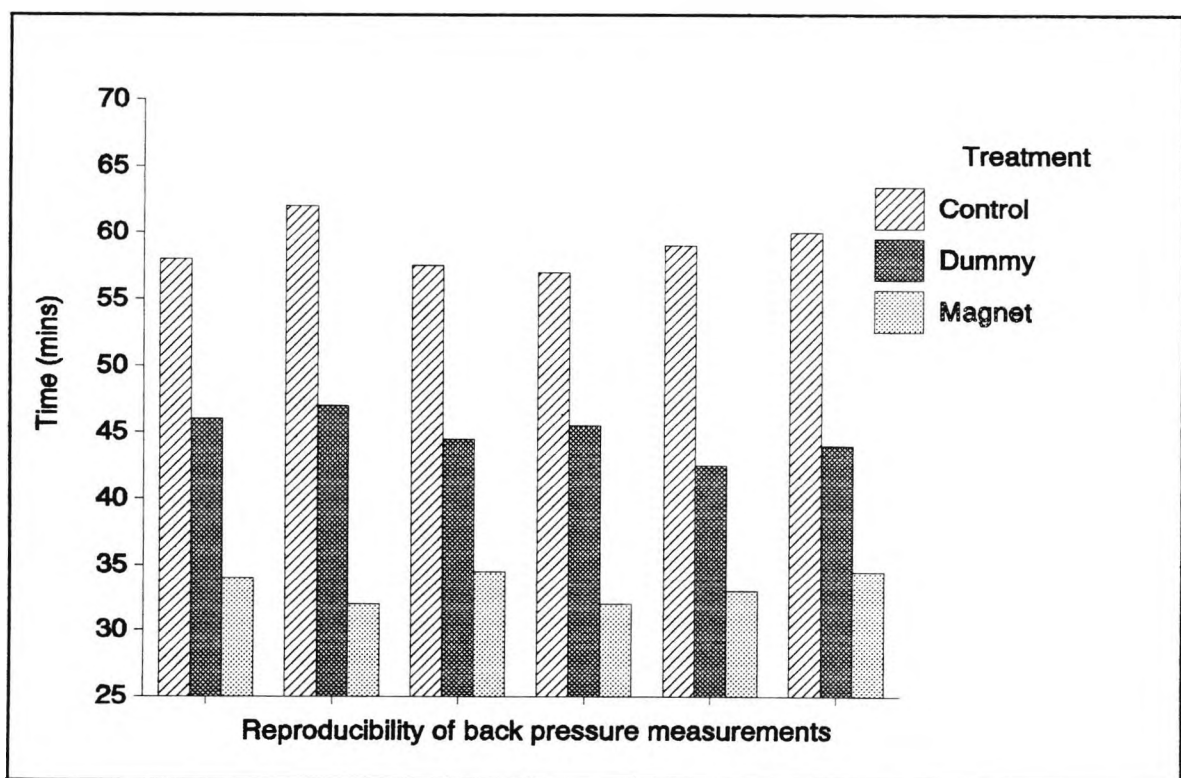


Figure 3.18 Reproducibility of propensity to scale measurements for the treatment of calcium solutions at 3 l/min.

The consistency of the measurements is shown in Figure 3.18, for six repeat runs of propensity to scale measurement, for the flow rate experiments of 3 l/min, for the three calcium solution treatments. Figure 3.19 shows the scaling profiles for the three treatments in this experiment.

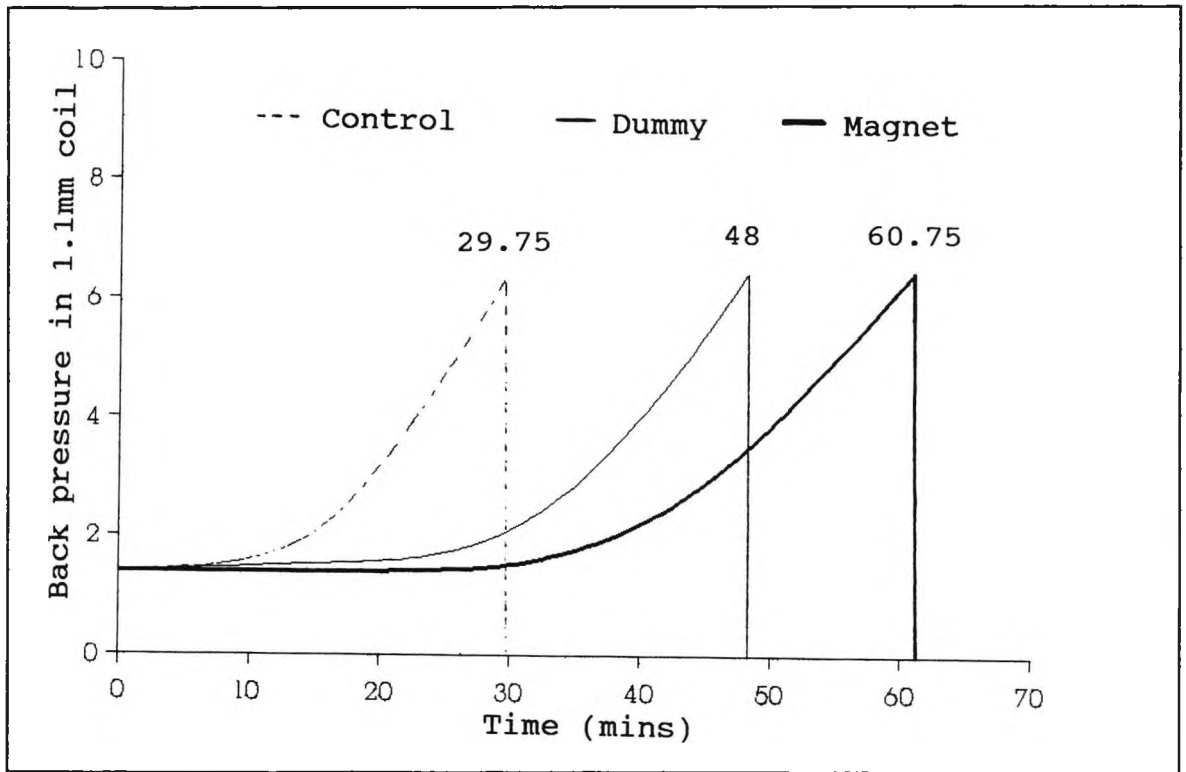


Figure 3.19 Scaling profiles in the propensity to scale measurements for the treatment of calcium solutions at 3 l/min.

The iron content for both magnetic and dummy solutions was  $<0.1$  ppm. The copper content for the dummy solution was greater than that for the magnetic samples in all the cases tested, averaging 0.5 and 0.3 ppm respectively.

The results for the flow rate experiments shown in Tables 3.11-3.13, show firstly that magnetic treatment of each calcium solution tested caused significant decreases in the rate of deposition of scale, when compared to the rate of deposition for the dummy and control treatments. Secondly, the decrease in the rate of deposition of scale was found to vary significantly with change in the flow rate of the calcium solutions through the

Hydromag DN15 unit. The data from Figures 3.11, 3.14 and 3.17, show clearly that the most effective flow rate for circulating a calcium solution through a Hydromag DN15 unit is 6 l/min. The propensity to scale measurements for the magnetic treatment of calcium solutions at 3, 9 and 12 l/min, were found to be lower than those for the flow rate of 6 l/min. The calculations of the percentage reduction in the propensity to scale for the magnetic solutions as compared to the control solutions for each calcium solution tested at each flow rate are shown in Table 3.14.

**Table 3.14 Percentage propensity reduction for the calcium solutions at each flow rate.**

% Propensity reduction for each flow rate l/min				
Calcium conc. ppm	3	6	9	12
250	70	119	54	15
500	89	112	59	38
750	42	72	43	26

The data confirm that the most effective flow rate for passing calcium solutions through the Hydromag DN15 unit is 6 l/min. At 3 l/min the percentage propensity reduction for calcium solutions is slightly lower, but still causes a significant decrease in the rate of deposition of scale. This reduction in effectiveness is caused by the calcium solution passing through the magnetic field too slowly, so that the magnetic effect on the solution is not at its maximum. For the flow rates of 9 and 12 l/min, the percentage propensity reduction for calcium solutions is significantly lower than that for the optimum flow rate. This reduction is caused by an increased turbulence within the Hydromag unit, reducing the magnetic field's effectiveness to treat the calcium solutions. Hydromag's published optimum flow rate for the DN15 unit is 6 l/min, which is consistent with the propensity to scale results.

The propensity to scale measurements for the calcium solutions treated in the dummy Hydromag DN15 unit showed that the lower flow rates (3 and 6 l/min) gave similar results. As the flow rate increased, the average scaling times increased significantly. This was attributed to the increase in turbulence as the calcium solution circulated through the dummy Hydromag unit. The control experiments for each calcium solution were found to be extremely accurate, displaying the reproducibility of the results obtained.

Analysis of the calcium solutions for copper showed that regular cleaning of the apparatus significantly reduced the copper contamination. The copper contamination was found to be higher in the calcium solutions passing through the dummy unit, when compared to the magnetically treated calcium solutions. Copper contamination is, therefore, not affecting the propensity to scale measurements for the magnetically treated calcium solutions.

The results of these experiments show clearly that the optimum flow rate for the Hydromag DN15 unit is 6 l/min and that all subsequent experiments using this unit should use this flow rate in the circulation of calcium solutions.

#### 3.7.4 The Effect of Sodium Hydrogen Carbonate Concentration on the Propensity to Scale

The aim of this set of experiments was to investigate the effect of varying the sodium hydrogen carbonate concentration on the propensity to scale measurements when mixed with calcium solutions at temperatures of 70, 80 and 90°C. Two different calcium solutions were used (500 and 750 ppm) in this investigation. The calcium solutions were circulated through the Hydromag DN15 unit with the power on (Magnet) and off (Dummy), and the results were compared with those from the control calcium solution. The effectiveness of magnetic treatment for both calcium solutions was assessed for each sodium hydrogen carbonate concentration and temperature investigated, using the propensity

to scale measurements.

The calcium solutions used in this section were circulated for 16 hours through the Hydromag unit at a flow rate of 6 l/min (as determined in Section 3.7.3), using the circulating apparatus described in Section 3.6.2. After each circulation of the calcium solution the PVC tubing and the glass vessel were cleaned as described in Section 3.7.2. Measurement of the copper and iron content for the magnet and dummy solutions were recorded for each experiment.

The sodium hydrogen carbonate concentrations used in this work were varied so that three different molar ratios of hydrogen carbonate to calcium were investigated. These were:

- (i) When the calcium ion and the hydrogen carbonate ion combined in **equimolar** amounts (Thus;  $\text{Ca}^{2+}:\text{HCO}_3^-$  react 1:2)
- (ii) When the **calcium ion** was in **excess** of the hydrogen carbonate ion (Thus;  $\text{Ca}^{2+}:\text{HCO}_3^-$  react  $> 1:2$ )
- (iii) When the **hydrogen carbonate ion** was in **excess** of the calcium ion (Thus;  $\text{HCO}_3^-:\text{Ca}^{2+}$  react  $> 2:1$ )

The flow rates into the P.M.A.C. microbore tube for the 500 and 750 ppm calcium solutions were fixed at  $1.3 \text{ lhr}^{-1}$  for all the experiments in this section. The concentration of calcium in moles per hour flowing into the microbore tube for a 500 ppm solution was approximately  $1.63 \times 10^{-2} \text{ M hr}^{-1}$ , giving an equimolar combination of  $\text{Ca}^{2+}:\text{HCO}_3^-$  of  $1.63 : 3.26 \times 10^{-2} \text{ M hr}^{-1}$ . For the 750 ppm calcium solution the concentration of calcium was  $2.44 \times 10^{-2} \text{ M hr}^{-1}$ , giving an equimolar combination of  $2.44:4.88 \times 10^{-2} \text{ M hr}^{-1}$ .

The flow rates into the P.M.A.C. microbore tube for the sodium hydrogen carbonate solutions were fixed at  $0.4 \text{ lhr}^{-1}$  for the experiments carried out at 70 and 80°C. The experiments at 90°C required a higher flow rate for the sodium hydrogen carbonate

solutions to gain reproducible results and to give a more uniform deposition of scale. The flow rate for these experiments was 0.5 lhr<sup>-1</sup>. The sodium hydrogen carbonate concentrations were reduced so that the number of moles per hour flowing into the microbore tube was equivalent to that used in the experiments at 70 and 80°C as shown in Table 3.15.

**Table 3.15 Difference in sodium hydrogen carbonate concentrations.**

Ca <sup>2+</sup> conc. ppm	Temp °C	NaHCO <sub>3</sub> conc. (M)	Flow rate lhr <sup>-1</sup>	NaHCO <sub>3</sub> conc. x 10 <sup>-2</sup> M hr <sup>-1</sup>
500	70	0.019	0.4	0.76
500	90	0.0152	0.5	0.76

Six different sets of sodium hydrogen carbonate concentration experiments were carried out for the two calcium concentrations and three temperatures used in this investigation. The results are given in the following sections.

**A. The effect of varying sodium hydrogen carbonate concentrations on a 500 ppm calcium solution at 70°C**

Nine concentrations of sodium hydrogen carbonate were investigated in this section of the work. These are given below and are in units of x 10<sup>-2</sup> Molar:

(i) 1.90; (ii) 2.38; (iii) 3.80; (iv) 4.75; (v) 5.63; (vi) 6.88; (vii) 8.40; (viii) 10.00; and (ix) 12.50.

Therefore, the concentrations in moles per hour of sodium hydrogen carbonate into the P.M.A.C. microbore tube were (in molar units x 10<sup>-2</sup> M hr<sup>-1</sup>).

(i) 0.76; (ii) 0.95; (iii) 1.52; (iv) 1.90; (v) 2.25; (vi) 2.75; (vii) 3.36; (viii) 4.00; and (ix) 5.00.

The results for the average scaling times for the sodium hydrogen carbonate concentration experiments for a 500 ppm calcium solution at 70°C are given in Table 3.16 and shown graphically in Figure 3.20. The details of replicate runs for the control, dummy and magnetic solution experiments are given in Appendix Tables A.18 to A.20.

**Table 3.16 Effect of sodium hydrogen carbonate concentration on the propensity to scale: Average scaling time (mins) at 70°C.**

NaHCO <sub>3</sub> conc. ( x 10 <sup>-2</sup> M hr <sup>-1</sup> )	Control	Dummy	Magnet
0.76	79.7	137.7	186.1
0.95	43.1	53.8	90.7
1.52	23.9	29.3	36.9
1.90	18.8	25.2	29.5
2.25	14.1	22.5	25.3
2.75	11.0	15.0	17.0
3.36	7.5	10.7	10.4
4.00	6.7	10.8	8.8
5.00	6.3	8.9	7.8

The scaling profiles of the propensity to scale measurements for the sodium hydrogen carbonate concentration of 0.95 x 10<sup>-2</sup> M hr<sup>-1</sup> are shown in Figure 3.21.

The iron content for both magnetic and dummy solutions was <0.1 ppm. The copper content for the dummy solution was greater than that for the magnetic samples in all the cases tested, averaging 0.6 and 0.4 ppm, respectively.

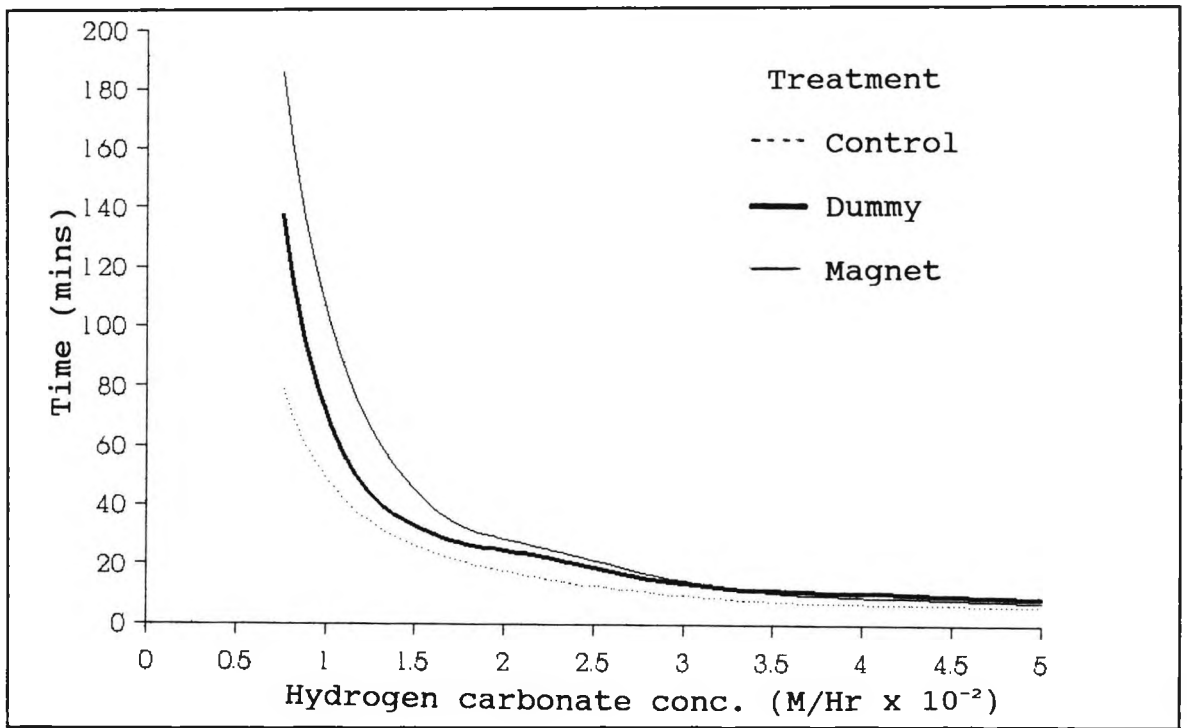


Figure 3.20 Effect of sodium hydrogen carbonate concentrations on the propensity to scale for a 500 ppm calcium solution: Average scaling time (mins) at 70°C.

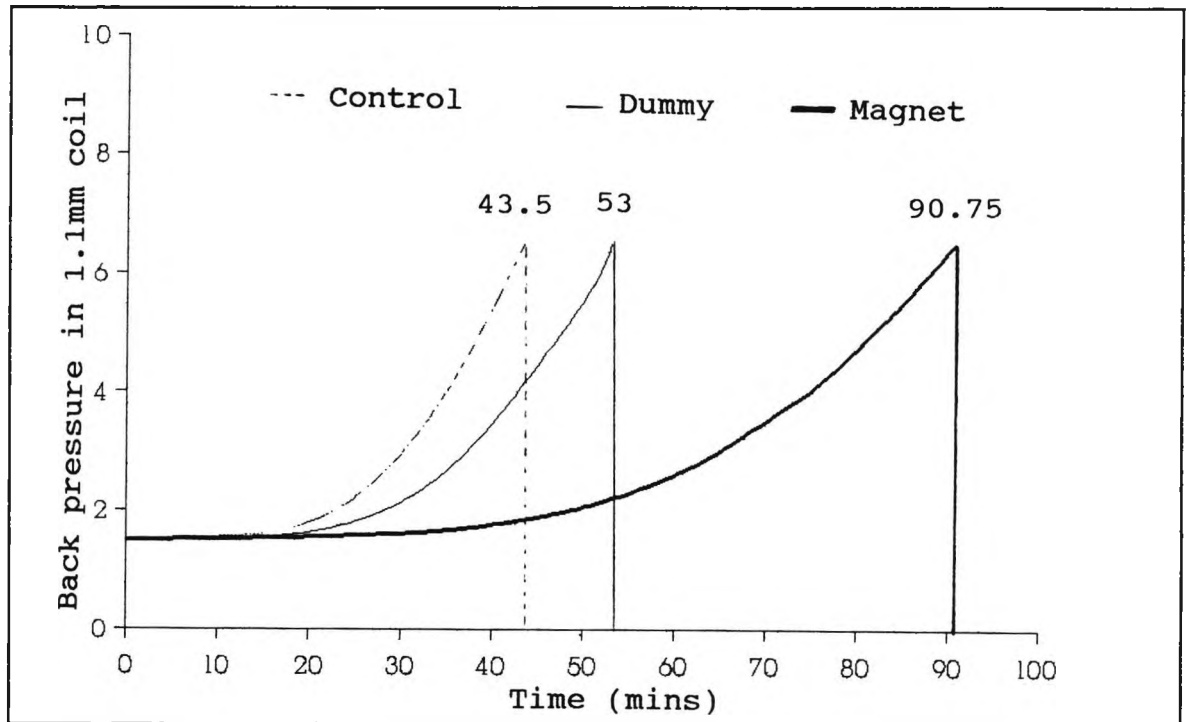


Figure 3.21 Scaling profiles for the propensity to scale measurements for the  $0.95 \times 10^{-2} \text{ M hr}^{-1} \text{ NaHCO}_3$  and 500 ppm calcium solution at 70°C.

**B. The effect of varying sodium hydrogen carbonate concentrations on a 500 ppm calcium solution at 80°C**

The nine sodium hydrogen carbonate concentrations investigated at 70°C were used again in the experiments at 80°C. The results for the average scaling times for the sodium hydrogen carbonate experiments with a 500 ppm calcium solution at 80°C are given in Table 3.17 and shown graphically in Figure 3.22. The details of replicate runs for the control, dummy and magnetic solution experiments are given in Appendix Tables A.21 to A.23.

**Table 3.17 Effect of sodium hydrogen carbonate concentration on the propensity to scale: Average scaling time (mins) at 80°C.**

NaHCO <sub>3</sub> conc. ( x 10 <sup>-2</sup> M hr <sup>-1</sup> )	Control	Dummy	Magnet
0.76	44.3	54.5	70.9
0.95	30.8	37.6	44.9
1.52	14.5	16.5	19.5
1.90	11.8	14.8	17.2
2.25	9.7	11.8	14.0
2.75	8.0	9.0	8.5
3.36	5.4	6.8	6.5
4.00	4.6	5.3	5.7
5.00	4.1	6.0	5.5

The consistency of the measurements is shown in Figure 3.23, for six repeat runs of propensity to scale measurements for the sodium hydrogen carbonate concentration of 0.76 x 10<sup>-2</sup> M hr<sup>-1</sup>.

The iron content for both magnetic and dummy solutions was <0.1 ppm. The copper content for the dummy solution was greater than that for the magnetic samples in all the cases tested, averaging 0.7 and 0.3 ppm, respectively.

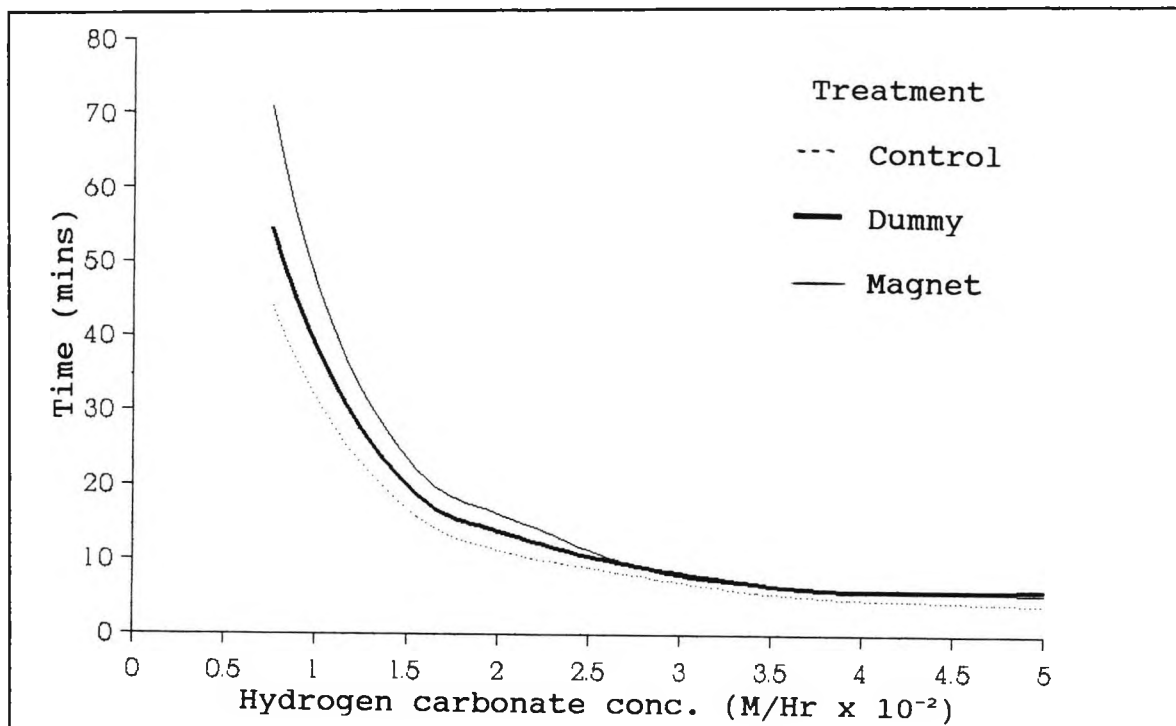


Figure 3.22 Effect of sodium hydrogen carbonate concentrations on the propensity to scale for a 500 ppm calcium solution: Average scaling time (mins) at 80°C.

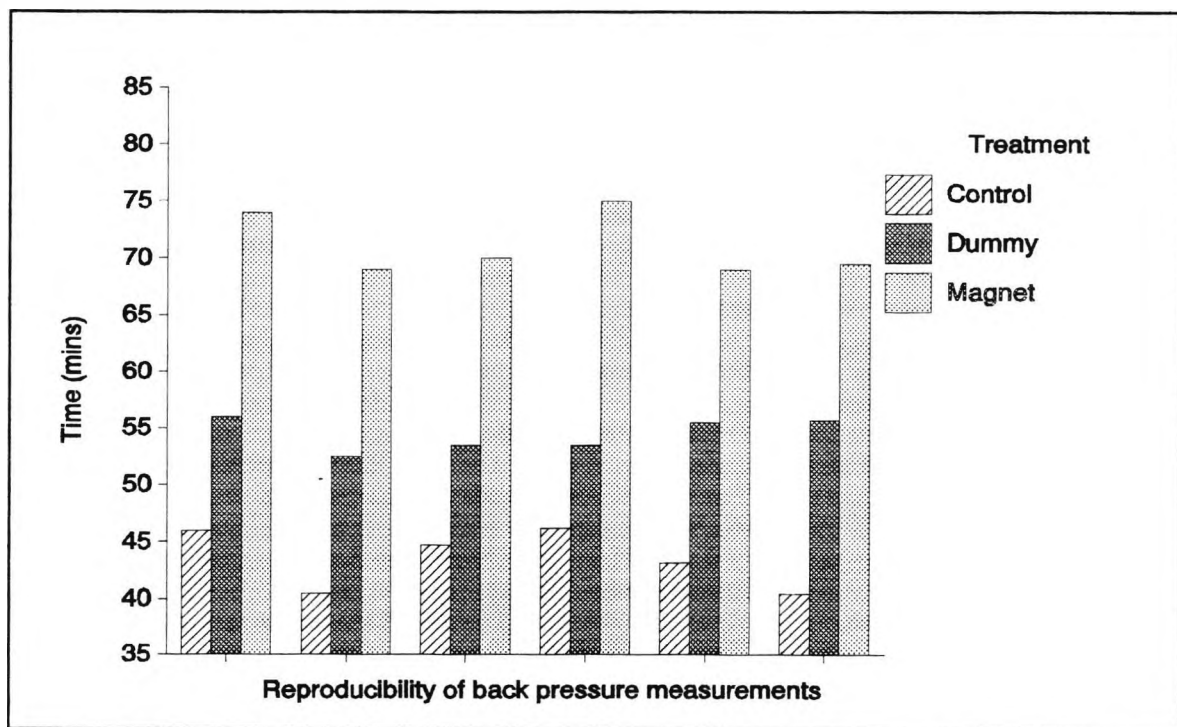


Figure 3.23 Reproducibility of propensity to scale measurements for the  $0.76 \times 10^{-2} \text{ M hr}^{-1} \text{ NaHCO}_3$  and 500 ppm calcium solution at 80°C.

**C. The effect of varying sodium hydrogen carbonate concentrations on a 500 ppm calcium solution at 90°C.**

Nine concentrations of sodium hydrogen carbonate were investigated in this section of the work. These are given below and are in units of  $\times 10^{-2}$  Molar:

(i) 1.52; (ii) 1.90; (iii) 3.04; (iv) 3.80; (v) 4.50; (vi) 5.50; (vii) 6.72; (viii) 8.00; and (ix) 10.00.

A higher flow rate into the P.M.A.C. microbore tube of  $0.5 \text{ lhr}^{-1}$  was used to give the same number of moles per hour of sodium hydrogen carbonate as that used in the experiments carried out at 70 and 80°C.

The results for the average scaling times for the sodium hydrogen carbonate concentration experiments with a 500 ppm calcium solution at 90°C are given in Table 3.18 and shown graphically in Figure 3.24.

**Table 3.18 Effect of sodium hydrogen carbonate concentration on the propensity to scale: Average scaling times (mins) at 90°C.**

NaHCO <sub>3</sub> conc. ( $\times 10^{-2}$ M hr <sup>-1</sup> )	Control	Dummy	Magnet
0.76	27.7	32.6	32.3
0.95	21.2	20.2	19.7
1.52	11.5	11.5	10.4
1.90	9.0	9.0	7.3
2.25	6.9	6.5	6.3
2.75	5.2	5.6	5.5
3.36	3.9	4.1	3.7
4.00	3.4	4.0	3.6
5.00	3.0	3.7	3.4

The details of replicate runs for the control, dummy and magnetic solution experiments are given in Appendix Tables A.24 to A.26.

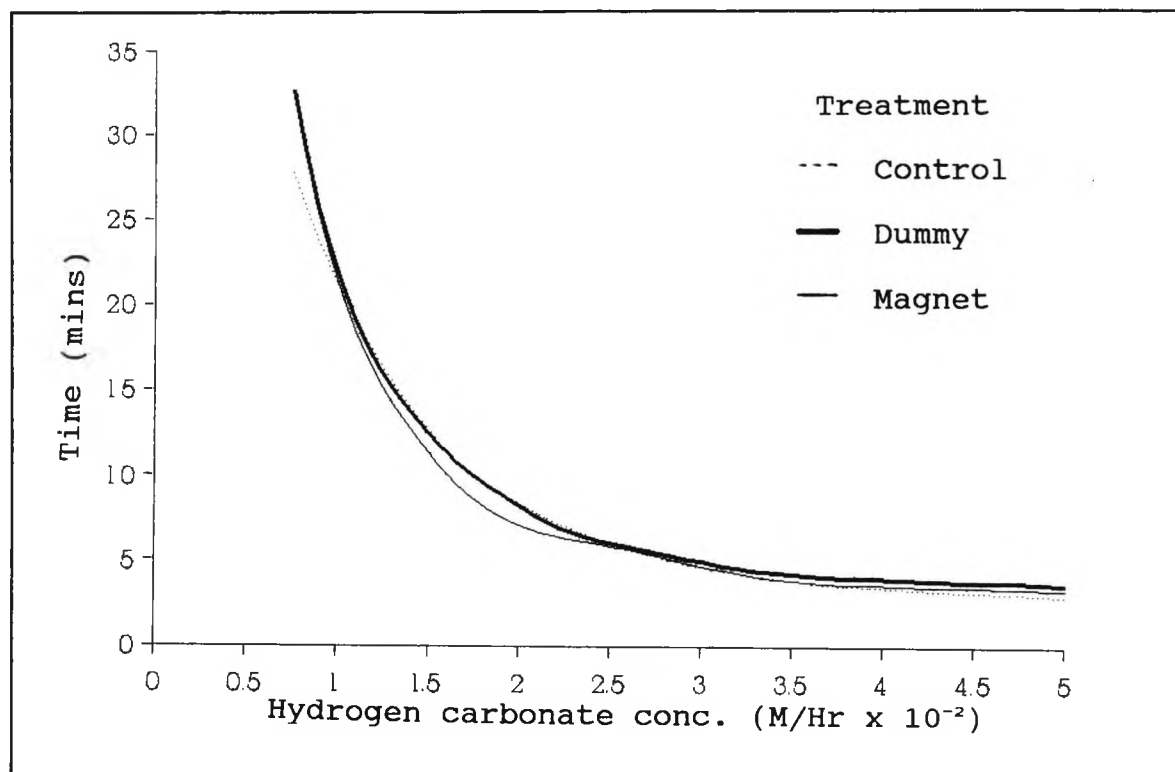


**Figure 3.24 Effect of sodium hydrogen carbonate concentrations on the propensity to scale for a 500 ppm calcium solution: Average scaling time (mins) at 90°C.**

The consistency of the measurements is shown in Figure 3.25, for six repeat runs of propensity to scale measurement for the sodium hydrogen carbonate concentration of  $2.75 \times 10^{-2} \text{ M hr}^{-1}$ , for the three calcium solution treatments. Figure 3.26 shows the scaling profiles for the three treatments in the experiments.

The iron content for both magnetic and dummy solutions was  $<0.1$  ppm. The copper content for the dummy solution was greater than that for the magnetic samples in all the cases tested, averaging 0.5 and 0.2 ppm, respectively.

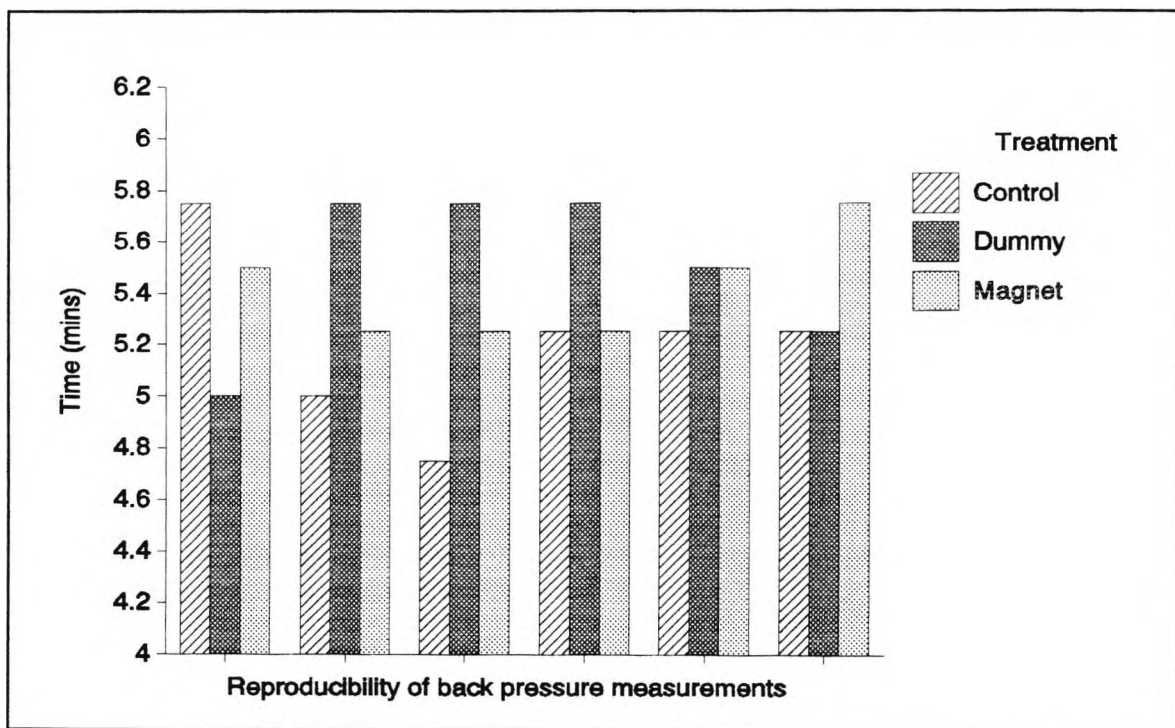


Figure 3.25 Reproducibility of propensity to scale measurements for the  $2.75 \times 10^{-2} \text{ M hr}^{-1} \text{ NaHCO}_3$  and 500 ppm calcium solutions at  $90^\circ\text{C}$ .

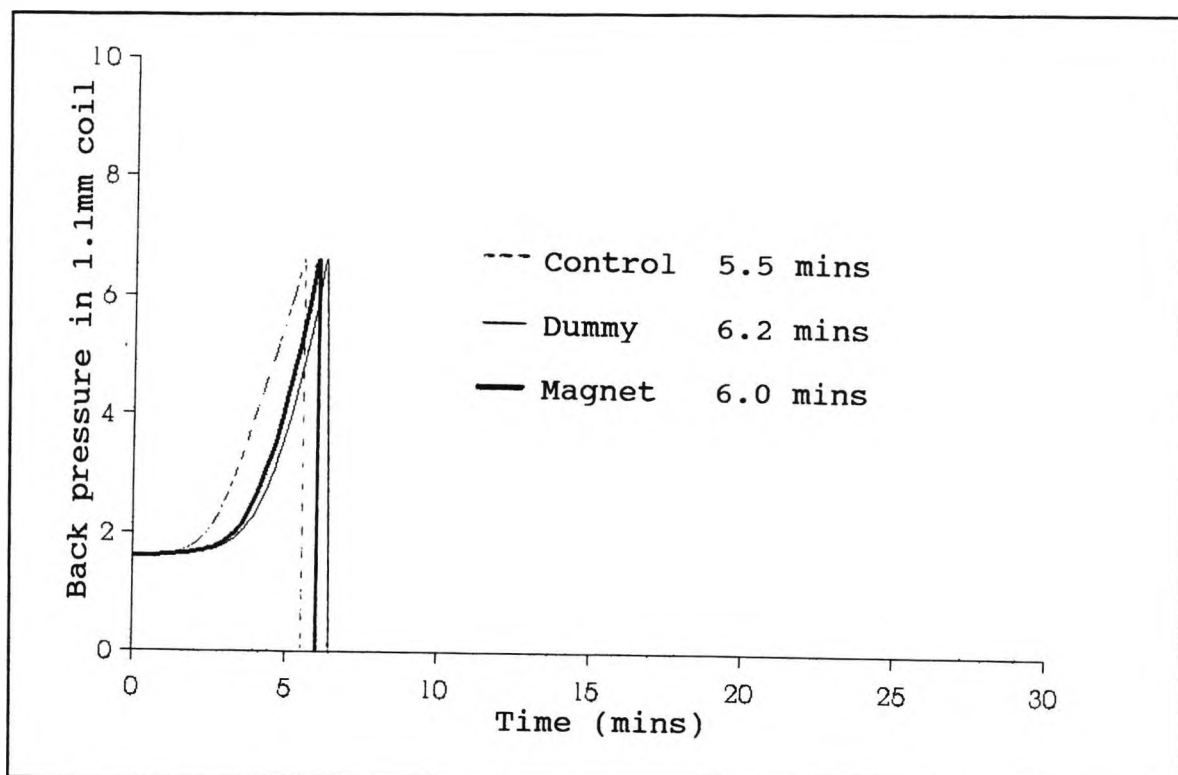


Figure 3.26 Scaling profiles for the propensity to scale measurements for the  $2.75 \times 10^{-2} \text{ M hr}^{-1} \text{ NaHCO}_3$  and 500 ppm calcium solutions at  $90^\circ\text{C}$ .

**D. The effect of varying sodium hydrogen carbonate concentrations on a 750 ppm calcium solution at 70°C.**

Eleven concentrations of sodium hydrogen carbonate were investigated in this section of the work. These are given below and are in units of  $\times 10^{-2}$  Molar:

(i) 1.87; (ii) 2.50; (iii) 3.75; (iv) 5.00; (v) 6.10; (vi) 7.50; (vii) 8.75; (viii) 10.00; (ix) 11.25; (x) 12.19; and (xi) 13.13.

Therefore, the concentrations in moles per hour of sodium hydrogen carbonate flowing into the P.M.A.C. microbore tube were (in molar units  $\times 10^{-2}$  M hr<sup>-1</sup>).

(i) 0.75; (ii) 1.00; (iii) 1.50; (iv) 2.00; (v) 2.44; (vi) 3.00; (vii) 3.50; (viii) 4.00; (ix) 4.50; (x) 4.88; and (xi) 5.25.

**Table 3.19 Effect of sodium hydrogen carbonate concentration on the propensity to scale: Average scaling times (mins) at 70°C.**

NaHCO <sub>3</sub> conc. ( $\times 10^{-2}$ M hr <sup>-1</sup> )	Control	Dummy	Magnet
0.75	55.0	71.3	125.5
1.00	30.1	41.4	63.4
1.50	18.0	30.6	39.7
2.00	14.1	22.3	29.9
2.44	10.4	17.4	21.5
3.00	8.3	14.0	15.5
3.50	7.6	10.6	12.6
4.00	6.3	9.1	10.5
4.50	6.1	8.3	9.3
4.88	6.0	7.9	8.4
5.25	6.1	7.9	7.9

The results for the average scaling times for the sodium hydrogen carbonate concentration experiments for a 750 ppm calcium solution at 70°C are given in Table 3.19 and are shown graphically in Figure 3.27. The details of replicate runs for the control, dummy and magnetic solution experiments are given in Appendix Tables A.27 to A.29.

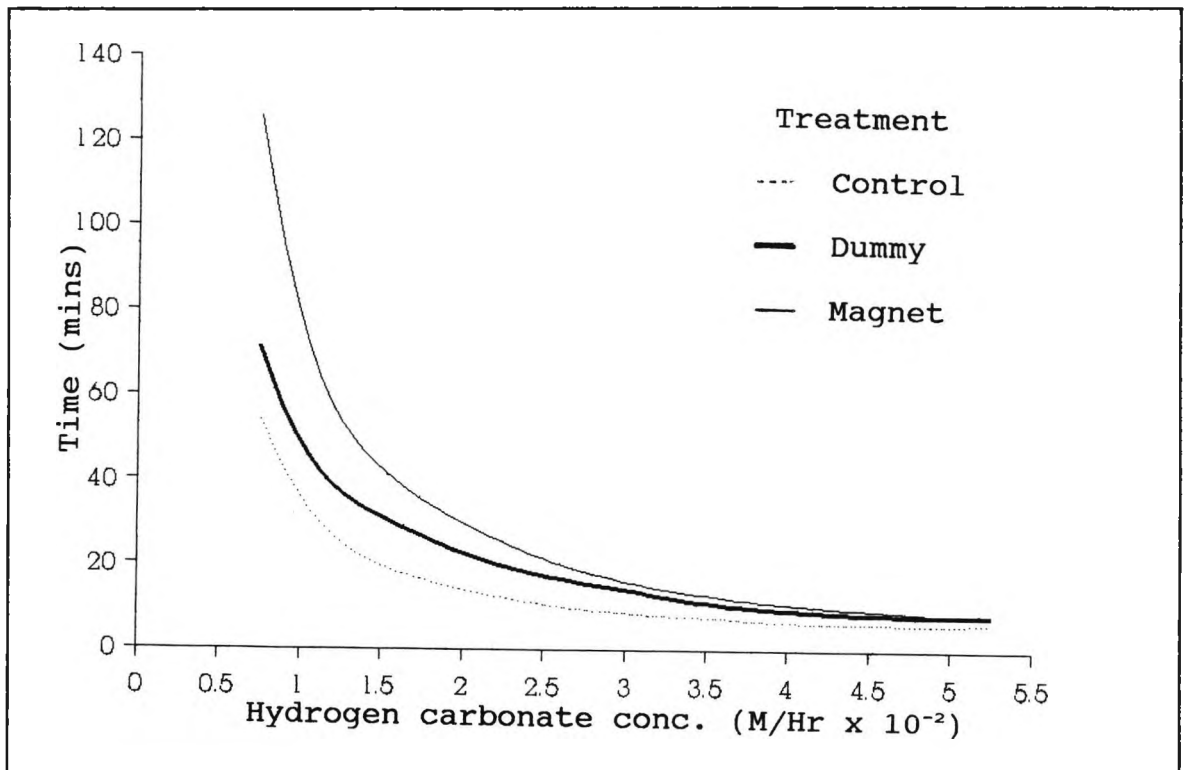


**Figure 3.27 Effect of sodium hydrogen carbonate concentrations on the propensity to scale for a 750 ppm calcium solution: Average scaling time (mins) at 70°C.**

The scaling profiles of the propensity to scale measurements for the sodium hydrogen carbonate concentration of  $0.75 \times 10^{-2} \text{ M hr}^{-1}$  are shown in Figure 3.28.

The iron content for both magnetic and dummy solutions was  $<0.1$  ppm. The copper content for the dummy solution was greater than that for the magnetic samples in all the cases tested, averaging 0.8 and 0.3 ppm, respectively.

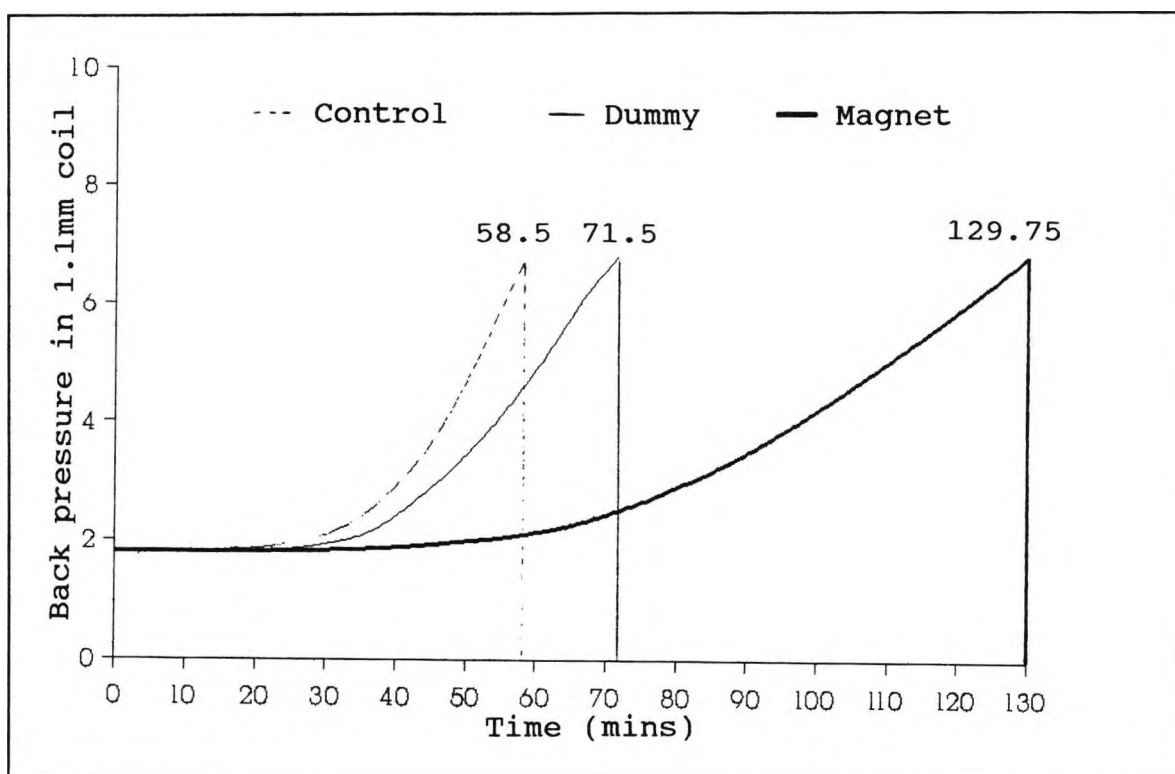


Figure 3.28 Scaling profiles for the propensity to scale measurements for the  $0.75 \times 10^{-2} \text{ M hr}^{-1} \text{ NaHCO}_3$ , and 750 ppm calcium solution at  $70^\circ\text{C}$ .

E. The effect of varying sodium hydrogen carbonate concentrations on a 750 ppm calcium solution at  $80^\circ\text{C}$

The eleven sodium hydrogen carbonate concentrations investigated at  $70^\circ\text{C}$  were used again in the experiments at  $80^\circ\text{C}$ . The results for the average scaling times for the sodium hydrogen carbonate concentration experiments for a 750 ppm calcium solution at  $80^\circ\text{C}$  are given in Table 3.20 and shown graphically in Figure 3.29. The details of replicate runs for the control, dummy and magnetic solutions are given in Appendix Tables A.30 to A.32.

The consistency of the measurements is shown in Figure 3.30, for seven repeat runs of propensity to scale measurement for the sodium hydrogen carbonate concentration of  $0.75 \times 10^{-2} \text{ M hr}^{-1}$ .

**Table 3.20 Effect of sodium hydrogen carbonate concentrations on the propensity to scale: Average scaling time (mins) at 80°C.**

NaHCO <sub>3</sub> conc. ( x 10 <sup>-2</sup> M hr <sup>-1</sup> )	Control	Dummy	Magnet
0.75	31.3	42.9	64.8
1.00	22.1	27.8	44.1
1.50	12.5	17.1	20.1
2.00	8.5	12.1	14.7
2.44	6.7	8.9	11.0
3.00	5.4	7.8	8.6
3.50	5.1	6.3	7.3
4.00	4.8	5.7	6.1
4.50	4.6	5.5	5.9
4.88	4.2	5.1	5.3
5.25	4.0	4.9	4.9

The iron content for both magnetic and dummy solutions was <0.1 ppm. The copper content for the dummy solution was greater than that for the magnetic samples in all the cases tested, averaging 0.5 and 0.2 ppm, respectively.

**F. The effect of varying sodium hydrogen carbonate concentrations on a 750 ppm calcium solution at 90°C**

Eleven concentrations of sodium hydrogen carbonate were investigated in this section of the work. These are given below and are in units x 10<sup>-2</sup> Molar:

(i) 1.50; (ii) 2.00; (iii) 3.00; (iv) 4.00; (v) 4.88; (vi) 6.00; (vii) 7.00; (viii) 8.00; (ix) 9.00; (x) 9.76; and (xi) 10.50.

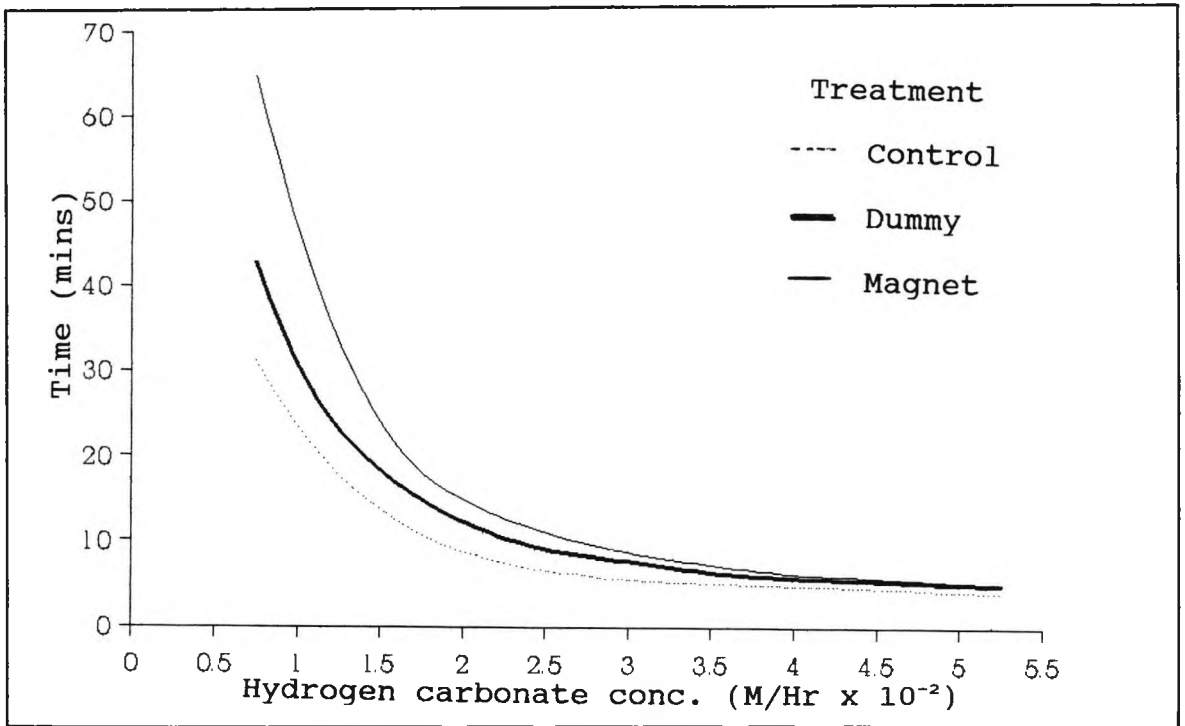


Figure 3.29 Effect of sodium hydrogen carbonate concentrations on the propensity to scale for a 750 ppm calcium solution: Average scaling time (mins) at 80°C.

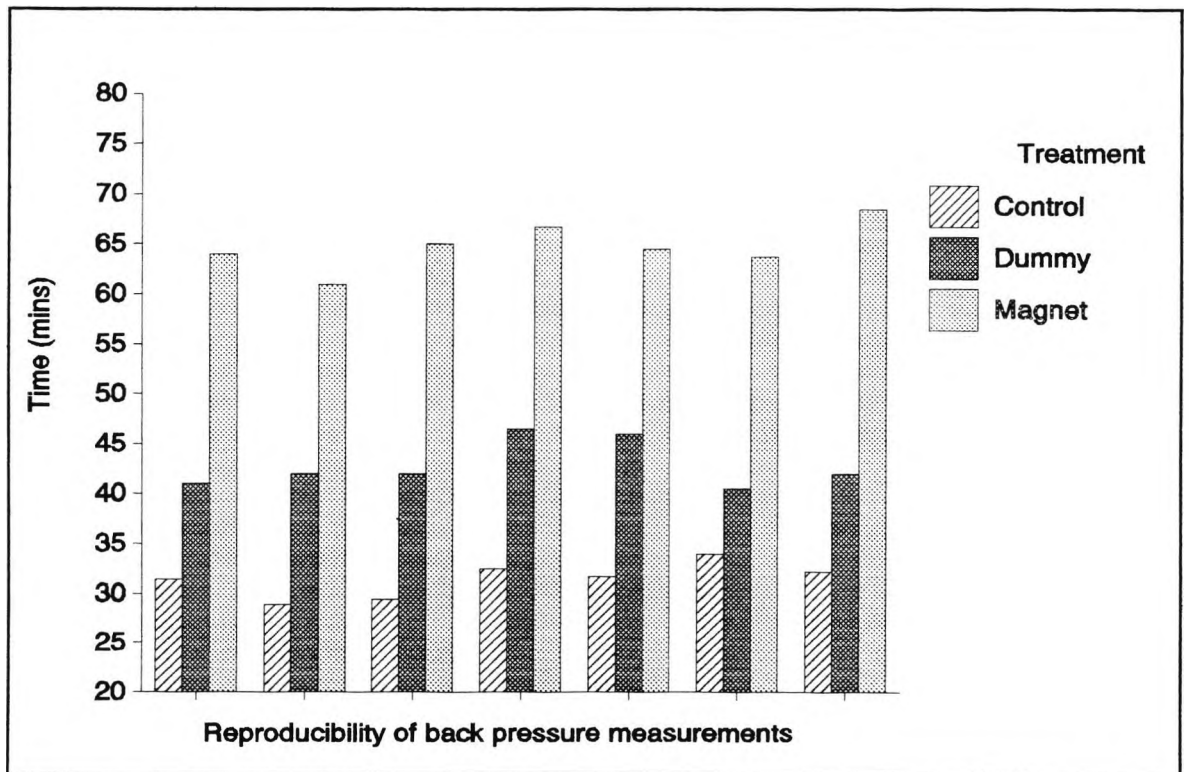


Figure 3.30 Reproducibility of propensity to scale measurements for the  $0.75 \times 10^{-2} \text{ M hr}^{-1} \text{ NaHCO}_3$  and 750 ppm calcium solutions at 80°C.

A higher flow rate into the P.M.A.C. microbore tube of  $0.5 \text{ l hr}^{-1}$  was used to give the same number of moles per hour of sodium hydrogen carbonate as that used in the experiments carried out at 70 and  $80^{\circ}\text{C}$ .

The results for the average scaling times for the sodium hydrogen carbonate concentration experiments for a 750 ppm calcium solution at  $90^{\circ}\text{C}$  are given in Table 3.21 and shown graphically in Figure 3.31. The details of replicate runs for the control, dummy and magnetic solution experiments are given in Appendix Tables A.33 to A.35.

**Table 3.21 Effect of sodium hydrogen carbonate concentration on the propensity to scale: Average scaling time (mins) at  $90^{\circ}\text{C}$ .**

NaHCO <sub>3</sub> conc. ( $\times 10^{-2} \text{ M hr}^{-1}$ )	Control	Dummy	Magnet
0.75	22.8	25.1	27.7
1.00	17.2	16.1	17.7
1.50	10.8	10.0	10.9
2.00	7.4	7.1	7.5
2.44	5.6	5.4	5.9
3.00	4.9	4.6	4.9
3.50	4.0	3.9	4.1
4.00	3.7	3.9	4.1
4.50	3.6	3.6	3.8
4.88	3.5	3.4	3.6
5.25	3.3	3.4	3.3

The consistency of the measurements is shown in Figure 3.32, for seven repeat runs of propensity to scale measurement for the sodium hydrogen carbonate concentration of  $1.5 \times 10^{-2} \text{ M hr}^{-1}$ , for the three calcium solution treatments. Figure 3.33 shows the

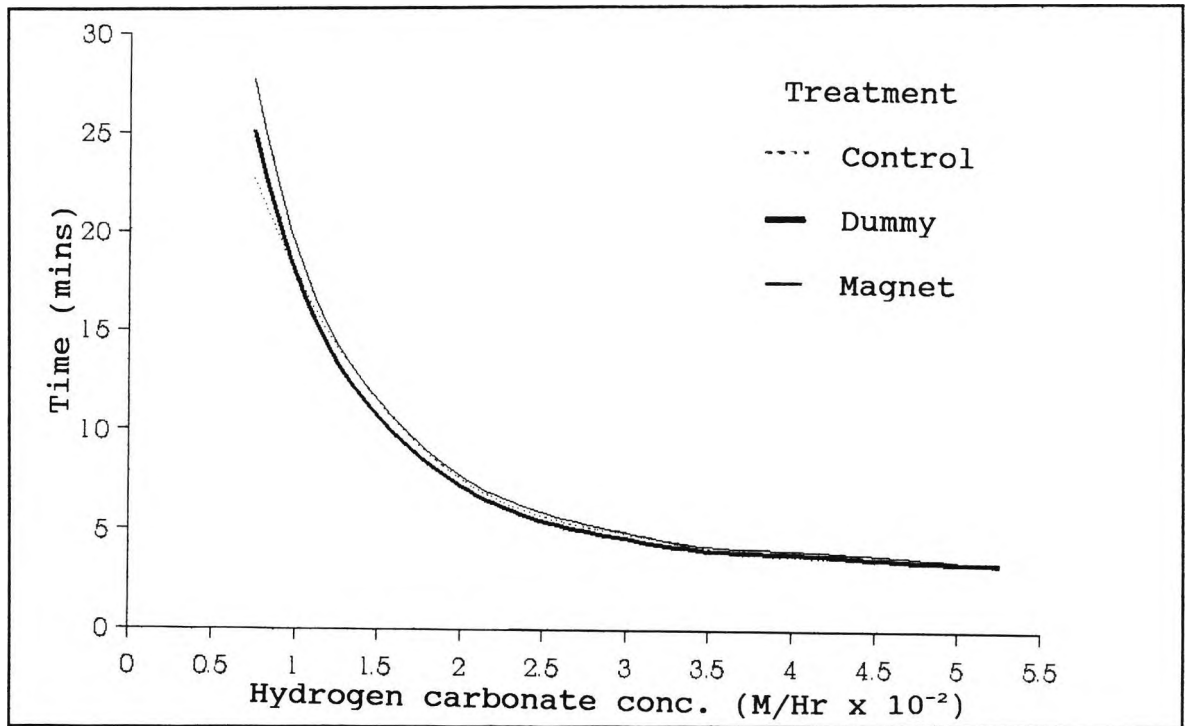


Figure 3.31 Effect of sodium hydrogen carbonate concentrations on the propensity to scale for a 750 ppm calcium solution: Average scaling time (mins) at 90°C.

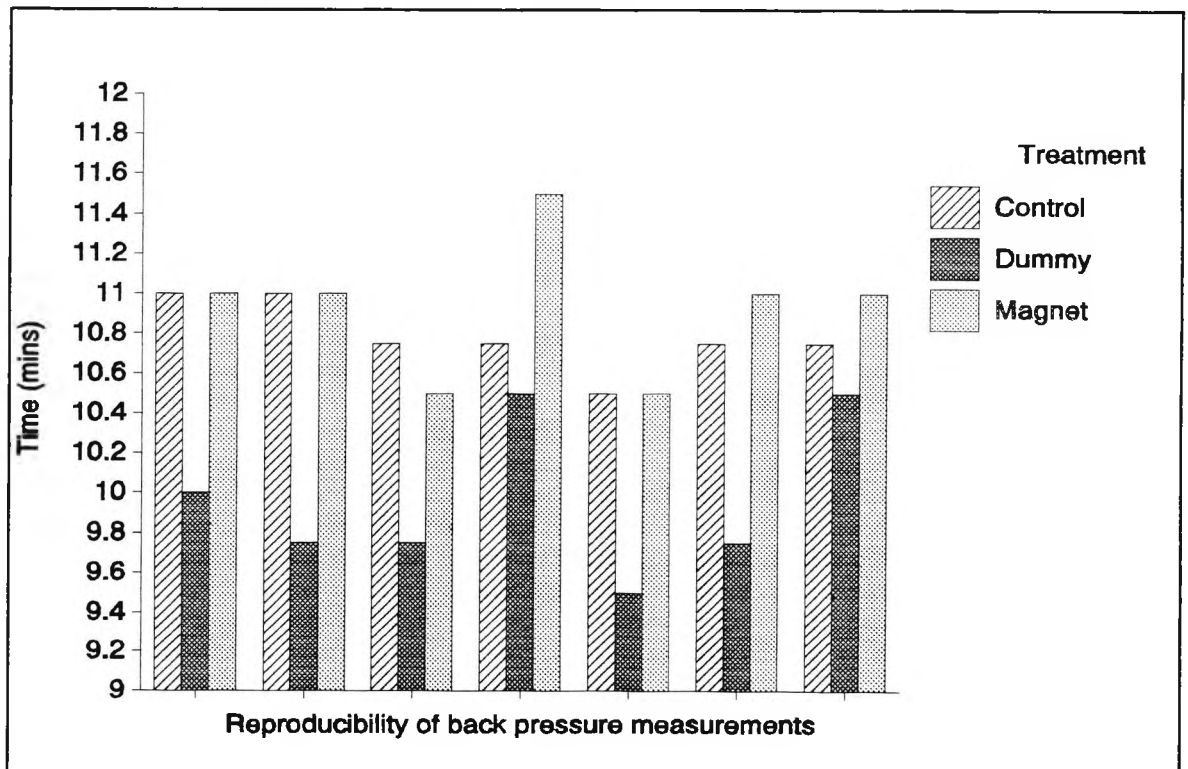


Figure 3.32 Reproducibility of propensity to scale measurements for the  $1.5 \times 10^{-2} \text{ M hr}^{-1} \text{ NaHCO}_3$  and 750 ppm calcium solutions at 90°C.

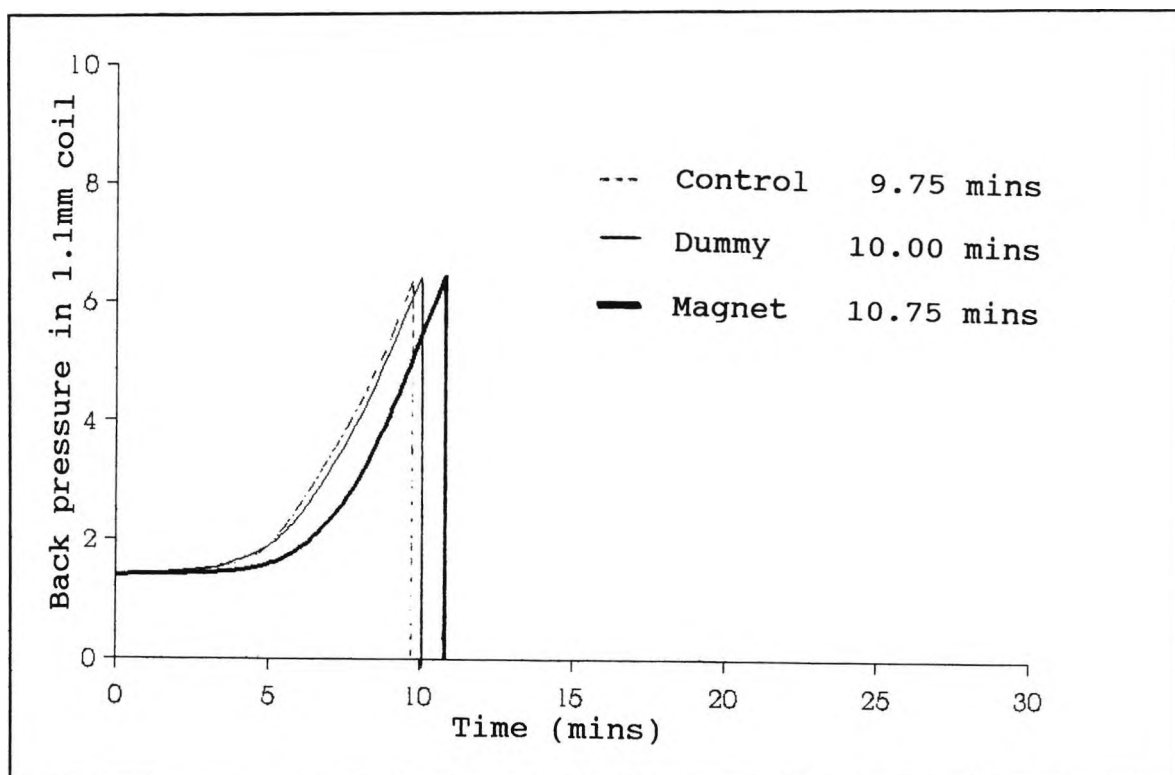


Figure 3.33 Scaling profiles for the propensity to scale measurements for the  $1.5 \times 10^{-2} \text{ M hr}^{-1} \text{ NaHCO}_3$ , and 750 ppm calcium solutions at  $90^\circ\text{C}$ .

scaling profiles for the three treatments in this experiment.

The iron content for both magnetic and dummy solutions was  $<0.1$  ppm. The copper content for the dummy solution was greater than that for the magnetic samples in all the cases tested, averaging 0.7 and 0.3 ppm, respectively.

All sodium hydrogen carbonate concentrations quoted here are given in units of  $\times 10^{-2} \text{ M hr}^{-1}$ .

The propensity to scale experiments carried out at  $70^\circ\text{C}$  for both calcium concentrations (500 and 750 ppm) showed generally that as the concentration of sodium hydrogen carbonate increased, the difference between the magnetic and both dummy and control treatments progressively decreased. The biggest differences

between the magnetic and the other treatments were observed when the calcium concentration was in excess of the sodium hydrogen carbonate concentration (i.e. between 0.76-3.36 for 500 ppm calcium and 0.75-4.88 for 750 ppm calcium). At the lowest sodium hydrogen carbonate concentrations tested the greatest time differences were observed, being 48 and 54 minutes respectively. At equimolar concentrations for each calcium concentration the difference between magnetic and dummy treatments was greatly reduced, with only marginal time differences being observed. When sodium hydrogen carbonate was in excess of calcium no time differences were observed.

The propensity to scale results at 80°C for all three treatments showed the same trends as those found at 70°C. The effect of increased temperature decreased the average scaling times for all three treatments over the range of sodium hydrogen carbonate concentrations investigated.

The data at 90°C for both calcium concentrations used showed that there was no significant difference between any of the three treatments for all the sodium hydrogen carbonate concentrations used, except for the lowest (0.76 for 500 ppm calcium and 0.75 for 750 ppm calcium). At both of these sodium hydrogen carbonate concentrations a noticeable time difference of 5 minutes was found between the magnetic and control treatments, but no difference was found between the magnetic and dummy treatments. The time differences between the magnetic and dummy treatments at lower temperatures were found to be significant and this illustrates that the cumulative effect of temperature and concentration at 90°C overrides the turbulence and magnetic effects, eliminating differences between the three treatments.

The individual effects of temperature and concentration on the precipitation rate are shown in Figures 3.34 and 3.35 respectively. Figure 3.34 shows the effect of increased temperature on magnetic treatment only for the calcium concentration of 500 ppm, when the sodium hydrogen carbonate

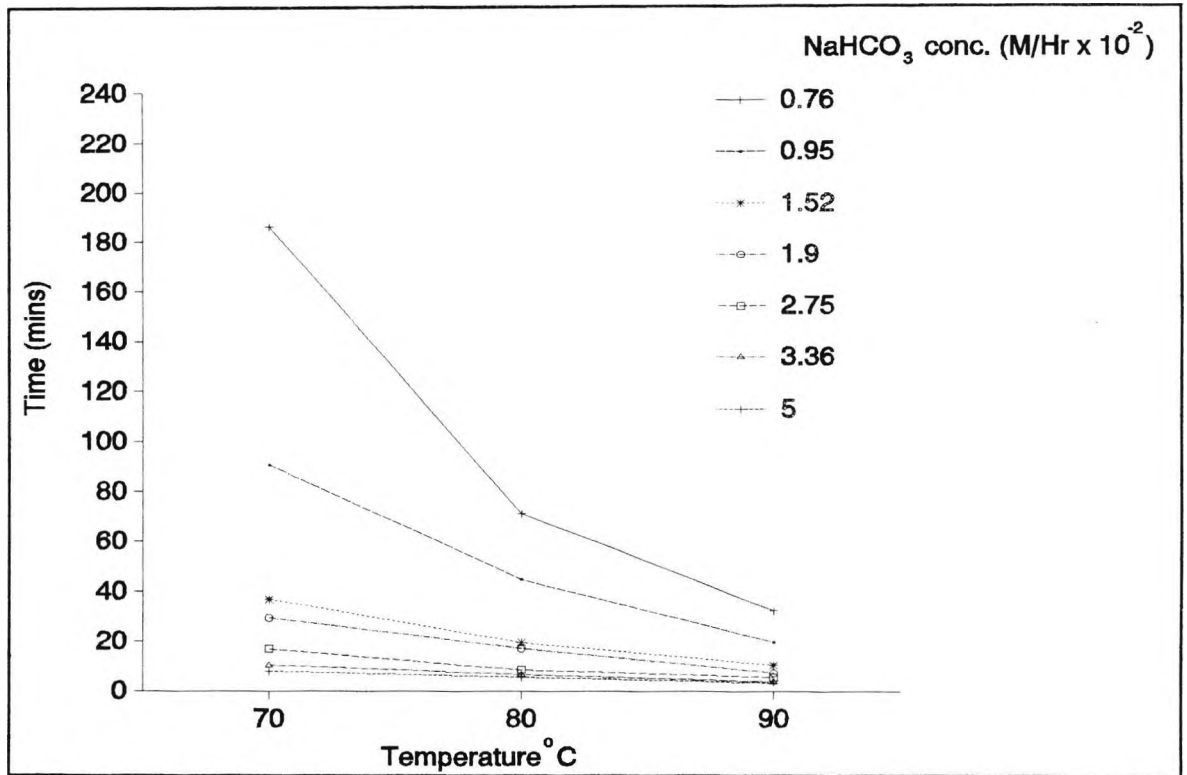


Figure 3.34 Effect of temperature on the propensity to scale measurements for magnetic treatment only.

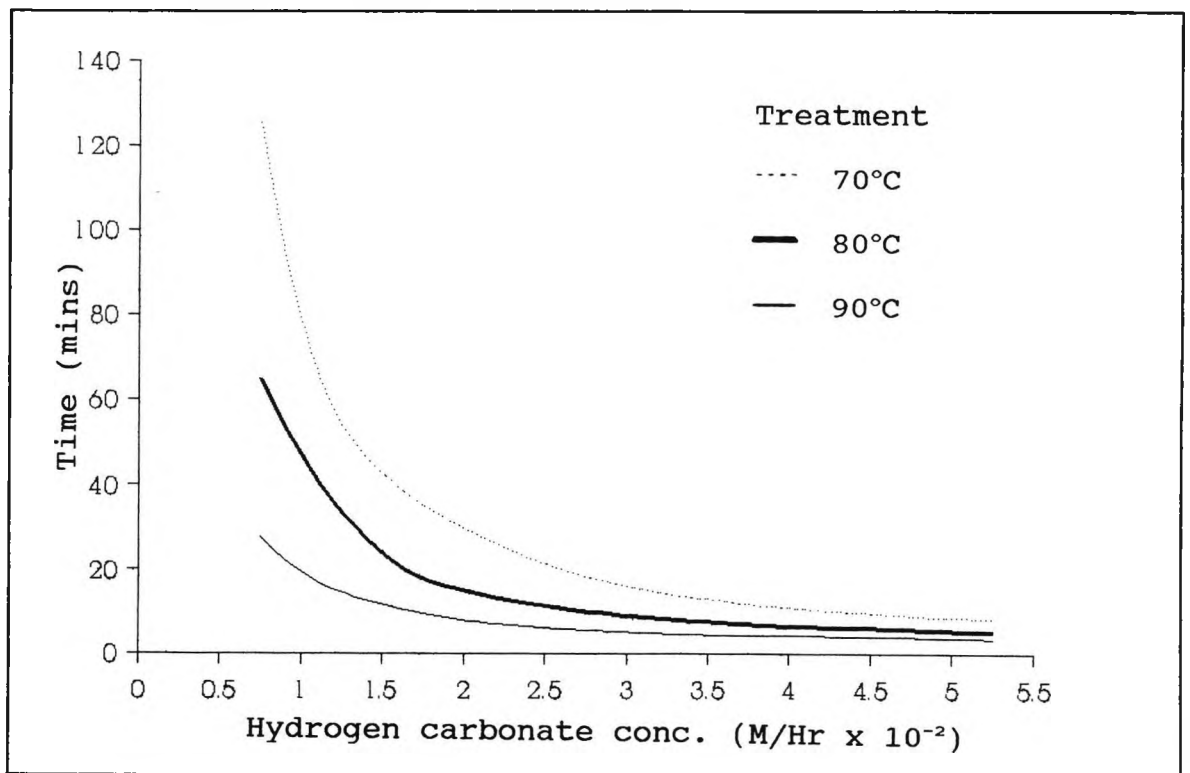


Figure 3.35 Effect of concentration on propensity to scale measurements for magnetic treatment only.

concentration was kept constant. The curves of the graph show that as the temperature increases from 70 to 90°C the magnetic effect is reduced for each increase in sodium hydrogen carbonate concentration. At 90°C, the difference between the higher sodium hydrogen carbonate concentrations is minimal.

Figure 3.35 shows the effect of sodium hydrogen carbonate concentration for a magnetically treated 750 ppm calcium solution, when the temperature is kept constant. The curves of this graph show that as the sodium hydrogen carbonate concentration increases the magnetic effect is progressively decreased. From these results it can be seen that both temperature and sodium hydrogen carbonate concentration have significant effects on (i) the rate of precipitation under normal conditions and (ii) the magnitude of the magnetic effect. It appears that temperature and sodium hydrogen carbonate have similar effects on (i) and (ii).

The results for the temperature and concentration experiments found in this work are consistent with those of Thomas [15], who found similar trends in the propensity to scale measurements between magnetic, dummy and control treatments. However, these experiments differed in that a permanent magnetic device was used, with the range of sodium hydrogen carbonate concentrations studied being smaller ( $0.24-1.90 \times 10^{-2} \text{ M hr}^{-1}$ ), and four temperatures being investigated (70, 75, 80 and 85°C).

In summary, the temperature and sodium hydrogen carbonate concentration experiments for each calcium concentration showed the following:

(1) When the concentration of sodium hydrogen carbonate is increased, the scaling times for all three treatments decreases. Equation 3.1 (pp 71) shows the equilibrium reaction for calcium carbonate, so that when more hydrogen carbonate ions are supplied to the left hand side of the equation, the equilibrium will move to the right to produce more calcium carbonate.

(2) As the temperature increases the average scaling time decreases, when the sodium hydrogen carbonate concentrations are compared for each temperature. The increased rate of reaction of hydrogen carbonate ions with calcium ions at higher temperatures moves the calcium carbonate equilibrium to the right (Equation 3.1), again increasing the production of calcium carbonate. At 90°C, there is no discernible difference in average scaling times for all three treatments (except at the lowest sodium hydrogen carbonate concentrations investigated). This is attributed to the cumulative effect of temperature and concentration which overrides the magnetic and turbulence effects.

(3) The magnetic effect is most pronounced at the lowest concentrations of sodium hydrogen carbonate and temperatures investigated. As the sodium hydrogen carbonate concentration and temperature are increased the magnetic effect is gradually diminished. Thus, at equimolar concentrations and at the highest temperature (90°C), the magnetic effect is minimal giving marginal time differences. The effects are due to either/or both temperature and concentration and the magnetic effect on the precipitation rate appears to reach some compromise at approximately equimolar conditions. Beyond this equimolar concentration the magnetic effect diminishes.

(4) A comparison of the sodium hydrogen carbonate curves for each calcium concentration and temperature investigated (Figures 3.20, 3.22, 3.24, 3.27, 3.29, and 3.31) shows an exponential relationship between the average scaling times for each treatment and the concentration of sodium hydrogen carbonate. This is most apparent in the magnetic treatment curves.

#### 3.7.5 The Effect of Temperature on the Propensity to Scale

The aim of this set of experiments was to investigate the effect of varying the temperature on the propensity to scale measurements, when mixing calcium solutions with fixed sodium hydrogen carbonate concentrations. Two different calcium

concentrations were used (500 and 750 ppm). The calcium solutions were circulated through the Hydromag DN15 unit with the power on (Magnet) and off (Dummy) and the results were compared with those from the control calcium solution. The effectiveness of magnetic treatment for both calcium solutions was assessed for a fixed sodium hydrogen carbonate concentration over a range of temperatures, 50, 55, 60, 70, 80 and 90°C, using propensity to scale measurements.

The two calcium concentrations used in this section were circulated for 16 hours through the Hydromag DN15 unit at a flow rate of 6 l/min (as determined in Section 3.7.3), using the circulating apparatus described in Section 3.6.2. After each circulation of the calcium solution the PVC tubing and the glass vessel were cleaned as described in Section 3.7.2. Measurements of the copper and iron contents for the magnet and dummy solutions were recorded for each experiment.

The sodium hydrogen carbonate concentrations used in this work were very concentrated to ascertain if magnetic fields reduce the propensity to scale at lower temperatures. The concentrations were  $3.5 \times 10^{-2} \text{ M hr}^{-1}$  for the 500 ppm calcium solution and  $3.25 \times 10^{-2} \text{ M hr}^{-1}$  for the 750 ppm calcium solution.

The flow rates into the P.M.A.C. microbore tube for this set of experiments were  $1.3 \text{ lhr}^{-1}$  for the calcium solutions and  $0.4 \text{ lhr}^{-1}$  for the sodium hydrogen carbonate solutions (except at 90°C, when  $0.5 \text{ lhr}^{-1}$  was used, as discussed in Section 3.7.4).

#### A. The effect of temperature for a 500 ppm calcium solution

The results for the average scaling times for the effect of temperature experiments for a 500 ppm calcium and  $3.5 \times 10^{-2} \text{ M hr}^{-1}$  sodium hydrogen carbonate solution are given in Table 3.22 and shown graphically in Figure 3.36. The details of replicate runs for the control, dummy and magnetic solution experiments are given in Appendix Tables A.36 to A.38.

Table 3.22 Effect of temperature on the propensity to scale for a 500 ppm calcium solution: Average scaling time (mins).

Temp°C	Control	Dummy	Magnet
50	28.0	62.0	82.6
55	17.6	32.9	43.1
60	11.9	19.6	23.2
70	6.4	8.8	10.3
80	4.4	5.0	6.3
90	3.6	3.9	3.9

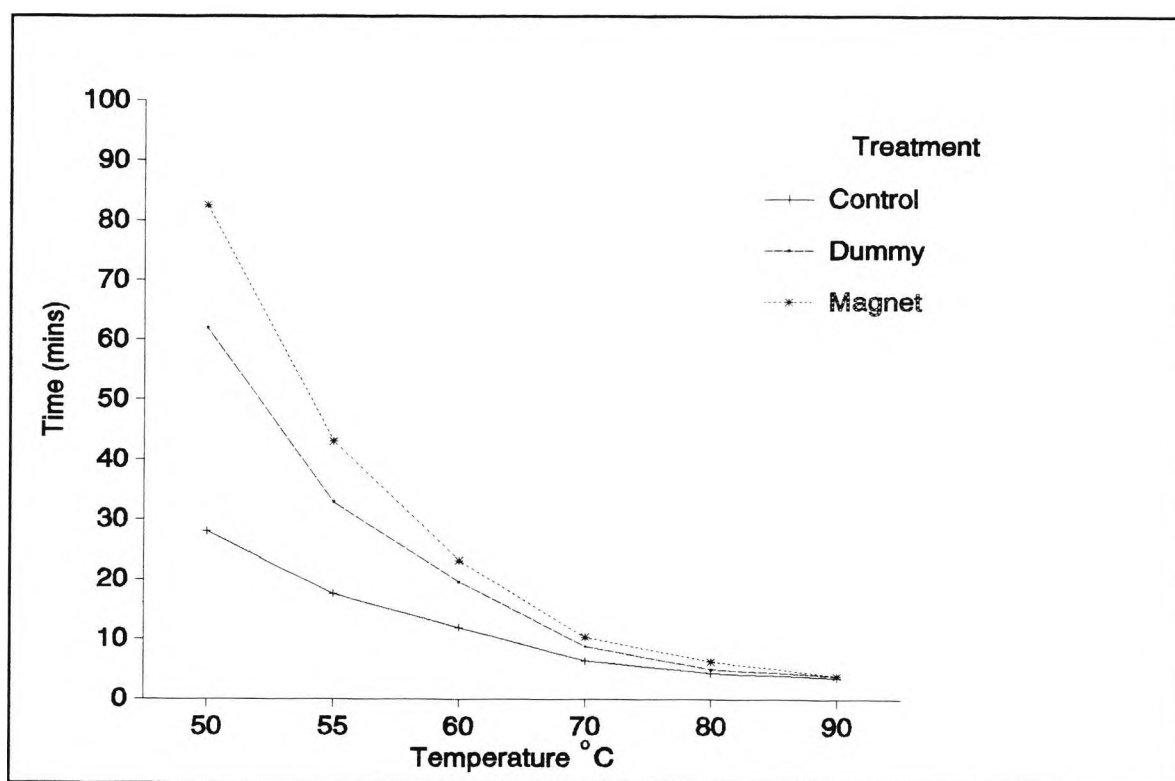


Figure 3.36 Effect of temperature on the propensity to scale for the 500 ppm calcium solution: Average scaling time (mins).

The consistency of the measurements is shown in Figure 3.37, for seven repeat runs of propensity to scale measurement at 50°C, for the three calcium solution treatments. Figure 3.38 shows the scaling profiles for the three treatments in these experiments.

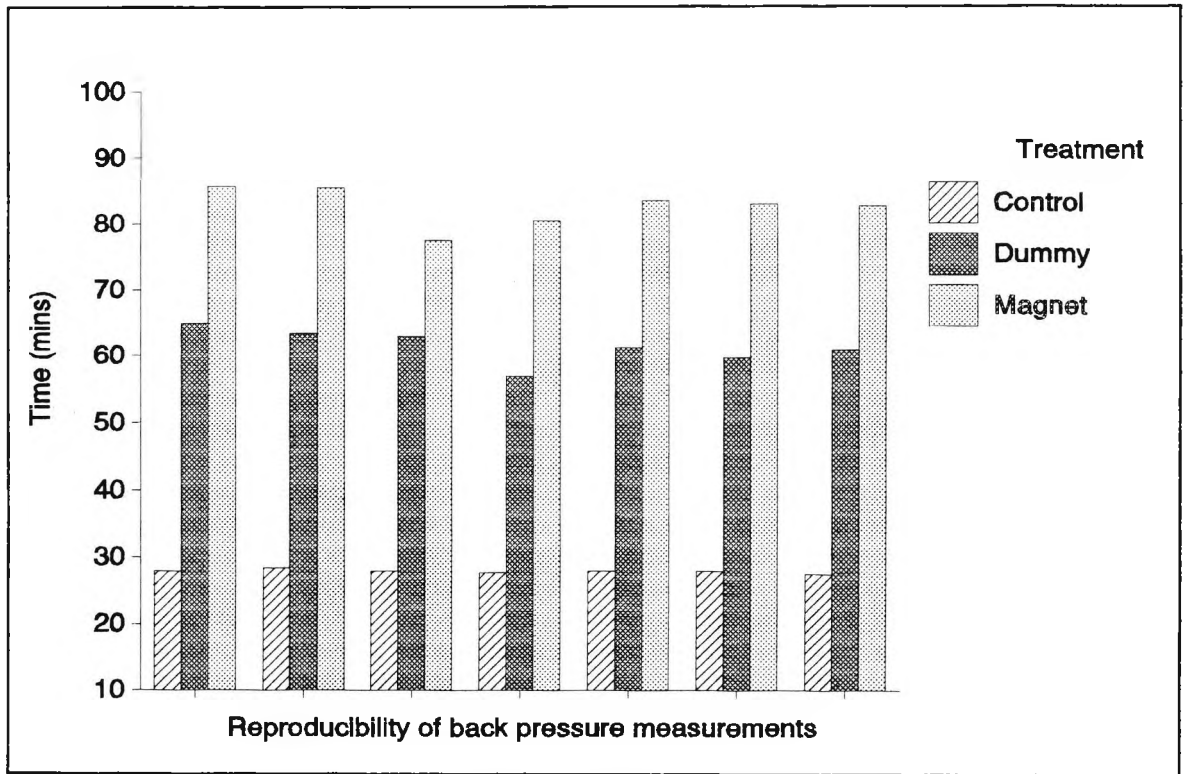


Figure 3.37 Reproducibility of propensity to scale measurements for the 500 ppm calcium solutions at 50°C.

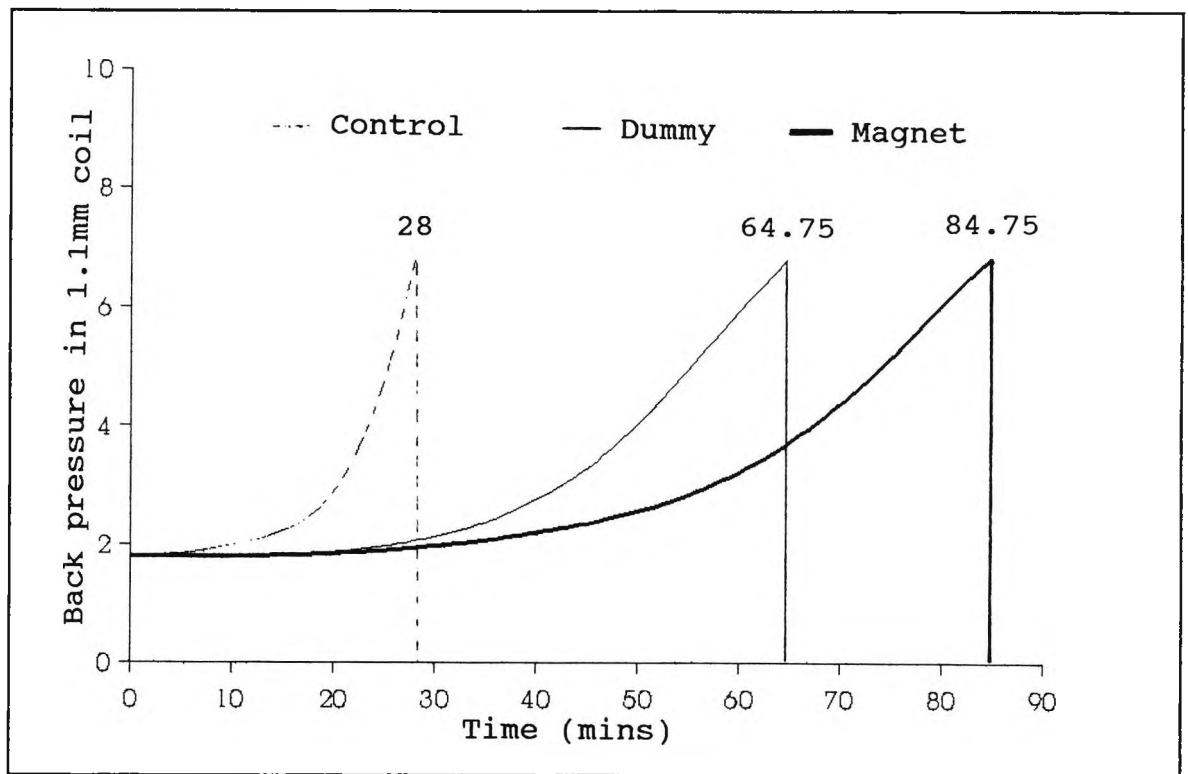


Figure 3.38 Scaling profiles for the propensity to scale measurements for the 500 ppm calcium solutions at 50°C.

The iron content for both magnetic and dummy solutions was <0.1 ppm. The copper content for the dummy solution was greater than that for the magnetic samples in all the cases tested, averaging 0.8 and 0.5 ppm, respectively.

**B. The effect of temperature for a 750 ppm calcium solution**

The results for the average scaling times for the temperature experiments for a 750 ppm calcium and  $3.25 \times 10^{-2}$  M hr<sup>-1</sup> sodium hydrogen carbonate solution are given in Table 3.23 and shown graphically in Figure 3.39. The details of replicate runs for the control, dummy and magnetic solution experiments are given in Appendix Tables A.39 to A.41.

**Table 3.23 Effect of temperature on the propensity to scale for a 750 ppm calcium solution: Average scaling time (mins).**

Temp°C	Control	Dummy	Magnet
50	30.6	48.9	66.0
55	20.8	27.9	40.9
60	11.6	19.0	24.4
70	6.9	8.4	9.6
80	4.7	5.4	5.9
90	3.5	4.1	4.1

The consistency of the measurements is shown in Figure 3.40, for seven repeat runs of propensity to scale measurement at 55°C, for the three calcium solution treatments. Figure 3.41 shows the scaling profiles for the three treatments in this experiment.

The iron content for both magnetic and dummy solutions was <0.1 ppm. The copper content for the dummy solution was greater than that for the magnetic samples in all the cases tested, averaging 0.7 and 0.4 ppm, respectively.

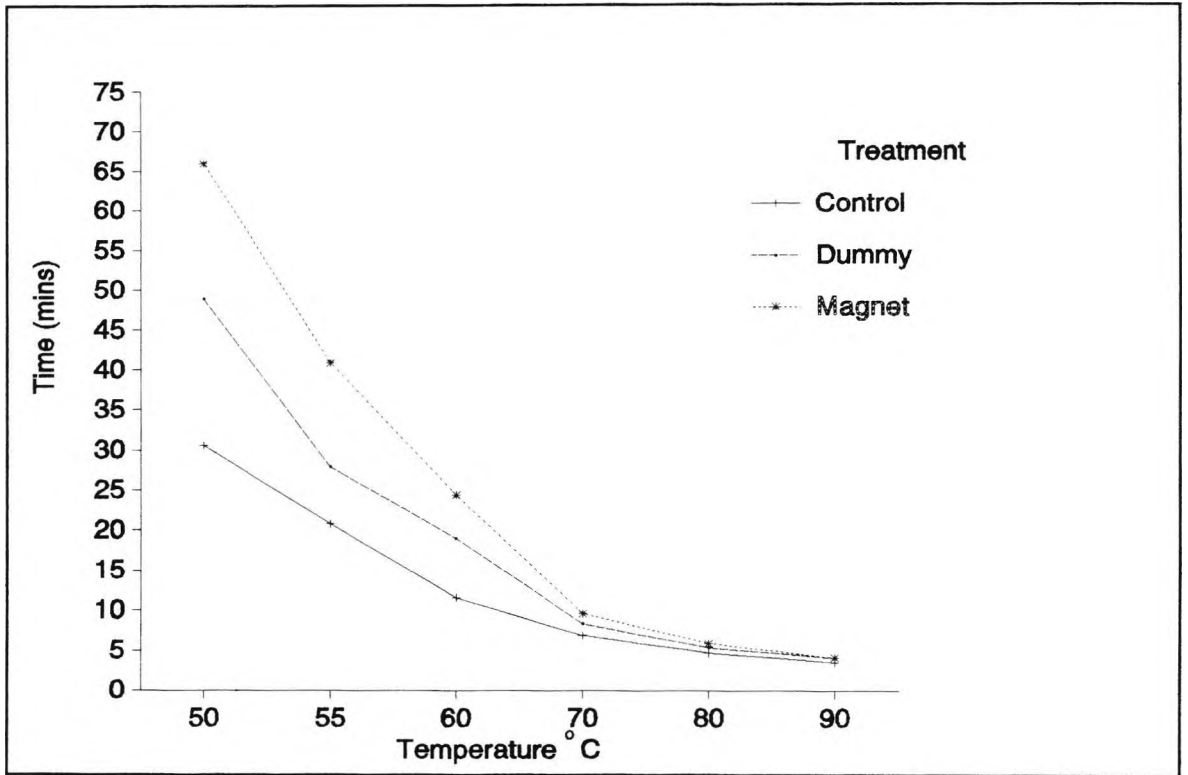


Figure 3.39 Effect of temperature on the propensity to scale for the 750 ppm calcium solution: Average scaling time (mins).

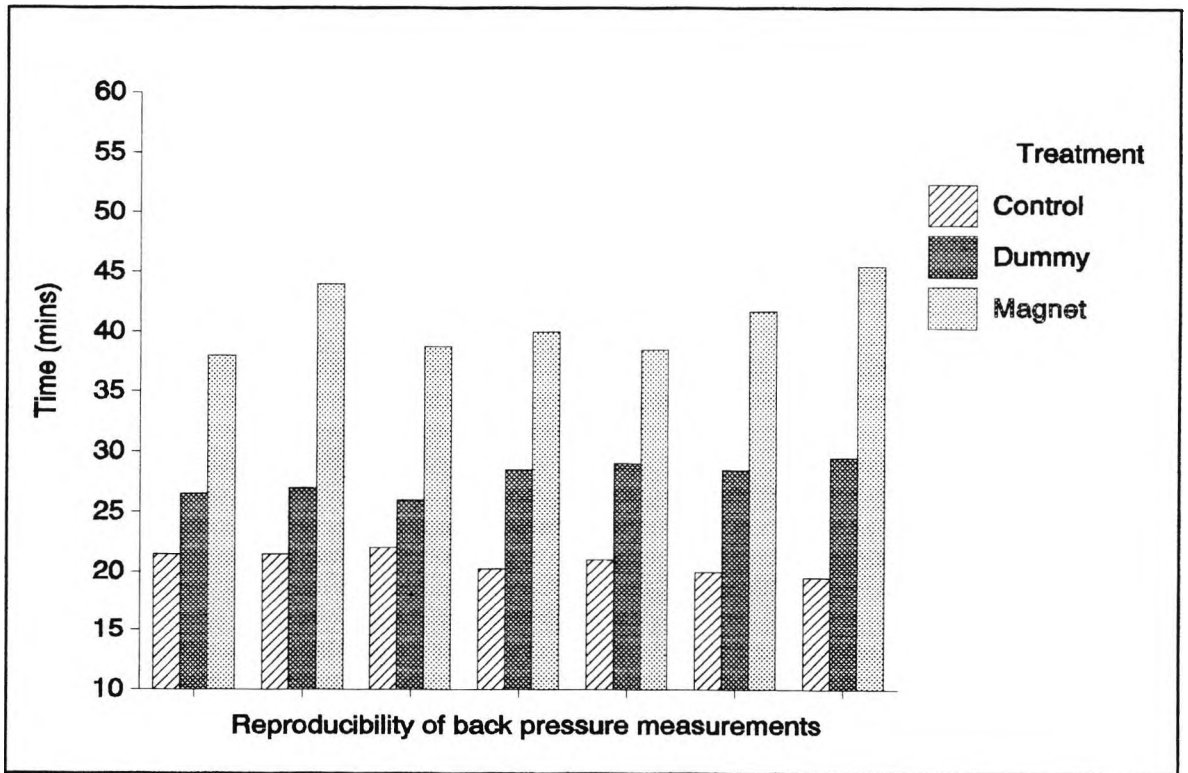
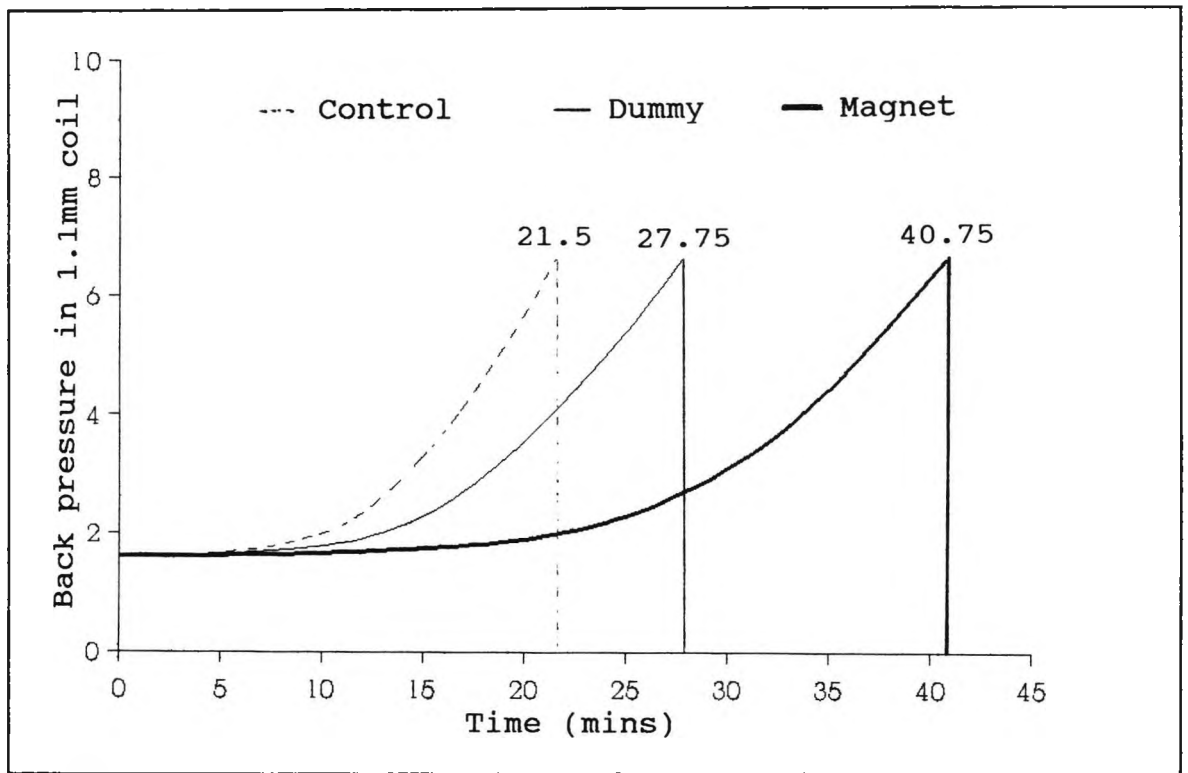


Figure 3.40 Reproducibility of propensity to scale measurements for the 750 ppm calcium solution at 55°C.



**Figure 3.41** Scaling profiles for the propensity to scale measurements for the 750 ppm calcium solution at 55°C.

The propensity to scale results for the effect of temperature experiments from 50 to 90°C for the calcium concentrations 500 and 750 ppm in Tables 3.22 and 3.23 and Figures 3.36 and 3.39 show that as the temperature was increased the difference between the magnetic and other treatments progressively decreased. Thus, the largest time differences between the magnetic and other treatments were observed at the lowest temperature used (50°C). At 50°C, the time differences between the magnetic and control treatments for the 500 ppm and 750 ppm calcium solutions were 54.6 minutes and 35.4 minutes, respectively. At 90°C, the difference between all three treatments was marginal, as seen in Section 3.7.4.

The calculation of the percentage reduction in the propensity to scale for the magnetic solutions, as compared to the control and dummy solutions for both 500 and 750 ppm calcium solutions tested over the range of temperatures, is shown in Table 3.24.

**Table 3.24 Percentage propensity reduction for each temperature.**

% Propensity reduction for each temperature °C						
Ca conc. ppm	50	55	60	70	80	90
500	74	58	30	23	29	0
750	56	63	47	17	10	0

The data show clearly that as the temperature is increased the percentage propensity reduction of each solution is reduced significantly until at 90°C, there is no difference between all three treatments. Also it demonstrates that the magnetic effect is significant at temperatures below 80°C for both calcium solutions and increases further as the temperature of the experiment is reduced. These results demonstrate that the magnetic effect of calcium solutions will give significant reductions in the propensity to scale even though the sodium hydrogen carbonate concentrations used were near to equimolar at all temperatures.

In summary the temperature experiments for both calcium concentrations showed the following:

(1) As the temperature increases the average scaling time decreases. The increased rate of reaction of hydrogen carbonate ions and calcium ions at higher temperatures moves the calcium carbonate equilibrium (Equation 3.1) to the right, increasing the production of calcium carbonate. At 90°C, there is no discernible difference in the average scaling times for all three treatments. This is attributed to the cumulative effect of temperature and concentration which overrides the magnetic and turbulence effects.

(2) The magnetic effect is most pronounced at the lowest temperatures used. As the temperature is increased the magnetic effect is gradually diminished, as shown in Table 3.24.

(3) A comparison of the temperature curves in Figures 3.36 and 3.39 for calcium solutions (500 and 750 ppm respectively) show an exponential relationship between the average scaling times for each treatment and the temperature of the reaction. This is most apparent in the magnetic treatment curves.

### 3.7.6 The Effect of Magnetic Treatment of Both Calcium and Sodium Hydrogen Carbonate Solutions on the Propensity to Scale

The aim of this experiment was to determine the effect of magnetically treating both the calcium and sodium hydrogen carbonate solutions on the propensity to scale. Both solutions were circulated for 16 hours through the Hydromag DN15 unit at the flow rates of 3, 6, and 9 l/min (as determined in Section 3.7.3), using the circulating apparatus described in Section 3.6.2. After each circulation the PVC tubing and the glass vessels were cleaned as described in Section 3.7.2.

The concentration of the calcium solution used in this investigation was 500 ppm which was mixed with a 0.025 M sodium hydrogen carbonate solution. Both solutions were circulated through the Hydromag unit with the power on only. Four different combinations of mixing the calcium and sodium hydrogen carbonate solutions were used for each flow rate, these being:

- (i) Magnet  $\text{Ca}^{2+}$  : Magnet  $\text{HCO}_3^-$  (Both)
- (ii) Magnet  $\text{Ca}^{2+}$  : Control  $\text{HCO}_3^-$  (Mag  $\text{Ca}^{2+}$ )
- (iii) Control  $\text{Ca}^{2+}$  : Magnet  $\text{HCO}_3^-$  (Mag  $\text{HCO}_3^-$ )
- (iv) Control  $\text{Ca}^{2+}$  : Control  $\text{HCO}_3^-$  (Control)

The terms for each combination are shown above. The magnetic calcium and magnetic sodium hydrogen carbonate solutions were both circulated through the Hydromag unit, whereas the control solutions had no flow treatment. The flow rates into the P.M.A.C. microbore tube at 70°C for this set of experiments were 1.3  $\text{hr}^{-1}$  for the calcium solutions and 0.4  $\text{hr}^{-1}$  for the sodium hydrogen carbonate solutions.

The results for the average scaling times for the flow rate experiments using each combination of mixing are given in Table 3.25 and shown graphically in Figure 3.42. The details of replicate runs for each flow rate experiment are given in Appendix Tables A.42 to A.44.

**Table 3.25 Effect of flow rate on the propensity to scale for each combination of mixing: Average scaling time (mins).**

Combination of mixing	Flow rate l/min		
	3	6	9
Control	32.3	32.7	30.8
Mag $\text{HCO}_3^-$	25.2	18.1	12.4
Mag $\text{Ca}^{2+}$	70.1	77.2	70.9
Both	44.1	47.9	33.5

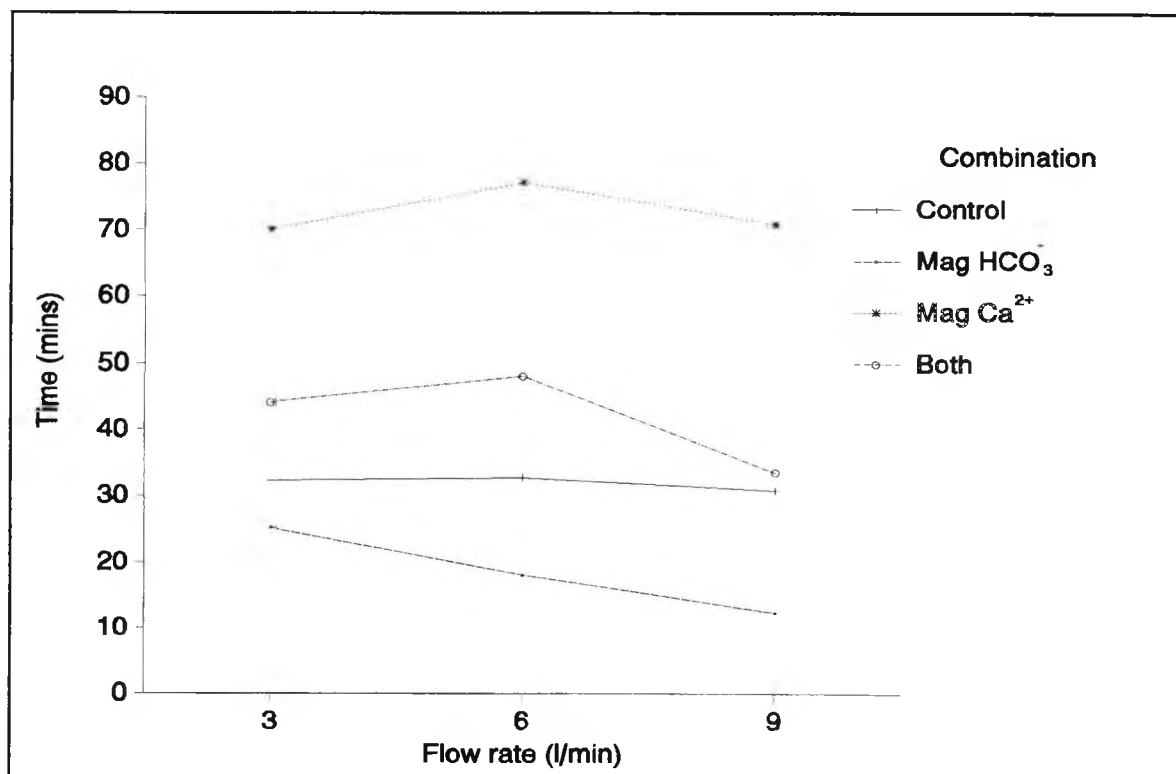


**Figure 3.42 Effect of flow rate on the propensity to scale for each combination of mixing: Average scaling time (mins).**

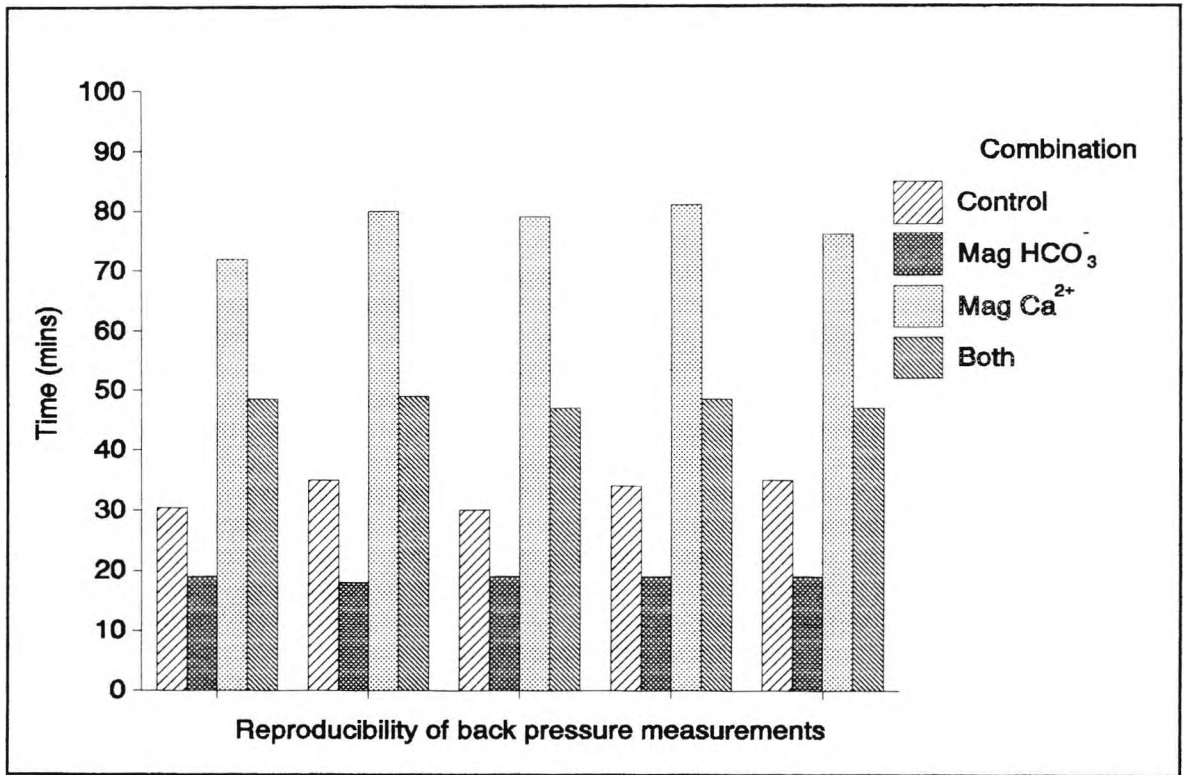


Figure 3.43 Reproducibility of propensity to scale measurements for each combination of mixing at 6 l/min.

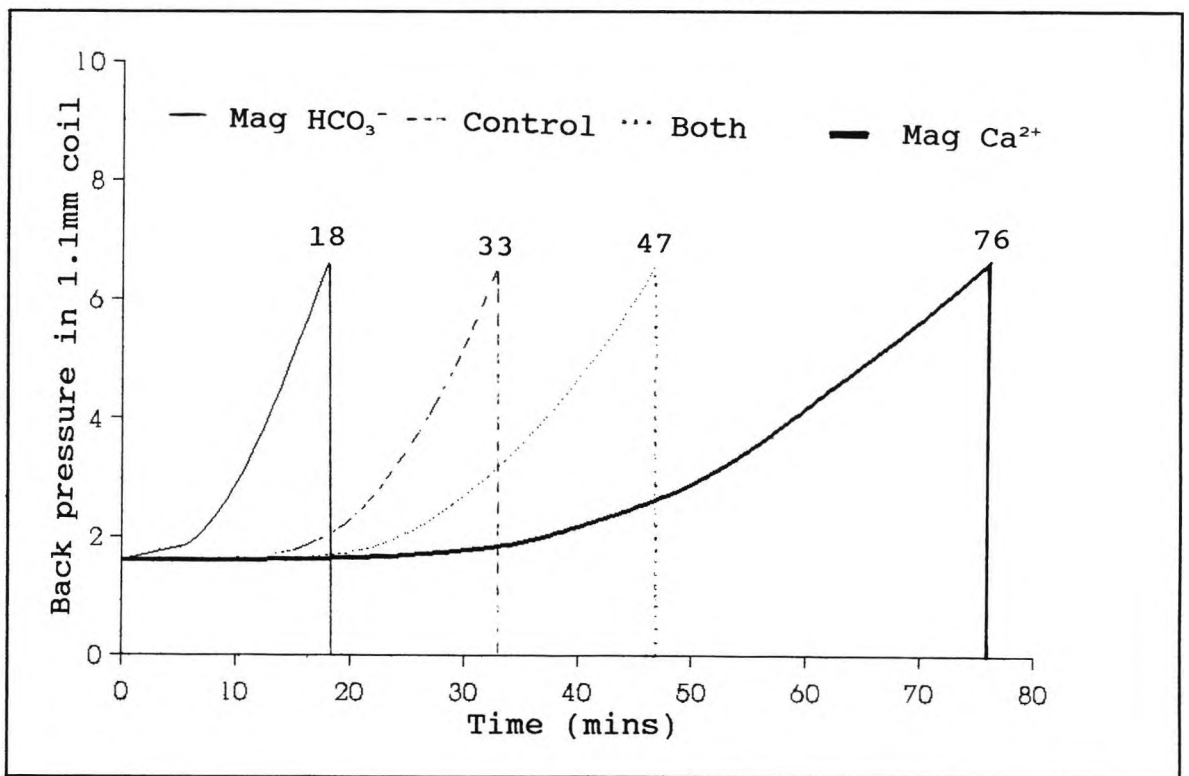


Figure 3.44 Scaling profiles in the propensity to scale measurements for each combination of mixing at 6 l/min.

The consistency of the measurements is shown in Figure 3.43, for five repeat runs of propensity to scale measurement for the flow rate experiment at 6 l/min, for the four combinations of mixing. Figure 3.44 shows the scaling profiles of the four treatments in this experiment.

The results of treating both solutions at different flow rates (Table 3.25) show firstly that magnetic treatment of the calcium solution only causes significant decreases in the rate of deposition of scale when compared to the other three treatments. The data in figure 3.14 show clearly that the most effective flow rate for circulating the calcium solution through the Hydromag DN15 unit is 6 l/min, in agreement with the data in Section 3.7.3. The propensity to scale measurements for the magnetic treatment of calcium solutions at 3 and 9 l/min are similar and have lower average scaling times than that for treating the calcium solution at 6 l/min.

Secondly the results show that the magnetic treatment of the sodium hydrogen carbonate solution only causes a significant increase in the rate of deposition of scale when compared to the other treatments. This increase in propensity to scale is greater as the flow rate of the sodium hydrogen carbonate solution is increased through the Hydromag DN15 unit. The average scaling time was reduced from 25 minutes at 3 l/min to 12 minutes at 9 l/min. This increase in propensity to scale is caused by the turbulence and aeration of the solution causing the hydrogen carbonate ions to decompose to carbonate ions in solution as shown in Equation 3.3.



The formation of carbonate ions in solution prior to mixing accelerates the rate of deposition of scale in the P.M.A.C. microbore tube and so lowers the average scaling times. In the experiments using control sodium hydrogen carbonate solutions this decomposition of hydrogen carbonate to carbonate is

controlled by the oven temperature forcing the reaction to the right. This causes the average scaling times of the control solutions to be higher than the control calcium: magnet sodium hydrogen carbonate solution.

Thirdly, when both solutions are magnetically treated and mixed in the P.M.A.C. microbore tube, the data shows the same trends found for treating each separately. The magnetic treatment of both causes a decrease in the rate of deposition of scale compared to the control at all the flow rates tested. The most effective flow rate for circulating both solutions is 6 l/min, as expected. At 3 l/min, mixing both magnetically treated solutions caused a small reduction in the average scaling times, as a result of the less effective magnetic treatment of the calcium solution and lower turbulence of the sodium hydrogen carbonate solution. However, at 9 l/min a significant increase in the propensity to scale was found, with the average scaling time being reduced to 33.5 minutes. This is mainly caused by the increased turbulence of the sodium hydrogen carbonate solution. Finally the control experiments for each experiment were found to be extremely accurate, displaying the reproducibility of the results obtained.

### 3.7.7 The Effect of Passing the Calcium Solutions and London Tap Water through the Magnetic field Once Only on the Propensity to Scale

The aim of this set of experiments was to determine the effect on the propensity to scale of passing a calcium solution or London tap water through the Hydromag DN15 unit once only. Two different calcium solutions were used (250 and 500 ppm) in this investigation. The calcium solutions were passed once through the unit with the power on (magnet) and off (dummy), comparing these with the control calcium solution. The calcium solutions were passed through the unit at a flow rate of 6 l/min (as determined in Section 3.7.3) using the circulating apparatus described in Section 3.6.2. The effectiveness of magnetic treatment for both

calcium solutions was assessed using a sodium hydrogen carbonate concentration of 0.05 M for the 250 ppm calcium solution and 0.03125 M for the 500 ppm calcium solution at 70°C, using the propensity to scale measurements.

The flow rates into the P.M.A.C. microbore tube for these experiments were 1.3 lhr<sup>-1</sup> for the calcium solutions and 0.4 lhr<sup>-1</sup> for the sodium hydrogen carbonate solution.

**A. The effect of passing a 250 ppm calcium solution once only through the magnetic field**

The results for this experiment are given in Table 3.26.

**Table 3.26 Effect of passing a 250 ppm calcium solution once through a magnetic field.**

Treatment	Time (mins)	S.D.	%	Range (mins)	No. of Runs
Control	24.2	1.39	5.76	22.3-26.0	14
Dummy	28.2	0.95	3.40	27.3-29.3	6
Magnet	32.5	1.00	3.10	31.5-34.8	9

The consistency of the measurements is shown in Figure 3.45, for six repeat runs of propensity to scale measurement for the three calcium solution treatments.

**B. The effect of passing a 500 ppm calcium solution once only through the magnetic field.**

The results for this experiment are given in Table 3.27. Figure 3.46 shows the scaling profiles for the three treatments in this experiment.

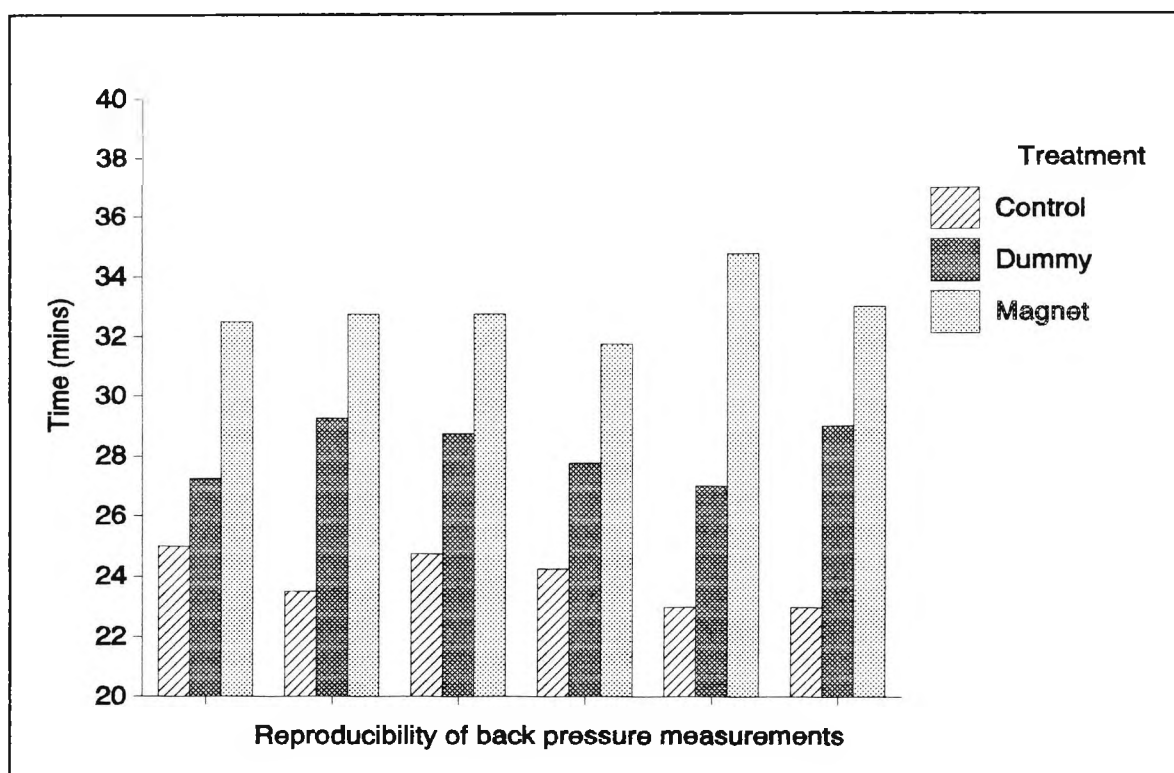


Figure 3.45 Reproducibility of propensity to scale measurements for the 250 ppm calcium solution passing once only through the magnetic field.

Table 3.27 Effect of passing a 500 ppm calcium solution once through the magnetic field.

Treatment	Time (mins)	S.D.	%	Range (mins)	No. of Runs
Control	32.8	1.22	3.74	30.8-34.0	8
Dummy	36.0	1.37	3.83	34.0-38.0	8
Magnet	38.0	1.09	2.90	36.0-39.0	7

The results for passing calcium solutions once only through the Hydromag magnetic field show a decrease in the rate of deposition of scale, when compared to the other treatments. The calculation of the percentage reduction in the propensity to scale for the magnetic solutions as compared to the other treatments for both calcium solutions tested are 18% for the 250 ppm calcium solution and 6% for the 500 ppm calcium solution. These differences are

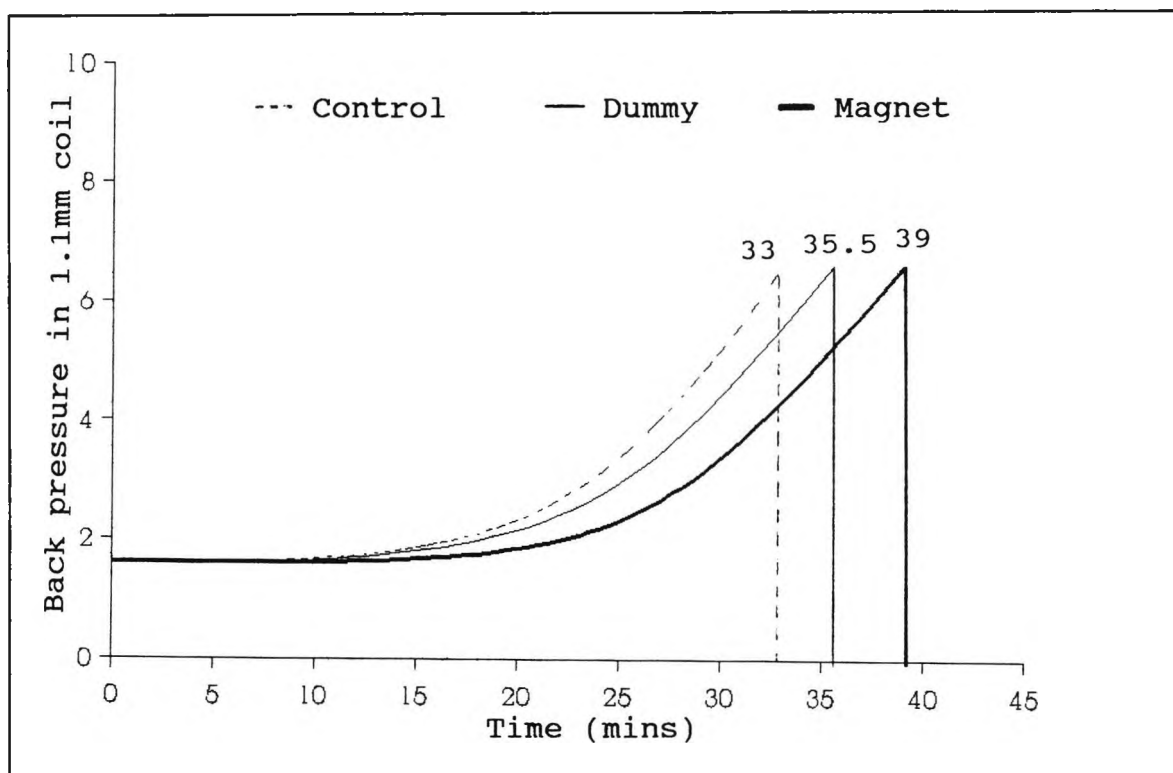


Figure 3.46 Scaling profiles for the propensity to scale measurements for the 500 ppm calcium solution once only through the magnetic field.

not as large as seen in the previous experiments where the calcium solutions were circulated for 16 hours through the magnetic field. These small differences can be increased by reductions in temperature and sodium hydrogen carbonate concentration. However, the results illustrate that the Hydromag DN15 unit does have an effect on the propensity to scale measurements even when the solutions are passed once only through the magnetic field.

### C. The effect of passing London tap water once only through the magnetic field.

London tap water was passed once only through the Hydromag DN15 unit at 6 l/min and then passed into the P.M.A.C. microbore tube at a rate of 1.8 lhr<sup>-1</sup> at a temperature of 90°C. Separate samples of London tap water were passed through the units with the power on or off. After four days of passing both samples of water

through the P.M.A.C. microbore tube neither sample had increased the back pressure measurement from its base line. These experiments were carried out in triplicate and illustrated that all the previous propensity to scale experiments greatly accelerate the scaling process when compared to normal tap water.

### 3.7.8 Summary of the Propensity to Scale Results

The results from the propensity to scale experiments show clearly that the magnetic treatment of both calcium and sodium hydrogen carbonate solutions prior to precipitation significantly affects the rate of deposition of calcium carbonate, in comparison to the rate of deposition from control experiments. The parameters which influence the observed magnetic phenomena, together with the main inferences from each experiment are summarised below:

1. The magnetic treatment of the calcium solution significantly reduces the rate of deposition of calcium carbonate when precipitated with sodium hydrogen carbonate solutions, as seen in the propensity to scale measurements. This significant reduction in the propensity to scale is seen when compared to treatments in zero field conditions.
2. The magnetic treatment of the calcium solution when passed through copper piping connected to the Hydromag DN15 unit significantly reduces the rate of deposition of calcium carbonate, when compared to the magnetically treated calcium solutions passed through polypropylene piping. The magnetic treatment of calcium solutions passing through polypropylene piping has no effect on the rate of deposition of calcium carbonate when compared to the control experiments.
3. The reduction in the rate of deposition of calcium carbonate, shown by the magnetic treatment or "magnetic effect", of the calcium solutions, was shown to be

significant over the range of flow rates tested, viz 3, 6, 9 and 12 l/min, as compared to measurements for zero field conditions. The magnitude of the reduction in the rate of deposition of calcium carbonate varied depending on the flow rate used. The flow rate of 6 l/min was shown to be the optimum flow rate for the Hydromag DN15 unit in the propensity to scale measurements.

4. The magnitude of the magnetic effect is also dependent on: (i) the concentration of sodium hydrogen carbonate used when mixing with the calcium solutions and (ii) the temperature at which the propensity to scale measurements are carried out. This work demonstrates that at both low temperature and sodium hydrogen carbonate concentrations over the ranges covered, magnetically treated calcium solutions gave significant reductions in the rate of deposition of calcium carbonate when compared to treatments in zero field conditions.
5. The magnetic treatment of sodium hydrogen carbonate solutions significantly increases the rate of deposition of calcium carbonate when precipitated with calcium solutions as seen in the propensity to scale measurements. This significant increase in propensity to scale is seen when compared to treatments in zero field conditions. The magnitude of the increase in the rate of deposition increased as the flow rate of magnetic treatment was increased.
6. The magnetic treatment of calcium solutions reduces the rate of deposition of calcium carbonate when it is passed through the Hydromag DN15 unit once only, when compared to treatments carried out in zero field conditions.
7. The propensity to scale measurements using calcium and hydrogen carbonate solutions show that the scaling process is greatly accelerated compared to London tap

water.

8. The magnetic effect of treating both solutions has been shown to be reproducible in all the propensity to scale experiments carried out.

### 3.8 HEAT EXCHANGER EXPERIMENTS

The heat exchanger experiments were carried out under laboratory and industrial conditions. These experiments were designed to determine whether the magnetic treatment of water would cause changes in the quantity of scale deposited under the same conditions. Optical microscopy and x-ray diffraction analysis were used to determine whether the magnetic treatment of water caused changes in the crystal size and morphology.

#### 3.8.1 Heat Exchanger Experiments Under Laboratory Conditions

The aim of this set of experiments was to determine whether the magnetic treatment of London tap water would affect the deposition of calcium carbonate scale under laboratory conditions. The experiments were carried out using the equipment shown in Figure 3.7 for periods of 3 and 7 days at 90°C, using the experimental technique discussed in Section 3.6.3. The results for the 3 day experiments are given in Table 3.28 and those for the 7 day experiments are given in Table 3.29.

**Table 3.28 Quantity of scale deposited after 3 days at 90°C.**

Magnetic treatment (g)	Dummy treatment (g)	% Weight difference
1.465	2.995	104
1.100	2.735	149
0.604	2.265	275
0.854	1.562	83
0.454	1.822	301

Table 3.29 Quantity of scale deposited after 7 days at 90°C.

Magnetic treatment (g)	Dummy treatment (g)	% Weight difference
1.388	4.193	202
1.354	3.707	174
3.125	9.162	193
2.676	4.733	77
1.539	7.129	363

The results indicate a significant difference in the weight of scale deposited between the magnetic and dummy treatments at 90°C. The results show a large discrepancy in the % weight difference of scale deposited, which is caused by the unpredictability of the crystallisation process, onto the beaker surface. The nature of the scale formed was different for the two treatments. The scale formed from Magnetically Treated Water (MTW), was like a very soft powder, which was easily removed from the beaker surface and formed a sludge on the bottom of the beaker. The scale formed from the non-Magnetically Treated Water (non-MTW) or dummy was hard and crystalline in nature; it was spread over the whole surface of the beaker and was difficult to remove.

Samples of the dried scale were examined by optical microscopy, Figures 3.47 and 3.48 show the optical micrographs of the scale from MTW and non-MTW, respectively. The optical micrographs of the scales show significant differences in their crystal and aggregate sizes. The crystals from MTW form a scale which consists of small individual crystals. These small crystals cause the scale to be a soft powder which is easily removed. The crystals from non-MTW form a scale which consists of small crystals clumped together to form larger aggregates. These clumps of crystals cause the scale to be hard and crystalline and very difficult to remove. X-ray diffraction powder patterns for each of the scales formed are shown in Figure 3.49.

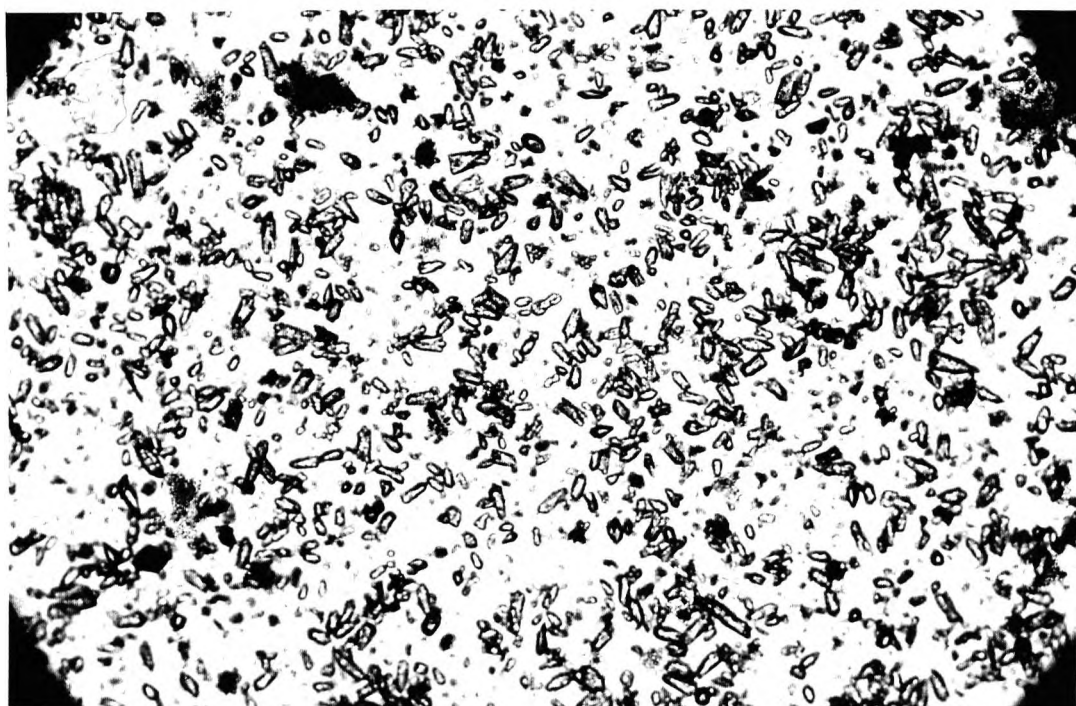
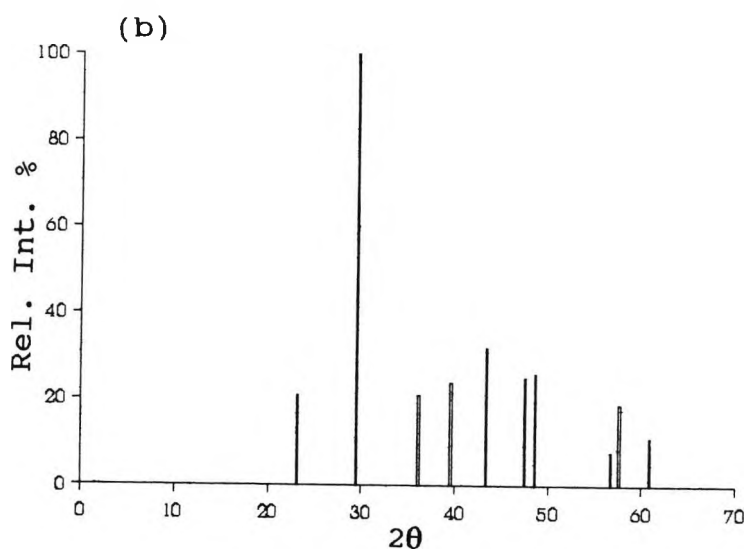
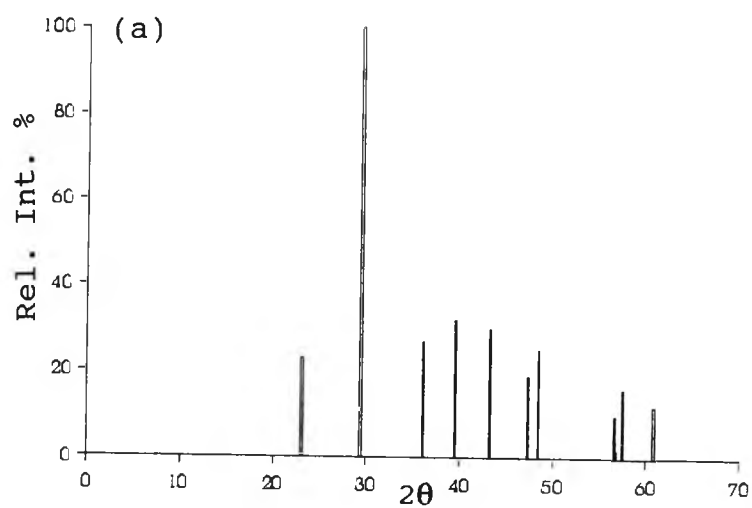


Figure 3.47 Optical micrograph of scale from MTW [ x100 ].



Figure 3.48 Optical micrograph of scale from non-MTW [ x100 ].



(a)			(b)		
$2\theta$	d	Rel. Int. %	$2\theta$	d	Rel. Int. %
23.08	4.450	23	23.12	4.440	21
29.39	3.394	100	29.49	3.381	100
36.06	2.719	27	36.15	2.713	21
39.49	2.471	32	39.57	2.465	24
43.27	2.246	30	43.37	2.241	32
47.40	2.046	19	47.47	2.043	25
48.51	1.998	25	48.60	1.995	26
56.70	1.711	10	56.76	1.708	8
57.56	1.686	16	57.60	1.684	19
60.80	1.598	12	60.89	1.596	11

Figure 3.49 X-ray diffraction powder patterns for the crystals deposited: (a) MTW crystals, (b) non-MTW crystals.

The x-ray diffraction powder patterns of the two treatments showed that the crystals were the calcite form of calcium carbonate. Also there is no evidence for a change in the morphology of the crystals for the water treated magnetically or non-magnetically.

### 3.8.2 Heat Exchanger Experiments Under Industrial Conditions

The heat exchanger experiments under industrial conditions were carried out at the Marks and Spencer store at Epsom, Surrey. A Hydromag DN15 unit was installed to the mains supplying water to a Hobarts Stills boiler in the staff canteen to provide hot water for making tea and coffee. The boiler operates for 14 hours each day at a temperature of 90°C and after 3 months of use (prior to installation of the Hydromag unit), the boiler would be opened to remove the scale which had deposited. This routine maintenance would remove up to 500 grams of scale and would take the maintenance engineer 2-3 hours to complete.

This experiment was started when the routine maintenance was carried out. The boiler was opened and a large quantity of scale was found at the bottom and sides, as shown in Figure 3.50. The heating element (not shown) was resting in this deposit and was also badly covered with scale, which was collected for examination. The sides of the boiler and the heat exchanger were scraped to remove as much scale as possible and the unit was reassembled and refilled with magnetically treated water (MTW), instead of untreated water. The boiler was used for a further 3 months using the MTW under the same conditions as before and reopened for its next routine maintenance. Figure 3.51 shows the inside of the boiler after 3 months of using MTW. The quantity of scale deposited at the bottom was significantly reduced. Also, on the back wall of the boiler the scrape marks from the previous maintenance were still visible. The heating element was almost clear of scale, whereas previously it was coated with scale. The engineer took only 30 minutes to complete the routine maintenance procedure and removed less than 50 grams of deposit

for examination. No scraping of the boiler walls was necessary as the deposit formed was easily removed with a brush. The Hydromag unit has now been installed for 3 years and the routine maintenance period for the boiler has been increased from 3 to 12 months.

Samples of the dried scale were examined by optical microscopy, Figures 3.52 and 3.53 show the optical micrographs of the scale from MTW and non-MTW, respectively.

The optical micrographs of the scales show significant differences in their crystal shape and size. The crystals from MTW form a scale which consists of individual crystals, which are mainly cubic in structure. The crystals from non-MTW form a scale which consists of larger individual crystals of cubic shape dispersed with needle-shaped crystals. This combination of crystals forms a hard scale which is very difficult to remove from the boiler walls, whereas the smaller cubic-shaped crystals from MTW are easily removed.

X-ray diffraction powder patterns for each of the scales formed are shown in Figure 3.54. The x-ray diffraction powder patterns for the crystals from the two treatments showed that they were predominantly the calcite form of calcium carbonate. The crystals from the non-MTW contained some aragonite. This can be seen from the powder patterns in Figure 3.54, where the  $2\theta$  values of 26.30 and 45.97 are the strongest peaks of aragonite. The presence of aragonite can also be seen by the needle-like crystals in the optical micrograph in Figure 3.53.

The x-ray diffraction powder patterns also display a change in crystal morphology between the two treatments. This change is seen at the  $2\theta$  value of 31.56 for non-MTW, which corresponds to the (006) Miller indices for calcite in Figure 3.54 (b). The crystals from the MTW contained no such strong peak at the  $2\theta$  value of 31.56.

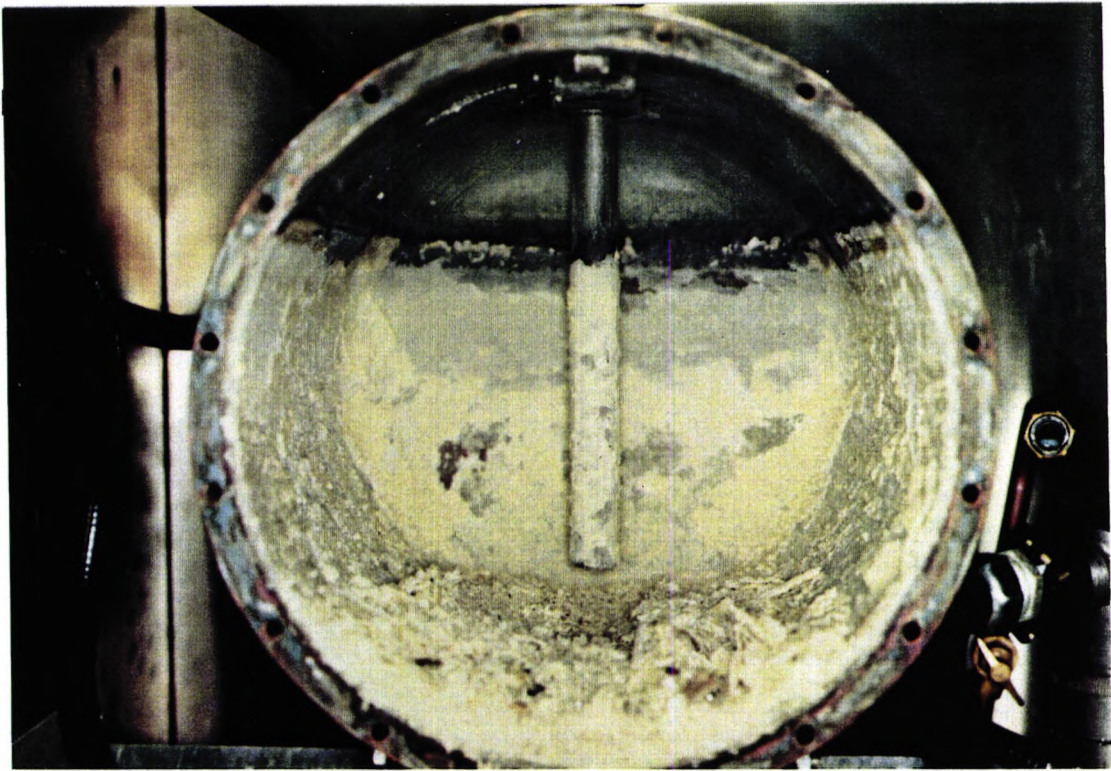


Figure 3.50 Stills boiler before the Hydromag unit was installed.

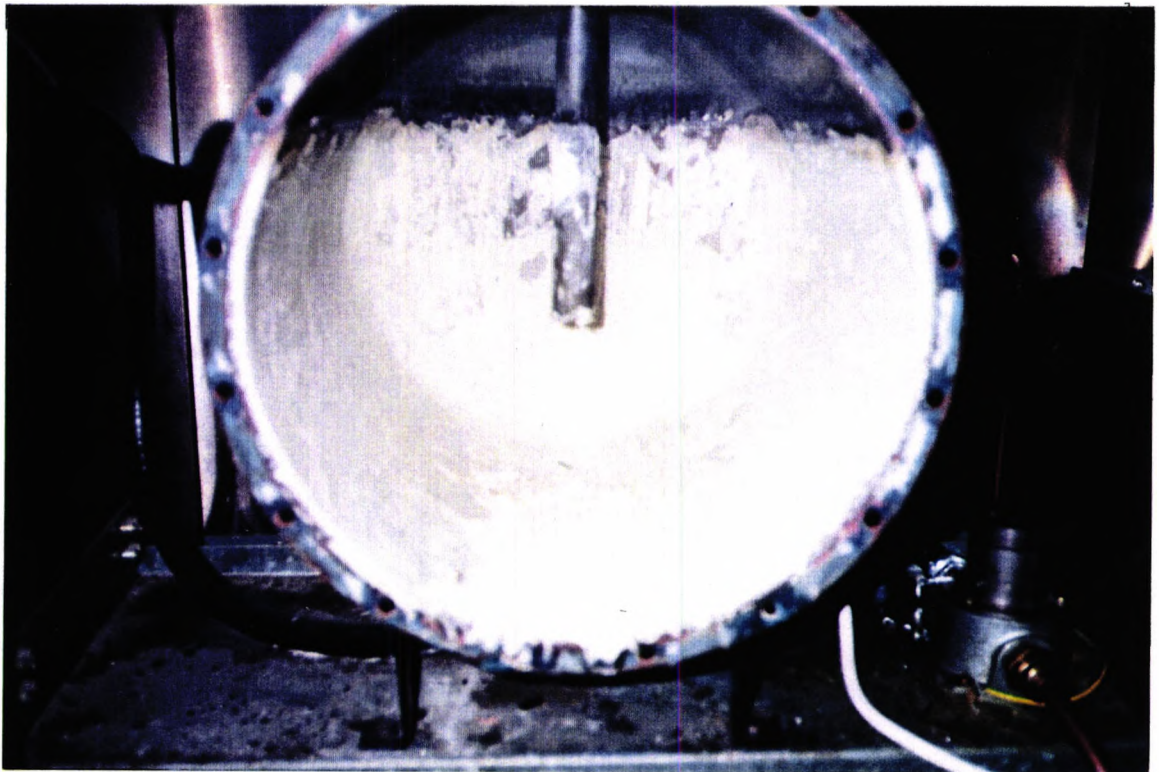


Figure 3.51 Stills boiler 3 months after the Hydromag was fitted.

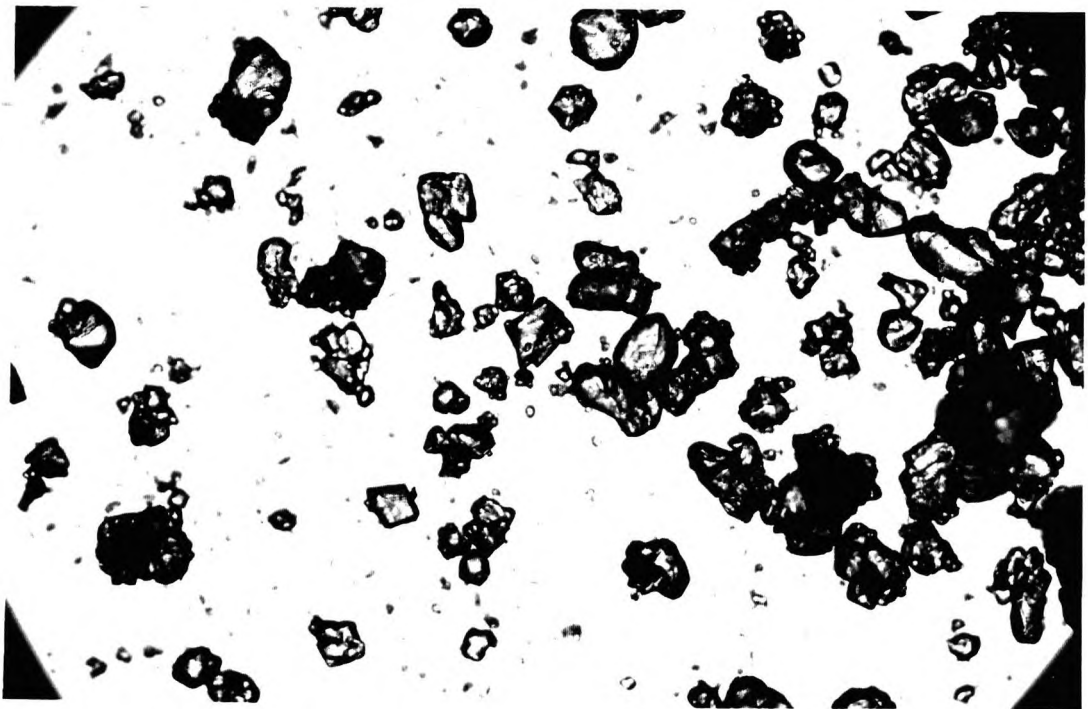


Figure 3.52 Optical micrographs of scale from MTW. [ x100 ].

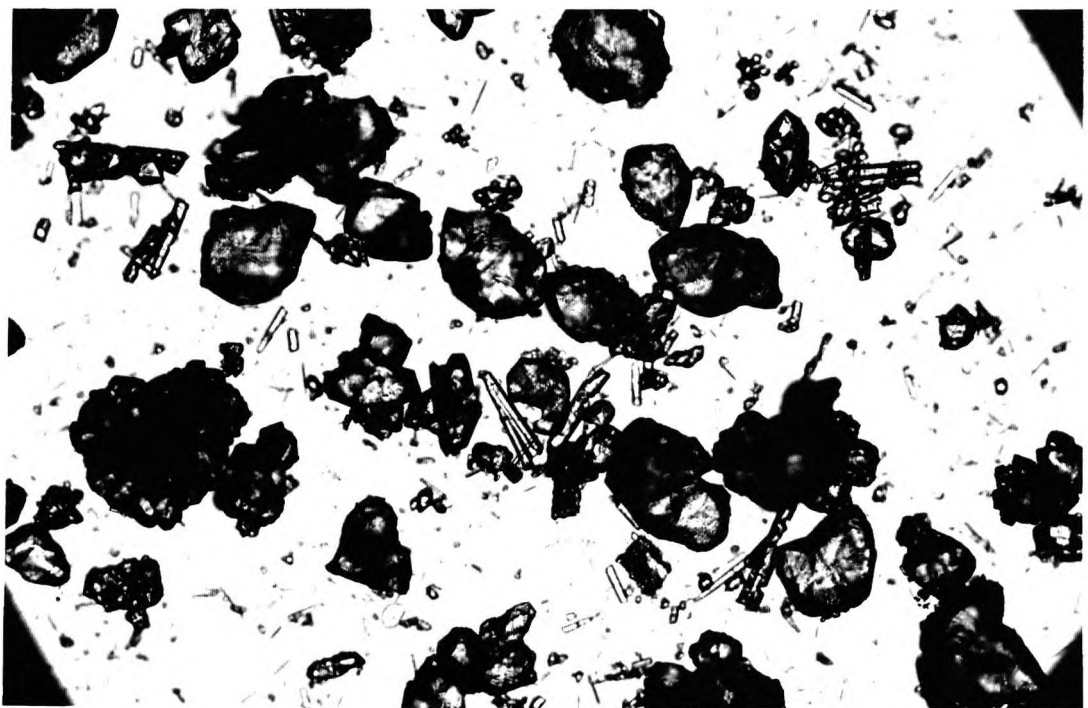
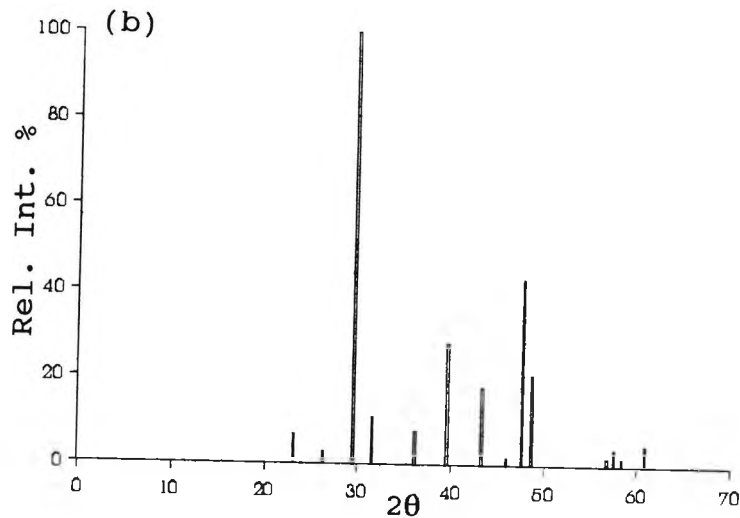
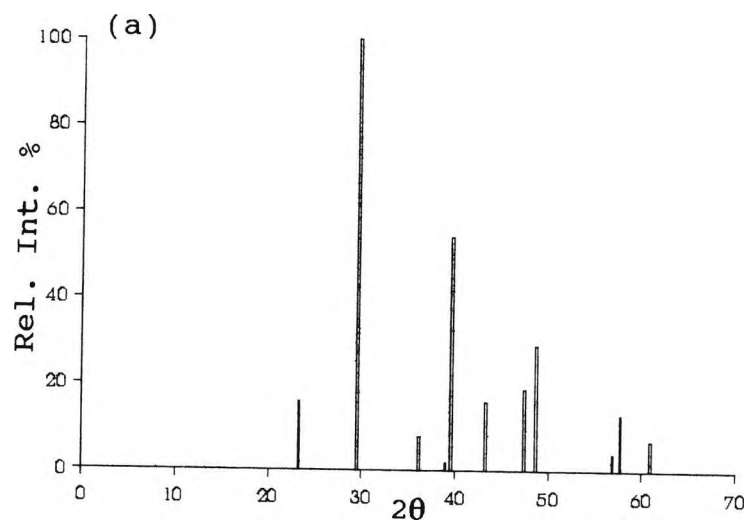


Figure 3.53 Optical micrographs of scale from non-MTW [ x100 ].



(a)				(b)			
$2\theta$	d	Rel. Int. %	hkl	$2\theta$	d	Rel. Int. %	hkl
23.26	4.411	16	102	23.16	4.432	7	102
29.57	3.371	100	104	26.30	3.839	3	
36.18	2.710	8	110	29.56	3.372	100	104
38.95	2.507	2		31.56	3.139	11	006
39.57	2.465	54	113	36.15	2.712	8	110
43.31	2.244	16	202	39.57	2.466	28	113
47.45	2.044	19		43.29	2.245	18	202
48.69	1.991	29	108	45.97	2.111	2	
56.83	1.707	4		47.68	2.034	43	108
57.66	1.683	13	211	48.69	1.991	21	116
60.95	1.595	7		56.78	1.708	2	211
				57.58	1.685	4	212
				58.37	1.663	2	
				60.89	1.596	5	

Figure 3.54 X-ray diffraction powder patterns for the crystals deposited: (a) MTW crystals and (b) non-MTW crystals.

### 3.8.3 Summary of the Results

The heat exchanger experiments have demonstrated that the use of magnetically treated water under both laboratory and industrial conditions significantly reduces the quantity of scale formed. In the laboratory experiments, although all the crystals formed were the calcite form of calcium carbonate, there was a significant difference in the crystal and aggregate sizes. The crystals from MTW consisted of small individual crystals, whereas the crystals from non-MTW were formed into clumps of larger aggregates. This difference in the formation of the crystals was displayed in the nature of the scale formed, with the MTW scale being a soft powder and the non-MTW scale being a hard crystalline deposit.

In the industrial experiments the crystals were again predominantly the calcite form of calcium carbonate. However, the crystals from non-MTW also contained some of the aragonite form. This was observed both in the optical and x-ray diffraction analysis. Also there was a change in the crystal morphology in the crystals for the two treatments, with the crystals from the non-MTW having a strong (006) crystal face, whereas the crystals from the MTW did not.

### 3.9 DISCUSSION

The results from this chapter show clearly that there is overwhelming evidence that the magnetic treatment of the cation scaling solutions and of water, prior to scale formation, significantly affects the rate of precipitation of calcium carbonate, in comparison to the normal precipitation of the scale. The parameters that influence the observed magnetic phenomena, together with the main inferences drawn from the propensity to scale experiments are discussed in Section 3.7.8. The effects of magnetically treating water in heat exchangers on the quantity of scale formed and the differences in crystal size and morphology are discussed in Section 3.8.3.

The following section attempts to ascribe a scientific basis to the magnetic phenomena which is both manifest in all of the summarised points and thought to affect the charged species present in calcium ion solutions and water.

### 3.9.1 Interpretation of the Observed Magnetic Phenomena

It is clear from the two types of experiment conducted in this work that when electromagnetic fields (using a Hydromag DN15 unit) are applied to (i) a circulating calcium ion solution, there is always a significant reduction in the propensity to scale of calcium carbonate when compared to calcium ion solutions treated in zero field conditions and (ii) water passing once through the electromagnetic field, there is always a substantial reduction in the quantity of scale formed in the heat exchanger experiments (under both laboratory and industrial conditions). The aggregate size of the scale formed from magnetically treated water is always smaller and the individual crystals are always separate and distinct when compared to scale from water treated in zero field conditions. The magnetic treatment of calcium ion solutions and water must, therefore affect the constituents of these solutions, which must then later act downstream away from the field to reduce the rate of precipitation of calcium carbonate and subsequent scale formation. Any explanation of the magnetic phenomena observed in this work must, therefore, attempt to explain both of the following:

- (a) The effect that the magnetic field has on the charged species in solution.
- (b) The downstream effect that the magnetically treated charged species has on the crystal growth processes.

Currently there are two possible theories to explain the general magnetic phenomenon for the reduction in the deposition of scale from scale-forming solutions, these being:

- (1) **The Lorentz Force** - which is the result of the interaction of charged species in moving solutions flowing through magnetic fields.
- (2) **Crystal Nucleation Modification** - by the direct interaction of the magnetic field on the nuclei and growing crystallites associated with crystal formation.

The merits of both of these possible theories in terms of encompassing explanations for both (a) and (b) and therefore elucidating the magnetic phenomena observed in this work are discussed in turn.

### (1) The Lorentz Force - Theoretical

The effects of magnetic fields on charged species in fluids is explained by the theory of magnetohydrodynamics (MHD) [53]. The phenomena of MHD has been sometimes referred to as magnetofluid dynamics (MFD) [54]. These theories are based upon the mutual interaction between the magnetic field and the velocity of the conducting fluid flowing across it. The fluid can conduct because it contains charged species, *viz.*, either ions, molecular dipoles or electrons, which if a current path is available allows an electric current to flow. In addition to this current, an electromagnetic force is produced when the fluid flows transversely through the magnetic field. The interaction of both the current and magnetic field produces a force that opposes the relative motion of the fluid. In addition, an induced magnetic field is generated by the current, termed self induction, which distorts the original magnetic field.

The charged species in the fluids are affected by three forces:

1. The **Electrostatic Field**,  $E_s$ , (volts/m), arising from the attractive and repulsive forces on charged particles.
2. The **Magnetic Force**,  $\mathbf{v} \times \mathbf{B}$ , (Newtons per unit charge), which arises from the interaction of the fluid velocity and the applied field and is orthogonal to the velocity,

$v$  and the magnetic field,  $B$ .

3. The **Induced Magnetic Field**,  $E_i$ , defined by the change in the magnetic field,  $B$ , with time.

The total force on the particle per unit charge is given by:

$$E_t = E + v B$$

$$\text{where } E = E_i + E_s$$

If a positively charged species of charge,  $Q$ , passes through a magnetic field of strength,  $B$ , with a velocity,  $v$ , the interaction between the field, the charge and the velocity causes a force,  $F$ , to act on the charged species such that:

$$F = QBv \qquad \text{Equation 3.4}$$

The force  $F$ , is termed the Lorentz force and is a modification of  $E_t = E + vB$ , which excludes the induced electric field component. The direction of the force,  $F$ , acts perpendicular to the plane established by the vectors  $v$  and  $B$ .

The physical basis of the interaction between a conducting medium and a magnetic field has been documented by Alfvén [55,56]. He states that "a magnetic field affects the random course of motion of charged particles (electrons and ions) but does not affect neutral particles." A charged particle moving in a plane perpendicular to the magnetic field executes a circular motion, the radius of the circle (the Larmor radius) being given by:

$$r = \frac{mc}{|||.B} \sqrt{\frac{8kT}{\pi m}}$$

where:  $m$ = Mass;  $B$ = Intensity of the Magnetic Field;  
 $|||$ = Linear Dimension;  $T$ = Temperature;  $c$ = Speed of light;  
and  $k$ = Boltzmann constant.

The radius increases with the mass of the particle and with its thermal energy, but decreases as the intensity of the field increases. The direction of motion is opposite for positive and negative particles. A particle which has a velocity component parallel to the field moves in a helix instead of a circle, as shown in Figure 3.55 (A). However, in a non-uniform magnetic field, the radius of curvature of the helix in which a particle moves is more complex and may even turn through 180°, as illustrated in Figure 3.55 (B). Figure 3.55 (A and B) demonstrates how the magnetic field contorts the random course of motion of the charged particles and reduces their freedom of movement.

### Possible Interpretation of the Magnetic Phenomena in terms of the Lorentz Effect

The Lorentz energy generated by the Lorentz Force on charged species in flowing fluids is theoretically of significance in influencing crystal growth processes at the crystal-solution interface.

The nucleation and subsequent crystal growth processes are comprised of a series of steps and include the setting up of diffusion layers between the solution and the faces of the growing crystals and the diffusion of ions across this layer to the solution-crystal interface. During this process the growing faces will carry a net charge which will differ from face to face or alter the way in which ions have access to the faces by way of the crystal-solution interface, which will affect the subsequent growth of the crystal. Theoretically the ions carrying the extra Lorentz energy could satisfy this criteria by:

(a) **Altering the diffusion of ions through the diffusion layer.** For a crystal to grow from a supersaturated solution, the constituent ions must cross a diffusion layer at the crystal surface which changes the concentration gradient of ions from the supersaturated level in the fluid to zero at the crystal (see Figure 3.56). Transport across the diffusion layer could be

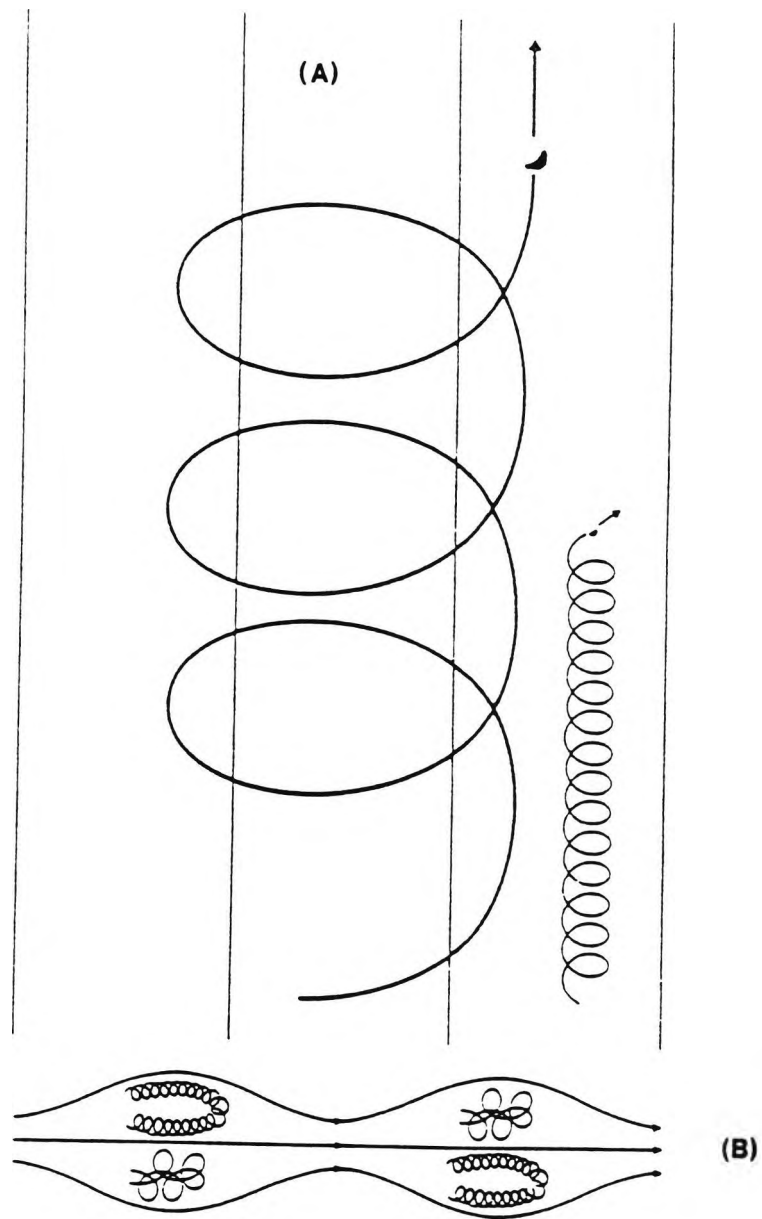


Figure 3.55 Motion of charged particles: (A) in an uniform magnetic field; (B) in a non-uniform magnetic field. The large sphere represents a positive ion, the small sphere an electron.

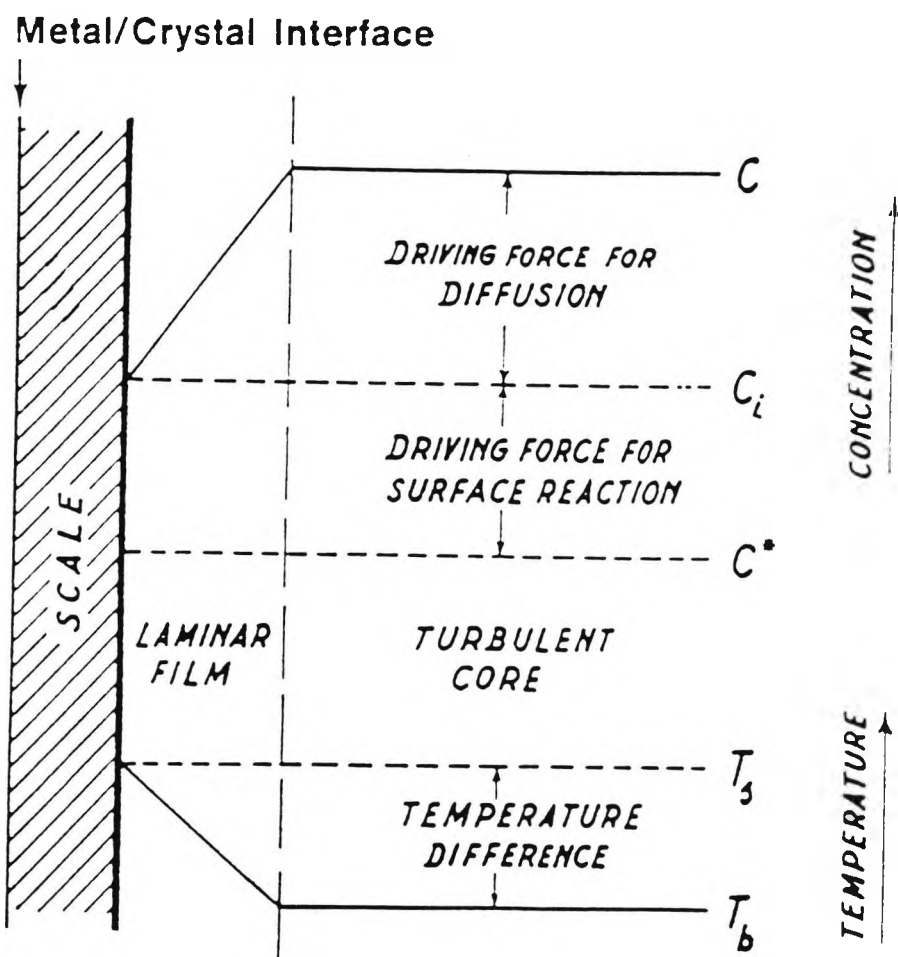


Figure 3.56 Schematic diagram of the diffusion layer set up at the crystal-solution interface, including the temperature and concentration gradients.

affected by the extra energy attributed to the ions by the Lorentz-type interactions, which could change its diffusion through the concentration layer or until the excess energy is dissipated by collisions.

(b) Lorentz effects at the crystal interface. Ions which have gained the additional Lorentz energy could dissipate this energy upon collision with the growing crystal surface. This energy, although small in magnitude could be significant at the point of contact and it is possible that the energy provided to the crystallising system from ions carrying the additional Lorentz energy may contribute in affecting the subsequent growth of the crystal.

The Lorentz effects described in (a) and (b) could theoretically influence crystal growth, but cannot account for the downstream effects of magnetically charged species observed in this work. For these effects to occur the ions in solution would have to carry the Lorentz energy downstream, away from the magnetic field, over a considerable distance to the point of crystallisation without losing this extra energy. This is very unlikely to occur because the Lorentz energy would be dissipated instantly upon the normal collisions between ions and water molecules and therefore processes (a) and (b) cannot possibly be significant factors in the phenomena observed in this work.

The Lorentz effect cannot be attributed to other magnetic phenomena, such as downstream descaling (the removal of existing scale deposits caused by magnetically treated fluids) which, although not investigated in this work, has been reported by other workers at City University [57]. Calculations of the Lorentz energy generated by  $M^{2+}$  ions flowing at  $0.95 \text{ m}^3 \text{ hr}^{-1}$  through a magnetic field of 2.5 kGauss [33] indicate that the Lorentz force is sufficient to influence particles in solution, but would not be enough to account for the downstream descaling, as a result of the collision processes between ions which would dissipate this energy.

## (2) Crystal Nucleation Modification

### Possible Interpretation of the Magnetic Phenomena in terms of Crystal Nucleation Modification

The magnetic treatment of fluids on calcium carbonate precipitation studied in this work, has focused on precipitations from supersaturated solutions and essentially on the magnetic effects at solid-fluid interfaces at the point of crystallisation. The magnetic phenomena observed in these studies are best explained in terms of the field-charge interactions of the magnetic field with the stable crystal nuclei, present in the fluid. The nuclei on which the crystals start growing are usually very small particles and have highly charged surfaces. These charged species would be subjected to interactions as they pass through a magnetic field. The growing nuclei consist of minute crystals of the precipitated material which have potentially growing faces, each with their own surface charge characteristics. The interaction between the magnetic field and the nuclei could modify the growth at the crystal face, both in general and specific planes. This modification process must favour certain growing crystal faces, so that these crystal faces would be significantly different from those growing in the absence of a magnetic field.

This theory provides a satisfactory explanation of the effects of magnetic fields on the crystallisation process, when the magnetic field acts at the point of crystallisation, but cannot account for the downstream phenomena observed in this work. It is unlikely that the unsaturated aqueous solutions which were magnetically treated in this work would contain any stable nuclei.

## Ascribing an Alternative Explanation to the Magnetic Phenomena Observed in this Work

The magnetic phenomena observed in the present work have been facilitated predominantly by the magnetic treatment of unsaturated aqueous calcium ion solutions, which were precipitated with hydrogen carbonate ions downstream away from the magnetic field in a microbore tube. The magnetic treatment of tap water under both laboratory and industrial conditions was also investigated with the formation of scale being downstream from the magnetic field. These solutions contain charged species, such as the dipole water molecule and the ions present which could be affected by the magnetic field. However, they will not contain stable nuclei to permit field-surface charge interactions.

The effects attributed to the ions in solution have been discussed (pp 147). The effects attributed to the water molecules because of their polarity and diamagnetic properties should be regarded as being negligible because any field-dipole interactions of this type are likely to be dissipated very rapidly. The downstream phenomena observed in this work must be due to other species present in the solutions on which the magnetic field acts.

It has been previously stated that the fluids treated in this work should not contain stable crystal nuclei. However, the concept of clusters of ions forming prior to the development of the nuclei is now widely accepted. Evidence for the formation of clusters comes from fundamental work on nickel chloride complexes in aqueous solution, where a comparison of the structure of the complex in solution was found to be very similar to that found in the solid state [58]. An explanation of the suggested importance of these clusters in influencing crystal growth processes is described here.

The clusters that form prior to stable nuclei would essentially consist of hydrated ions (for the solutions used in this work clusters of hydrated calcium ions would be present) in close proximity to each other. These clusters would have a high surface charge and be stable enough to have a finite lifetime in the fluid. Both of these factors are significant in determining the effect that these species have on the subsequent nucleation process, especially in terms of explaining the observed downstream phenomena. Therefore, it has been suggested that the interaction between the field and the clusters would be important because field-charge interactions would result in the formation and destruction of clusters, which would subsequently affect the nature of the nuclei formed from them and the final crystallisation process. This is shown in the following scheme whereby clusters are thought to be in equilibrium with both the ions and nuclei in the fluid.



**PROPOSED SCHEME FOR THE EQUILIBRIUM OF CLUSTERS IN A FLUID**

The stability of the clusters is very important as it would influence the formation of nuclei and hence the precipitation and crystallisation processes which lead to scale formation. It is further suggested that the magnetic field must, therefore influence the kinetics of the equilibrium process (essentially the proposed equilibrium constants  $K'$  and  $K''$ ) which control the rate of deposition of scale.

**3.10 CONCLUSION**

In conclusion, the reduction in the propensity to scale of unsaturated calcium ion solutions and hence the reduction in the rate of deposition of calcium carbonate, in combination with the reduction in the quantity and nature of the scale deposited in the industrial and laboratory heat exchanger experiments observed

in this work, resulting from the application of an electromagnetic field using a Hydromag DN15 unit has been explained in terms of the field-charge interactions of cluster species present in the fluid that forms prior to the formation of stable nuclei. It is suggested that the stability of these cluster species is influenced by the applied field which subsequently affects the precipitation and crystallisation processes.

## REFERENCES

1. Donaldson, J.D. and Grimes, S.M., New Scientist, Feb. 1988, 43-46.
2. Hay, A.T., U.S.Pat. No. 140196; June 24, 1873.
3. Joshi, K.M. and Kamat, P.V., J. Indian Chem. Soc., 1966, 43, (9), 620-2.
4. Klassen, V.I., Doklady Akademii Nauk. SSSR, 1971, 197, 1104-5.
5. Duffy, E.A., Ph.D. Thesis, Clemson University, 1977.
6. Gonet, B., Bioelectromagnetics, 1985, 6, 169.
7. Drost-Hansen, W. and Kavjic, G., "Conference on Electrolyte Precipitation in Aqueous Solution", University of Copenhagen, Proceeding abstr. Book II (supplement), 1978.
8. Eliassen, R., Skrinde, R.T. and Davis, W.B., J. Amer. Water Works Assoc., 1958, 50, (10), 1371-85.
9. Minenko, V.I. and Petrov, S.M., Teploenergetica, 1962, 9, (9) 63.
10. Ellingsen, F.T. and Fjeldsend, O., Water Supply, 1983, 1 (2/3), SS8 12-19.
11. Ellingsen, F.T. and Kristiansen, H., Vatten, 1979, 35, (4), 309-15.
12. American Petroleum Institute, "Evaluation of the Principles of Magnetic Water Treatment", 1985, API Publication 960.
13. Herzog, R.E., Shi, Q., Patil, J.N. and Katz, J.L., Langmuir, 1989, 5, (3), 861-7.
14. Speranskiy, B.A., Vikhrev, V.V., Vinogradov, V.N. and Dolya, Y.I., Prom. Enerq., 1973, 8, 43-4.
15. Thomas, A.P.A., Ph.D. Thesis, City University, 1992.
16. Lychagin, N.I., Belavina, I.G., Potapova, E.S., Semenov, A.S., Yushkova, I.K., Obukhov, A.A., Cherkasov, N.Kh., and Grigorova, G.I., Koks. Khim., 1979, , 47.
17. Marko, J.A., Mekh. Kampoz Mater., 1984, 589.
18. Negmatov, S.S. and Usmanov, D.I., Mater. Vses. Symp. Mekhaneomiss, Mekhanokhim. Iverd., 1975.
19. Lee, H. and Labes, M.M., Mol. Cryst. Liq. Crvst., 1982, 84 (1-4), 137.

20. Samarskaya, T.G., Skrunts, L.K., Kiprianova, L.A., Levit, A.F. and Gragerov, I.P., Dokl. Akad. Nauk., SSSR, 1985, 283 (2), 424.
21. Gray, M., Unpublished Manuscript.
22. Steiner, U.E. and Ulrich, T., Chem. Rev., 1989, 89, 51.
23. Weller, A., Nolting, F. and Staerk, F., Chem. Phys. Letts., 1983, 96, 24.
24. Turro, N.J. and Weed, G.C., J. Amer. Chem. Soc., 1983, 105, 1861.
25. Baretz, B.H. and Turro, N.J., J. Amer. Chem. Soc., 1983, 105, 1309.
26. Margulis, L.A., Khudyakov, I.V. and Kuz'min, V.A., Chem. Phys. Lett., 1986, 124 (5), 483.
27. Evans, G.J., J. Chem. Soc. Faraday Trans. I., 1985, 81, 673.
28. Donaldson, J.D., Grimes, S.M. and Prosser, J., Unpublished Manuscript.
29. Grimes, S.M., Tube International, March 1988, 111.
30. Donaldson, J.D., Grimes, S.M. and Menezes, A., Unpublished Manuscript.
31. Donaldson, J.D., Grimes, S.M., Prosser, J. and Stokes, F., Unpublished Manuscript.
32. Kronenberg, K.J., Magnets in your future, 1987, 2 (8), 6-15.
33. Ekaireb, S., Ph.D. Thesis, City University, 1988.
34. Donaldson, J.D., Tube International, January 1988, 42.
35. Rudert, M. and Müller, G., Chem. Ztg., 1982, 106, 191.
36. Lippmann, F., "Sedimentary Carbonate Minerals", In: Minerals Rocks and Inorganic Materials; Springer-Verlag: New York, 1973, Vol. 6.
37. Kohlschütter, V. and Egg, C., Helvetica Chim. Acta., 1925, 8, 470-90.
38. Cowan, J.C. and Weintritt, D.J., "Water Formed Scale Deposits", Gulf Publishing Co., Texas, 1976.
39. Wray, J.L. and Daniels, F., J. Amer. Chem. Soc., 1957, 79, 2031-4.
40. Meigen, W., Chem. Ztg., 1911, 34, 1015.
41. Faivre, R., Compt. Rend., 1946, 222, 140-1.
42. Kelley, V.C., Amer. Min., 1940, 25 (5), 357-67.

43. Krieger, P., Amer. Min., 1930, 15, 23.
44. Huggins, M.L., Phys. Rev., 1922, 19, 354.
45. Alexander, A.E., Gem., 1941, 10, 93.
46. Alexander, A.E., Am. J. Sci., 1940, 238, 366.
47. Miller, J.P., Am. J. Sci., 1952, 250, 161.
48. Ellis, A.J., Am. J. Sci., 1959, 257, 354.
49. Pytkowicz, R. and Connors, D., Science, 1964, 144, 840-1.
50. Kitano, Y., Bull. Chem. Soc. Japan., 1962, 35, 1973-80.
51. Hydromag Factsheet on Flow Rates, 1989.
52. Stumper, R., Anorg. u. allgen. Chem., 1932, 204, 365-77.
53. Shercliff, J.A., "A Textbook of Magnetohydrodynamics", Pergamon Press, London, 1965.
54. Cramer, K.R. and Pai, S.I., "Magnetofield Dynamics for Engineers and Applied Physicists", Scripta Publishing Co. Ltd., U.S.A., 1973.
55. Alfvén, G., "Worlds and Anti-worlds", Moscow, 1968.
56. Alfvén, G., "Magnetohydrodynamics", Symposium Proceedings, Moscow, 1958.
57. Donaldson, J.D., HDL Fluid Dynamics Symposium, Harwell, 1986.
58. Neilson, G.W. and Enderby, J.E., Proc. R. Soc., London, 1983, 390, 353-71.

## CHAPTER 4

### PRECIPITATION STUDIES OF FORMATION WATER AND SEA WATER AS ENCOUNTERED IN THE PETROLEUM INDUSTRY

	Page
4.1 INTRODUCTION	162
4.2 SCALE DEPOSITS IN PETROLEUM PRODUCTION	162
4.2.1 Production	163
4.2.2 Maintenance	163
4.2.3 Disposal of Scale	164
4.3 SCALE FORMATION IN THE PETROLEUM INDUSTRY	164
4.3.1 Formation Waters	165
4.3.2 Sea Water	166
4.3.3 Problems Encountered when Mixing Incompatible Waters	168
4.3.4 The Composition and Tendency of Formation Waters to Scale in Offshore Production	170
4.4 MONITORING AND COMBATTING SCALE FORMATION	171
4.4.1 Prediction	172
4.4.2 Monitoring Scale Formation	173
4.4.3 Removal Techniques	174
4.4.4 Chemical Inhibition	176
4.5 LABORATORY STUDIES IN OILFIELD PRECIPITATES	176
4.5.1 Solubility Studies	177
4.5.2 Deposition Studies	181
4.5.3 Uses of Laboratory Studies	183
4.6 OBJECTIVES	187
4.7 EXPERIMENTAL TECHNIQUES	188
4.7.1 Propensity to Scale Measurements	188

4.7.2	Precipitation Studies	191
4.8	PROPENSITY TO SCALE EXPERIMENTS	192
4.9	THE EFFECT OF VARYING THE CONCENTRATIONS OF CONSTITUENT IONS IN SIMULATED FORMATION WATERS ON THE PROPENSITY TO SCALE	193
4.9.1	The Effect of Varying the Sodium Chloride Concentration in Simulated Formation Water on the Propensity to Scale	194
4.9.2	The Effect of Varying the Potassium Ion Concentration in Simulated Formation Water on the Propensity to Scale	199
4.9.3	The Effect of Varying the Magnesium Ion Concentration in Simulated Formation Water on the Propensity to Scale	202
4.9.4	The Effect of Varying the Calcium Ion Concentration in Simulated Formation Water on the Propensity to Scale	207
4.9.5	The Effect of Varying the Strontium Ion Concentration in Simulated Formation Water on the Propensity to Scale	211
4.9.6	The Effect of Varying the Barium Ion Concentration in Simulated Formation Water on the Propensity to Scale	216
4.9.7	Summary of the Propensity to Scale Experiments	220
4.10	THE EFFECT OF VARYING THE CONCENTRATIONS OF CONSTITUENT IONS IN SIMULATED SEA WATERS ON THE PROPENSITY TO SCALE	221
4.10.1	The Effect of Varying the Sodium Chloride Concentration in Simulated Sea Water on the Propensity to Scale	221
4.10.2	The Effect of Varying the Potassium Ion Concentration in Simulated Sea Water on the Propensity to Scale	226

4.10.3	The Effect of Varying the Magnesium Ion Concentration in Simulated Sea Water on the Propensity to Scale	229
4.10.4	The Effect of Varying the Calcium Ion Concentration in Simulated Sea Water on the Propensity to Scale	234
4.10.5	The Effect of Varying the Strontium Ion Concentration in Simulated Sea Water on the Propensity to Scale	238
4.10.6	The Effect of Varying the Hydrogen Carbonate Ion Concentration in Simulated Sea Water on the Propensity to Scale	243
4.10.7	The Effect of Varying the Sulphate Ion Concentration in Simulated Sea Water on the Propensity to Scale	247
4.10.8	Summary of the Propensity to Scale Experiments	251
4.10.9	Overall Summary of the Propensity to Scale Experiments	252
4.11	THE EFFECT OF MIXING THE MOST AND LEAST SCALE-FORMING FORMATION AND SEA WATERS AS DETERMINED IN SECTIONS 4.9 AND 4.10.	253
4.12	THE EFFECT OF RATIO MIXING OF SIMULATED FORMATION AND SEA WATERS ON THE PROPENSITY TO SCALE	259
4.13	THE EFFECT OF VARYING THE CONCENTRATIONS OF CONSTITUENT IONS IN SIMULATED FORMATION WATERS ON THE PROPENSITY TO SCALE FOR THE $\text{CaSO}_4$ - $\text{CaCO}_3$ SYSTEM	268
4.13.1	The Effect of Varying the Sodium Chloride Concentration in Simulated Formation Water on the Propensity to Scale	269
4.13.2	The Effect of Varying the Potassium Ion Concentration in Simulated Formation Water on the Propensity to Scale	271

4.13.3	The Effect of Varying the Magnesium Ion Concentration in Simulated Formation Water on the Propensity to Scale	274
4.13.4	The Effect of Varying the Calcium Ion Concentration in Simulated Formation Water on the Propensity to Scale	276
4.13.5	Summary of the Propensity to Scale Experiments	278
4.14	THE EFFECT OF VARYING THE CONCENTRATIONS OF CONSTITUENT IONS IN SIMULATED SEA WATERS ON THE PROPENSITY TO SCALE FOR THE $\text{CaSO}_4$ - $\text{CaCO}_3$ SYSTEM	279
4.14.1	The Effect of Varying the Sodium Chloride Concentration in Simulated Sea Waters on the Propensity to Scale	280
4.14.2	The Effect of Varying the Potassium Ion Concentration in Simulated Sea Waters on the Propensity to Scale	282
4.14.3	The Effect of Varying the Magnesium Ion Concentration in Simulated Sea Water on the Propensity to Scale	284
4.14.4	The Effect of Varying the Hydrogen Carbonate Ion Concentration in Simulated Sea Waters on the Propensity to Scale	287
4.14.5	The Effect of Varying the Sulphate Ion Concentration in Simulated Sea Water on the Propensity to Scale	290
4.14.6	Summary of the Propensity to Scale Measurements	293
4.15	CONCLUSIONS	293
	REFERENCES	295

## CHAPTER 4

### PRECIPITATION STUDIES OF FORMATION WATER AND SEA WATER AS ENCOUNTERED IN THE PETROLEUM INDUSTRY

#### 4.1 INTRODUCTION

Scale formation has been a common problem in the petroleum industry since the birth of the industry. The first observed deposition was of barite oolites in some producing oil wells in the Saratoga Field, Texas in 1914. As petroleum production has increased, more oilfields are operating using new techniques. Waterflooding (discussed in Section 4.3.3) tends to result in higher water production and more scale. American legislation in the 1930s forced operators to reinject produced brines; this enforced practice resulted in scale formation due to the mixing of incompatible brines. Since the 1970s offshore oil production has become more common; this uses sea water as the injection brine. Due to its high sulphate content, when it is reinjected it is prone to scaling because of its chemical incompatibility with the reservoir brine, which contains barium, strontium and calcium.

Therefore, as petroleum production has grown, the increase in scale formation has become a major economic factor, especially in offshore fields. An estimated loss in revenue, caused by the flow restrictions arising from scale formation, was in the order of \$1 billion/year in the U.S. alone in 1976 [1]. This sum is considered a minimum.

#### 4.2 SCALE DEPOSITS IN PETROLEUM PRODUCTION

Scale deposits in the petroleum industry can begin with the drilling of an oil well, with drill pipe, centrifuges and other drilling equipment being scaled-up in certain conditions. Once the well is in production problems are encountered from the formation to the refinery. Scale deposition can occur when the

produced fluids (which contain water with high levels of dissolved mineral matter) move through fractures near the wellbore, causing a reduction in oil flow. This is known as formation damage. The biggest problem with scale is encountered when the subsurface fluid is brought to the surface, causing blockages to the tubing string in chokes and flowlines at the wellhead. Further problems are encountered when the produced fluid is separated either in the transmission lines to the refinery or to a gathering system, where the water is either disposed of or conditioned and reinjected for further recovery of oil by waterflooding.

#### **4.2.1 Production**

Scale deposition in oil production equipment is a major operational problem. Scale can contribute to equipment wear, corrosion and flow restrictions, thus resulting in a decrease in oil production. The flow restrictions occur because of scale deposition within the oil-producing formation and down-hole equipment. As scale deposits around the wellbore, the porous formation can become plugged and rendered impermeable to any fluids. Surface production equipment also becomes blocked, causing its life to be shortened. Blockages cause a reduction of carrying capacity in pipes due to a decrease in their diameter, which consequently restricts oil production, making it less economic.

#### **4.2.2 Maintenance**

As scale builds up it must be removed in order to avoid decreases in fluid flow, increased safety hazards and other deposit related problems, within production equipment. Maintenance programmes are used to prevent scale formation; these programmes can be either mechanical (reaming or drilling) or chemical treatments discussed in Section 4.4.3. The mechanical method is expensive (cost of equipment), but can be used regardless of scale type. Chemical cleaning is preferred as there are many chemicals available for

scale removal. In cases where no maintenance is carried out, entire lengths of surface piping can become plugged (sometimes up to several miles long), necessitating replacement and causing expensive shutdowns in production.

#### 4.2.3 Disposal of Scale

The disposal of solid scale and scale-removing solutions is a serious consideration in today's ecologically conscious society, resulting in greater costs for the operators. The solid scale found in the North Sea consists of barium sulphate which can contain small quantities of radioactive radium [2]. In Kansas, radium-bearing precipitates have been found in deposits of celestite, iron oxide, gypsum and barite [3]. This leads to highly specialised and costly forms of disposal by government approved companies. Scale-removing solutions also need to be treated with extreme care and in-plant water treatment facilities are needed to handle such wastes. Specialised companies also treat and dispose of these highly toxic solutions. As environmental legislation is tightened up on the disposal of radioactive scale, costs will rise in the petroleum industry and new acceptable methods of scale prevention will need to be developed.

#### 4.3 SCALE FORMATION IN THE PETROLEUM INDUSTRY

Scale and other deposits are a major concern in the petroleum industry where substantial quantities of water are produced with the oil. The average wells in the petroleum industry are becoming deeper and more expensive to maintain, as oil reserves are depleted. As wells age, more water is used to produce oil, increasing scale formation until excessive sea water breakthrough eventually reduces the problem by dilution.

The primary cause of scale deposition is supersaturation. When the solubility product of a deposit-forming material is exceeded, it precipitates and may aggregate to form scale. The key

requirements that influence scale formation have already been discussed in Chapter 1. Therefore, the waters used in the petroleum industry will affect the rate of scale formation. The two main waters used in oil production and the consequences of mixing them are described in the following sections.

#### 4.3.1 Formation Waters

Formation water exists as connate brines in hydrocarbon reservoirs and is produced in varying quantities with oil and gas. These waters can vary greatly in their chemical composition from field to field and even within the same field, because as subsurface brines they become highly mineralised by contact with the formation rock, coupled with high pressures and temperatures, and, in some cases, bacterial activity over long periods of geological time. Formation waters change constantly with time, although these changes may be so minute that the waters are considered to be in an equilibrium condition. However, when the formation is tapped with a drill and the formation fluids are brought to the surface, the water undergoes rapid and drastic changes in temperature and pressure which affect the supersaturation of the chemical constituents. These changes cause the formation water to dissolve or deposit solids with which it comes into contact. It is common for several ions to co-exist at varying concentrations in formation waters in oil production. Table 4.1 shows some typical chemical compositions encountered in oilfields.

The scales found in oil production wells are caused by the ions dissolved in formation waters, especially the concentrations of barium, strontium and calcium mixing with sulphate and hydrogen carbonate ions in sea water. The main scales found in oil production are, therefore, mixtures of barium sulphate, strontium sulphate, calcium sulphate and calcium carbonate, depending on the brine chemistry. Examples of reported barium levels (mg/l) in various North Sea oilfields are listed in order of increasing potential scaling severity: Fulmar (15), Cormorant (15), Magnus

(20), Brent (39), Murchison (42), Thistle (54), Dunlin (60), Nelson (74), Forties (210), Brea (700), and Millar (1050). High strontium levels have also been reported for some fields including Dunlin (55), Millar (110), Forties (570) and Fulmar (660).

The fields shown in Table 4.1 are the T-Block Field (North Sea, U.K. sector) [2], the Ramadan Nubia Field (Gulf of Suez, Egypt) [4], the Wilmington Field (California, U.S.A.) [3] and the two Arab-D Fields (Ghawar, Saudi Arabia) [5].

**Table 4.1 Chemical composition of some formation waters in oilfields around the world.**

mg/l Water Analysis					
Ion	T-Block	Ramadan Nubia	Wilmington	Low salinity Arab-D	High salinity Arab-D
Na <sup>+</sup>	36360	32547	10485	29680	51187
K <sup>+</sup>	1720	N/A	297	N/A	N/A
Mg <sup>2+</sup>	365	3270	362	1575	4264
Ca <sup>2+</sup>	3790	20800	507	13574	29760
Sr <sup>2+</sup>	355	1050	21	557	1035
Ba <sup>2+</sup>	930	2	68	8	10
Cl <sup>-</sup>	65840	96400	18528	73861	143285
SO <sub>4</sub> <sup>2-</sup>	2	190	4	404	108
HCO <sub>3</sub> <sup>-</sup>	560	5	916	369	351

#### 4.3.2 Sea Water

Sea waters are probably one of the most complex systems known to man. Their complexity stems from the variety of elements that make up its composition; 72 elements occur with many being found

in trace quantities. Sea waters also vary with depth and geographical location. Significant variations can occur in dissolved and suspended solids as one gets closer to shore, especially near river estuaries and bays, where the concentration gradient is affected by tidal movements. There are several major ions which co-exist at varying concentrations in sea water. Table 4.2 shows the chemical composition of some sea waters.

**Table 4.2 Chemical composition of some sea waters in oil fields around the world.**

mg/l Water Analysis				
Ion	North Sea water	Gulf of Suez water	Wilmington Sea water	Arab-D Sea water
Na <sup>+</sup>	11150	13162	9010	18043
K <sup>+</sup>	380	N/A	306	N/A
Mg <sup>2+</sup>	1350	1490	1567	2159
Ca <sup>2+</sup>	410	512	505	652
Sr <sup>2+</sup>	7	0	6	11
Ba <sup>2+</sup>	0	0	0	0
Cl <sup>-</sup>	18950	23100	17887	31808
SO <sub>4</sub> <sup>2-</sup>	2850	3200	2207	4450
HCO <sub>3</sub> <sup>-</sup>	148	134	329	119

The data in Table 4.2 show that the chemical composition of sea water varies around the world. However, comparing Table 4.2 with Table 4.1, it is found that the sea water composition is far more consistent than that found in formation waters. The principal ions involved in scale formation from sea water are hydrogen carbonate and sulphate. The high sulphate content is responsible for the major scale problems encountered in the petroleum industry when sea water is mixed with formation water.

#### 4.3.3 Problems Encountered when Mixing Incompatible Waters

In the petroleum industry, as much oil as possible will be produced from wells by primary production methods. However, as some oil remains in the formation, operators opt for secondary recovery techniques to flush out all the remaining oil. The technique is better known as waterflooding and was discovered by accident in 1912 [6]. The technique involves injecting water into the formation through injection wells. As the injected water moves towards the producing well, it flushes trapped oil from the formation and carries it along to the producing well, thus enhancing oil production levels. Initially the oil industry used fresh or natural surface waters for waterflooding, but as they became less available, operators turned to waters produced with the oil to reinject. However, in most fields saltwater formations exist near the oil zones, so that wells are dug and water is pumped to the surface for reinjection. If the oil field is near an ocean, sea water is used.

In waterflooding operations, it is unusual to obtain waters that are chemically compatible, and so when incompatible streams are mixed substantial solid precipitation and subsequent scale formation can result. In general, the scale formed is a mixture of barium, calcium and strontium sulphates. The amount of solid formed by mixing incompatible waters and the nature of the problems these solids cause are dependent upon the concentrations of the various constituents in the waters, the ratio of mixing, and other factors such as time, temperature and pressure. The sulphate scales may result from changes in temperature and pressure while water flows through the formation, but the major cause is chemical incompatibility between the injected sea water, which is high in sulphate ions and the formation water which contains high concentrations of barium, calcium and strontium ions.

The example of scale formation resulting from mixing incompatible waters detailed in Table 4.3 is taken from a petroleum operation

at Boston Pool, Oklahoma, U.S.A. [7]. Analysis shows that the Bartlesville brine is high in barium, whereas the Arbuckle brine is high in sulphate. On mixing the two brines, scale formation occurs. The analysis of the scale formed shows that  $\text{BaSO}_4$  is the predominant scale (80.1%) deposited along with the minor scale phases  $\text{MgCO}_3$  (8.12%),  $\text{SrCO}_3$  (4.45%), and  $\text{SrSO}_4$  (3.60%). There are other materials which can form deposits and scale and cause operating problems. These deposits can be complex silicates, clays, iron compounds such as  $\text{FeCO}_3$ , corrosion products like rust and even waxes from the produced oil.

**Table 4.3 An example of mixing incompatible waters used in a petroleum operation, Oklahoma, U.S.A.**

Ion	ANALYSIS OF BRINE		ANALYSIS OF SCALE	
	Milligrams/ Litre		Scale type	Percent
	Bartsville	Arbuckle		
Sodium	52000	58400	-	-
Calcium	10700	13900	$\text{CaCO}_3$	0.65
Magnesium	1807	2182	$\text{MgCO}_3$	8.12
Barium	250	nil	$\text{BaSO}_4$	80.10
Sulphates	nil	194	-	-
Chlorides	104750	120750		
Alkalinity	44	50		
			$\text{SrCO}_3$	4.45
			$\text{SrSO}_4$	3.60
			Others	2.68
			Total	99.6

#### 4.3.4 The Composition and Tendency of Formation Waters to Scale in Offshore Production

A formation water will have a natural tendency to scale formation if it contains concentrations of all the component ions of the scale in excess of the solubility of the scale material. That is when the product of the concentrations of the component ions exceeds the solubility product for the solid in the fluid containing ions. The formation waters from several North Sea oil fields illustrate this point; for example, Murchison formation water has the reported composition:

Ion	Ca <sup>2+</sup>	Ba <sup>2+</sup>	Sr <sup>2+</sup>	HCO <sub>3</sub> <sup>-</sup>	SO <sub>4</sub> <sup>2-</sup>
mg/l	212	42	42	960	<5

which contains levels of calcium and hydrogen carbonate high enough to give calcium carbonate scaling in the well as the temperature reduces from the reservoir. The Murchison formation water, however, contains only low levels of sulphate ions, and because of this, does not have a natural tendency to form barium or strontium sulphate type scales. Barium and strontium sulphates can be deposited from a formation water of this composition when sea water breakthrough contains about 2800 mg/l of sulphate. Under these circumstances, the tendency to form scale will depend upon the concentrations of barium, strontium and sulphate (particularly barium) and the percentage of sea water breakthrough. Sea water breakthrough has two possible effects on scaling: (a) the supply of sulphate ions for scale formation and (b) a dilution effect. Very small amounts of sea water breakthrough (about 1%) can provide the conditions for sulphate scale formation even with barium levels of 40 mg/l. This becomes more acute with increasing levels of barium and strontium in the formation water because of the increased amount of solid that can be deposited. For formation waters with significantly low levels of barium and strontium, the dilution effects on the sea water may eventually lead to a reduction in sulphate scaling-tendency.

An example of this effect has been reported in the Cormorant Field which has low levels of barium and strontium (about 15 mg/l of each) and high sea water breakthrough levels.

#### 4.4 MONITORING AND COMBATTING SCALE FORMATION

If scale represents a problem in an oilfield, engineers are confronted with four distinctly different problem areas, and they are forced to fight simultaneously on four different fronts.

**(a) Prediction:** They have to determine the extent of the damage that has already occurred. This includes detailed chemical analysis of the past, present and future sets of conditions that could lead to scale deposition.

**(b) Monitoring:** They can use a number of laboratory and field methods to monitor scale formation for comparison with the prediction methods or to check the effectiveness of scale prevention methods.

**(c) Removal:** If scale has formed, they have to remove it to restore the field to full productivity as best they can. They can use either chemical, mechanical or a combination of methods to remove deposited scale.

**(d) Inhibition:** They can decide upon preventative methods, such as chemical scale inhibition procedures, specific to their field's requirements.

These are the four areas to be discussed in this section. The engineers in the field need to consider all four areas to remove any potential scaling problems in oil production. Unfortunately, there seem to be no two identical sets of scale-forming conditions in any two fields. Every field has its own specific set of conditions that requires its own treatment.

#### 4.4.1 Prediction

In recent years the widespread use of computers has enabled prediction methods to become more sophisticated, quicker and easier to use. Many different methods for oilfield scale prediction have been devised [4,8,9,10,11], and used as aids in selection of an effective scale prevention technique through the prediction of scaling tendency, type, and potential severity. The scaling models use actually measured solubilities in various solution compositions (oilfield brines) at various temperatures and pressures. They can take into account all the major parameters leading to scale formation at various locations within the reservoir, well, and surface equipment. Accurate water analysis of all the brines used within the prediction models are of prime importance, because any errors are carried throughout the calculations and lead to erroneous results in scale prediction.

The scaling models can predict the deposition of all the major scales, such as  $\text{BaSO}_4$ ,  $\text{SrSO}_4$ ,  $\text{CaSO}_4$  and  $\text{CaCO}_3$ . The three cations compete for available sulphate ions at differing rates due to their differences in solubility and solubility products. To avoid these differences the models use an iteration method to calculate the simultaneous deposition of more than one sulphate. The ease of predicting the major scales is as follows:  $\text{BaSO}_4 > \text{SrSO}_4 > \text{CaSO}_4 > \text{CaCO}_3$ . This is the reverse to the degree of difficulty in their removal by chemicals; in other words the easiest to remove,  $\text{CaCO}_3$ , is the hardest to predict. The newer models predict precipitations of scale forming compounds as a function of (a) mixing ratios of various waters, (b) compositions of injection and reservoir waters, (c) temperatures at any point or location in the field and (d) pressures at any point or location in the field.

One problem with these scaling models is that they only predict the precipitation of scale-forming compounds and not the adherence of the precipitated compound to metal or rock surfaces.

In some cases, severe scaling was expected from the prediction model but no scale was found in the well. Until this problem has been solved the models will only be predictions giving scaling tendencies and not actual scaling conditions found in production wells.

#### 4.4.2 Monitoring Scale Formation

A number of methods are used to monitor scale formation for comparison with predictions or to check the effectiveness of scale prevention methods. Examples of field monitoring methods include:

**Scale Coupons:** these are perforated plates placed into the field stream; they are orientated so that fluid flow impinges on the coupon creating turbulence. This causes scaling tendencies, if present, to accelerate. The coupons are initially cleaned and weighed, inserted into the system for a set specified time, dried and reweighed with the quantity of scale deposited being recorded.

**Caliper Measurement:** these measurements are conducted by running a special tool into the production tube by wire. The tool has a series of spreading fingers which measure the hole diameter for comparison with the installed diameter, hence giving a measure of scale thickness.

**Strain Gauge Monitoring:** these permanently installed instruments measure mechanical stress which varies in proportion to the weight of the production string. As scale builds up as a coating on the production tube, an increase in the string weight occurs.

**Material Balances:** water analysis is used to determine material balance calculations where scale deposition is expected. Any deposition of  $\text{BaSO}_4$  in the production tube would result in a decrease in the level of barium determined in the produced water and is a potential measure of scale production. Another ion,

usually  $\text{Cl}^-$ , known not to deposit, is used as a base line so that errors from evaporation, sampling, etc. are taken into account. However, other problems still occur with this method of measuring scale formation because (a) barium levels can vary and (b) the method does not distinguish between removal of barium as a scale in the production tube or as a deposit deeper in the formation.

Other methods used for monitoring scale formation are test nipples and differential thermocouples which are both used within the production pipelines.

#### **4.4.3 Removal Techniques**

Once scale deposits are encountered in a production well, there are three different types of remedial measures which can be taken. These are (a) mechanical methods, (b) chemical methods and (c) a combination of mechanical and chemical methods. Examples of the mechanical and chemical methods are discussed in the following section.

##### **(a) Mechanical methods:**

Many mechanical methods have been used to remove scale deposits. Drilling, scraping and hammering out are the oldest methods used. When severe scale deposits occur, they may be removed by underreaming, which removes the scale, resulting in an undesirable widening of the tubing. High pressure jets using compressed air and water or, in severe cases, sand jetting/blasting can be used to remove scale. Explosives have been used to remove downhole scale deposits but care is required to ensure enough explosive is used to pulverise the scale without damaging any piping. Newer methods like ultrasonic cleaning to break up scale deposits are becoming very popular. If scaling occurs in the formation rock it can be bypassed by fracturing. Mechanical scale removal is expensive (cost of equipment), but it can be used regardless of scale type. Mechanical workover is not an effective method for well restimulation because it does not entirely remove scale and may result in a residual

impermeable skin caused by scale cuttings squeezed into the formation.

**(b) Chemical methods:**

Chemical removal of scale is different for each scale type encountered. Each of the four major types of scale need different chemical treatments to remove them from a wellbore or a formation, and each of these will be discussed in this section.

**BaSO<sub>4</sub>:** chemical removal of BaSO<sub>4</sub> scale is notoriously difficult because of its insolubility in acids and poor solubility in strong complexing agents like EDTA (ethylene diamine tetra-acetic acid), NTA (nitrilotriacetic acid) and similar chelating agents. The main disadvantage with the complexing agents is that it takes too much time to dissolve enough BaSO<sub>4</sub> to obtain a measurable beneficial effect. Mechanical techniques are the only effective removal methods for BaSO<sub>4</sub> scale at present.

**SrSO<sub>4</sub>:** strontium sulphate scale is normally found with BaSO<sub>4</sub>, or as a mixed scale, (Ba,Sr)SO<sub>4</sub>. As SrSO<sub>4</sub> behaves like BaSO<sub>4</sub>, it is difficult to treat chemically as already discussed and is removed like BaSO<sub>4</sub> by mechanical methods.

**CaSO<sub>4</sub>:** this scale can be removed with several types of chemical agent. Strong alkaline solutions (NaOH, KOH), various sequestrants (EDTA, NTA) and salt converters (proprietary compounds containing low molecular weight organic acids as major ingredients) are effective in removing CaSO<sub>4</sub>. Problems can occur because some treating agents are effective only on gypsum and not on anhydrite or vice versa, but other treatments can remove both forms of CaSO<sub>4</sub>.

**CaCO<sub>3</sub>:** this scale is the easiest to remove. It is acid soluble and dissolves rapidly in many types and strengths of acids. Selection is based on cost, safety, disposal, corrosion, etc.

#### 4.4.4 Chemical Inhibition

Many chemicals can inhibit scale formation. Among these are inorganic phosphates (sodium hexametaphosphate and sodium tripolyphosphate), organo-phosphorus compounds (phosphonic acid salts and organic phosphate esters) and organic polymers (low molecular weight acrylic acid salts and polyacrylamides). These inhibitors come as either solids or liquids and have been used in the applications described in the following paragraphs [4].

Solid inhibitors (phosphates) can be applied by bypass feeders, baskets and filler packs, bottom hole well packs and formation squeeze fracturing. The liquid scale inhibitors (phosphonates and polymers) are applied by continuous injection into downhole production tubing or with fracturing fluids. Formation squeeze treatment techniques with liquid inhibitors involve slow introduction of the chemical into the formation matrix for storage and reproduction with the produced brines. The inhibitors function by interfering with the crystal growth mechanism of the scale forming solids. Weintritt and Cowan [12] showed that the crystal growth habit of  $BaSO_4$  was altered by using the organophosphorus inhibitor, ATMP, the sodium salt of aminotrimethylene phosphoric acid. The inhibitor was found to absorb onto the  $BaSO_4$  particles almost as soon as they nucleated, and decreased preferential crystal growth along the (010) face.

The use of chemical inhibitors is a very efficient method for controlling scale formation. However, using these complex compounds does involve substantial recurrent costs. This cost is small compared to a complete shutdown of a production well.

#### 4.5 LABORATORY STUDIES IN OILFIELD PRECIPITATES

When mixing incompatible waters in the oilfield, the precipitation of  $BaSO_4$ ,  $SrSO_4$ ,  $CaSO_4$  and  $CaCO_3$  occurs when the solubility product is exceeded. In formation waters, the potential scale-forming materials remain in solution because they

are in conditions of high temperature and pressure. However, on moving these waters from the formation to the surface, vast differences will occur in their physical conditions which will change their solubility product. These changes in conditions result in a decrease in the solubility in these waters, and can lead to the formation of scale.

The most obvious physical conditions affecting the numerical value of the solubility product of scale-forming materials are:

- (1) Chemical composition of brine
- (2) Temperature
- (3) Pressure

When the brine composition, temperature or pressure changes, there is also a change in the solubility product. Other factors which affect the solubility are particle sizes, time, complexing agents, mechanical agitation and pH. Many investigators have looked at the solubility of these scales in different environments, as well as trying to form scale in the laboratory. These are discussed in the following sections.

#### 4.5.1 Solubility Studies

Templeton [13] studied the solubility of  $\text{BaSO}_4$  at temperatures from 25 to 95°C in sodium chloride solutions ranging in molality between 0.1 and 5.0. For a given NaCl concentration, he found that the solubility of  $\text{BaSO}_4$  increased with increasing temperature. Templeton's data show that there are three important factors governing the solubility of  $\text{BaSO}_4$  and therefore, the possibility of forming scale, they are:

- (1) The higher the NaCl concentration of the brine, the larger the effect of temperature on  $\text{BaSO}_4$  solubility.
- (2) The higher the NaCl concentration and the higher the absolute temperature, the larger the effect of a given temperature change on the amount of precipitation.
- (3) A given change of the NaCl concentration has a larger effect

on BaSO<sub>4</sub> solubility at low NaCl concentration (below 5g NaCl/100ml brine), than at higher NaCl concentrations (above 5g NaCl/100ml brine).

Uchameyshvili *et al* [14] studied the solubility of BaSO<sub>4</sub> at temperatures from 100 to 370°C. However, the data from this work is not in good agreement with Templeton's results. At the 100°C mark, Uchameyshvili's findings are almost 25% lower than Templeton's data.

These studies did not include the effects of pressure and the presence of strontium, both of which are important in BaSO<sub>4</sub> scale formation. Collins and Zelinski [15] showed that BaSO<sub>4</sub> is soluble up to 60mg/l in some synthetic brines, and that SrSO<sub>4</sub> is soluble up to 900mg/l.

Davis and Collins [16] used sulphates tagged with <sup>35</sup>S to study the solubility of barium and strontium sulphates in strong electrolyte solutions containing NaCl, KCl, KBr, Na<sub>2</sub>B<sub>4</sub>O<sub>7</sub>, CaCl<sub>2</sub>, MgCl<sub>2</sub>, and NaHCO<sub>3</sub>. They found that the solubilities reached a maximum at concentration levels near an ionic strength of 1. They also showed that the solubility of BaSO<sub>4</sub> and SrSO<sub>4</sub> in three synthetic brines (representing formation waters) corresponded to the values predicted from the total ionic strength.

Gates and Caraway [3] also investigated the solubility and supersaturation of BaSO<sub>4</sub> in Wilmington brine, sodium chloride and distilled water. The equilibrium solubilities of BaSO<sub>4</sub> in distilled water, sodium chloride and Wilmington brine are shown in Figure 4.1. The BaSO<sub>4</sub> solubility in the sodium chloride was 6 times that of distilled water and 4 times that of the Wilmington brine under the conditions tested. They also investigated the effect of time on BaSO<sub>4</sub> supersaturation. It was shown that the barium concentration in the Wilmington brine decreased with time in supersaturated sulphate solutions. The decrease of barium concentration is shown in Figure 4.2.

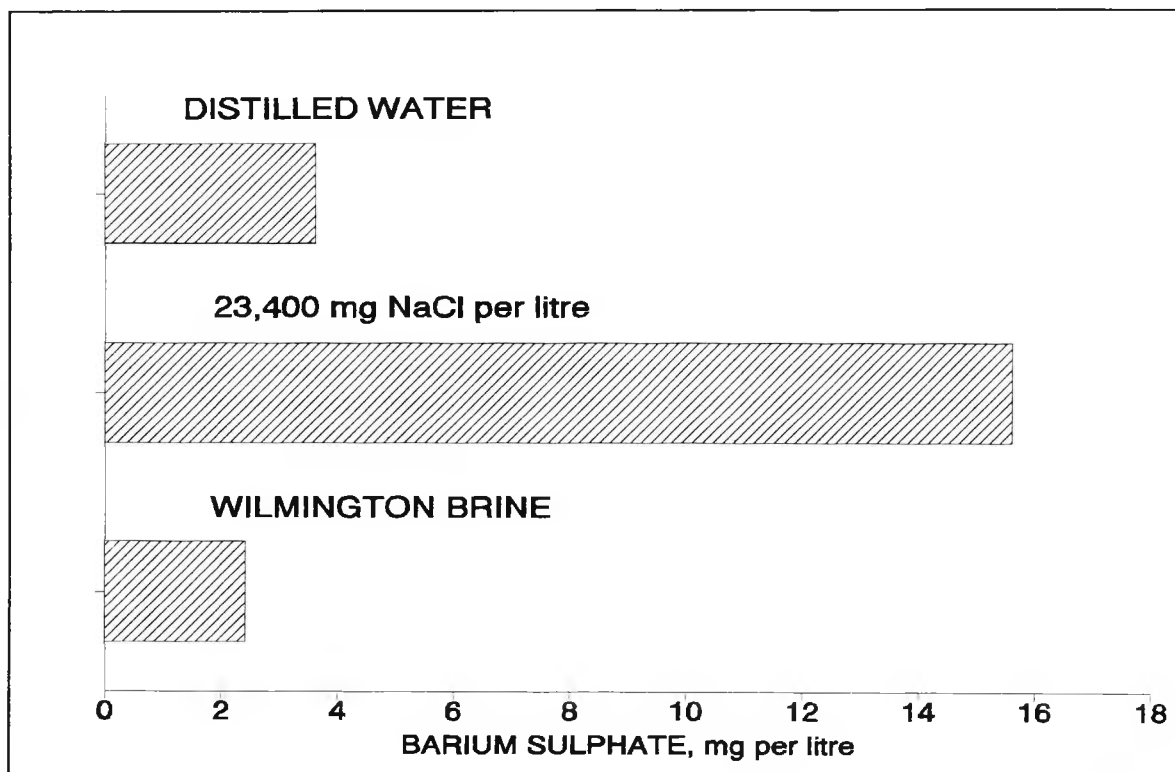


Figure 4.1 Equilibrium solubility of barium sulphate in Wilmington brine, NaCl solution (0.4M) and distilled water.

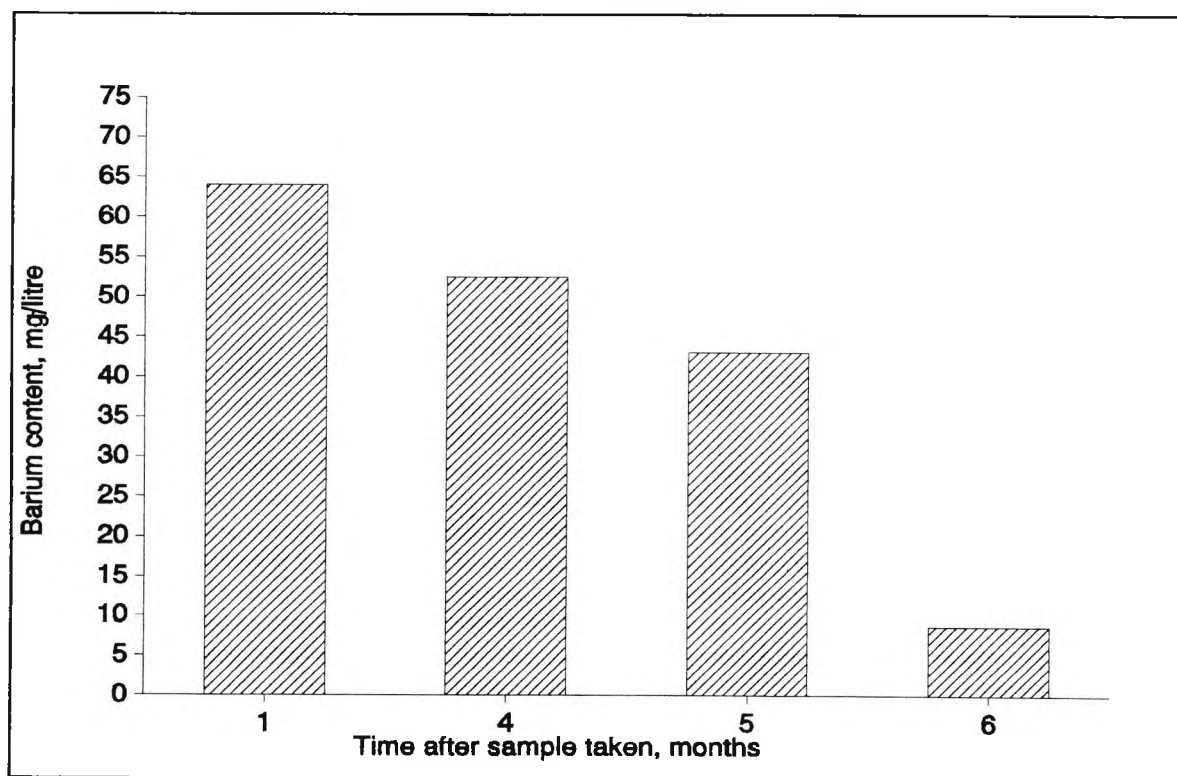


Figure 4.2 Effect of time on barium sulphate solubility in Wilmington brine.

The effects of pressure on BaSO<sub>4</sub> solubility are shown in Table 4.4 [17]. The data show that there is a 20-fold increase in the solubility of BaSO<sub>4</sub> at 500°C and 1000 bars in superheated steam, and a 50-fold increase in NaCl solution, compared to ambient temperature and atmospheric pressure data in neutral pH, salt-free water.

**Table 4.4 Solubility of BaSO<sub>4</sub> in supersaturated steam at high pressures.**

SOLUBILITY	mg/l
BaSO <sub>4</sub> in water	2
BaSO <sub>4</sub> at 206°C in water	10
BaSO <sub>4</sub> at 500°C in steam	40
BaSO <sub>4</sub> with 100g NaCl	105

Calcium sulphate crystallises from an aqueous solution in three different forms: gypsum, CaSO<sub>4</sub>.2H<sub>2</sub>O, calcium sulphate hemihydrate, CaSO<sub>4</sub>.½H<sub>2</sub>O and anhydrite, CaSO<sub>4</sub>, with each form differing in solubility. Figure 4.3 is a comparison of their solubility data in pure water at different temperatures [18], with calcium sulphate precipitation increasing as temperature increases.

Calcium sulphate solubility in sodium chloride solutions increases with increasing salinity up to 100 000 ppm chloride concentration, and then decreases again at 25°C [8,10,19]. Vetter and Phillips [20] found that at each sodium chloride concentration there is a certain pressure (critical pressure) at which calcium sulphate becomes more soluble in fresh water than in brine. This pressure depends on the sodium chloride concentration, i.e. the greater the NaCl concentration, the lower the pressure it occurs.

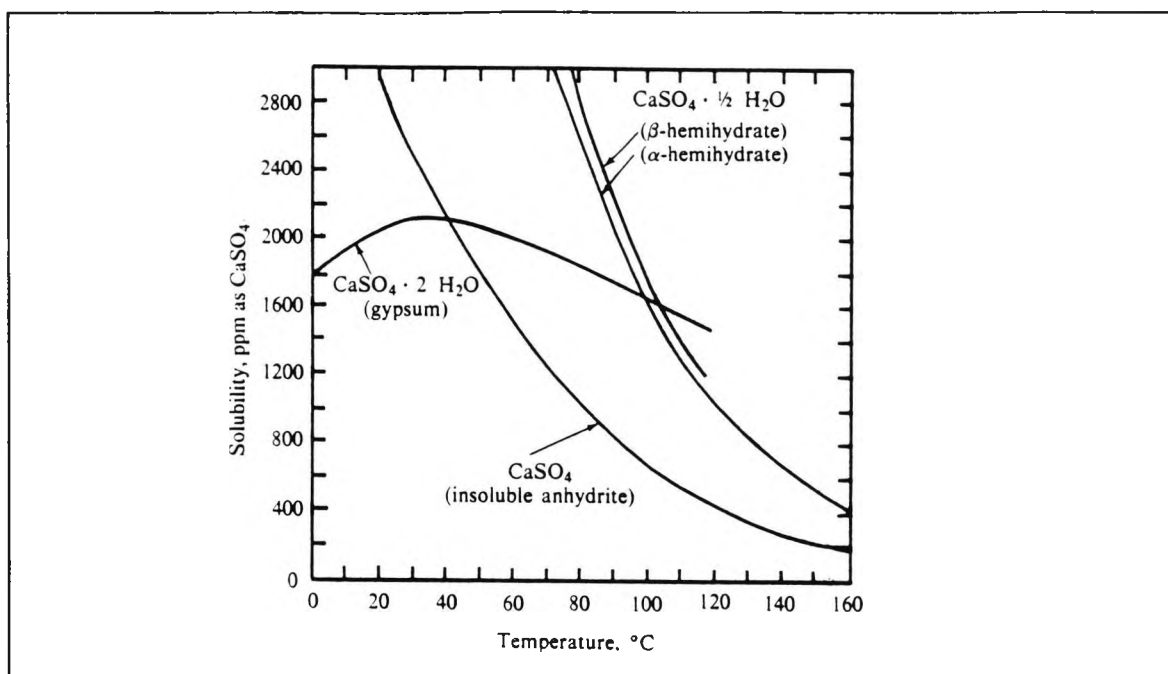


Figure 4.3 Solubility of calcium sulphate in pure water.

Higher magnesium ion concentrations greatly affect calcium sulphate solubility, as more sulphate ions are said to be tied up in the form of magnesium sulphate ion pairs. This results in greater calcium sulphate solubility [21,22]. Another factor which alters calcium sulphate solubility is pH, with an increase in solubility at lower pH values [19].

#### 4.5.2 Deposition Studies

Weintritt and Cowan [12] attempted to study the deposition rate of BaSO<sub>4</sub> under laboratory conditions, comparing the rate of deposition with the results from deposition studies of CaSO<sub>4</sub> and CaCO<sub>3</sub>. A Baroid Scale Deposition Test Cell was used for the study, which involved passing 8 litres of a 300me/l potential scaling solution at 160°F through the test cell, leaving via a 0.5 inch tubular coupon. The effluents were allowed to impinge on unetched glass slides, and both CaSO<sub>4</sub> and CaCO<sub>3</sub> deposited scale on the coupons and on the glass slides. However, BaSO<sub>4</sub> yielded profuse quantities of precipitate showing virtually no adherence to the glass slide or tubular coupon. They also attempted a series of tests, to determine the effects of pH,

catalyst, electricity, seeding, concentration, surfaces and temperature on the deposition rate of  $\text{BaSO}_4$ . All these variations led to no scale deposit, but all produced large amounts of precipitate.

These effects found by Weintritt and Cowan are the same as those found in the initial propensity to scale measurements discussed in Section 4.8., where large amounts of  $\text{BaSO}_4$  were precipitated, but no  $\text{BaSO}_4$  scale was formed. The formation of  $\text{BaSO}_4$  scale is assisted by placing  $\text{Ba}^{2+}$  and  $\text{SO}_4^{2-}$  ions in a mixed brine environment as found in formation and sea waters. However, placing  $\text{Ba}^{2+}$  and  $\text{SO}_4^{2-}$  in this environment not only forms  $\text{BaSO}_4$ , but also  $\text{SrSO}_4$ ,  $\text{CaSO}_4$  and  $\text{CaCO}_3$ , depending on the brine composition used.

Todd and Yuan [23,24] have investigated  $(\text{Ba,Sr})\text{SO}_4$  scale formation in a porous medium to gain an insight into the scale and its effect on rock permeability. They mixed two brines uniformly before passing them into a rock core (Clashach sandstone) and measuring sectional pressure differentials along the core, to permit a detailed study of permeability decline distribution. The experiments were carried out at room temperature using artificial brines and at  $70^\circ\text{C}$  with artificial brines and full component synthetic sea water and two formation waters.

The room temperature experiments considered the distribution of permeability decline rate, the effect of supersaturation and the effect of Sr/Ba ratio. Their tests indicated that  $(\text{Ba,Sr})\text{SO}_4$  solid solution scale caused significant permeability alteration in the rock cores. The formation damage was complex, with the rate of decline being a function of depth into the core.  $\text{BaSO}_4$  and  $\text{SrSO}_4$  supersaturation in a brine significantly affected permeability decline, with higher supersaturations causing more damage. Changes in strontium concentration were reported to have little influence on permeability reduction, unless the ratio of strontium to barium was high (1000:1), where drastic permeability

decline occurred.

The experiments at 70°C showed that permeability damage occurred more rapidly, the effect being more evident when cores were injected with SrSO<sub>4</sub> supersaturated brines (Sr/Ba ratio of 100) because higher temperatures not only accelerated scale formation but also created a more supersaturated solution. The increased scale formation decreased the time required to reduce the core permeability decline rate to less than half its initial value ( $t_{1/2}$ ). At 20°C the average  $t_{1/2}$  value was 122.4 minutes, but at 70°C the average value was 13 minutes. The crystal morphology of (Ba,Sr)SO<sub>4</sub> was also reported to change with higher temperatures.

The field waters used at elevated temperatures also caused severe loss of core permeability, which underlines the severity of potential formation damage arising from mixing incompatible injection sea water with formation water in the producing wellbore. The permeability decline rate was similar to that of the simple brines used, but entirely different scaling crystals from those produced from the simple brines were precipitated by mixing field waters. Yuan and Todd claimed that the distinct difference in crystal habit and size between the crystals precipitated was probably caused by the presence of ions, such as calcium, magnesium and hydrogen carbonate in the mixed waters.

Precipitation studies carried out in the City University laboratories [25], showed that there are considerable time delays in the formation of CaSO<sub>4</sub>.2H<sub>2</sub>O nuclei when solutions of calcium ion and sulphate ion are mixed.

#### 4.5.3 Uses of Laboratory Studies

The results obtained in laboratory studies can be used to estimate the precipitation tendencies of barium sulphate. Templeton's solubility studies [13] can be used to estimate the precipitation of barium sulphate due to supersaturation. His studies were limited to sodium chloride brines. Since natural

waters contain many other ionic species, the solubility data can only be used to provide an approximation of brine supersaturation with respect to barium sulphate. Templeton's solubility data for the  $\text{BaSO}_4 - \text{NaCl} - \text{H}_2\text{O}$  system at various temperatures are shown in Table 4.5. To obtain a graph of the data over a wide temperature range, the data in Table 4.5 were converted to  $\text{pK}_{\text{sp}}$  values at three temperatures, as shown in Figure 4.4. An example of the use of these data in estimating barium sulphate precipitation tendencies is shown below for the standard barium, sulphate and chloride ion concentrations used in the propensity to scale measurements.

**Table 4.5 Solubility data for  $\text{BaSO}_4 - \text{NaCl} - \text{H}_2\text{O}$  system at various temperatures.**

NaCl (M)	Molal Basis					
	25°C	35°C	50°C	65°C	80°C	95°C
0.000	1.08	1.25	1.44	1.54	1.62	1.68
0.001	1.28	1.46	1.69	1.83	1.92	1.97
0.005	1.60	1.81	2.10	2.31	2.47	2.55
0.01	1.84	2.08	2.43	2.70	2.90	3.05
0.05*	3.02	3.49	4.00	4.37	4.67	4.85
0.1	3.92	4.47	5.20	5.78	6.13	6.30
0.2	5.2	5.8	6.9	7.7	8.4	8.8
0.4	6.7	7.5	8.9	10.3	11.7	12.7
0.6	7.8	8.8	10.5	12.4	14.3	15.8
0.8	8.8	9.8	11.7	14.2	16.3	18.3
1.0	9.6	10.6	12.8	15.5	18.1	20.5
1.5	11.2	12.4	14.9	18.0	21.2	24.9
2.0	12.5	13.8	16.5	19.9	23.7	28.1
2.5	13.5	14.8	17.7	21.2	25.2	30.6
3.0	14.4	15.7	18.7	22.3	26.5	32.8
3.5	15.3	16.6	19.7	23.2	27.7	34.7
4.0	16.1	17.5	20.6	24.1	28.8	36.4
4.5	16.9	18.5	21.4	25.1	29.9	38.0
5.0	17.7	19.4	22.2	26.0	30.9	39.7

\* Approximate lowest ionic strength experimentally studied in the present work.

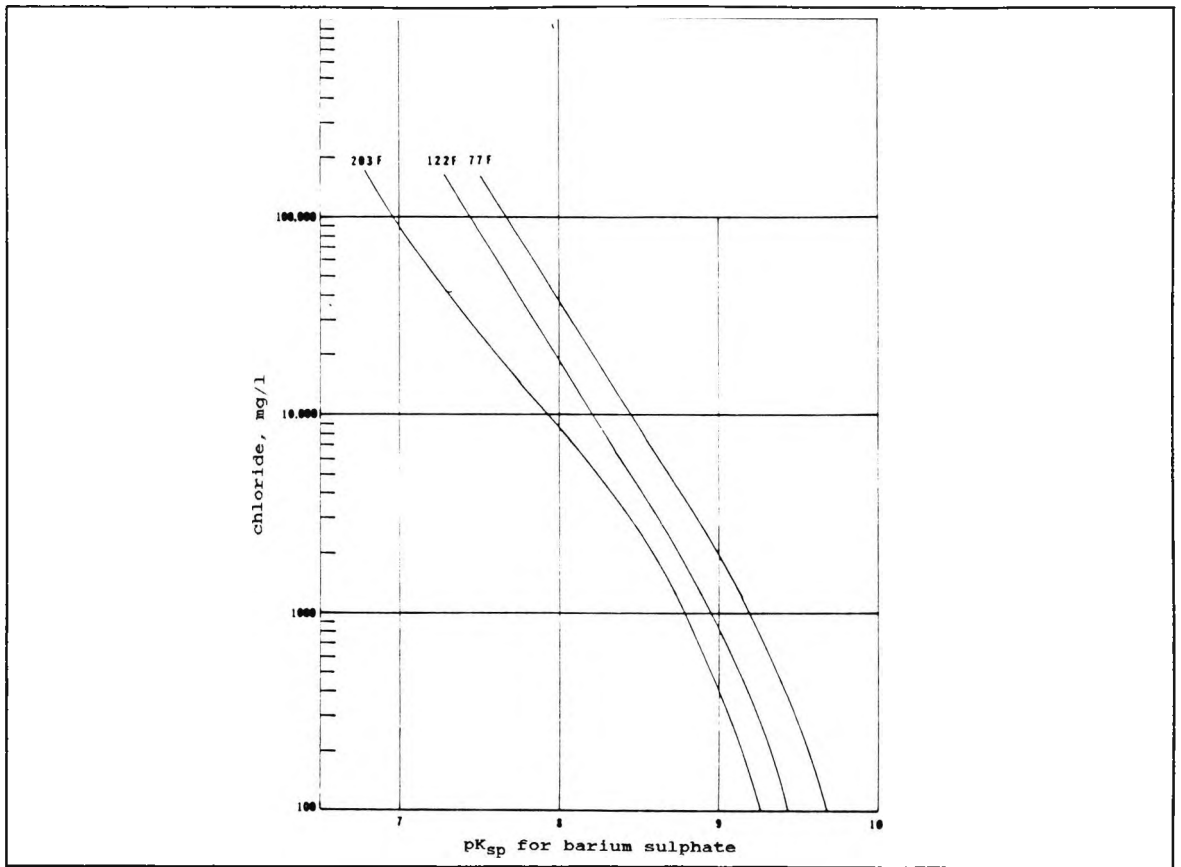


Figure 4.4 Graph showing  $pK_{sp}$  for barium sulphate against chloride concentration taken from Table 4.5.

$$Cl^{-}, \text{ mg/l} = 17309 \quad SO_4^{2-}, \text{ mg/l} = 1350 \quad Ba^{2+}, \text{ mg/l} = 75.0$$

The following is an example to calculate the solubility of barium sulphate at 95°C in standard formation and sea water.

The  $pK_{sp}$  value was found from Figure 4.4, and was 7.70 for a chloride concentration of 17309 mg/l.

1. Calculate the  $K_{sp}$  at 203°F. (Figure 4.4)

$$pK_{sp} = 7.70$$

$$- \log K_{sp} = 7.70 = 10 - 2.30$$

$$\log K_{sp} = 2.30 - 10$$

$$\text{antilog } 2.30 = 199$$

$$K_{sp} = 199 \times 10^{-10}$$

2. Calculate the observed molar concentrations of barium and sulphate:

$$\begin{aligned}\text{Ba}^{2+} &= (75 \text{ mg/l}) / (1000 \text{ mg/g} \times 137.36 \text{ g/mole}) \\ &= 0.000546 \text{ moles/litre} = 5.46 \times 10^{-4}\end{aligned}$$

$$\begin{aligned}\text{SO}_4^{2-} &= (1350 \text{ mg/l}) / (1000 \text{ mg/g} \times 96 \text{ g/mole}) \\ &= 0.0140625 \text{ moles/litre} = 1.41 \times 10^{-2}\end{aligned}$$

3. Satisfy the calculated  $K_{sp}$  with the general equation:

$$(\text{Ba}^{2+} - x) (\text{SO}_4^{2-} - x) = 199 \times 10^{-10} = K_{sp}$$

Where  $\text{Ba}^{2+}$  is the observed barium concentration in moles/litre;  
 $\text{SO}_4^{2-}$  is the observed sulphate concentration in moles/litre;  
 $x$  is the amount of  $\text{Ba}^{2+}$ , or  $\text{SO}_4^{2-}$ , or  $\text{BaSO}_4$  in  
moles/litre which must precipitate to satisfy the  $K_{sp}$ .

$$(5.46 \times 10^{-4} - x) (1.461 \times 10^{-2} - x) = K_{sp} = 199 \times 10^{-10}$$

$$(7.678 \times 10^{-6}) - (1.461 \times 10^{-2})x - (5.46 \times 10^{-4})x + x^2 = K_{sp}$$

$$x^2 - (1.406 \times 10^{-2})x + 7.678 \times 10^{-6} = 0.0199 \times 10^{-6}$$

$$x^2 - 0.01406x + 7.6582 \times 10^{-6} = 0$$

4. This quadratic equation can be solved with:

$$x = [-b \pm (b^2 - 4ac)^{1/2}] / 2a$$

$$x = \frac{7.658 \times 10^{-6} \pm [(7.658 \times 10^{-6})^2]^{1/2}}{2 \times 0.0141} = 5.445 \times 10^{-4}$$

5. Solving for  $x$ :

$$5.445 \times 10^{-4} \text{ mols/litre} \times 233.42 = 127.1 \text{ mg/l barium sulphate precipitated from the water.}$$

#### 4.6 OBJECTIVES

The work described in this chapter is a detailed study into scale formation in the off-shore oil industry. It determines the effects of all ions in formation and sea waters on the precipitation and crystallisation processes of the scale precipitates formed from simulated formation and sea water fluids. Work was carried out looking at two different systems which form scale in the off-shore oil industry. The first system investigated was the  $\text{BaSO}_4$ - $\text{SrSO}_4$ - $\text{CaCO}_3$  scale formation system, which consisted of mixing formation waters containing  $\text{Ba}^{2+}$  and  $\text{Sr}^{2+}$  with sea waters containing  $\text{HCO}_3^-$  and  $\text{SO}_4^{2-}$  (with both waters having low  $\text{Ca}^{2+}$  concentrations to precipitate  $\text{CaCO}_3$  only). The work carried out for this system involved changing one ion in either formation or sea water to determine what effect this would have on the rate at which these scales form at differing temperatures. The ratios at which formation and sea waters were mixed together were also studied to determine which scales predominate at a particular ratio, and to find the maximum and minimum scale-forming ratios. The effects of chemical changes on the crystallisation and precipitation processes were measured quantitatively, using two techniques:

- (i) Propensity to scale measurements of the precipitates formed (Dynamic test).
- (ii) Precipitation studies to evaluate the precipitates formed (Static test).

The second system investigated was the  $\text{CaSO}_4$ - $\text{CaCO}_3$  scale formation system, which consisted of mixing formation waters containing high  $\text{Ca}^{2+}$  concentrations with sea waters containing  $\text{HCO}_3^-$  and high  $\text{SO}_4^{2-}$  concentrations, with neither water containing  $\text{Ba}^{2+}$  or  $\text{Sr}^{2+}$  ions. The work carried out for this system involved changing one ion in either formation or sea water to determine what effect this would have on the rate at which these scales would form at differing temperatures, keeping the ratio of mixing constant. The effects of chemical changes on the crystallisation

and precipitation processes were measured quantitatively using the propensity to scale measurements.

#### 4.7 EXPERIMENTAL TECHNIQUES

##### 4.7.1 Propensity to Scale Measurements

The propensity to scale measurements were carried out using the P.M.A.C. pressure measurement and control equipment described in Chapter 2 (Section 2.1), for the  $\text{BaSO}_4$ - $\text{SrSO}_4$ - $\text{CaCO}_3$  scaling system. The initial experiments were based on mixing solutions of  $\text{Ba}^{2+}$  and  $\text{SO}_4^{2-}$  in sodium chloride, which produced copious quantities of  $\text{BaSO}_4$  precipitate, but no scale. The formation of  $\text{BaSO}_4$  scale was induced by placing  $\text{Ba}^{2+}$  and  $\text{SO}_4^{2-}$  in mixed brine environments as found in formation and sea waters. The concentrations of the waters were set so that only  $\text{BaSO}_4$ ,  $\text{SrSO}_4$  and  $\text{CaCO}_3$  would deposit. The measurements were based on the time taken for the scale formed from the mixing of formation water and sea water solutions to build up to back pressures of 1.0 or 4.0 pounds per square inch (psi) in the microbore tube above the distilled water base line. The changes in back pressure measurements were recorded on a chart recorder set at a chart speed of  $6 \text{ cm hr}^{-1}$ . In the concentration experiments the simulated solutions of formation water and sea water were pumped into the microbore tube at a fixed temperature and at set flow rates using single channel pumps for both fluids. However, in the ratio experiments, depending on the ratio used, either single or double channel pumps were used for the two waters. Details of the chemical content of both of these fluids are given in Section 4.9. The recorded outputs for the propensity to scale measurements for this system are shown in Figure 4.5 for the time taken for scale to form to pressures of 1 and 4 psi, for the experiments discussed in Section 4.10.3 for the magnesium ion concentrations of 375 and 2250 ppm at 40 and 50°C.

The microbore tube was cleaned by (i) continuously circulating 20% EDTA disodium salt solution containing 5% potassium hydroxide

through the microbore tube until the back pressure baseline returned to the lowest attainable value, (the function of the EDTA is to dissolve the  $\text{BaSO}_4$  and  $\text{SrSO}_4$  formed), (ii) distilled water was then run through the microbore tube to remove any traces of EDTA together with dissolved salts, (iii) 10ml of 10% dilute nitric acid was then injected to dissolve any remaining  $\text{CaCO}_3$ , returning the baseline to its base value and finally (iv) the microbore tube was again flushed through with distilled water.

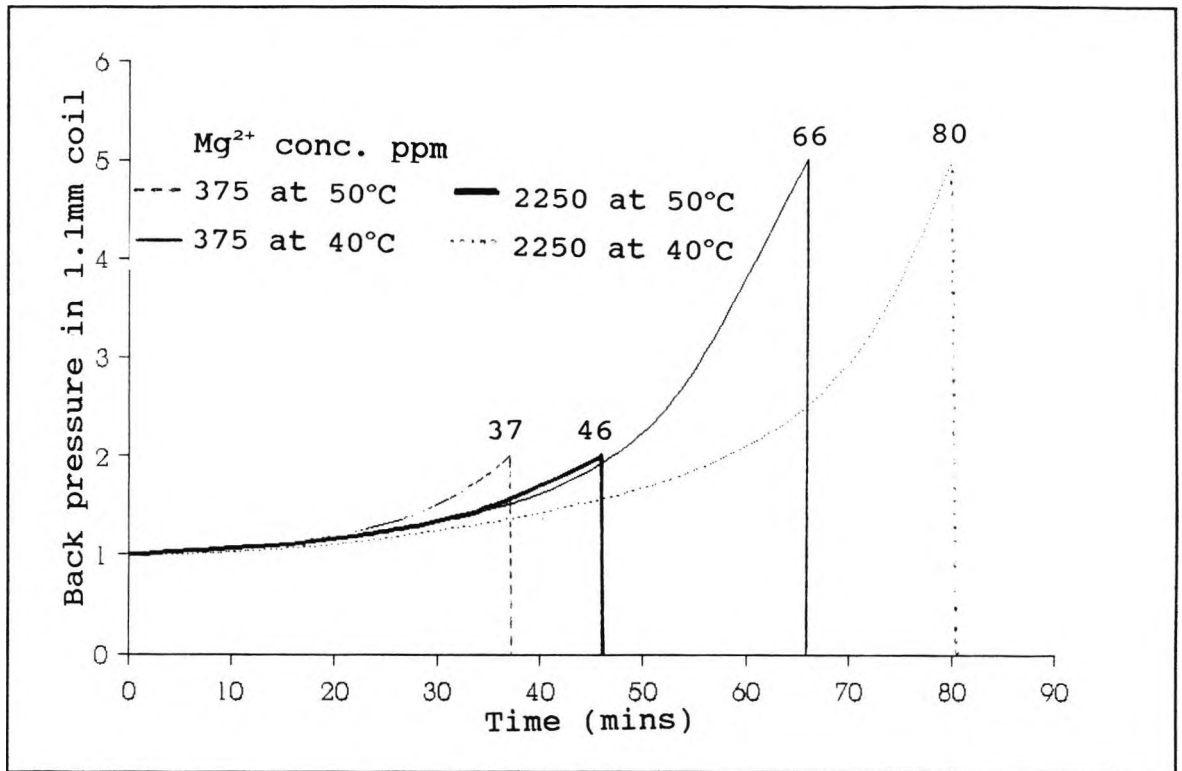


Figure 4.5 Scaling profile for the  $\text{BaSO}_4$ - $\text{SrSO}_4$ - $\text{CaCO}_3$  system.

The propensity to scale measurements for the  $\text{CaSO}_4$ - $\text{CaCO}_3$  system were carried out using the P.M.A.C. pressure measurement and control equipment described in Chapter 2 (Section 2.1). Initial experiments were based on mixing solutions of formation water containing  $\text{Ca}^{2+}$  with sea waters containing  $\text{SO}_4^{2-}$  and  $\text{HCO}_3^-$ . No reproducible results were obtained until both solutions were filtered prior to mixing. The measurements for this system were based on the time taken for the scale to form from mixing formation and sea waters to increase the back pressure by 3 psi

in the microbore tube. The changes in back pressure measurements were recorded on a chart recorder set at a chart speed of 6 cm hr<sup>-1</sup>. In these experiments the simulated solutions of formation and sea water were pumped into the microbore tube at a fixed temperature and at set flow rates, using single channel pumps for both fluids. The recorded outputs for the propensity to scale measurements for this system are shown in Figure 4.6 for the time taken to form a scale in the experiments discussed in Section 4.13.4, for the calcium ion concentrations of 5500 and 7000 ppm at 50 and 65°C. The outputs show that there is a considerable time delay in the formation of scale when the two solutions are mixed and this was observed throughout these experiments.

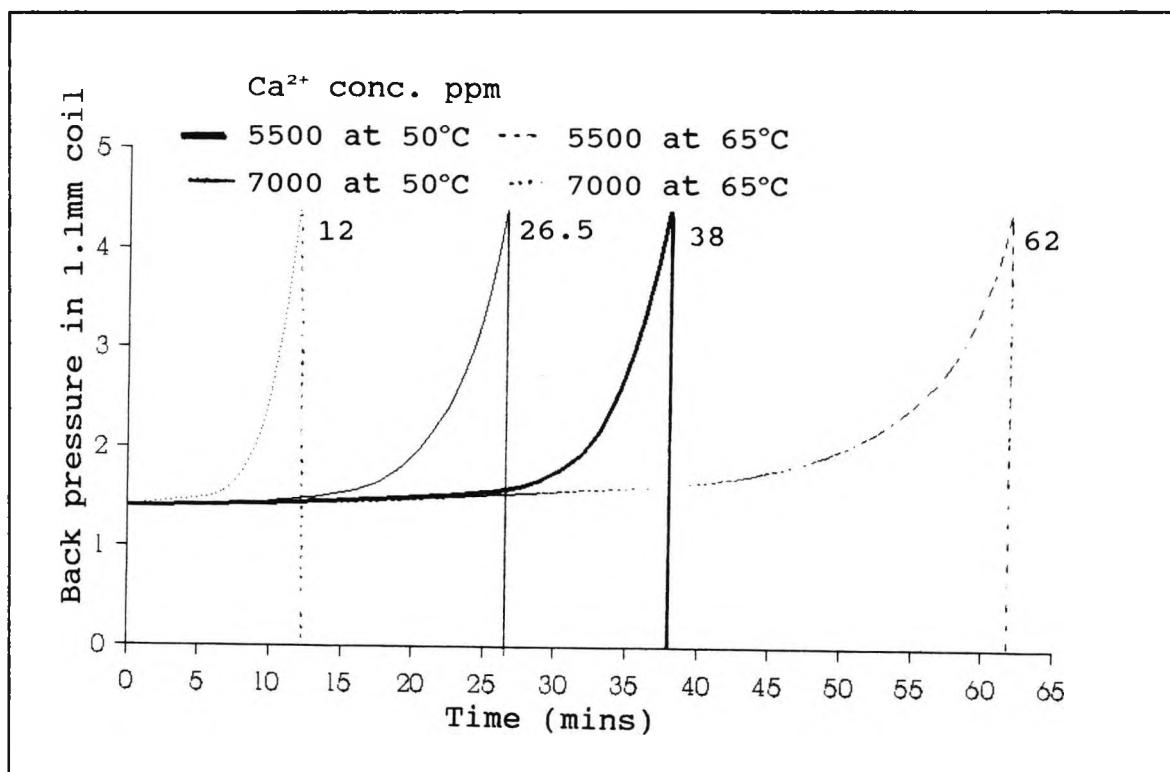


Figure 4.6 Scaling profile for the CaSO<sub>4</sub>-CaCO<sub>3</sub> system.

The microbore tube was cleaned by (i) injecting 15 ml of 10% dilute nitric acid to dissolve CaSO<sub>4</sub> and CaCO<sub>3</sub>, returning the baseline to its base value and (ii) flushing the tube with distilled water to remove any traces of nitric acid together with dissolved salts.

#### 4.7.2 Precipitation Studies

The propensity to scale data for the  $\text{BaSO}_4$ - $\text{SrSO}_4$ - $\text{CaCO}_3$  scaling system were used to indicate which fluid compositions needed to be further studied by precipitation experiments. Precipitation studies were carried out when unexplained but significant differences were found in the propensity to scale measurements arising from either changing one component in the formation or sea waters, or their ratio of mixing. The precipitation studies were designed to determine which precipitates formed when the waters were mixed at a given temperature. The initial chemical compositions of the waters were known so that after mixing them analysis of the remaining solution provided information on the amounts of  $\text{BaSO}_4$ ,  $\text{SrSO}_4$  and  $\text{CaCO}_3$  deposited. The tests were only carried out for the highest and lowest ion concentrations being investigated in order to maximise potential differences. No precipitation studies were carried out for the  $\text{CaSO}_4$ - $\text{CaCO}_3$  system because the predominant scale was  $\text{CaSO}_4$  and all the differences were either solubility or kinetic effects on  $\text{CaSO}_4$  deposition.

The precipitation tests were carried out in triplicate in closed 250ml glass jars, containing 100ml of formation water and 100ml of sea water. The glass jars were shaken to ensure complete mixing and placed in an oven for 36 hours at 40, 60 and 80°C to equilibrate precipitation. The jars were cooled to ambient temperature and the precipitates were filtered to leave clear solutions for analysis. The three main cations, barium, strontium and calcium were analysed by A.A.S. (Section 2.2). The only anion to be analysed was sulphate and this was determined by ion-exchange chromatography, (Section 2.3).

The results of the precipitation study were compared with data from a scaling prediction model for mixed brines [26]. The scaling prediction was carried out using computer models which forecast the types of scale that were likely to form and the quantity of each type in mg scale/kg mixed brines. These forecasts were made from a knowledge of the solubility product

of each scale type and the conditions under which precipitation was likely to occur. The model included allowances for temperature, pH and specific gravity of each water, the concentrations of ions and the ratio of formation water to sea water mixing.

#### 4.8 PROPENSITY TO SCALE EXPERIMENTS

For the  $\text{BaSO}_4$ - $\text{SrSO}_4$ - $\text{CaCO}_3$  scaling system, four sets of propensity to scale experiments were carried out to determine:

- (i) The effect of varying the concentrations of constituent ions in simulated formation water on the propensity to scale (Section 4.9).
- (ii) The effect of varying the concentrations of constituent ions in simulated sea water on the propensity to scale (Section 4.10).
- (iii) The effect of mixing the most and least scale-forming formation water and sea water concentrations as determined in (i) and (ii) (Section 4.11).
- (iv) The effect of ratio mixing of simulated formation and sea waters on the propensity to scale (Section 4.12).

For the  $\text{CaSO}_4$ - $\text{CaCO}_3$  scaling system, two sets of propensity to scale experiments were carried out to determine:

- (i) The effect of varying the concentrations of constituent ions in simulated formation water on the propensity to scale (Section 4.13).
- (ii) The effect of varying the concentrations of constituent ions in simulated sea water on the propensity to scale (Section 4.14).

Sufficient replicate propensity to scale runs were carried out in each set of experiments to obtain statistically significant results, taken as being situations in which the standard deviation was less than 9% of the mean (the detailed S.D. calculations are given in Appendix B).

#### 4.9 THE EFFECT OF VARYING THE CONCENTRATIONS OF CONSTITUENT IONS IN SIMULATED FORMATION WATERS ON THE PROPENSITY TO SCALE

The standard simulated formation and sea waters used in the propensity to scale experiments were made up by dissolving the quantities of salts shown in Table 4.6 and 4.7 to give the significant ion concentrations listed.

**Table 4.6 Standard simulated formation water composition used in the propensity to scale measurements.**

Salt compound	Weight used g/l	Significant cation ppm
NaCl	23.0	9048
KCl	0.477	250
MgCl <sub>2</sub> .6H <sub>2</sub> O	1.297	155
CaCl <sub>2</sub> .2H <sub>2</sub> O	1.65	450
SrCl <sub>2</sub> .6H <sub>2</sub> O	0.6846	225
BaCl <sub>2</sub> .2H <sub>2</sub> O	0.2669	150

The standard formation water was used as the base line against which waters of other concentrations were compared. It had a chloride concentration of 15686 ppm, a pH of 5.59 and a specific gravity of 1.018. The aim of this set of experiments was to determine the effects of varying each significant cation concentration in the formation water separately leaving the other concentrations unchanged. The propensity to scale of each formation water was then measured using the standard sea water as the precipitant, which had a chloride concentration of 18932 ppm, a pH of 7.56 and a specific gravity of 1.025. Ten litres of each simulated water were used in each set of propensity to scale measurements carried out over a range of temperatures.

The mixing flow rates for the experiments in this section were kept constant at 50:50, with each delivering 0.5 litres per hour of formation or sea water into the P.M.A.C. microbore tube

(except for the variation of barium ion concentration experiments described in Section 4.9.6). The propensity to scale was measured for an increase in back pressure of 1 or 4 psi above the distilled water base line for each concentration investigated at temperatures of 40, 50, 60, 70, 80, and 90°C. For each set of conditions, four or five experiments were carried out to ensure that statistically significant results were achieved. After each experiment, the normal cleaning procedure was carried out as described in Section 4.7.1.

**Table 4.7 Standard simulated sea water composition used in the propensity to scale measurements.**

Salt compound	Weight used g/l	Significant ion ppm
NaCl	23.0	10529
KCl	0.753	395
MgCl <sub>2</sub> .6H <sub>2</sub> O	11.209	1340
CaCl <sub>2</sub> .2H <sub>2</sub> O	1.467	400
SrCl <sub>2</sub> .6H <sub>2</sub> O	0.0243	8
NaHCO <sub>3</sub>	0.688	500
Na <sub>2</sub> SO <sub>4</sub>	3.995	2700

**4.9.1 The Effect of Varying the Sodium Chloride Concentration in Simulated Formation Water on the Propensity to Scale**

The sodium chloride concentrations used and the physical properties of the formation waters studied are given in Table 4.8. All other ion concentrations in the formation water were kept constant. The pump speeds were set at Pump A, 54.5% and Pump B, 57.0%.

The data for the average scaling times for the sodium chloride concentration experiments are given in Table 4.9 and shown graphically in Figure 4.7. The details of replicate runs for each

sodium chloride concentration experiment are given in Appendix Tables B.1 to B.4.

**Table 4.8 Changes in chemical composition on varying the sodium chloride concentration in formation water.**

Na <sup>+</sup> ppm	Cl <sup>-</sup> ppm	NaCl wt. (g/l)	pH	S.G.
3934	7800	10.0	5.68	1.009
7868	13866	20.0	5.89	1.016
11802	19932	30.0	5.91	1.022
15736	25998	40.0	5.93	1.029

The results indicate that varying the concentration of sodium chloride in simulated formation waters significantly influences the rate of deposition of scale. The rate is significantly increased as the sodium chloride concentration is decreased. The three lowest concentrations tested (NaCl concentrations of 10, 20, 30 g/l) show this trend at all of the temperatures tested. The biggest differences were at 40°C, where the formation water containing 30 g/l NaCl took 16 minutes longer than the formation water containing 10 g/l NaCl to form scale. At 90°C, the time difference was reduced to 5.4 minutes. However, when the sodium chloride concentration in the formation water was increased to 40 g/l, no significant differences in propensity to scale were found when compared to the formation water containing 30 g/l NaCl, at temperatures up to 60°C. At temperatures above 60°C, slight time differences were observed for the formation water containing 40 g/l NaCl. The effect of temperature on the propensity to scale measurements is also evident, and as expected the rate of deposition of scale was shown to increase with temperature.

The results of varying the sodium chloride concentration in a formation water show that there are statistically significant increases in the rate of deposition as the sodium chloride

Table 4.9 Effect of different sodium chloride concentrations on an increase in back pressure of 1 psi: Average scaling times (mins).

Temp °C	NaCl (10 g/l)	NaCl (20 g/l)	NaCl (30 g/l)	NaCl (40 g/l)
40	36.6	41.4	53.2	53.6
50	32.4	34.6	45.0	44.4
60	25.2	30.2	35.2	35.0
70	22.6	25.4	28.4	31.6
80	19.6	23.6	25.8	28.4
90	18.4	21.0	23.8	26.0

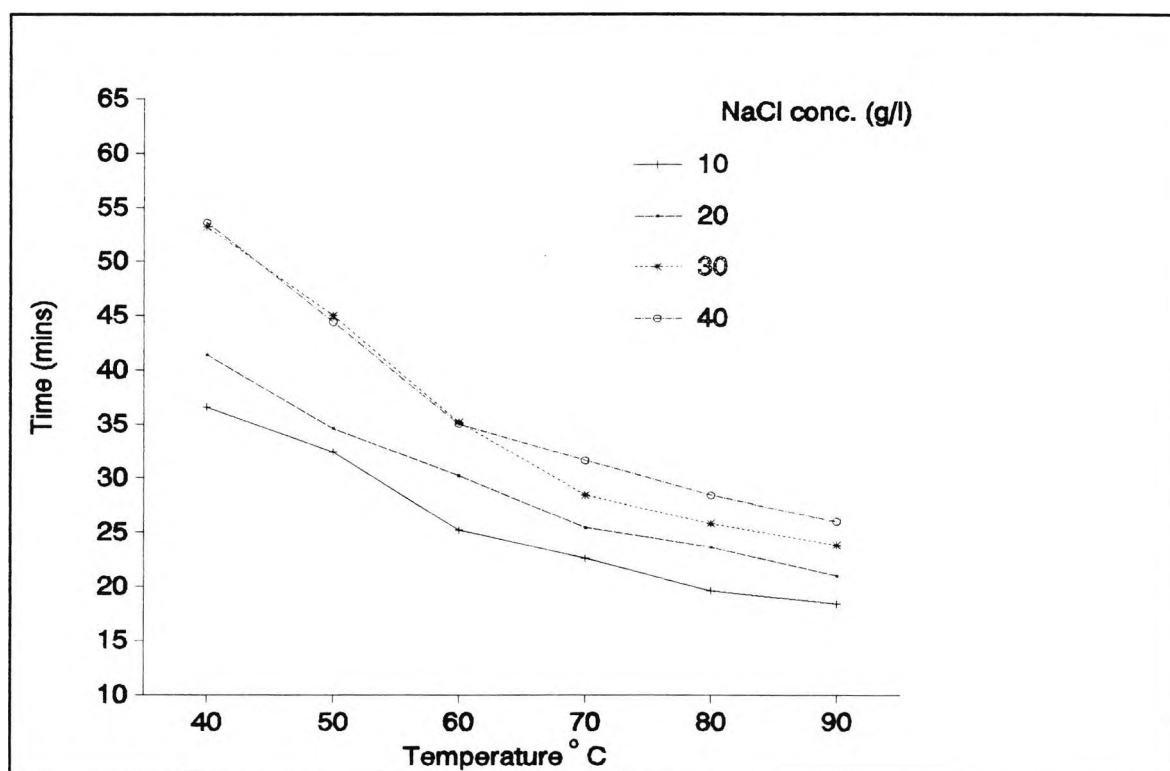


Figure 4.7 Effect of different sodium chloride concentrations on the average scaling times.

concentration is decreased. Therefore precipitation studies were carried out to determine which precipitates were forming at the

highest and lowest sodium chloride concentrations in the formation waters used. The experimental procedure for the precipitation tests is described in Section 4.7.2 and the results (mg scale/ kg mixed brines) are given in Table 4.10.

**Table 4.10 Weights (mg scale/ kg mixed brines) of each precipitate deposited.**

NaCl 10 g/l				NaCl 40 g/l			
Temp°C	CaCO <sub>3</sub>	SrSO <sub>4</sub>	BaSO <sub>4</sub>	Temp°C	CaCO <sub>3</sub>	SrSO <sub>4</sub>	BaSO <sub>4</sub>
40	76	112	127	40	75	93	127
60	115	141	127	60	111	116	127
80	149	167	127	80	139	148	127

The results show that at both sodium chloride concentrations and at each temperature there were no significant differences in the weights of calcium carbonate precipitated. The effect of temperature on calcium carbonate deposition is, however, apparent and increases as the temperature rises because of the increased decomposition of hydrogen carbonate ion to carbonate ion (see Chapter 3). For strontium sulphate there is a noticeable reduction in the weights precipitated between the high and low sodium chloride solutions at all three temperatures. This reduction is caused by the increased solubility of strontium sulphate in waters containing higher sodium chloride concentrations [16]. The rate of deposition of strontium sulphate increases with temperature. The data show that barium sulphate precipitation is not affected by an increase in sodium chloride concentration or temperature; this is possibly an unexpected result considering suggestions that barium sulphate is more soluble in higher sodium chloride concentrations and at higher temperatures [13,14]. The differences detected in the work containing these suggestions, however, corresponded to less than 1 mg/kg of barium sulphate precipitate formed for the conditions used in the precipitation tests carried out in the present work.

The data from Tables 4.9 and 4.10, in combination with Figure 4.7, demonstrate that as the sodium chloride concentration increases in formation waters the propensity to scale and the weight of precipitate are reduced. These effects are controlled by two main factors: the precipitation of  $\text{CaCO}_3$ ,  $\text{SrSO}_4$  and  $\text{BaSO}_4$  and the aggregation of these precipitates to form scale. In the precipitation studies the two solutions have ample time to mix and produce the maximum quantity (in weight) of each precipitate. To further explain the differences found, the scaling prediction model [26] was used for the sodium chloride concentrations of 10 and 40 g/l at temperatures of 40, 60 and 80°C, and the predicted results (mg scale/ kg mixed brines) are given in Table 4.11.

**Table 4.11 Predicted weight (mg scale/ kg mixed brines) of each precipitate deposited.**

NaCl 10 g/l				NaCl 40 g/l			
Temp°C	$\text{CaCO}_3$	$\text{SrSO}_4$	$\text{BaSO}_4$	Temp°C	$\text{CaCO}_3$	$\text{SrSO}_4$	$\text{BaSO}_4$
40	3.7	138.5	125.2	40	32.8	88.5	123.9
60	60.5	145.9	125.1	60	79.2	100.4	123.8
80	101.4	157.3	125.0	80	112.8	117.3	123.6

The experimental data for the weights of precipitates (Table 4.10) can be compared with those predicted by a scaling model (Table 4.11). There are significant differences between the observed and calculated weights for calcium carbonate and strontium sulphate deposition. The differences for calcium carbonate can be explained in terms of the increased time allowed for equilibration in the precipitation experiments which permits increased decomposition of hydrogen carbonate ion to carbonate ion. The smaller differences for strontium sulphate must also arise from the extra time allowed for equilibration which would maximise the deposition of strontium sulphate (the most soluble compound in the scale system). There were no differences in the observed and calculated weights of barium sulphate deposition.

The precipitation tests and the scaling prediction model results illustrate that the quantity of precipitate formed is reduced as the sodium chloride concentration is increased in formation waters. This is confirmed in the propensity to scale experiments.

#### 4.9.2 The Effect of Varying the Potassium Ion Concentration in Simulated Formation Water on the Propensity to Scale

The potassium chloride concentrations used and the physical properties of the formation waters studied are given in Table 4.12. All the other ion concentrations in the formation water were unchanged. The pump speeds were set at Pump A, 54.5% and Pump B, 57.0%.

**Table 4.12 Changes in chemical composition on varying the potassium chloride concentration in formation water.**

K <sup>+</sup> ppm	Cl <sup>-</sup> ppm	KCl wt. (g/l)	pH	S.G.
100	15550	0.1907	5.59	1.017
500	15912	0.9535	5.65	1.018
1000	16366	1.907	5.60	1.019
1500	16819	2.8605	5.85	1.020

The data for the average scaling times for the potassium ion concentration experiments are given in Table 4.13, and shown graphically in Figure 4.8. The details of replicate runs for each potassium ion concentration experiment are given in Appendix Tables B.5 to B.8.

The results indicate that varying the concentration of potassium ion in formation water does not have any effect on the rate of deposition of scale. At all the temperatures tested, except 40°C, the average scaling time for an increase of back pressure of 1 psi varied by less than 2 minutes at all concentrations. The consistency of the measurements is shown in Figure 4.9, for five repeat runs of propensity to scale measurement for a potassium

ion concentration of 500 ppm at temperatures of 40, 60 and 80°C, giving standard deviations of 1.95, 0.71 and 0.55, respectively.

**Table 4.13 Effect of different potassium ion concentrations on an increase in back pressure of 1 psi: Average scaling times (mins)**

Temp °C	K <sup>+</sup> 100ppm	K <sup>+</sup> 500ppm	K <sup>+</sup> 1000ppm	K <sup>+</sup> 1500ppm
40	50.6	49.6	48.8	46.8
50	39.4	40.2	39.6	39.4
60	32.6	34.0	32.8	32.8
70	29.4	29.0	28.0	28.2
80	25.2	26.6	25.4	27.8
90	23.4	24.6	24.0	25.0

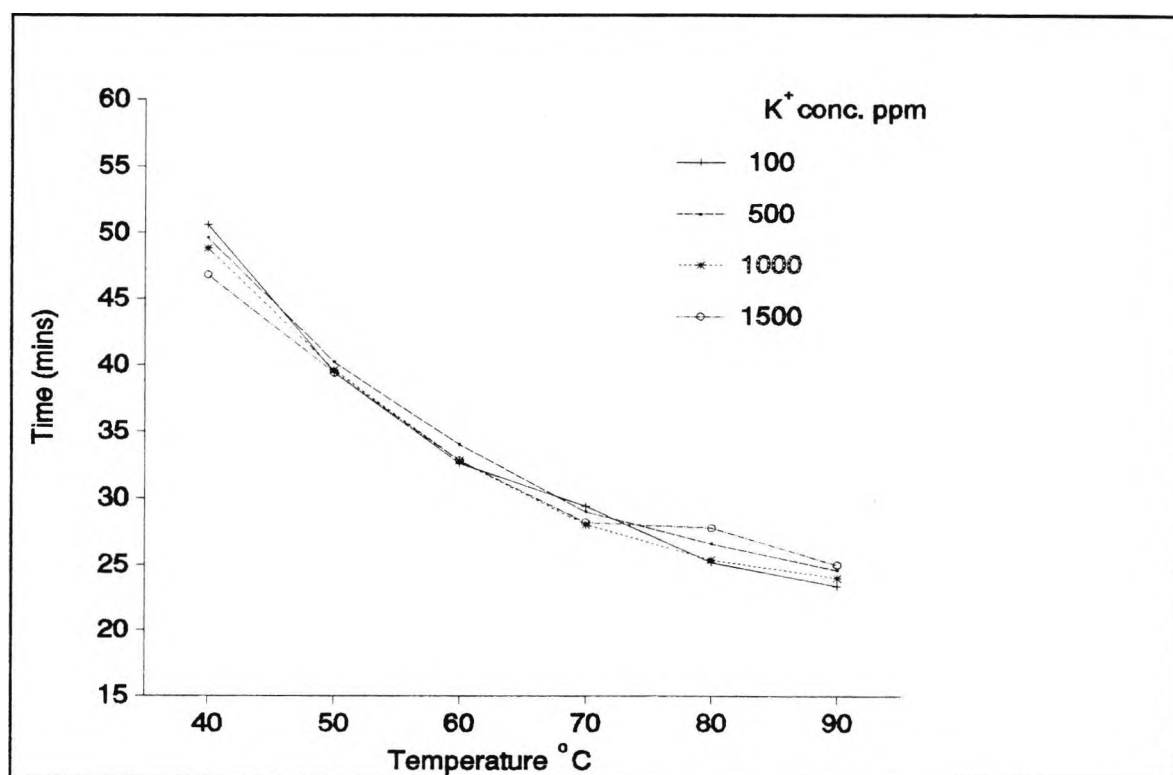


**Figure 4.8 Effect of different potassium ion concentrations on the average scaling times.**

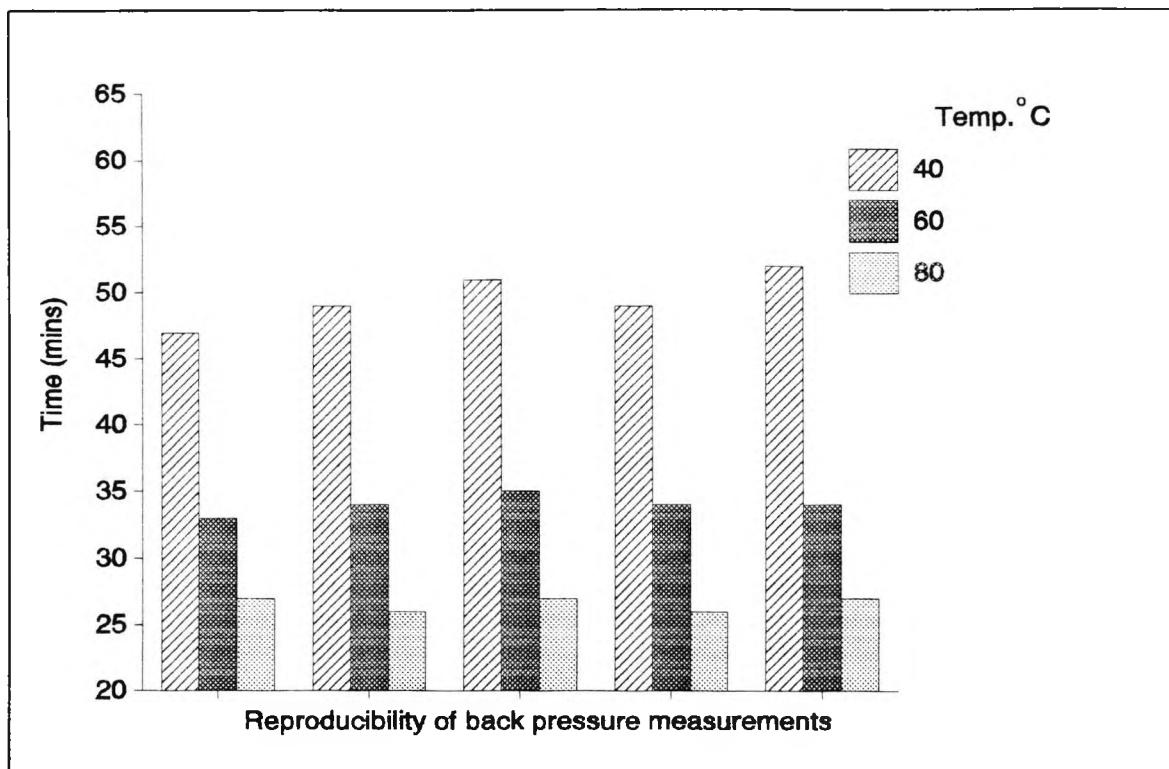


Figure 4.9 Reproducibility of propensity to scale measurements for the potassium ion concentration of 500 ppm in formation water.

The effect of temperature on the propensity to scale was as expected, with the rate of deposition increasing at higher temperatures. Because no differences were found in the propensity to scale measurements for changes in the potassium ion concentration, no precipitation studies were carried out. Calculations based on the scaling prediction model for mixed brines [26], were carried out for potassium ion concentrations of 100 and 1500ppm at temperatures of 40, 60 and 80°C, the data (mg scale/ kg mixed brines) are given in Table 4.14.

The data show that at all potassium concentrations and temperatures studied there are no significant differences in the predicted quantities for strontium sulphate and barium sulphate deposition.

At the higher potassium ion concentration, the predicted amount of calcium carbonate increases significantly and this is

Table 4.14 Predicted weight (mg scale/ kg mixed brines) of each precipitate deposited.

K <sup>+</sup> 100ppm				K <sup>+</sup> 1500ppm			
Temp°C	CaCO <sub>3</sub>	SrSO <sub>4</sub>	BaSO <sub>4</sub>	Temp°C	CaCO <sub>3</sub>	SrSO <sub>4</sub>	BaSO <sub>4</sub>
40	0.0	117.1	124.7	40	20.9	113.4	124.5
60	52.8	126.3	124.5	60	71.6	122.9	124.3
80	94.8	140.2	124.4	80	108.3	137.2	124.2

reflected in a slight increase in the propensity to scale at 40°C (Table 4.13 and Figure 4.8).

The propensity to scale experiments and the scaling prediction model indicate that increasing the potassium ion concentration in formation waters has no significant effect on the propensity to scale on mixing with a sea water.

#### 4.9.3 The Effect of Varying the Magnesium Ion Concentration in Simulated Formation Water on the Propensity to Scale

The magnesium chloride concentrations used and the physical properties of the formation waters studied are given in Table 4.15. All other ion concentrations in the formation water were kept constant. The pump speeds were set at Pump A, 61.0% and Pump B, 63.5%. The propensity to scale was measured for increases in back pressure of 1 and 4 psi above the distilled water base line.

The results for the average scaling times for the magnesium ion concentration experiments for an increase in back pressure of 1 psi are given in Table 4.16, and shown graphically in Figure 4.10. The results for an increase in back pressure of 4 psi are given in Table 4.17, and shown graphically in Figure 4.11. The details of replicate runs for each magnesium ion concentration experiment are given in Appendix Tables B.9 to B.12 for an increase in back pressure of 1 psi, and in Appendix Tables B.13 to B.16 for an increase in back pressure of 4 psi.

**Table 4.15 Changes in chemical composition on varying the magnesium chloride concentration in formation water.**

Mg <sup>2+</sup>	Cl <sup>-</sup>	MgCl <sub>2</sub> .6H <sub>2</sub> O wt. (g/l)	pH	S.G.
155	15686	1.297	6.22	1.019
300	16110	2.51	5.98	1.018
600	16987	5.02	5.72	1.018
1200	18740	10.04	5.44	1.022

The results indicate that varying the concentration of magnesium ion in formation waters only slightly influences the rate of deposition of scale. At the lowest temperature used, 40°C, no apparent trend can be seen. However, at 50°C and above there is a clear trend as the magnesium ion concentration in formation water is increased to 1200ppm, with a slight but noticeable decrease in the propensity to scale, which is observed most clearly in experiments increasing the back pressure by 4 psi. Comparison of the propensity to scale data in Table 4.18 for initial scale deposition (1 psi back pressure) and scale buildup (4 psi back pressure) shows that the time for buildup of scale is considerably shorter than that required to deposit the initial precipitate on which the scale subsequently grows.

**Table 4.16 Effect of different magnesium ion concentrations on an increase in back pressure of 1 psi: Average scaling times (mins).**

Temp°C	Mg <sup>2+</sup> 155ppm	Mg <sup>2+</sup> 300ppm	Mg <sup>2+</sup> 600ppm	Mg <sup>2+</sup> 1200ppm
40	53.6	55.4	57.4	49.8
50	43.8	45.2	43.4	44.6
60	35.6	37.0	36.2	38.2
70	30.6	31.6	31.6	33.6
80	27.4	28.6	27.6	30.0
90	24.8	26.6	26.2	26.8

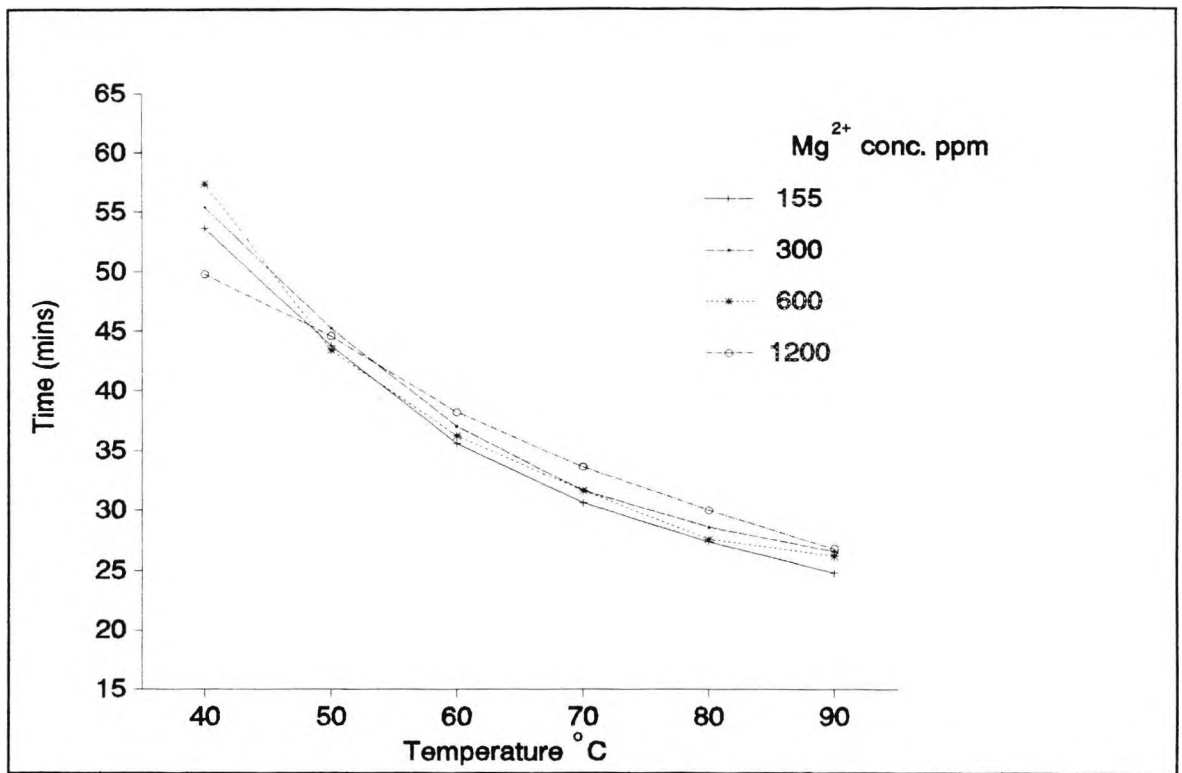


Figure 4.10 Effect of different magnesium ion concentrations on the average scaling times for an increase in back pressure of 1 psi.

Table 4.17 Effect of different magnesium ion concentrations on an increase in back pressure of 4 psi: Average scaling times (mins)

Temp °C	Mg <sup>2+</sup> 155ppm	Mg <sup>2+</sup> 300ppm	Mg <sup>2+</sup> 600ppm	Mg <sup>2+</sup> 1200ppm
40	70.8	73.0	74.2	73.2
50	56.2	57.8	57.6	63.0
60	46.2	47.0	49.0	53.2
70	40.6	41.4	42.2	45.8
80	37.8	38.6	38.4	43.0
90	37.0	36.6	38.2	42.0

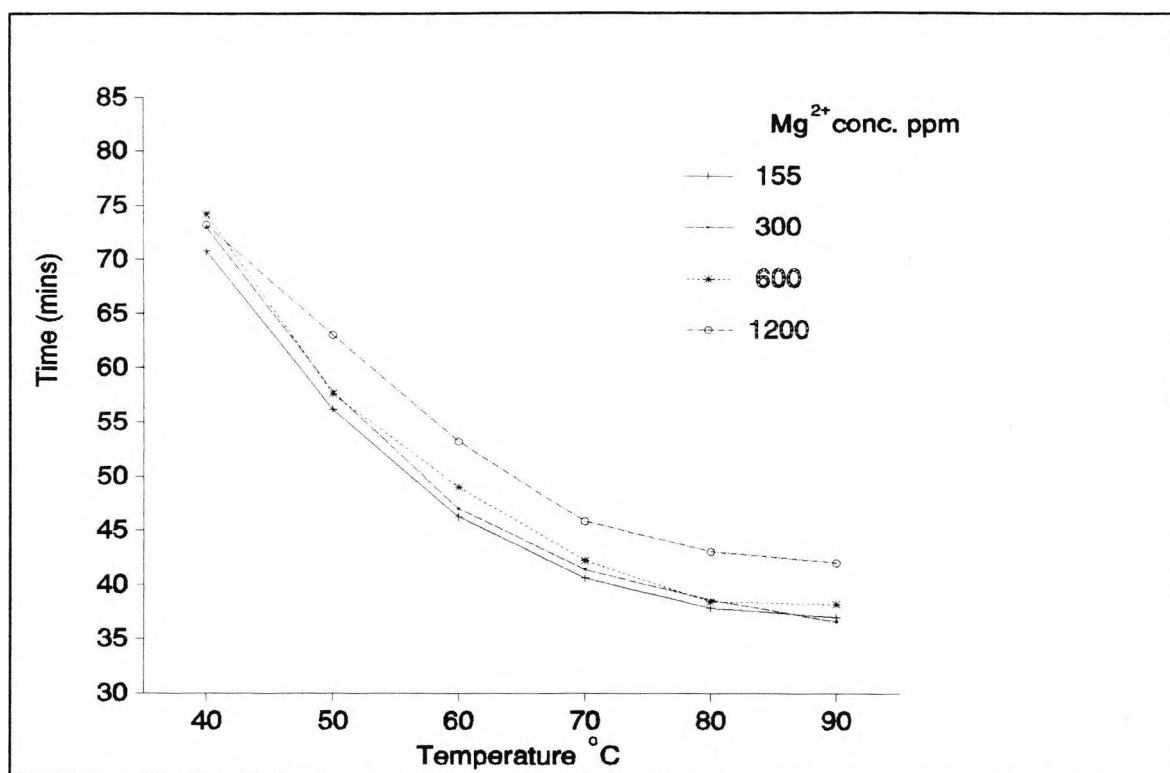


Figure 4.11 Effect of different magnesium ion concentrations on the average scaling times for an increase in back pressure of 4 psi.

At 40°C, the formation water containing 1200 ppm magnesium ion took on average 49.8 minutes for the back pressure to increase by 1 psi. This initial scale deposition is a complex crystallisation process. The formation of the initial scale layer and its subsequent rate of growth are determined by the interaction of several rate processes: chemical reaction, supersaturation, nucleation, crystal growth and ordering of the scale crystal lattice.

These processes are all taking place inside the microbore tube and account for the relatively long time for the initial layer of scale to deposit. When the experiment was extended to increase the back pressure to 4 psi above the base line, it took a further 23.4 minutes for scale to form in the microbore tube. This phenomenon is easily explained, because once scale has formed inside the microbore tube, the deposition rate, for the same degree of supersaturation and same contact time, is greater than

it is during nucleation.

**Table 4.18 Average scaling times (mins) for a formation water containing 1200 ppm of magnesium ion for increases in back pressure of 1 and 4 psi.**

Temp °C	Time for a 1 psi increase	Time for a 4 psi increase	Time difference for extra 3 psi increase
40	49.8	73.2	23.4
60	38.2	53.2	15.0
80	30.0	43.0	13.0

Because no significant differences were found in the propensity to scale measurements for changes in the magnesium ion concentration, no precipitation studies were carried out. However, the scaling prediction model calculations [26] were carried out for magnesium concentrations of 155 and 1200 ppm at temperatures of 40, 60 and 80°C, and the results (mg scale/ kg mixed brines) are given in Table 4.19.

**Table 4.19 Predicted weights (mg scale/ kg mixed brines) of each precipitate deposited.**

Mg <sup>2+</sup> 155ppm				Mg <sup>2+</sup> 1200ppm			
Temp°C	CaCO <sub>3</sub>	SrSO <sub>4</sub>	BaSO <sub>4</sub>	Temp°C	CaCO <sub>3</sub>	SrSO <sub>4</sub>	BaSO <sub>4</sub>
40	34.0	116.5	124.5	40	0.0	86.1	124.3
60	81.3	125.8	124.4	60	41.3	94.5	124.2
80	115.4	139.7	124.3	80	85.8	109.5	124.0

The data indicate that at both of the magnesium ion concentrations studied, there was no difference in the predicted quantity of barium sulphate. For the higher magnesium ion concentration the model suggests that there should be a significant reduction in the precipitation of strontium sulphate and calcium carbonate at the three temperatures studied. These

predictions are consistent with the overall changes in propensity to scale measured in the present work. The reduction in the amount of strontium sulphate precipitated has been linked to its increased solubility in the presence of high magnesium ion concentrations [27] caused by the formation of magnesium sulphate ion pairs [21,22], which would reduce the availability of sulphate ions to form strontium sulphate. Similar effects were observed in sea water solutions containing high magnesium ion levels (Section 4.10.3). The predicted reduction in the amount of calcium carbonate precipitate is consistent with earlier solubility data [28].

#### 4.9.4 The Effect of Varying the Calcium Ion Concentration in Simulated Formation Water on the Propensity to Scale

The calcium chloride concentrations used and the physical properties of the formation waters studied are given in Table 4.20. All other ion concentrations in the formation water were unchanged. The pump speeds were set at Pump A, 61.0% and Pump B, 63.5%.

**Table 4.20 Changes in chemical composition on varying the calcium chloride concentration in formation water.**

Ca <sup>2+</sup>	Cl <sup>-</sup>	CaCl <sub>2</sub> .2H <sub>2</sub> O wt. (g/l)	pH	S.G.
500	15776	1.834	6.29	1.019
1000	16661	3.6682	5.96	1.019
1500	17547	5.502	5.61	1.020
2000	18433	7.3363	5.44	1.021

The data for the average scaling times for the calcium ion concentration experiments are given in Table 4.21, and shown graphically in Figure 4.12. The details of replicate runs for each calcium ion concentration experiment are given in Appendix Tables B.17 to B.20.

**Table 4.21 Effect of different calcium ion concentrations on an increase in back pressure of 1 psi: Average scaling times (mins).**

Temp °C	Ca <sup>2+</sup> 500ppm	Ca <sup>2+</sup> 1000ppm	Ca <sup>2+</sup> 1500ppm	Ca <sup>2+</sup> 2000ppm
40	50.50	54.50	66.75	73.75
50	42.75	48.50	54.25	64.00
60	36.25	41.50	46.50	55.25
70	31.75	37.50	41.00	48.50
80	29.00	33.50	35.50	42.50
90	27.25	30.75	32.75	38.25

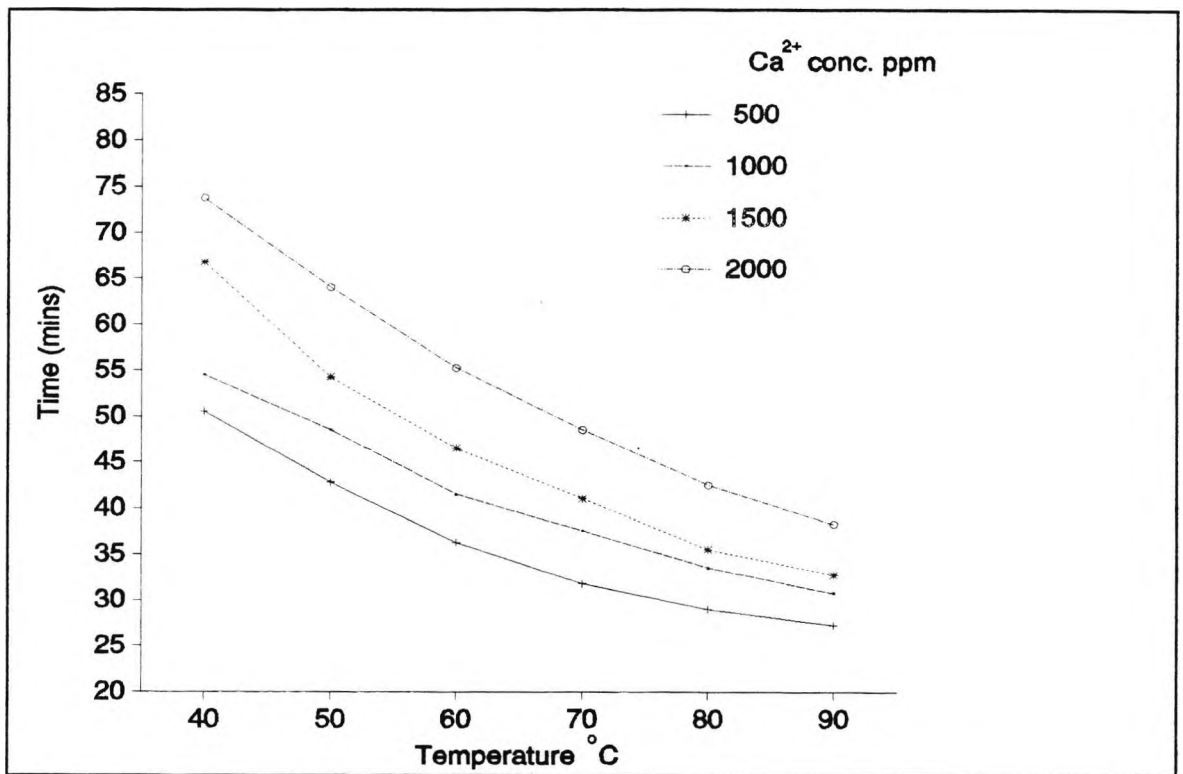


**Figure 4.12 Effect of different calcium ion concentrations on the average scaling times.**

The results show that varying the concentration of calcium ion in formation waters significantly influences the rate of deposition of scale, the rate increasing as the calcium ion

concentration is decreased. This trend is found at all the concentrations and temperatures studied. The formation water containing 2000ppm of calcium ion, took 23 minutes longer than the formation water containing 500 ppm of calcium ion to form a scale at 40°C. This was reduced to 11 minutes at 90°C. The effect of temperature on the propensity to scale measurements was also evident, and as expected the rate of deposition of scale was shown to increase with temperature.

As statistically significant decreases in the rate of deposition were found as the calcium ion concentration was increased, precipitation studies were carried out to determine which precipitates were forming at the highest and lowest calcium ion concentrations. The experimental procedure for the precipitation tests is described in Section 4.7.2 and the results (mg scale/kg mixed brines) are given in Table 4.22.

**Table 4.22** Weights (mg scale/ kg mixed brines) of each precipitate deposited.

Ca <sup>2+</sup> 500ppm				Ca <sup>2+</sup> 2000ppm			
Temp°C	CaCO <sub>3</sub>	SrSO <sub>4</sub>	BaSO <sub>4</sub>	Temp°C	CaCO <sub>3</sub>	SrSO <sub>4</sub>	BaSO <sub>4</sub>
40	82	106	127	40	108	91	127
60	114	135	127	60	138	112	127
80	134	158	127	80	163	139	127

The results show that at the higher calcium ion concentration (2000ppm), for the three temperatures, there is a noticeable increase in the weight of calcium carbonate precipitated. This effect is easily explained because there were more calcium ions in the mixed brine to react with the carbonate ions available. In this set of experiments the amount of calcium carbonate formed was limited by the low level of hydrogen carbonate ion (500ppm) in the sea water. The effect of temperature on calcium carbonate deposition is apparent; as the temperature rises the rate of precipitation increases because of the increased decomposition

of hydrogen carbonate ion to carbonate ion. For strontium sulphate there is a noticeable reduction in the weights precipitated between the high and low calcium ion solutions at all three temperatures. This reduction is consistent with an increased solubility of strontium sulphate in waters containing higher calcium ion concentrations [27]. On analysis of the solutions the sulphate ion concentration was found to be reduced only by precipitation with barium and strontium ions and not through the formation of calcium sulphate which is much more soluble. Barium sulphate precipitation is not affected by increases in either calcium ion concentration or temperature.

The results from Tables 4.21 and 4.22 in combination with Figure 4.12 demonstrate that as the calcium ion concentration increases in formation waters, the propensity to scale is reduced. To further explain the differences found, the scaling prediction model [26] was used for mixed brines for calcium ion concentrations of 500 and 2000ppm at temperatures of 40, 60 and 80°C, and the predictions (mg scale/ kg mixed brines) are given in Table 4.23.

**Table 4.23 Predicted weights (mg scale/ kg mixed brines) of each precipitate deposited.**

Ca <sup>2+</sup> 500ppm				Ca <sup>2+</sup> 2000ppm			
Temp°C	CaCO <sub>3</sub>	SrSO <sub>4</sub>	BaSO <sub>4</sub>	Temp°C	CaCO <sub>3</sub>	SrSO <sub>4</sub>	BaSO <sub>4</sub>
40	61.4	116.1	124.5	40	66.7	105.6	124.4
60	101.3	125.4	124.4	60	106.0	115.9	124.3
80	130.6	139.4	124.3	80	133.6	131.0	124.2

The scaling prediction model data show the same trends found in the precipitation tests *viz.*, (a) no significant difference in the predicted quantity of barium sulphate, (b) a noticeable reduction in the weight of strontium sulphate precipitated and (c) a noticeable increase in the weight of calcium carbonate predicted. As discussed in Section 4.9.1, the precipitation tests

gave higher quantities of calcium carbonate precipitate than the prediction scaling model because of the increased time allowed in the precipitation tests for equilibration.

#### 4.9.5 The Effect of Varying the Strontium Ion Concentration in Simulated Formation Water on the Propensity to Scale

The strontium chloride concentrations used and the physical properties of the formation waters studied are given in Table 4.24. All the other ion concentrations in the formation water were unchanged. The pump speeds were set at Pump A, 61.0% and Pump B, 63.5%.

**Table 4.24 Changes in chemical composition on varying the strontium chloride concentration in formation water.**

Sr <sup>2+</sup>	Cl <sup>-</sup>	SrCl <sub>2</sub> .6H <sub>2</sub> O wt. (g/l)	pH	S.G.
225	15686	0.6846	5.59	1.018
500	15909	1.5214	5.68	1.018
750	16112	2.2822	5.67	1.019
1000	16314	3.0429	5.84	1.019

The results for the average scaling times for the strontium ion concentration experiments are given in Table 4.25, and shown graphically in Figure 4.13. The details of replicate runs for each strontium ion concentration experiment are given in Appendix Tables B.21 to B.24.

The results show that varying the concentration of strontium ion in formation waters significantly influences the rate of deposition of scale. At temperatures below 70°C, the rate of deposition is reduced as the strontium ion concentration is increased, but at temperatures above 70°C a rise in strontium ion concentration increases the rate of scale deposition. The results show that three factors affect the propensity to scale. These are (a) strontium ion concentration, (b) temperature and (c) the effect of temperature at each strontium ion concentration.

Table 4.25 Effect of different strontium ion concentrations on an increase in back pressure of 1 psi: Average scaling times (mins).

Temp °C	Sr <sup>2+</sup> 225ppm	Sr <sup>2+</sup> 500ppm	Sr <sup>2+</sup> 750ppm	Sr <sup>2+</sup> 1000ppm
40	47.50	50.75	53.75	65.50
50	38.50	44.50	44.75	49.00
60	32.00	33.50	31.75	36.50
70	27.75	27.50	26.00	28.50
80	24.25	23.50	21.50	22.50
90	22.25	21.75	17.75	19.00

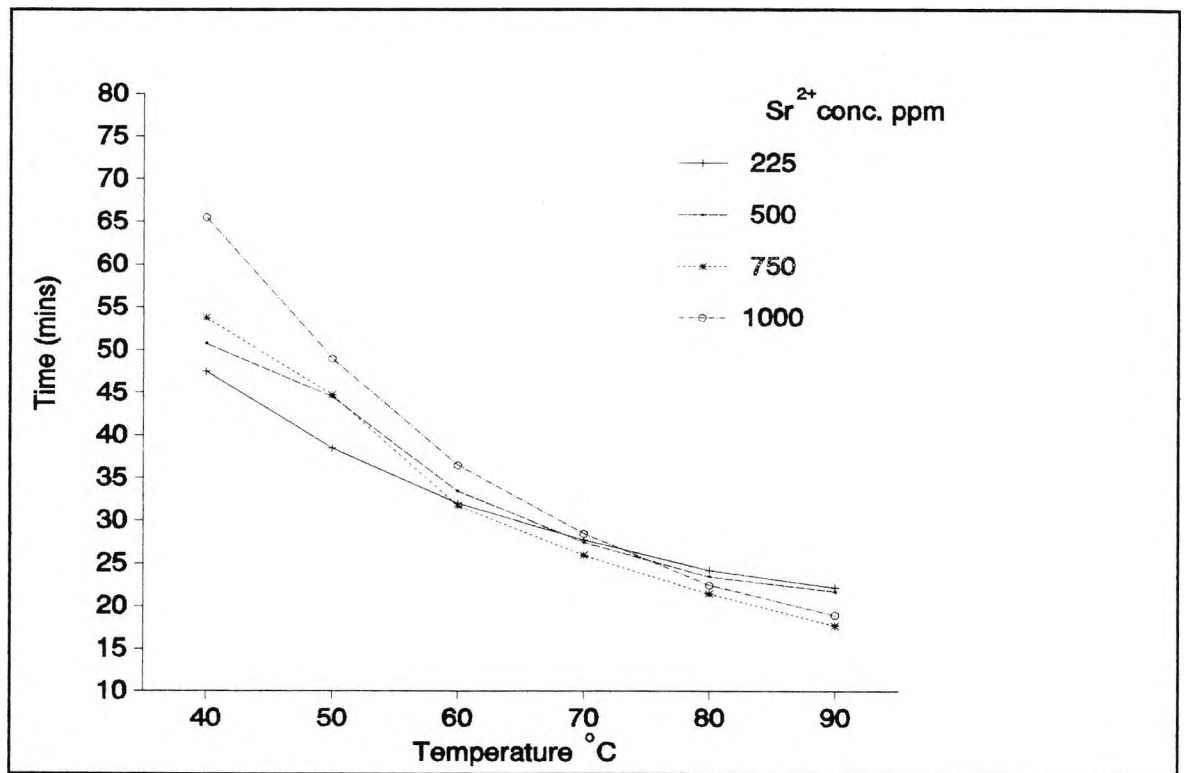


Figure 4.13 Effect of different strontium ion concentrations on the average scaling times.

At higher strontium ion concentrations it was expected that the rate of deposition would increase because more strontium sulphate would be precipitated, but this was not found for temperatures below 70°C. The results show that as the strontium ion concentration is increased from 225 ppm to 1000 ppm, the scaling time takes 18 minutes longer at 40°C. As the temperature increases, the time reductions (mins) in the propensity to scale were 10.5 at 50°C, 4.5 at 60°C and 0.75 at 70°C. Above 70°C an increase in propensity to scale is found for formation water with the higher strontium ion concentration. The effect of temperature on the propensity to scale measurements was as expected, with the rate of deposition increasing at higher temperatures. At the lowest strontium ion concentration (225ppm), the scaling time was reduced by 25 minutes when the temperature was raised from 40 to 90°C. At higher strontium ion concentrations, this time difference was increased so that formation water containing 1000ppm strontium ion showed a reduction of 47 minutes in scaling time between 40 and 90°C.

The results of varying the strontium ion concentration in formation waters show clearly that there are statistically significant differences in the rate of deposition as the strontium ion concentration is increased. Therefore, precipitation studies were carried out to determine which precipitates were forming at the highest and lowest strontium ion concentrations in formation waters. The experimental procedure for the precipitation tests is described in Section 4.7.2 and the results (mg scale/ kg mixed brines) are given in Table 4.26.

The data indicate that at the higher strontium ion concentration (1000ppm) for the three temperatures, there is a noticeable decrease in the weight of calcium carbonate precipitate formed, when compared to the formation water containing 225ppm of strontium ion. At the higher strontium ion concentrations the formation of calcium carbonate is inhibited either by the strontium ions affecting the decomposition of hydrogen carbonate ions or by the precipitation of strontium carbonate.

Table 4.26 Weights (mg scale/ kg mixed brines) of each precipitate deposited.

Sr <sup>2+</sup> 225 ppm				Sr <sup>2+</sup> 1000 ppm			
Temp°C	CaCO <sub>3</sub>	SrSO <sub>4</sub>	BaSO <sub>4</sub>	Temp°C	CaCO <sub>3</sub>	SrSO <sub>4</sub>	BaSO <sub>4</sub>
40	102	108	127	40	47	773	127
60	134	137	127	60	95	874	127
80	164	154	127	80	132	932	127

The effect of temperature on calcium carbonate deposition is clear: as the temperature rises the rate of precipitation increases, because of the faster rate of decomposition of hydrogen carbonate ions to carbonate ions. For strontium sulphate there is a very significant increase in the weight precipitated between the high and low strontium solutions at the three temperatures studied. At 40°C, the quantity of strontium sulphate precipitate formed was 108 mg/kg compared to 773 mg/kg for the formation waters containing 225 and 1000ppm strontium ion, respectively. The effect of temperature on strontium sulphate deposition was similar to that for calcium carbonate; as the temperature rises the rate of deposition increases because of changes in solubility. Barium sulphate precipitation studies suggest that the deposition of barium sulphate is not affected by increases in strontium ion concentration or temperature. To further explain the differences found, the scaling model predictions [26] for mixed brines were carried out for strontium ion concentrations of 225 and 1000ppm at temperatures of 40, 60 and 80°C, and the results (mg scale/ kg mixed brines) are given in Table 4.27.

The data for calcium carbonate precipitation is not in agreement with the experimental results. The precipitation tests show that for formation waters with higher strontium concentrations calcium carbonate precipitation is lower than for formation waters with lower strontium concentrations, whereas the scaling prediction model shows the opposite. This reversal was totally unexpected

Table 4.27 Predicted weights (mg scale/ kg mixed brines) of each precipitate deposited.

Sr <sup>2+</sup> 225ppm				Sr <sup>2+</sup> 1000ppm			
Temp°C	CaCO <sub>3</sub>	SrSO <sub>4</sub>	BaSO <sub>4</sub>	Temp°C	CaCO <sub>3</sub>	SrSO <sub>4</sub>	BaSO <sub>4</sub>
40	0.0	116.6	124.6	40	20.0	850.0	124.4
60	52.7	125.9	124.5	60	70.9	862.8	124.3
80	94.7	139.8	124.4	80	107.8	882.5	124.1

as the precipitation tests and prediction models showed the same trends in other sets of data described in Sections 4.9.1 and 4.9.4. The scaling prediction model for strontium sulphate is in fairly close agreement with the precipitation results, showing that formation waters with higher strontium concentrations deposit more strontium sulphate than formation waters containing lower strontium concentrations. Barium sulphate precipitation was in close agreement with the precipitation tests.

The data from Tables 4.25, 4.26 and 4.27 in combination with Figure 4.13 show that the propensity to scale measurements and precipitation studies for changes in strontium ion concentrations in formation waters appear to give conflicting results. In the propensity to scale experiments, at temperatures below 70°C, the rate of scale deposition is significantly reduced as the strontium ion concentration is increased. Above 70°C, the rate of scale deposition increases for formation waters with higher strontium ion concentrations. Whereas the precipitation tests and the prediction model suggest that the higher the strontium ion concentration in formation waters, then more strontium sulphate should be deposited. The results demonstrate that higher strontium ion concentrations in formation water enhance the precipitation of the three main precipitates but this does not subsequently increase scale formation.

The differences in the data obtained between propensity to scale measurements and precipitation results (in agreement with the

scale prediction model) highlight the fact that kinetic effects must be important in scale formation. The precipitation experiments are carried out over a long enough time span to ensure that the equilibrium scale mixture is totally precipitated. The scale prediction model should mirror these results because it is based on the available solubility data for the compounds being precipitated. The propensity to scale measurements, however, result from instantaneous precipitation reactions within the microbore tube with no time allowance to achieve equilibrium. The nature of the scale obtained must, therefore, depend not only on composition but also on the rate of formation of nuclei of the potential components of the scale. It is known, for example, from other work carried out in the City University laboratories [25] that there is a considerable time delay in the formation of  $\text{CaSO}_4 \cdot 2\text{H}_2\text{O}$  nuclei when solutions containing calcium and sulphate ions are mixed. It seems likely that a similar delay in the formation of strontium sulphate nuclei is responsible for the absence of the predicted amounts of strontium sulphate in the instantaneous precipitation situation. Other workers studying the co-precipitation of strontium sulphate with barium sulphate have found similar effects at high strontium/barium ratios [23].

#### 4.9.6 The Effect of Varying the Barium Ion Concentration in Simulated Formation Water on the Propensity to Scale

The barium chloride concentrations used and the physical properties of the formation waters studied are given in Table 4.28. All other ion concentrations in the formation waters were kept constant. The pump speeds were set at Pump A, 90.5% and Pump B, 93.0%, with each delivering 0.85 litres per hour of formation or sea water into the P.M.A.C. microbore tube. In these experiments the simulated sea water contained 100 ppm hydrogen carbonate ion, not 500 ppm as used in all the other experiments.

Table 4.28 Changes in chemical composition on varying the barium chloride concentration in formation water.

Ba <sup>2+</sup>	Cl <sup>-</sup>	BaCl <sub>2</sub> .2H <sub>2</sub> O wt. (g/l)	pH	S.G.
100	15661	0.1778	5.55	1.018
125	15674	0.2224	5.70	1.018
150	15686	0.2669	5.56	1.018
175	15699	0.3113	5.82	1.018

The results for the average scaling times for the barium ion concentration experiments are given in Table 4.29 and shown graphically in Figure 4.14. The details of replicate runs for each barium ion concentration experiment given in Appendix Tables B.25 to B.28.

The results show that varying the concentration of barium ion in formation waters significantly influences the rate of deposition of scale. The rate is increased as the barium ion concentration is increased. This trend is displayed at all concentrations and temperatures studied. At 40°C, the formation water containing 100 ppm of barium ion took 29.8 minutes longer to scale than the formation water with 175 ppm of barium ion. However, at 90°C the time difference in the propensity to scale is 17.6 minutes between the formation waters. These results are consistent with those of Thomas [29], who investigated the effect of barium ion concentrations (100-200ppm) on mixed brine solutions. The results showed that the rate of deposition increased as the barium concentration was increased. The consistency of these measurements is shown in Figure 4.15, for five repeat runs of propensity to scale measurements for a barium ion concentration of 125 ppm at temperatures of 40, 60 and 80°C, giving standard deviations of 1.51, 0.45 and 0.71, respectively.

The results of varying the barium ion concentration in a formation water clearly show that there are statistically significant increases in the rate of deposition as the barium ion

Table 4.29 Effect of different barium ion concentrations on an increase in back pressure of 1 psi: Average scaling times (mins).

Temp °C	Ba <sup>2+</sup> 100ppm	Ba <sup>2+</sup> 125ppm	Ba <sup>2+</sup> 150ppm	Ba <sup>2+</sup> 175ppm
40	50.0	31.4	25.0	20.2
50	44.0	28.4	21.0	16.2
60	35.6	23.2	17.6	13.2
70	31.8	20.0	14.6	11.4
80	28.2	17.0	13.2	9.2
90	25.8	14.6	11.2	8.2

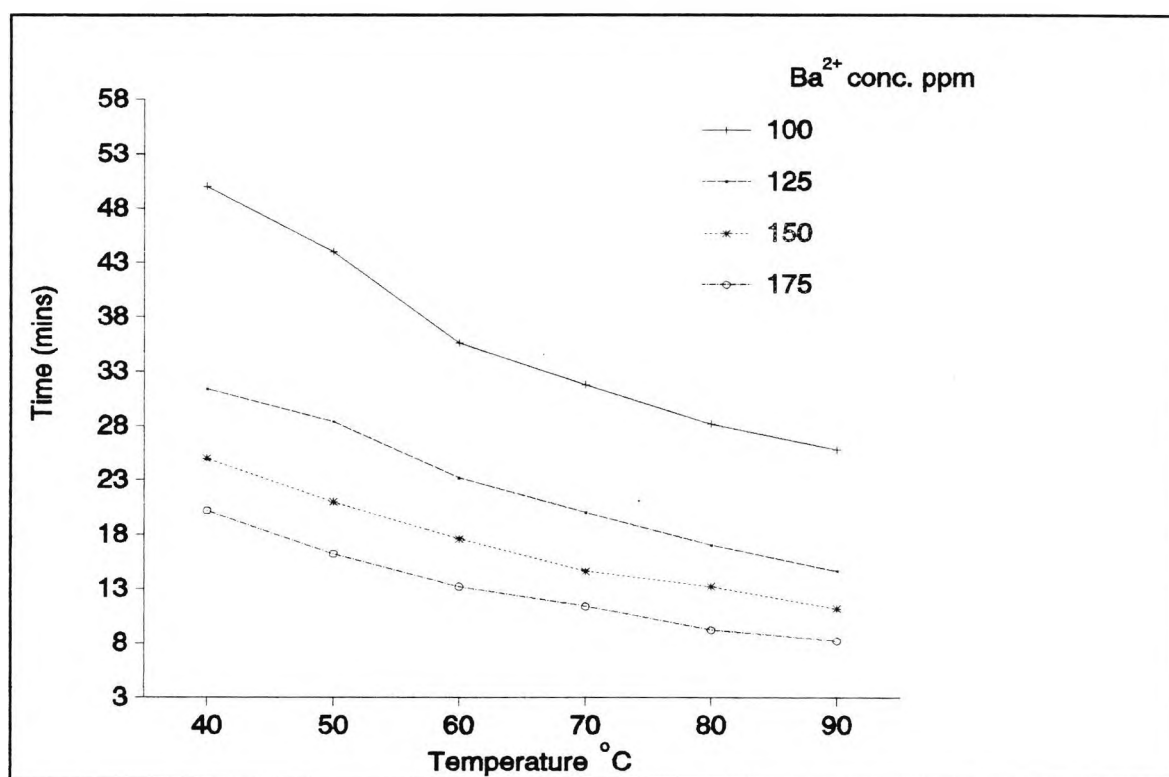


Figure 4.14 Effect of different barium ion concentrations on the average scaling times.

concentration is increased. No precipitation studies were carried out as the effects found were caused only by the increased deposition of barium sulphate at higher barium ion concentrations. However, scaling prediction model

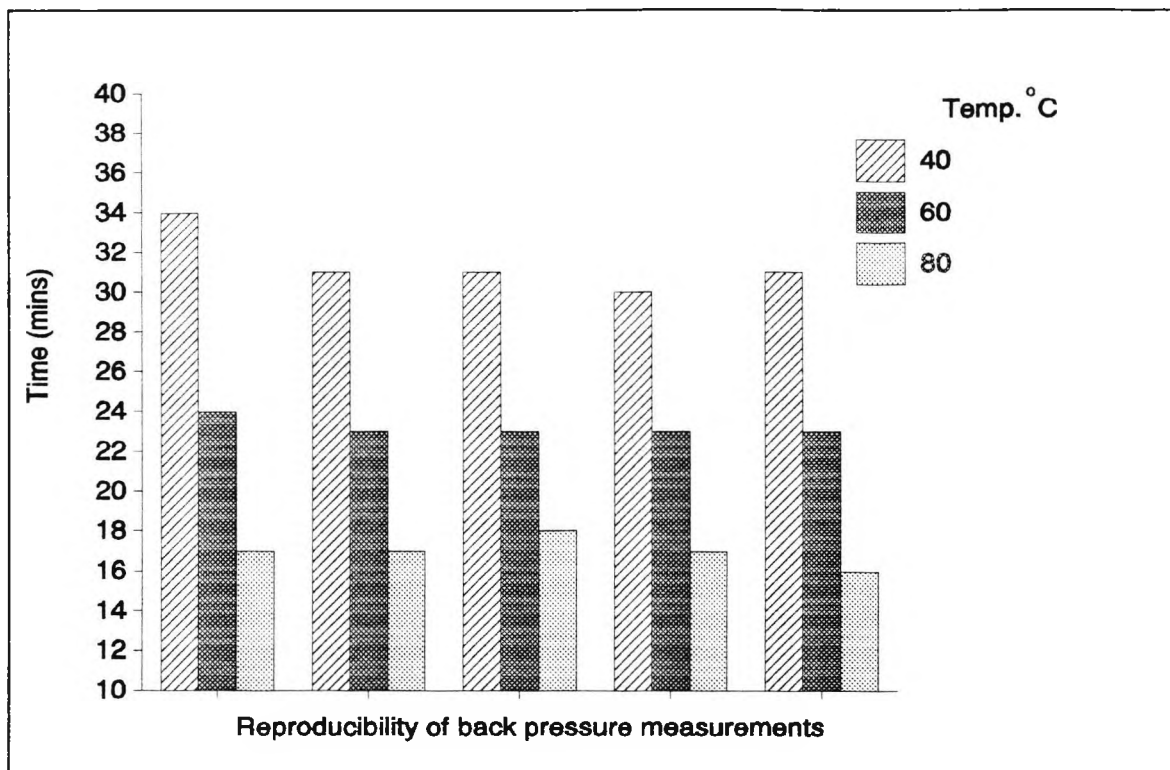


Figure 4.15 Reproducibility of propensity to scale measurements for the barium ion concentration of 125 ppm in formation water.

calculations [26] for mixed brines were carried out for barium ion concentrations of 100 and 175 ppm at 40, 60 and 80°C to prove this and the results (mg scale/ kg mixed brines) are given in Table 4.30.

Table 4.30 Predicted weights (mg scale/ kg mixed brines) of each precipitate deposited.

Ba <sup>2+</sup> 100ppm				Ba <sup>2+</sup> 175ppm			
Temp°C	CaCO <sub>3</sub>	SrSO <sub>4</sub>	BaSO <sub>4</sub>	Temp°C	CaCO <sub>3</sub>	SrSO <sub>4</sub>	BaSO <sub>4</sub>
40	0	118.9	83.0	40	0	116.3	145.4
60	0	128.0	82.9	60	0	125.6	145.3
80	0	141.7	82.8	80	0	139.5	145.2

The scaling model predicts that no calcium carbonate should be precipitated at either barium ion concentration, because of the

low hydrogen carbonate ion concentration (100ppm) in the sea water used during these experiments.

The model also indicates that there is no difference in the predicted quantity of strontium sulphate at the three temperatures shown but that the quantity of barium sulphate should increase significantly with increase in the barium ion concentration.

#### 4.9.7 Summary of the Propensity to Scale Experiments

The effects of changing each significant cation in simulated formation water separately, leaving the other concentrations unchanged, have yielded many interesting results. Every significant cation changed has been shown to have a different effect on the propensity to scale, as measured in the P.M.A.C. unit, when formation and sea waters are mixed. The details of propensity to scale data have been further characterised by precipitation tests and a scaling prediction model for mixed brines. The combined results show that kinetic effects can be more important than concentration effects in some cases. Table 4.31 summarises the general trends found in the propensity to scale measurements by increasing each significant cation concentration.

**Table 4.31 Summary of the general trends found in the propensity to scale.**

Cation	General trend in propensity to scale
Na <sup>+</sup>	Significant decrease
K <sup>+</sup>	No difference
Mg <sup>2+</sup>	Slight decrease at higher Mg <sup>2+</sup> concentrations
Ca <sup>2+</sup>	Significant decrease
Sr <sup>2+</sup>	Significant decrease below 70°C, significant increase above 70°C
Ba <sup>2+</sup>	Significant increase

#### 4.10 THE EFFECT OF VARYING THE CONCENTRATIONS OF CONSTITUENT IONS IN SIMULATED SEA WATERS ON THE PROPENSITY TO SCALE

The standard simulated formation and sea waters used in the propensity to scale experiments were made up by dissolving the quantities of salts shown in Tables 4.6 and 4.7 (Section 4.9), to give the significant ion concentrations listed. The standard sea water was used as the base line against which waters of other concentrations were compared. It had a chloride concentration of 18932 ppm, a pH of 7.56 and a specific gravity of 1.025. The aim of this set of experiments was to determine the effects of varying each significant ion concentration in the sea water separately leaving the other concentrations unchanged. The propensity to scale of each sea water was then measured using the standard formation water as a precipitant, having a chloride concentration of 15686 ppm, a pH of 5.59 and a specific gravity of 1.018.

The mixing flow rates for the experiments in this section were kept constant at 50:50, with each delivering 0.5 litres per hour of sea or formation water into the microbore tube (except for the variation of hydrogen carbonate ion concentration experiments described in Section 4.10.6). The propensity to scale was measured for an increase of 1 or 4 psi above the distilled water base line, for each concentration investigated at temperatures of 40, 50, 60, 70, 80 and 90°C. For each set of conditions, four or five experiments were carried out to ensure statistically significant results were achieved. After each experiment, the normal cleaning procedure was carried out as described in Section 4.7.1.

##### 4.10.1 The Effect of Varying the Sodium Chloride Concentration in Simulated Sea Water on the Propensity to Scale

The sodium chloride concentrations used and the physical properties of the simulated sea waters studied are given in Table 4.32. All the other ion concentrations in the sea water were kept

constant. The pump speeds were set at Pump A, 54.5% and Pump B, 57.0%.

**Table 4.32 Changes in chemical composition on varying the sodium chloride concentration in sea water.**

Na <sup>+</sup> ppm	Cl <sup>-</sup> ppm	NaCl wt. (g/l)	pH	S.G.
5415	11046	10	7.68	1.016
9349	17112	20	7.33	1.022
13283	23178	30	7.31	1.028
17217	26244	40	7.56	1.035

The data for the average scaling times for the sodium chloride experiments are given in Table 4.33, and shown graphically in Figure 4.16. The details of replicate runs for each sodium chloride concentration experiment are given in Appendix Tables B.29 to B.32.

**Table 4.33 Effect of different sodium chloride concentrations on an increase in back pressure of 1 psi: Average scaling times (mins).**

Temp °C	NaCl	NaCl	NaCl	NaCl
	10 g/l	20 g/l	30 g/l	40 g/l
40	41.4	45.8	48.4	60.0
50	33.8	36.6	42.0	48.0
60	27.6	32.8	35.8	37.2
70	24.2	27.2	32.6	33.4
80	21.6	25.2	27.8	29.6
90	19.8	23.6	25.6	28.8

The results show that varying the concentration of sodium chloride in sea waters significantly influences the rate of deposition of scale. The rate is significantly decreased as the

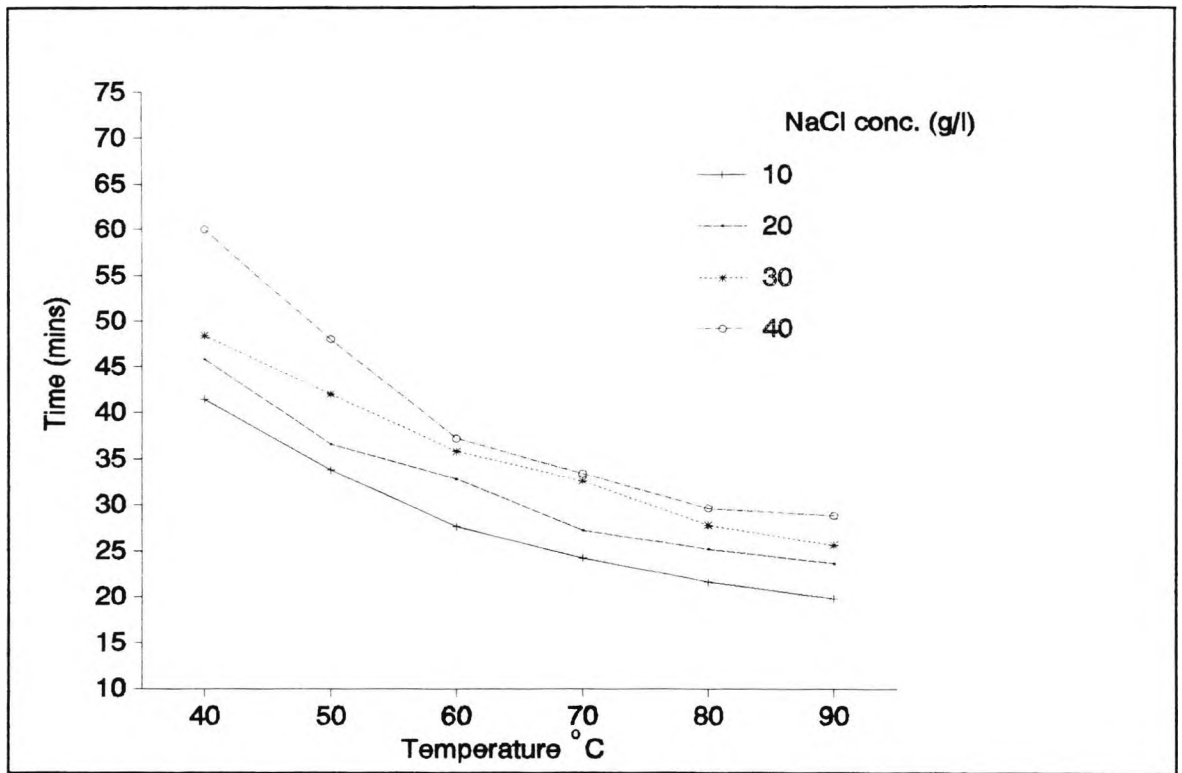


Figure 4.16 Effect of different sodium chloride concentrations on the average scaling times.

sodium chloride concentration is increased. This trend is displayed at all the concentrations and temperatures studied. The biggest time differences were shown at 40°C, where the sea water containing 40 g/l sodium chloride took 19.6 minutes longer than the sea water containing 10 g/l to form scale. At 90°C, this time difference was reduced to 9 minutes. The sea water containing 40 g/l sodium chloride showed slight differences in propensity to scale when compared to the sea water containing 30 g/l sodium chloride at temperatures above 60°C. At temperatures below 60°C, significant time differences were observed. The effect of temperature on the propensity to scale measurements is also evident, and as expected the rate of deposition of scale was shown to increase with temperature.

The results of varying the sodium chloride concentration in sea water show that there are statistically significant increases in the rate of deposition as the concentration is decreased. Therefore precipitation studies were carried out to determine

which precipitates were forming at the highest and lowest sodium chloride concentrations in the sea waters. The experimental procedure of the precipitation tests is described in Section 4.7.2 and the results (mg scale/ kg mixed brines) are given in Table 4.34.

**Table 4.34** Weights (mg scale/ kg mixed brines) of each precipitate deposited.

NaCl 10 g/l				NaCl 40 g/l			
Temp°C	CaCO <sub>3</sub>	SrSO <sub>4</sub>	BaSO <sub>4</sub>	Temp°C	CaCO <sub>3</sub>	SrSO <sub>4</sub>	BaSO <sub>4</sub>
40	40	102	127	40	30	91	127
60	90	146	127	60	87	120	127
80	130	173	127	80	107	158	127

The results show at the higher sodium chloride concentration, and at each temperature there is a noticeable decrease in the weight of calcium carbonate precipitated. The effect of temperature on calcium carbonate deposition is, however, apparent and increases as the temperature rises because of the increased decomposition of hydrogen carbonate ion to carbonate ion (see Chapter 3). For strontium sulphate there is a significant reduction in the weights precipitated between the high and low sodium chloride solutions at all three temperatures. This reduction is caused by the increased solubility of strontium sulphate in waters containing higher sodium chloride concentrations [16]. The rate of deposition of strontium sulphate increases with temperature. The data shows that barium sulphate precipitation is not affected by an increase in sodium chloride concentration or temperature. This is possibly an unexpected result considering suggestions that imply barium sulphate is more soluble in higher sodium chloride concentrations and at higher temperatures [13,14]. The differences detected in the work containing these suggestions, however, correspond to less than 1 mg/kg of barium sulphate precipitate formed for the conditions used in precipitation tests carried out in the present work.

The data from Tables 4.33 and 4.34, in combination with Figure 4.16, demonstrate that as the sodium chloride concentration increases in sea waters, the propensity to scale and the weight of precipitate is reduced. These effects are controlled by two main factors: the precipitation of  $\text{CaCO}_3$ ,  $\text{SrSO}_4$  and  $\text{BaSO}_4$  and the aggregation of these precipitates to form scale. To further explain the differences found, the scaling prediction model [26] was used for mixed brines for sodium chloride concentrations of 10 and 40 g/l at temperatures of 40, 60 and 80°C, and the prediction results (mg scale/ kg mixed brines) are given in Table 4.35.

**Table 4.35 Predicted weight (mg scale/ kg mixed brines) of each precipitate deposited.**

NaCl 10 g/l				NaCl 40 g/l			
Temp°C	$\text{CaCO}_3$	$\text{SrSO}_4$	$\text{BaSO}_4$	Temp°C	$\text{CaCO}_3$	$\text{SrSO}_4$	$\text{BaSO}_4$
40	6.7	138.5	125.2	40	0.0	92.5	124.0
60	62.6	145.9	125.1	60	54.5	104.0	123.8
80	103.0	157.3	125.0	80	94.8	120.5	123.7

The experimental data for the weights of precipitates (Table 4.34) can be compared with the weights predicted by the scaling model (Table 4.35). There are significant differences between the observed and calculated weights for calcium carbonate and strontium sulphate deposition. The difference for calcium carbonate can be explained in terms of the increased times allowed for equilibration in the precipitation experiments, which permit increased decomposition of hydrogen carbonate ion to carbonate ion. The smaller differences for strontium sulphate must also arise from the extra time allowed for equilibration. This would maximise the deposition of strontium sulphate, which is the most soluble compound in the scale system. There was no difference in the observed and calculated weights of barium sulphate deposition.

#### 4.10.2 The Effect of Varying the Potassium Ion Concentration in Simulated Sea Water on the Propensity to Scale

The potassium chloride concentrations used and the physical properties of the formation waters studied are given in Table 4.36. All the other ion concentrations in the sea water were unchanged. The pump speeds were set at Pump A, 54.5% and Pump B, 57.0%.

**Table 4.36 Changes in chemical composition on varying the potassium chloride concentration in sea water.**

K <sup>+</sup>	Cl <sup>-</sup>	KCl wt. (g/l)	pH	S.G.
250	18801	0.477	7.59	1.024
500	19208	0.954	7.48	1.024
1000	19482	1.907	7.89	1.025
1500	19936	2.861	7.72	1.025

The data for the average scaling times for the potassium ion concentration experiments are given in Table 4.37, and shown graphically in Figure 4.17. The details of replicate runs for each potassium ion concentration experiment are given in Appendix Tables B.33 to B.36.

The results show that varying the concentration of potassium ion in sea water only slightly influences the rate of deposition of scale. At the highest potassium ion concentration there is a slight, but noticeable decrease in the propensity to scale. At 40°C, no trend can be seen, but at 50°C and above there is a clear trend. The consistency of the measurements is shown in Figure 4.18, for five repeat runs of propensity to scale measurements for a potassium concentration of 1000 ppm at temperatures of 40, 60 and 80°C, giving standard deviations of 0.89, 0.55 and 1.14, respectively. The effect of temperature on propensity to scale is as expected with the rate of deposition increasing at higher temperatures.

Table 4.37 Effect of different potassium ion concentrations on an increase in back pressure of 1 psi: Average scaling times (mins).

Temp °C	K <sup>+</sup> 250 ppm	K <sup>+</sup> 500 ppm	K <sup>+</sup> 1000 ppm	K <sup>+</sup> 1500 ppm
40	52.6	51.2	49.6	51.2
50	42.6	40.8	40.8	44.0
60	35.2	32.8	34.6	39.7
70	31.0	28.4	29.4	32.8
80	27.6	26.2	28.6	30.2
90	26.8	25.0	25.4	28.4

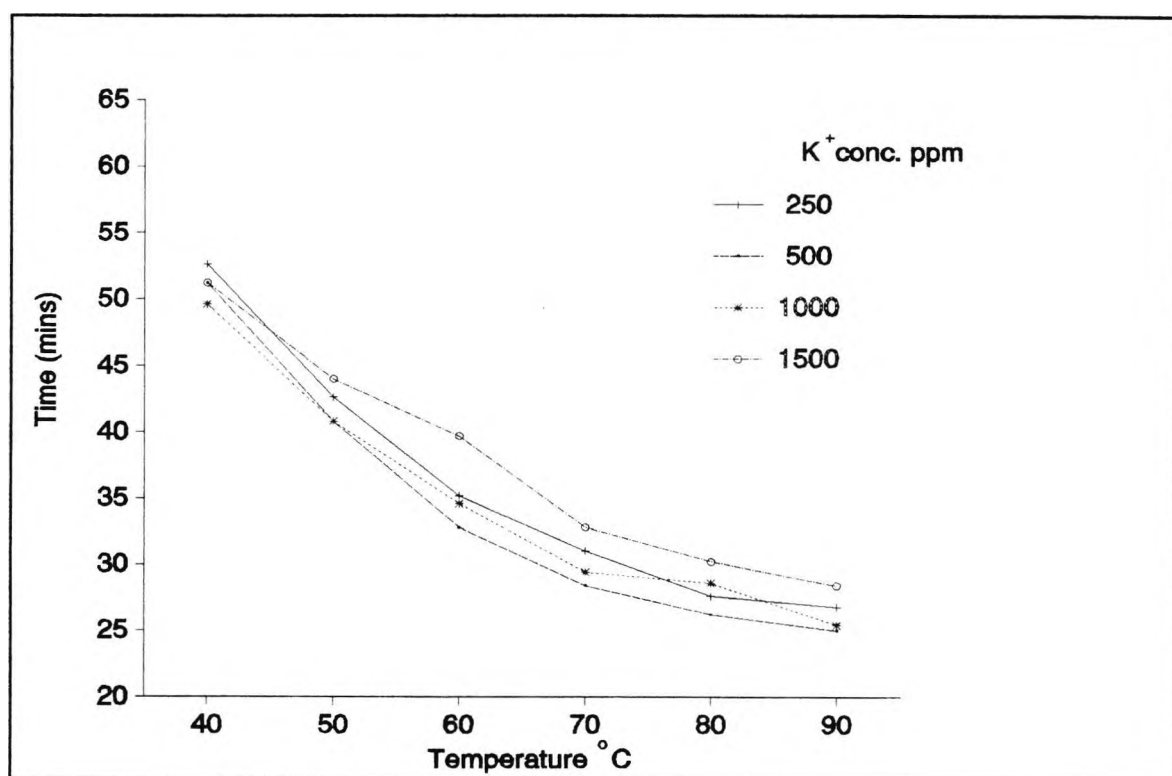


Figure 4.17 Effect of different potassium ion concentrations on the average scaling times.

Because no significant differences were found in the propensity to scale measurements for changes in the potassium ion concentration, no precipitation tests were carried out.

Calculations based on the scaling prediction model [26] for mixed brines were carried out for potassium ion concentrations of 250 and 1500 ppm at temperatures of 40, 60 and 80°C. The data (mg scale/ kg mixed brines) are given in Table 4.38.

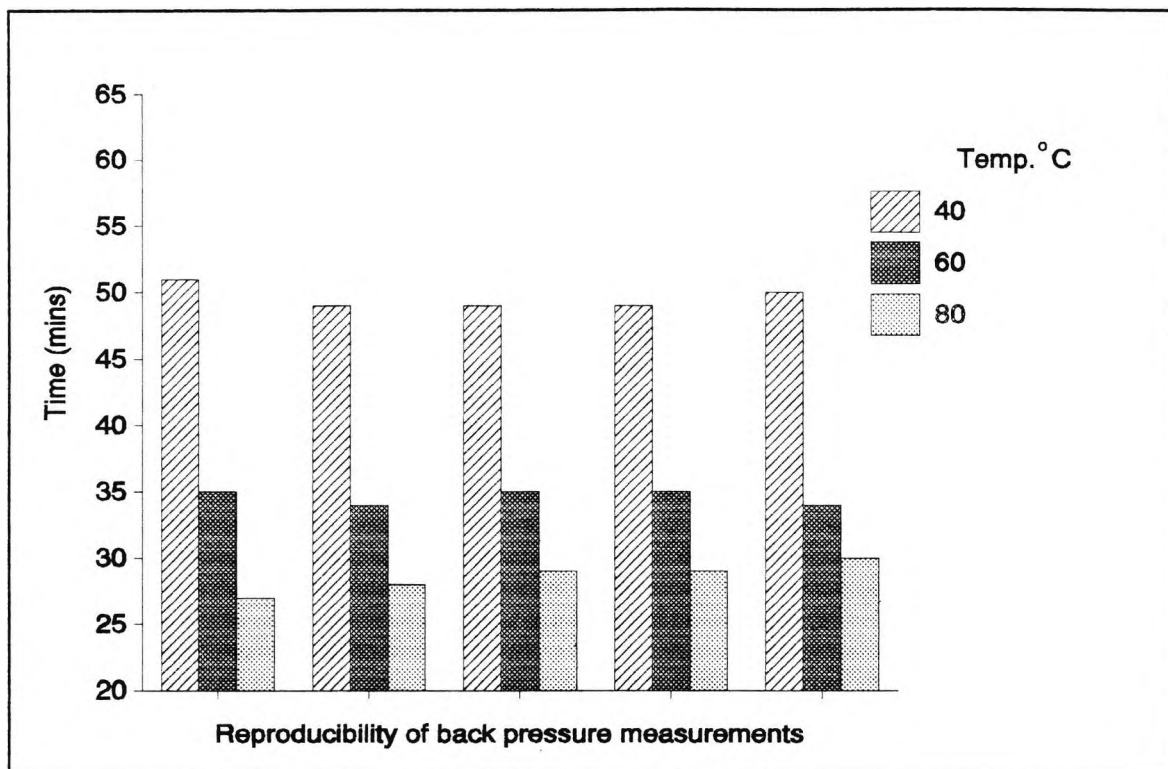


Figure 4.18 Reproducibility of propensity to scale measurements for the potassium ion concentration of 1000 ppm in sea water.

Table 4.38 Predicted weight (mg scale/ kg mixed brines) of each precipitate deposited.

K <sup>+</sup> 250ppm				K <sup>+</sup> 1500ppm			
Temp°C	CaCO <sub>3</sub>	SrSO <sub>4</sub>	BaSO <sub>4</sub>	Temp°C	CaCO <sub>3</sub>	SrSO <sub>4</sub>	BaSO <sub>4</sub>
40	0.0	117.0	124.7	40	11.5	114.0	124.6
60	55.1	126.3	124.5	60	64.8	123.5	124.5
80	96.4	140.1	124.3	80	103.4	137.7	124.4

The data show that at all potassium ion concentrations and temperatures studied there are no significant differences in the

predicted quantities for strontium and barium sulphate deposition. At the higher potassium ion concentration the predicted amount of calcium carbonate is increased slightly at 40°C, but this is not reflected in the propensity to scale measurements.

The propensity to scale experiments and the scaling prediction model indicate that increasing potassium ion concentrations in sea water has no significant effect on the propensity to scale on mixing with formation water.

#### 4.10.3 The Effect of Varying the Magnesium Ion Concentration in Simulated Sea Water on the Propensity to Scale

The magnesium chloride concentrations used and the physical properties of the sea waters studied are given in Table 4.39. All the other ion concentrations in the sea water were kept constant. The pump speeds were set at Pump A, 61.0% and Pump B, 63.5%. The propensity to scale was measured for increases in back pressure of 1 and 4 psi above the distilled water base line.

**Table 4.39 Changes in chemical composition on varying the magnesium chloride concentration in sea water.**

Mg <sup>2+</sup>	Cl <sup>-</sup>	MgCl <sub>2</sub> .6H <sub>2</sub> O wt. (g/l)	pH	S.G.
375	16119	3.138	7.96	1.021
750	17214	6.275	7.87	1.023
1500	19406	12.550	7.76	1.024
2250	21597	18.825	7.46	1.027

The results for the average scaling times for the magnesium ion concentration experiments for an increase in back pressure of 1 psi are given in Table 4.40, and shown graphically in Figure 4.19. The results for an increase in back pressure of 4 psi are given in Table 4.41, and shown graphically in Figure 4.20. The details of replicate runs for each magnesium ion concentration

experiment are given in Appendix Tables B.37 to B.40 for an increase in back pressure of 1 psi, and given in Appendix Tables B.41 to B.44 for an increase in back pressure of 4 psi.

**Table 4.40 Effect of different magnesium ion concentrations on an increase in back pressure of 1 psi: Average scaling times (mins).**

Temp °C	Mg <sup>2+</sup> 375ppm	Mg <sup>2+</sup> 750ppm	Mg <sup>2+</sup> 1500ppm	Mg <sup>2+</sup> 2250ppm
40	42.6	41.4	48.2	58.4
50	35.8	36.2	39.2	44.8
60	30.6	33.0	33.8	37.2
70	26.0	25.8	27.4	32.2
80	23.2	22.4	24.6	28.2
90	21.0	21.0	23.8	25.4

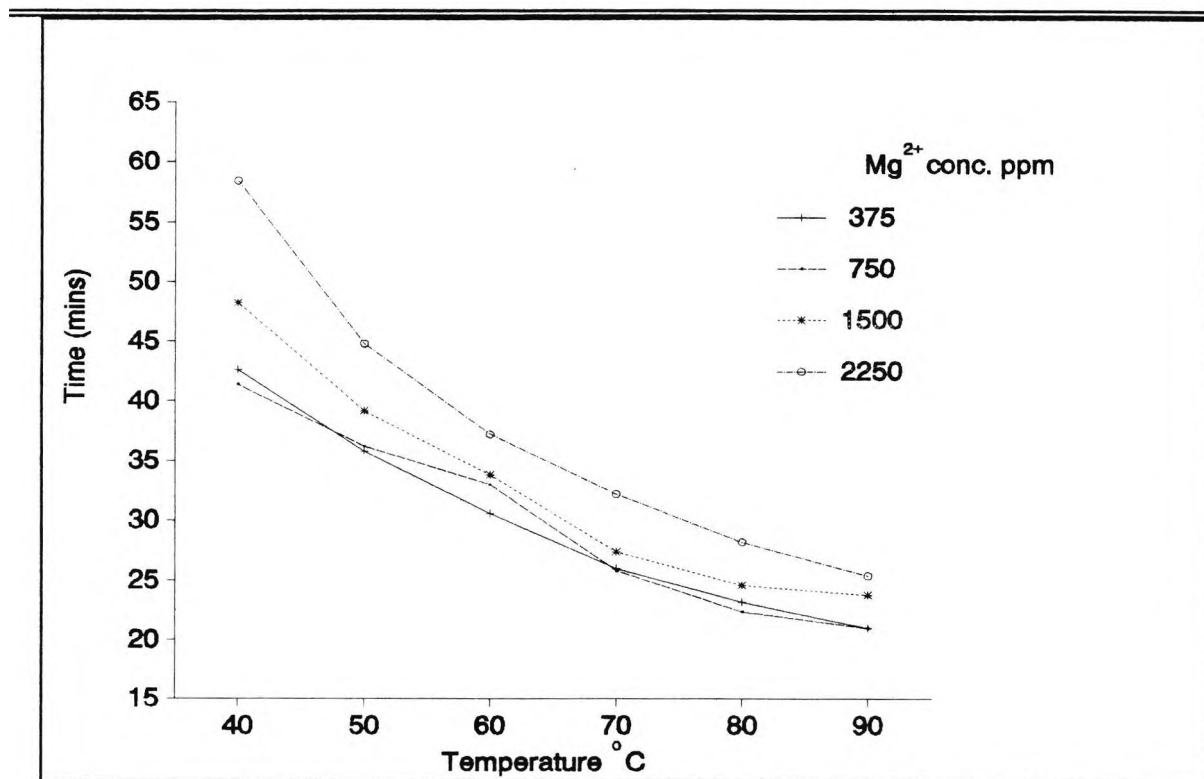


**Figure 4.19 Effect of different magnesium ion concentrations on the average scaling times for an increase in back pressure of 1 psi.**

Table 4.41 Effect of different magnesium ion concentrations on an increase in back pressure of 4 psi: Average scaling times (mins).

Temp °C	Mg <sup>2+</sup> 375ppm	Mg <sup>2+</sup> 750ppm	Mg <sup>2+</sup> 1500ppm	Mg <sup>2+</sup> 2250ppm
40	60.8	59.6	68.8	80.6
50	49.8	50.0	57.6	63.0
60	42.2	44.6	50.2	54.4
70	36.8	37.2	42.8	45.6
80	32.4	34.2	39.6	41.8
90	32.8	33.4	38.2	41.6

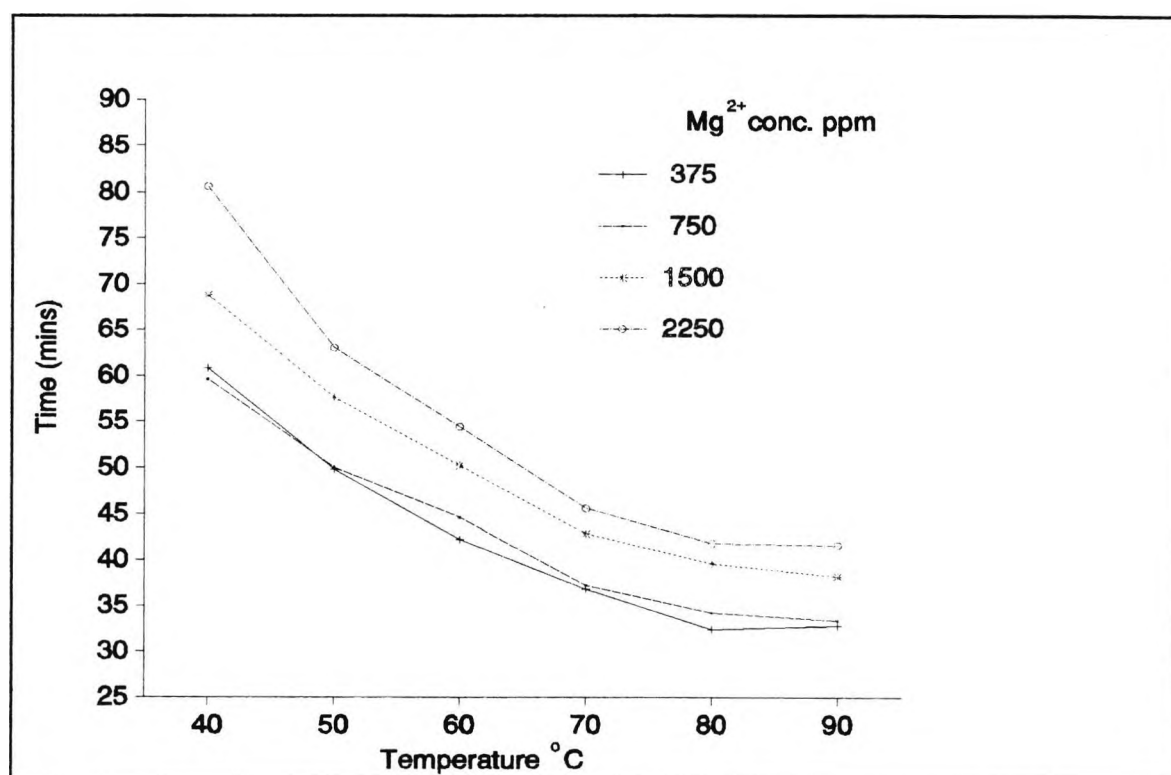


Figure 4.20 Effect of different magnesium ion concentrations on the average scaling times for an increase in back pressure of 4 psi.

The results show that varying the concentration of magnesium ion in simulated sea waters significantly influences the rate of

deposition of scale, the rate decreasing as the magnesium ion concentration increases. At the two lowest concentrations tested, no apparent trend can be seen, but as the concentration is raised to 1500 ppm and above a clear trend can be seen. The sea water containing 2250 ppm of magnesium ion took 15.8 minutes longer than the sea water containing 375 ppm of magnesium ion at 40°C to form a scale, increasing the back pressure by 1 psi. For an increase in back pressure of 4 psi, the time difference was 19.8 minutes. Comparison of the propensity to scale data in Table 4.42 for initial scale deposition (1 psi back pressure) and scale buildup (4 psi back pressure) shows that the time for buildup of scale is considerably shorter than that required to deposit the initial precipitate on which the scale subsequently grows.

**Table 4.42 Average scaling times (mins) for a sea water containing 2250 ppm of magnesium ion for increases in back pressure of 1 and 4 psi.**

Temp °C	Time for a 1 psi increase	Time for a 4 psi increase	Time difference for extra 3 psi increase
40	58.4	80.6	22.2
60	37.2	54.4	17.2
80	28.4	41.8	13.4

These results confirm the effects found in changing the magnesium ion concentrations in formation water (Section 4.9.3), which proved that the initial scale deposition accounted for the relatively long time for the initial layer of scale to deposit. Extending the experiment to increase the back pressure by an extra 3 psi, confirmed that the deposition rate for the same degree of supersaturation and contact time was greater than during its nucleation stage. Finally, it confirmed that the rate of scale deposition increased at higher temperatures, which in turn increased the propensity to scale.

The results of varying the magnesium ion concentration show

clearly that there are statistically significant decreases in the rate of deposition as the magnesium ion concentration is increased. Precipitation studies were carried out to determine which precipitates were forming at the highest and lowest magnesium concentrations. The experimental procedure for the precipitation tests is described in Section 4.7.2 and the results (mg scale/ kg mixed brines) are given in Table 4.43.

**Table 4.43 Weight (mg scale/ kg mixed brines) of each precipitate deposited.**

Mg <sup>2+</sup> 375ppm				Mg <sup>2+</sup> 2250ppm			
Temp°C	CaCO <sub>3</sub>	SrSO <sub>4</sub>	BaSO <sub>4</sub>	Temp°C	CaCO <sub>3</sub>	SrSO <sub>4</sub>	BaSO <sub>4</sub>
40	113	95	127	40	73	76	127
60	137	139	127	60	124	108	127
80	169	164	127	80	154	137	127

The results show that at both magnesium ion concentrations studied, there was no difference in the quantity of barium sulphate precipitated. But at the higher magnesium ion concentration, significant reductions in the precipitation of strontium sulphate and calcium carbonate at the temperatures studied were found. To confirm the differences found, the scaling prediction model [26] was used for mixed brines for magnesium ion concentrations of 375 and 2250 ppm at temperatures of 40, 60 and 80°C and the predictions (mg scale/ kg mixed brines) are given in Table 4.44.

The scaling prediction model data show the same trends as those found in the precipitation tests *viz.*, (1) no significant difference in the predicted quantity of barium sulphate, (2) a noticeable reduction in the predicted weight of calcium carbonate and (3) a noticeable reduction in the weight of strontium sulphate precipitated.

Table 4.44 Predicted weight (mg scale/ kg mixed brines) of each precipitate deposited.

Mg <sup>2+</sup> 375ppm				Mg <sup>2+</sup> 2250ppm			
Temp°C	CaCO <sub>3</sub>	SrSO <sub>4</sub>	BaSO <sub>4</sub>	Temp°C	CaCO <sub>3</sub>	SrSO <sub>4</sub>	BaSO <sub>4</sub>
40	12.3	144.5	124.9	40	0.0	90.2	124.4
60	66.1	154.5	124.8	60	45.5	98.7	124.3
80	104.9	167.2	124.7	80	88.9	113.6	124.1

The precipitation and scaling prediction model results are consistent with the overall changes in propensity to scale measured in the present work. The reduction in the amount of strontium sulphate precipitated has been linked to its increased solubility in the presence of high magnesium ion concentrations [27], caused by the formation of magnesium sulphate ion pairs [21,22], which would reduce the availability of sulphate ions to form strontium sulphate. Similar effects have been seen in the formation water solutions containing high magnesium ion levels (Section 4.9.3). The reduction in the amount of calcium carbonate precipitate is consistent with earlier solubility data [28].

#### 4.10.4 The Effect of Varying the Calcium Ion Concentration in Simulated Sea Water on the Propensity to Scale

The calcium chloride concentrations used and the physical properties of the sea waters studied are given in Table 4.45. All the other ion concentrations in the sea water were kept constant. The pump speeds were set at Pump A, 61.0% and Pump B, 63.5%.

The results for the average scaling times for the calcium ion concentration experiments are given in Table 4.46, and shown graphically in Figure 4.21. The details of replicate runs for each calcium ion concentration experiment are given in Appendix Tables B.45 to B.48.

**Table 4.45 Changes in chemical composition on varying the calcium chloride concentration in sea water.**

Ca <sup>2+</sup> ppm	Cl <sup>-</sup> ppm	CaCl <sub>2</sub> .2H <sub>2</sub> O wt. (g/l)	pH	S.G.
250	18668	0.917	7.90	1.023
500	19111	1.834	7.52	1.024
1000	19996	3.668	7.24	1.025
1500	20882	5.502	7.20	1.025

**Table 4.46 Effect of different calcium ion concentrations on an increase in back pressure of 1 psi: Average scaling times (mins).**

Temp °C	Ca <sup>2+</sup> 250ppm	Ca <sup>2+</sup> 500ppm	Ca <sup>2+</sup> 1000ppm	Ca <sup>2+</sup> 1500ppm
40	44.4	51.4	55.6	61.0
50	37.4	40.6	43.8	51.2
60	31.8	36.0	37.6	44.6
70	27.6	29.6	33.2	39.6
80	23.8	26.0	28.6	35.8
90	22.4	25.4	29.0	33.0

The results indicate that varying the concentration of calcium ion in sea waters significantly influences the rate of deposition of scale with the rate decreasing as the calcium ion concentration is increased. This trend was found at all temperatures and concentrations studied. The sea water containing 1500 ppm calcium ion took 16.6 minutes longer than the sea water containing 250 ppm to form a scale at 40°C. However, at 90°C the time difference in the propensity to scale was 10.6 minutes between the two sea waters. The effect of temperature on the propensity to scale measurements is also evident and, as expected, the rate of deposition of scale was shown to increase with temperature.

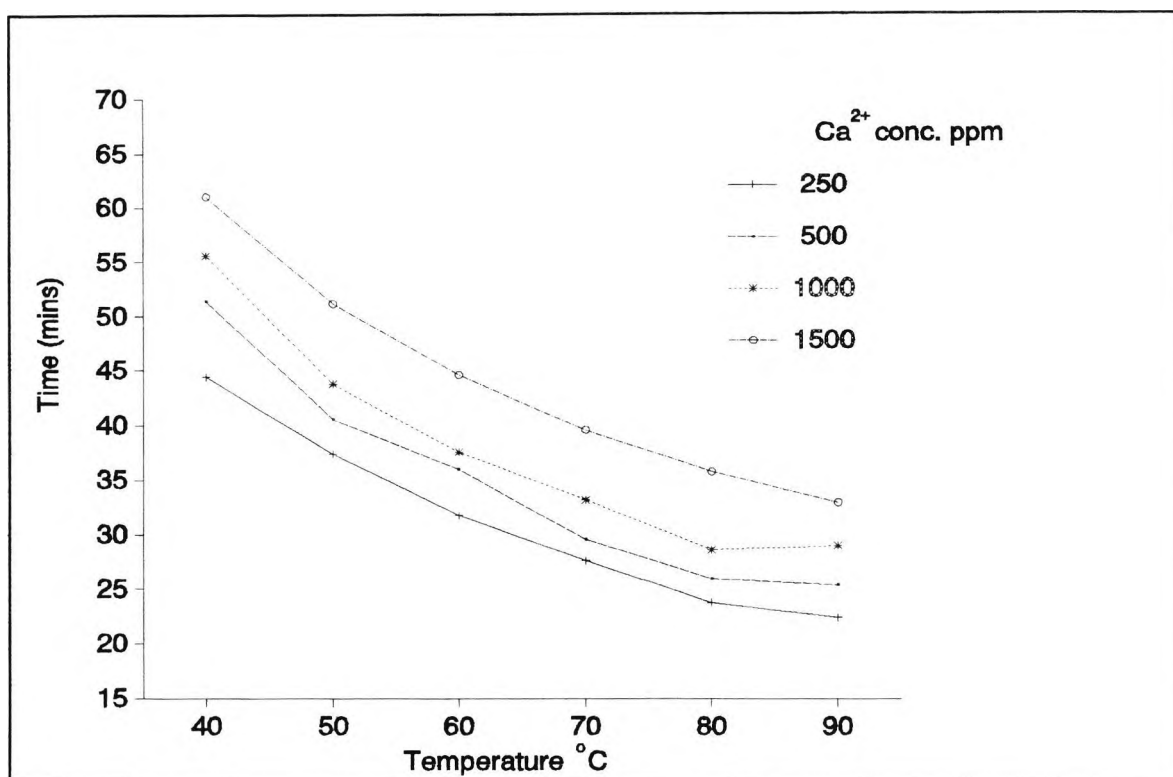


Figure 4.21 Effect of different calcium ion concentrations on the average scaling times.

As a statistically significant decrease was found in the rate of deposition as the calcium ion concentration was increased, precipitation studies were carried out to determine which precipitates were forming at the highest (1500 ppm) and lowest (250 ppm) calcium ion concentrations. The experimental procedure for the precipitation tests is described in Section 4.7.2, and the results (mg scale/ kg mixed brines) are given in Table 4.47.

The results show that at the higher calcium ion concentration (1500ppm) there is a significant increase in the weight of calcium carbonate precipitated because there were more calcium ions in the mixed brine to react with the carbonate ions available. In this set of experiments the amount of calcium carbonate formed was limited by the low level of hydrogen carbonate ion (500 ppm) in sea water. The effect of temperature is apparent for as the temperature rises, the rate of precipitation increases because of the increased decomposition of hydrogen carbonate ion to carbonate ion. For strontium

Table 4.47 Weight (mg scale/ kg mixed brines) of each precipitate deposited.

Ca <sup>2+</sup> 250ppm				Ca <sup>2+</sup> 1500ppm			
Temp°C	CaCO <sub>3</sub>	SrSO <sub>4</sub>	BaSO <sub>4</sub>	Temp°C	CaCO <sub>3</sub>	SrSO <sub>4</sub>	BaSO <sub>4</sub>
40	3	92	127	40	112	84	127
60	27	133	127	60	125	107	127
80	46	165	127	80	135	139	127

sulphate there was a noticeable reduction in the weights precipitated between the two sea waters at all three temperatures. This reduction is consistent with an increased solubility of strontium sulphate in waters containing high calcium ion concentrations [27]. On analysis of the solutions, the sulphate ion concentration was found to be reduced only by precipitation with barium and strontium ions and not by forming calcium sulphate, which is more soluble. Barium sulphate precipitation is not affected by an increase in either calcium ion concentration or temperature.

The results in Table 4.46 and 4.47, in combination with Figure 4.21, demonstrate that as the calcium ion concentration increases in sea waters the propensity to scale is reduced. To further explain the differences found, the scaling prediction model [26] was used for mixed brines for calcium ion concentrations of 250 and 1500 ppm at 40, 60 and 80°C, and the predicted results (mg scale/ kg mixed brines) are given in Table 4.48.

The scaling prediction model data show the same trends as those found in the precipitation tests *viz.*, (1) no difference in the predicted quantity of barium sulphate, (2) a slight decrease in the predicted weight of strontium sulphate and (3) a noticeable increase in the weight of calcium carbonate. The precipitation tests gave higher quantities of calcium carbonate precipitate than the prediction scaling model because of the increased time allowed in the precipitation tests for equilibration. This has

Table 4.48 Predicted weight (mg scale/ kg mixed brines) of each precipitate deposited.

Ca <sup>2+</sup> 250ppm				Ca <sup>2+</sup> 1500ppm			
Temp°C	CaCO <sub>3</sub>	SrSO <sub>4</sub>	BaSO <sub>4</sub>	Temp°C	CaCO <sub>3</sub>	SrSO <sub>4</sub>	BaSO <sub>4</sub>
40	11.6	117.8	124.7	40	33.9	109.0	124.6
60	64.3	127.0	124.6	60	82.6	119.0	124.5
80	102.8	140.8	124.5	80	117.0	133.8	124.3

been discussed previously in Section 4.9.1.

#### 4.10.5 The Effect of Varying the Strontium Ion Concentration in Simulated Sea Water on the Propensity to Scale

The strontium chloride concentrations used and the physical properties of the sea waters studied are given in Table 4.49. All the other ion concentrations were unchanged. The pump speeds were set at Pump A, 52.5% and Pump B, 55.0%.

Table 4.49 Changes in chemical composition on varying the strontium chloride concentration in sea water.

Sr <sup>2+</sup>	Cl <sup>-</sup>	SrCl <sub>2</sub> .2H <sub>2</sub> O wt. (g/l)	pH	S.G.
0	18926	0.0	7.62	1.024
100	19007	0.3043	7.61	1.024
250	19128	0.7607	7.65	1.025

The results for the average scaling times for the strontium ion concentration experiments are given in Table 4.50, and shown graphically in Figure 4.22. The details of replicate runs for each strontium ion concentration experiment are given in Appendix Tables B.49. to B.51.

Table 4.50 Effect of different strontium ion concentrations on an increase in back pressure of 1 psi: Average scaling times (mins).

Temp °C	Sr <sup>2+</sup> 0ppm	Sr <sup>2+</sup> 100ppm	Sr <sup>2+</sup> 250ppm
40	51.0	53.4	60.4
50	41.0	43.0	46.2
60	34.4	38.6	40.6
70	31.4	32.4	33.2
80	26.6	29.2	27.0
90	25.4	26.8	25.2

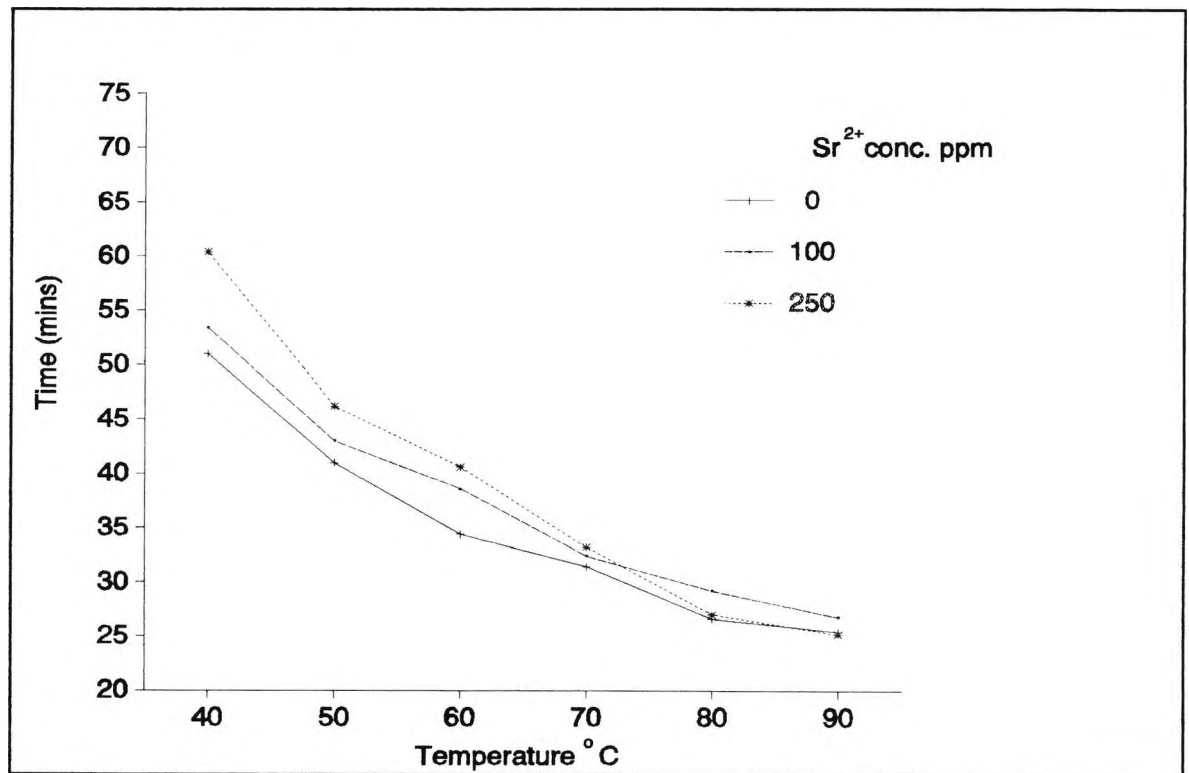


Figure 4.22 Effect of different strontium ion concentrations on the average scaling times.

The results show that varying the concentration of strontium ion in sea waters significantly influences the rate of deposition of scale. At temperatures below 70°C, the rate of deposition was

reduced as the strontium ion concentration was increased, but at temperatures above 70°C no trend was found. These results show the same three factors found when changing strontium ion concentrations in formation water. These are: (1) strontium ion concentration, (2) temperature and (3) the effect of temperature at each strontium ion concentration. At higher strontium ion concentrations it was expected that the rate of deposition would increase because more strontium sulphate would be precipitated, but this was not found for temperatures below 70°C.

The results show that as the strontium ion concentration is increased from 0 to 250 ppm, the scaling time takes 9.4 minutes longer at 40°C, for the propensity to scale measurements. As the temperature was increased, this time reduction was decreased until at 70°C and above there was no difference. The effect of temperature on the propensity to scale measurements was as expected, with the rate of deposition increasing at higher temperatures. At the lowest strontium ion concentration, 0 ppm, the scaling time was reduced by 25.6 minutes when the temperature was raised from 40 to 90°C. At higher strontium ion concentrations this time difference was increased so that sea water containing 250 ppm strontium ion showed a reduction of 35.2 minutes in scaling time between 40 and 90°C.

The strontium ion concentration was only changed three times from 0 to 250 ppm. When the concentration was increased to 500 ppm, strontium sulphate began to precipitate within the sea water, affecting the propensity to scale measurements with the scaling time increasing from 59 to 78 minutes overnight.

The results of varying the strontium ion concentration in sea water clearly show that there are statistically significant differences in the rate of deposition as the strontium ion concentration is increased. Precipitation studies were carried out to determine which precipitates were forming at the highest and lowest strontium ion concentrations. The experimental procedure for the precipitation tests is described in Section

4.7.2, and the results (mg scale/ kg mixed brines) are given in Table 4.51.

**Table 4.51 Weight (mg scale/ kg mixed brines) of each precipitate deposited.**

Sr <sup>2+</sup> 0ppm				Sr <sup>2+</sup> 250ppm			
Temp°C	CaCO <sub>3</sub>	SrSO <sub>4</sub>	BaSO <sub>4</sub>	Temp°C	CaCO <sub>3</sub>	SrSO <sub>4</sub>	BaSO <sub>4</sub>
40	39	97	127	40	47	309	127
60	89	125	127	60	87	369	127
80	126	152	127	80	132	395	127

The results indicate that an increase in strontium ion concentration does not affect calcium carbonate precipitation. The effect of temperature is clear: as the temperature rises, the rate of precipitation increases, because of the faster decomposition of hydrogen carbonate ion to carbonate ion. For strontium sulphate there is a very significant increase in the weight precipitated between the highest and lowest strontium ion concentrations for the three temperatures studied. At 40°C, the quantity of strontium sulphate precipitate formed was 97 mg/kg compared to 309 mg/kg for the sea waters containing 0 and 250 ppm strontium ion, respectively. The effect of temperature on strontium sulphate deposition was similar to that for calcium carbonate. As the temperature rises, the rate of deposition increases, because of changes in solubility. Barium sulphate precipitation is not affected by increases in either strontium ion concentration or temperature. To further explain the differences found, the scaling model predictions for mixed brines [26] were carried out for strontium ion concentrations of 0 and 250 ppm at temperatures of 40, 60 and 80°C, and the results (mg scale/ kg mixed brines) are given in Table 4.52.

Table 4.52 Predicted weight (mg scale/ kg mixed brines) of each precipitate deposited.

Sr <sup>2+</sup> 0ppm				Sr <sup>2+</sup> 250ppm			
Temp°C	CaCO <sub>3</sub>	SrSO <sub>4</sub>	BaSO <sub>4</sub>	Temp°C	CaCO <sub>3</sub>	SrSO <sub>4</sub>	BaSO <sub>4</sub>
40	23.5	108.9	124.7	40	37.6	350.1	124.6
60	73.7	118.2	124.5	60	83.9	360.3	124.4
80	110.0	132.0	124.4	80	117.3	375.6	124.3

The data indicate that there is no difference in the predicted quantity of barium sulphate deposited. The quantity of calcium carbonate deposited was predicted to increase slightly at higher strontium ion concentrations at the three temperatures. The scaling prediction model for strontium sulphate is in fairly close agreement with the precipitation results, showing that the sea water containing 250 ppm of strontium ion deposits an increased quantity of strontium sulphate, when compared to the sea water containing 0 ppm of strontium.

The data in Tables 4.50, 4.51 and 4.52, in combination with Figure 4.22, show that the propensity to scale measurements and precipitation studies appear to give conflicting results. In the propensity to scale experiments, at temperatures below 70°C, the rate of scale deposition is significantly reduced as the strontium ion concentration is increased. Above 70°C, the rate of scale deposition is not affected by increases in strontium ion concentration, whereas the precipitation tests and the scaling prediction model suggest that the higher the strontium ion concentration in sea waters, then more strontium sulphate should be precipitated. The results demonstrate that higher strontium concentrations in sea water enhance the precipitation of the three main precipitates, but this does not subsequently increase scale formation.

The differences in the data obtained between propensity to scale measurements and precipitation results (in agreement with the

scale prediction model) highlight the fact that kinetic effects must be important in scale formation. The precipitation experiments are carried out over a long enough time span to ensure that the equilibrium scale mixture is totally precipitated. The scale prediction model should mirror these results because it is based on the available solubility data for the compounds being precipitated. The propensity to scale measurements, however, result from instantaneous precipitation reactions within the microbore tube with no time allowance to achieve equilibrium. The nature of the scale obtained must, therefore, depend not only on composition but on the rate of formation of nuclei of the potential components of the scale. It is known, for example, from other work carried out in the City University laboratories [25], that there is a considerable time delay in the formation of  $\text{CaSO}_4 \cdot 2\text{H}_2\text{O}$  nuclei when solutions containing calcium and sulphate ions are mixed. It seems likely that a similar delay in the formation of strontium sulphate nuclei is responsible for the absence of the predicted amounts of strontium sulphate in the instantaneous precipitation situation. Other workers studying the co-precipitation of strontium sulphate with barium sulphate have found similar effects at high strontium/barium ratios [23].

#### 4.10.6 The Effect of Varying the Hydrogen Carbonate Ion Concentration in Simulated Sea Water on the Propensity to Scale

The sodium hydrogen carbonate concentrations used and the physical properties of the sea waters studied are given in Table 4.53. All the other ion concentrations in the sea water were kept constant. The pump speeds were set at Pump A, 90.5% and Pump B, 93.0%, with each delivering 0.85 litres per hour of formation or sea water into the P.M.A.C. microbore tube. In these experiments the simulated formation water contained 100 ppm of barium ion not 150 ppm as used in all the other experiments.

**Table 4.53 Changes in chemical composition on varying the sodium hydrogen carbonate concentration in sea water.**

Na <sup>+</sup>	HCO <sub>3</sub> <sup>-</sup>	NaHCO <sub>3</sub> wt. (g/l)	pH	S.G.
10379	100	0.1377	7.35	1.024
10435	250	0.3443	7.41	1.024
10529	500	0.6885	7.56	1.025
10718	1000	1.3770	7.17	1.025

The results for the average scaling times for the hydrogen carbonate ion concentration experiments are given in Table 4.54, and shown graphically in Figure 4.23. The details of replicate runs for each hydrogen carbonate ion concentration experiment are given in Appendix Tables B.52 to B.55.

**Table 4.54 Effect of different hydrogen carbonate ion concentrations on an increase in back pressure of 1 psi: Average scaling times (mins).**

Temp °C	HCO <sub>3</sub> <sup>-</sup>	HCO <sub>3</sub> <sup>-</sup>	HCO <sub>3</sub> <sup>-</sup>	HCO <sub>3</sub> <sup>-</sup>
	100ppm	250ppm	500ppm	1000ppm
40	50.00	47.50	42.25	54.00
50	44.00	39.75	41.25	44.75
60	35.75	37.00	37.50	37.25
70	31.75	31.00	31.00	35.00
80	27.75	28.00	28.25	30.00
90	25.50	23.50	24.75	28.00

The results indicate that varying the concentration of hydrogen carbonate ion in sea waters does not have any noticeable effect on the rate of deposition of scale. At all temperatures except 40°C, the average scaling times for an increase in back pressure of 1 psi, varied by less than 5 minutes at all concentrations. The effect of temperature on the propensity to scale measurements

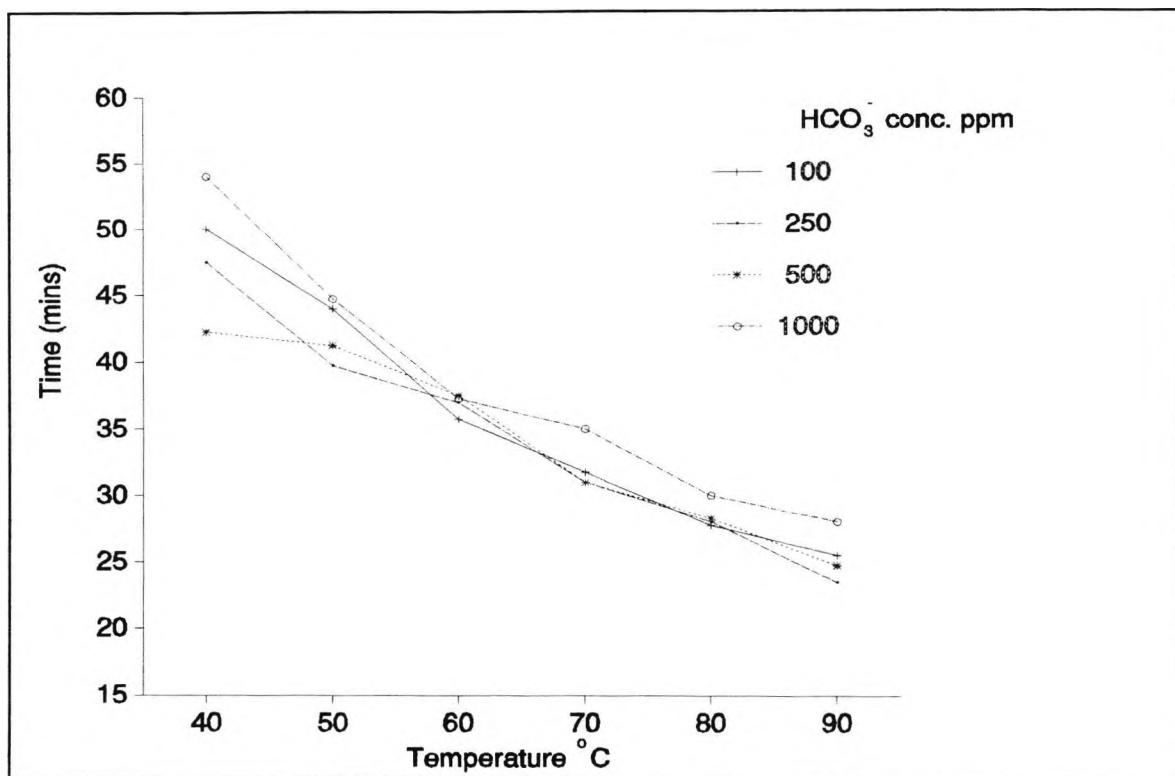


Figure 4.23 Effect of different hydrogen carbonate ion concentrations on the average scaling times.

was also evident, and as expected the rate of deposition of scale was shown to increase with temperature.

The results of varying the hydrogen carbonate ion concentration in a sea water clearly show that there is no significant difference in the rate of deposition of scale. At higher hydrogen carbonate ion concentrations it was expected that the rate of deposition would increase because more calcium carbonate would be precipitated, but this was not found. Precipitation studies were, therefore, carried out to determine which precipitates were forming at the highest and lowest hydrogen carbonate ion concentrations. The experimental procedure for the precipitation test is described in Section 4.7.2 and the results (mg scale/ kg mixed brines) are given in Table 4.55.

The results show that at the higher hydrogen carbonate ion concentration (1000ppm), there is a significant increase in the weight of calcium carbonate precipitated at the three

**Table 4.55 Weight (mg scale/ kg mixed brines) of each precipitate deposited.**

HCO <sub>3</sub> <sup>-</sup> 100ppm				HCO <sub>3</sub> <sup>-</sup> 1000ppm			
Temp°C	CaCO <sub>3</sub>	SrSO <sub>4</sub>	BaSO <sub>4</sub>	Temp°C	CaCO <sub>3</sub>	SrSO <sub>4</sub>	BaSO <sub>4</sub>
40	23	97	85	40	135	93	85
60	21	114	85	60	172	120	85
80	29	144	85	80	228	156	85

temperatures, because there were more hydrogen carbonate ions in the mixed brine to react with the calcium ions available. The effect of temperature increases precipitation as the temperature rises because of the increased decomposition of hydrogen carbonate ion to carbonate ion. There is no difference in the weights of strontium sulphate precipitated between the high and low hydrogen carbonate ion solutions. The effect of temperature on strontium sulphate deposition was similar to that for calcium carbonate. As the temperature rises the rate of deposition increases because of changes in solubility. Barium sulphate precipitation is not affected by increases in hydrogen carbonate ion concentration or temperature. To further explain the differences found, the scaling model predictions for mixed brines [26] were carried out for hydrogen carbonate ion concentrations of 100 and 1000 ppm at temperatures of 40, 60 and 80°C and the results (mg scale/ kg mixed brines) are given in Table 4.56.

**Table 4.56 Predicted weight (mg scale/ kg mixed brine) of each precipitate deposited.**

HCO <sub>3</sub> <sup>-</sup> 100ppm				HCO <sub>3</sub> <sup>-</sup> 1000ppm			
Temp°C	CaCO <sub>3</sub>	SrSO <sub>4</sub>	BaSO <sub>4</sub>	Temp°C	CaCO <sub>3</sub>	SrSO <sub>4</sub>	BaSO <sub>4</sub>
40	0	118.9	83.0	40	35.4	117.6	83.0
60	0	128.0	82.9	60	132.3	126.8	82.9
80	0	141.7	82.8	80	204.6	140.6	82.8

The scaling prediction model data show the same trends as those found in the precipitation tests viz., (1) no difference in the predicted quantity of barium sulphate, (2) no difference in the predicted quantity of strontium sulphate and (3) a noticeable increase in the predicted weight of calcium carbonate at higher hydrogen carbonate ion concentrations. The precipitation tests gave higher quantities of calcium carbonate precipitate than the prediction scaling model because of the increased time allowed in the precipitation tests for equilibration.

The data in Tables 4.54, 4.55 and 4.56, in combination with Figure 4.23, show that the propensity to scale measurements and precipitation studies for changing hydrogen carbonate ion concentrations in sea waters appear to give conflicting results. In the propensity to scale experiments no difference was found as the hydrogen carbonate ion concentration was increased, whereas in the precipitation tests the higher the hydrogen carbonate ion concentration, then more precipitate was formed when the sea water was mixed with formation water. The results demonstrate that higher hydrogen carbonate ion concentrations in sea water enhance the precipitation of calcium carbonate, but this has no effect on the aggregation of the barium and strontium sulphate precipitates to form scale.

#### 4.10.7 The Effect of Varying the Sulphate Ion Concentration in Simulated Sea Water on the Propensity to Scale

The sodium sulphate concentrations used and the physical properties of the sea waters studied are given in Table 4.57. All the other ion concentrations in the sea water were kept constant. The pump speeds were set at Pump A, 63.5% and Pump B, 65.0%.

The results for the average scaling times for the sulphate ion concentration experiments are given in Table 4.58 and shown graphically in Figure 4.24. The details of replicate runs for each sulphate ion concentration experiment are given in Appendix Tables B.56 to B.59.

**Table 4.57 Changes in chemical composition on varying the sodium sulphate concentration in sea water.**

Na <sup>+</sup>	SO <sub>4</sub> <sup>2-</sup>	Na <sub>2</sub> SO <sub>4</sub> wt. (g/l)	pH	S.G.
9954	1500	2.219	7.60	1.024
10194	2000	2.959	7.56	1.025
10433	2500	3.699	7.57	1.025
10672	3000	4.439	7.52	1.025

**Table 4.58 Effect of different sulphate ion concentrations on an increase in back pressure of 1 psi: Average scaling times (mins).**

Temp °C	SO <sub>4</sub> <sup>2-</sup>	SO <sub>4</sub> <sup>2-</sup>	SO <sub>4</sub> <sup>2-</sup>	SO <sub>4</sub> <sup>2-</sup>
	1500ppm	2000ppm	2500ppm	3000ppm
40	92.25	67.75	54.50	49.25
50	84.50	54.75	42.50	40.50
60	71.00	44.75	29.25	34.00
70	62.00	40.50	27.00	27.75
80	54.50	36.00	24.75	25.75
90	46.25	32.75	23.75	24.00

The results show that varying the concentration of sulphate ion in sea waters significantly influences the rate of deposition of scale. However, the sulphate ion concentrations of 2500 and 3000 ppm do not cause any changes in the rate of deposition, but as the sulphate ion concentration is reduced to 1500 ppm a significant reduction in the propensity to scale is found. At 40°C, the sea water containing 1500 ppm of sulphate ion took 43 minutes longer to scale than the sea water with 3000 ppm of sulphate ion. This time difference at 90°C is reduced to 22.25 mins between the two sea waters. These results appear to be consistent with those of Thomas [29], who investigated the effect of sulphate ion concentrations on mixed brine solutions of 2400-3000 ppm. The results showed that the rate of deposition

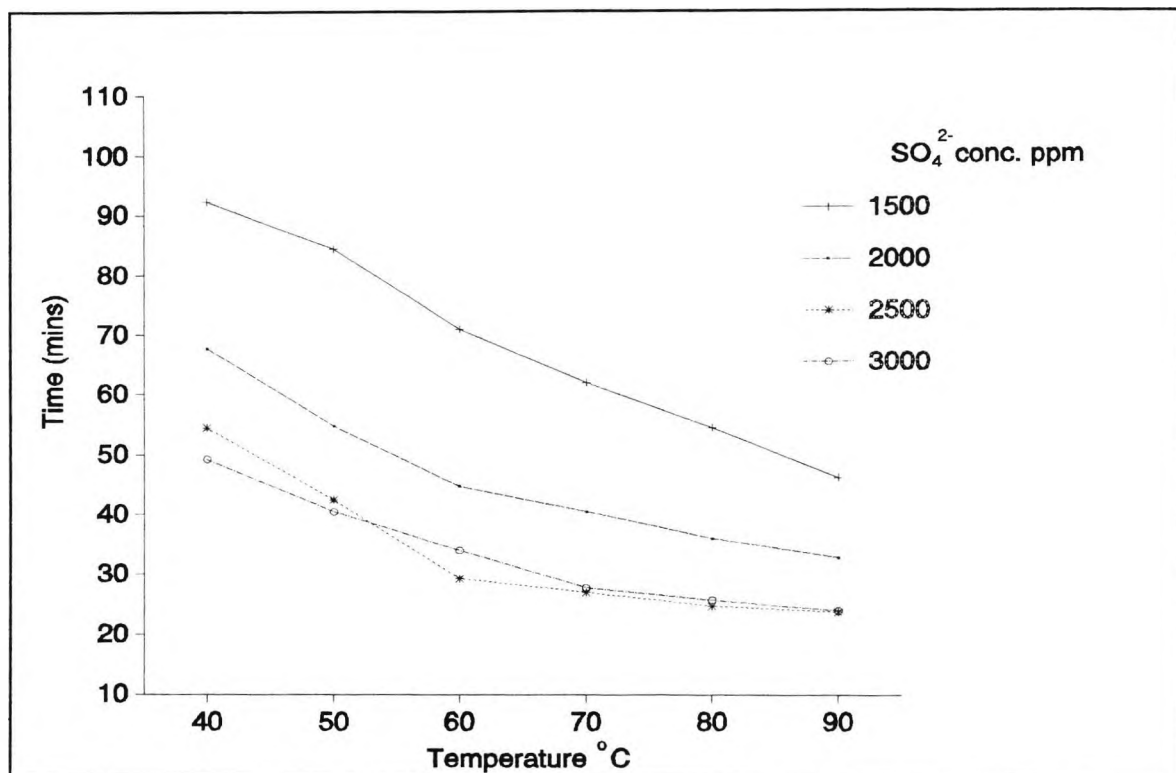


Figure 4.24 Effect of different sulphate ion concentrations on the average scaling times.

decreases as the sulphate ion concentration is reduced. The consistency of the measurements are shown in Figure 4.25, for four repeat runs of propensity to scale measurement for a sulphate ion concentration of 2000ppm at temperatures of 40, 60 and 80°C, giving standard deviations of 1.70, 1.26 and 1.15, respectively. The effect of temperature on the propensity to scale measurements was also evident and, as expected, the rate of deposition of scale was shown to increase with temperature.

The results of varying the sulphate ion concentration in a sea water clearly show that there are statistically significant increases in the rate of deposition as the concentration of the anion is increased. No precipitation studies were carried out as the effects found were caused by the sulphate ions affecting the deposition of strontium and barium sulphate. However, scaling prediction model calculations for mixed brines [26] were carried out for sulphate ion concentrations of 1500 and 3000 ppm at 40, 60 and 80°C. The results (mg scale/ kg mixed brines) are given in Table 4.59.

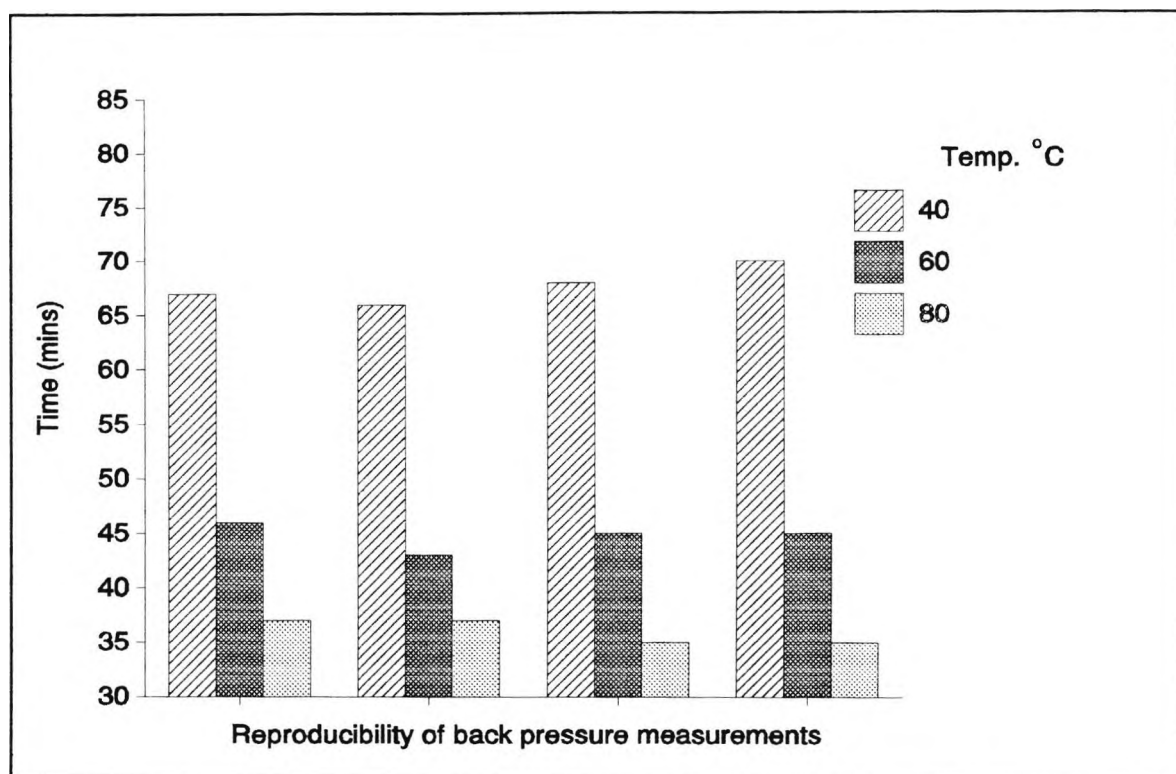


Figure 4.25 Reproducibility of propensity to scale measurements for the sulphate ion concentration of 2000 ppm in sea water.

Table 4.59 Predicted weight (mg scale/ kg mixed brines) of each precipitate deposited.

SO <sub>4</sub> <sup>2-</sup> 1500ppm				SO <sub>4</sub> <sup>2-</sup> 3000ppm			
Temp°C	CaCO <sub>3</sub>	SrSO <sub>4</sub>	BaSO <sub>4</sub>	Temp°C	CaCO <sub>3</sub>	SrSO <sub>4</sub>	BaSO <sub>4</sub>
40	0.0	22.1	124.3	40	0.0	128.8	124.6
60	55.3	36.1	124.1	60	49.6	137.4	124.5
80	96.6	58.1	123.8	80	92.4	150.1	124.4

The scaling model predicts that there is no significant difference in the quantity of calcium carbonate precipitated. The model also indicates that there is no difference in the predicted quantity of barium sulphate, but that the predicted quantity of strontium sulphate should significantly increase with higher

sulphate ion concentrations. This significant decrease in strontium sulphate precipitation causes a reduction in the deposition of scale as confirmed by the propensity to scale experiments.

#### 4.10.8 Summary of the Propensity to Scale Experiments

The effects of changing each significant ion concentration in simulated sea water separately, leaving the other concentrations unchanged, have yielded many interesting results. Every significant ion changed has been shown to have a different effect on the propensity to scale, as measured in the P.M.A.C. unit, when formation and sea waters are mixed.

The details of propensity to scale data have been further characterised by the precipitation tests and a scaling prediction model for mixed brines. The combined results show that kinetic effects can be more important than concentration effects in some cases. Table 4.60 summarises the general trends for increasing each significant ion concentration in the propensity to scale measurements.

**Table 4.60 Summary of the general trends found in the propensity to scale.**

Ion	General trend in propensity to scale
Na <sup>+</sup>	Significant decrease
K <sup>+</sup>	Slight decrease at higher K <sup>+</sup> concentrations
Mg <sup>2+</sup>	Significant decrease
Ca <sup>2+</sup>	Significant decrease
Sr <sup>2+</sup>	Significant decrease below 70°C, no difference above 70°C
HCO <sub>3</sub> <sup>-</sup>	Slight decrease at higher HCO <sub>3</sub> <sup>-</sup> concentrations
SO <sub>4</sub> <sup>2-</sup>	Significant increase

#### 4.10.9 Overall Summary of the Propensity to Scale Experiments

The effects found in the propensity to scale experiments, precipitation tests and the scaling prediction model data in Sections 4.9.1 to 4.9.6 and 4.10.1 to 4.10.7, show that increasing the concentration of an ion in either formation or sea water can have significant effects on the precipitation of  $\text{CaCO}_3$ ,  $\text{SrSO}_4$  and  $\text{BaSO}_4$ , and on the aggregation of the precipitates to form scale.

Table 4.61 Salt and common ion effects on changing each ion in formation and sea waters.

Ion	Formation water changes			Sea water changes		
	$\text{CaCO}_3$	$\text{SrSO}_4$	$\text{BaSO}_4$	$\text{CaCO}_3$	$\text{SrSO}_4$	$\text{BaSO}_4$
$\text{Na}^+$	N	S	S	N	S	S
$\text{K}^+$	N	S	S	N	S	S
$\text{Mg}^{2+}$	N	S	S	N	S	S
$\text{Ca}^{2+}$	C	S	S	C	S	S
$\text{Sr}^{2+}$	N	C	S	N	C	S
$\text{Ba}^{2+}$	N	S	C	-	-	-
$\text{HCO}_3^-$	-	-	-	C	S	N
$\text{SO}_4^{2-}$	-	-	-	S	C	C

C denotes a common ion effect, S denotes a salt effect and N denotes no effect was found.

Two main effects are identified in these experiments. The first occurs when the added ion does not have an ion in common with the sparingly soluble salt (the **salt effect**) and results in an increase in solubility of the sparingly soluble salt. The second occurs when the added ion is a component of the sparingly soluble salt (the **common ion effect**) and results in a reduction of solubility of the sparingly soluble salt. These effects are

illustrated in Table 4.61 for all the ions changed in formation and sea waters in the work described in Sections 4.9 and 4.10.

These experiments have shown the concentrations at which each ion is at its most and least scale-forming.

**4.11 THE EFFECT OF MIXING THE MOST AND LEAST SCALE-FORMING FORMATION AND SEA WATERS AS DETERMINED IN SECTIONS 4.9 and 4.10.**

In these experiments the barium and sulphate ion concentrations were fixed at 150 and 2700 ppm respectively, so that any potential differences were caused by the other ions. The most and least scale-forming simulated formation and sea waters used in these experiments were made up to the compositions shown in Table 4.62 and 4.63, giving the significant ion concentrations listed.

**Table 4.62 Most and least scale-forming formation waters used in the propensity to scale measurements.**

Salt compound	Most scale-forming		Least scale-forming	
	wt. g/l	sig.ion ppm	wt. g/l	sig.ion ppm
NaCl	10.0	3934	40.0	15736
KCl	0.954	500	0.954	500
MgCl <sub>2</sub> .6H <sub>2</sub> O	1.297	155	10.04	1200
CaCl <sub>2</sub> .2H <sub>2</sub> O	1.834	500	7.3363	2000
SrCl <sub>2</sub> .6H <sub>2</sub> O	0.6846	225	3.0429	1000
BaCl <sub>2</sub> .2H <sub>2</sub> O	0.2669	150	0.2669	150

The mixing flow rates for the experiments described in this section were kept constant at 50:50, with Pump A, 54.5% and Pump B, 57.0%, each delivering 0.5 litres per hour of formation or sea water into the P.M.A.C. microbore tube. The propensity to scale was measured for an increase of 1 psi above the distilled water base line for each combination investigated at temperatures of 40, 50, 60, 70, 80 and 90°C. For each set of conditions, five

experiments were carried out to ensure statistically significant results were achieved. After each experiment the normal cleaning procedure was carried out as described in Section 4.7.1. The physical properties of the waters studied are listed in Table 4.64.

**Table 4.63 Most and least scale-forming sea waters used in the propensity to scale measurements.**

Salt compound	Most scale-forming		Least scale-forming	
	wt. g/l	sig.ion ppm	wt. g/l	sig.ion ppm
NaCl	10.0	5265	40.0	17065
KCl	0.9535	500	2.8605	1500
MgCl <sub>2</sub> .6H <sub>2</sub> O	3.1375	375	18.825	2250
CaCl <sub>2</sub> .2H <sub>2</sub> O	0.917	250	5.5022	1500
SrCl <sub>2</sub> .6H <sub>2</sub> O	0.0	0	0.7607	250
NaHCO <sub>3</sub>	1.377	1000	0.1377	100
Na <sub>2</sub> SO <sub>4</sub>	3.995	2700	3.995	2700

**Table 4.64 Chemical composition of the waters used.**

Water type	Cl <sup>-</sup> ppm	pH	S.G.
MSF Formation water	8114	6.52	1.008
LSF Formation water	32642	6.32	1.037
MSF Sea water	8055	7.89	1.013
LSF Sea water	35044	7.11	1.042

LSF least scale-forming and MSF most scale-forming.

The results for the average scaling times for each combination are given in Table 4.65 and shown graphically in Figure 4.26. The details of replicate runs for each combination are given in Appendix Tables B.60. to B.63.

The propensity to scale experiments carried out were:

- (i) LSF Formation water : LSF Sea water
- (ii) LSF Formation water : MSF Sea water
- (iii) MSF Formation water : LSF Sea water
- (iv) MSF Formation water : MSF Sea water

**Table 4.65 Effect of different water combinations on increasing the back pressure by 1 psi: Average scaling times (mins).**

Temp °C	LSF : LSF	LSF : MSF	MSF : LSF	MSF : MSF
40	188.4	79.4	84.0	27.8
50	144.2	67.4	61.6	22.4
60	108.8	53.0	49.8	18.8
70	85.6	48.6	47.2	16.0
80	66.0	41.8	39.2	15.0
90	49.0	36.0	37.2	14.2

The results show that varying the combinations of most and least scale-forming formation and sea waters significantly influences the rate of deposition of scale. These experiments produced large time differences in the propensity to scale measurements, with the biggest differences being at 40°C, where the LSF formation and sea waters took 161 minutes longer than the MSF formation and sea waters to scale. However, at 90°C the time difference in the propensity to scale was 34.8 minutes for the same water combinations. When the combinations of MSF and LSF formation and sea waters and vice versa were mixed, there was no noticeable difference in their propensity to scale. The effect of temperature on propensity to scale was as expected, with the rate of deposition increasing with temperature.

The results of varying the combinations of most and least scale-forming formation and sea waters clearly show that there are statistically significant differences in their rate of

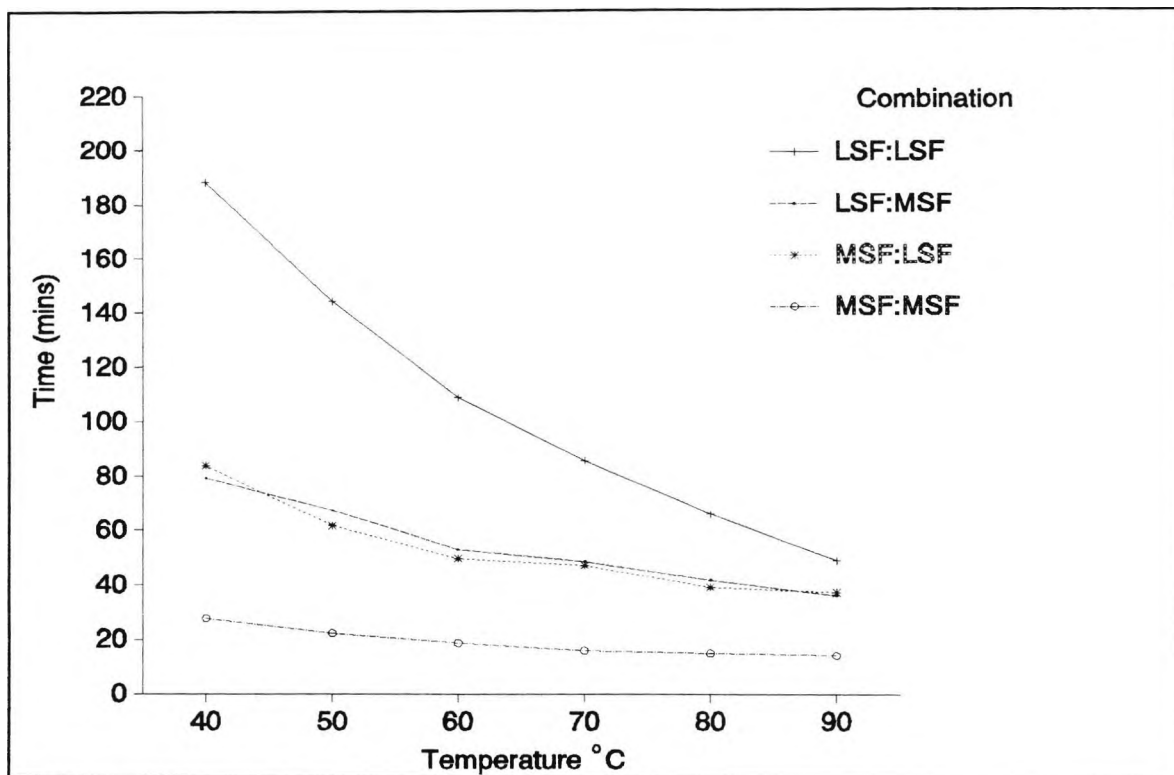


Figure 4.26 Effect of different formation and sea water combinations on the average scaling times.

deposition, depending on which combinations are used. No precipitation tests were carried out because from the previous experiments (Sections 4.9 and 4.10), it was possible to predict how much of the three precipitates form when each combination is mixed.

These predictions were carried out on a ranking system determining which of the combinations would produce the most precipitate (No.1) and least precipitate (No.4). The barium sulphate predictions are based on its solubility in sodium chloride. Strontium sulphate predictions are based on total strontium ion concentration. Calcium carbonate predictions are based on the ratio of calcium to hydrogen carbonate ions in each combination. Table 4.66 contains the results of these predictions and, to check their validity, the scaling prediction model [26] was used for each of the four combinations, providing the data in Tables 4.67 to 4.69 for comparison with the ranking data in Table 4.66.

The predictions made in Table 4.66 are consistent with the scaling model data and show that the extent of precipitation is not necessarily a measure of the ability to aggregate and form scale. The predictions further demonstrate that there are presumably kinetic effects involved in barium sulphate: strontium sulphate nucleation and co-precipitation effects for calcium carbonate that play a major part in the aggregation to scale process. This is illustrated in the following discussion on the four water combinations.

**Table 4.66 Scaling predictions for each precipitate at different formation and sea water combination.**

Precipitate	LSF : LSF	LSF : MSF	MSF : LSF	MSF : MSF
CaCO <sub>3</sub>	3	1	4	2
SrSO <sub>4</sub>	1	2	3	4
BaSO <sub>4</sub>	4	2	3	1

**Table 4.67 Scaling predictions for calcium carbonate (mg scale/kg mixed brine).**

Temp °C	LSF : LSF	LSF : MSF	MSF : LSF	MSF : MSF
40	0.0	181.2	0.0	130.8
60	0.3	244.2	0.0	207.7
80	11.1	289.1	8.7	264.4

**Table 4.68 Scaling predictions for strontium sulphate (mg scale/kg mixed brine).**

Temp °C	LSF : LSF	LSF : MSF	MSF : LSF	MSF : MSF
40	865.2	814.1	300.2	177.1
60	886.2	828.8	311.2	183.3
80	918.4	850.9	329.6	191.0

Table 4.69 Scaling predictions for barium sulphate (mg scale/ kg mixed brine).

Temp °C	LSF : LSF	LSF : MSF	MSF : LSF	MSF : MSF
40	122.2	124.1	123.8	125.7
60	121.8	123.9	123.7	125.6
80	121.3	123.7	123.5	125.6

Comparison of the scale prediction data for the LSF:LSF and MSF:LSF combinations for calcium carbonate (Table 4.67) shows that the effect of calcium carbonate should be negligible so that any changes must be due to strontium or barium sulphate. The scale prediction data for barium sulphate (Table 4.69) shows little variance, and any difference in propensity to scale must, therefore, be due to differences in the strontium ion concentrations. The data show that the LSF:LSF combination took 104.8 minutes longer to scale than the MSF:LSF combination at 40°C, and this confirms that the difference is caused by the different strontium ion concentrations. It is thus concluded that high strontium ion concentrations do modify the rate of aggregation of barium sulphate to form scale.

Comparison of the scale prediction data for the LSF:MSF and MSF:MSF combinations for calcium carbonate (Table 4.67) shows that the effect of calcium carbonate should be equally significant. The scale prediction data for barium sulphate (Table 4.69) show little variance, and therefore any difference in propensity to scale must be due to differences in the strontium ion concentration. The data show that the LSF:MSF combination took 51.6 minutes longer to scale than the MSF:MSF combination at 40°C, and this confirms that the time difference is caused by the different strontium ion concentrations. Thus it is again concluded that high strontium ion concentrations do modify the rate of aggregation of barium sulphate to form scale.

The presence of calcium carbonate in the precipitant material

leads to an increase in the propensity to scale. This is shown by comparison of the data for the LSF:LSF and LSF:MSF combinations, which indicates that the effect of strontium and barium sulphates shows little variance, and any differences in propensity to scale must, therefore, be due to differences in the calcium and hydrogen carbonate ion concentrations. The data show that the LSF:LSF combination took 109.4 minutes longer to scale than the LSF:MSF combination at 40°C, and this confirms that the time difference is caused by the different calcium and hydrogen carbonate ion concentrations. Thus it is concluded that high calcium and hydrogen carbonate ion concentrations do modify the rate of aggregation of barium sulphate to form scale.

#### 4.12 THE EFFECT OF RATIO MIXING OF SIMULATED FORMATION AND SEA WATERS ON THE PROPENSITY TO SCALE

The compositions of the standard simulated formation and sea waters used in this part of the work were the same as shown in Tables 4.6 and 4.7, and were kept constant throughout these experiments. The ratio of mixing was changed from 10:90 to 90:10 formation water:sea water (FW:SW) in steps of 10% for each water. The total flow rate through the P.M.A.C. microbore tube was 1.0 litre per hour and Table 4.70 lists the ratios and pump speeds used (2P denotes double channel pumps were used for the water).

The propensity to scale was measured for increases of 1 and 4 psi above the distilled water base line for each of the ratios investigated at temperatures of 40, 50, 60, 70, 80 and 90°C. For each set of conditions five experiments were carried out to ensure statistically significant results were achieved. After each experiment the normal cleaning procedure was carried out as described in Section 4.7.1, except for the ratios 80:20 and 90:10 where a 30% EDTA disodium salt solution containing 10% potassium hydroxide was used, due to the difficulty of cleaning the microbore tube.

Table 4.70 Ratio of mixing and pump speeds used in the propensity to scale measurements.

Ratio	FW:SW	Pump A %	Pump B %	Flow rate l/hr
10:90		7.4	58.3(2P)	0.1:0.9
20:80		21.5	50.8(2P)	0.2:0.8
30:70		35.0	93.0	0.3:0.7
40:60		46.5	76.1	0.4:0.6
50:50		61.0	63.5	0.5:0.5
60:40		76.0	50.8	0.6:0.4
70:30		91.0	37.5	0.7:0.3
80:20		48.7(2P)	24.5	0.8:0.2
90:10		55.9(2P)	10.5	0.9:0.1

The results for the average scaling times for each ratio of mixing experiment for an increase in the back pressure of 1 psi are given in Table 4.71 and shown graphically in Figure 4.27. The results for an increase in the back pressure of 4 psi are given in Table 4.72 and shown graphically in Figure 4.28. The details of replicate runs for each ratio of mixing experiment are given in Appendix Tables B.64 to B.71 for an increase in back pressure of 1 psi and in Appendix Tables B.72 to B.79 for an increase in back pressure of 4 psi.

The results indicate that varying the ratio of mixing the standard formation and sea waters significantly influences the rate of deposition of scale. The least scale-forming ratio was 10:90 FW:SW, which took 515 minutes for the back pressure to increase by 1 psi at 40°C, whereas the most scale-forming ratios at 40°C were 60:40 and 70:30, both of which took 44 minutes. The time difference between the two most extreme ratios for propensity to scale was 471 minutes. The data demonstrate (Figures 4.27 and 4.28) that the propensity to scale increases as the formation water ratio is increased to 60-70%, but then

Table 4.71 Effect of different ratios of mixing on an increase in back pressure of 1 psi: Average scaling times (mins).

FW:SW	Temperature °C					
	40	50	60	70	80	90
10:90	515	-	-	-	-	-
20:80	157	137	124	111	104	97
30:70	82	67	59	55	51	-
40:60	59	49	42	38	34	-
50:50	52	43	34	29	26	24
60:40	44	33	27	25	24	23
70:30	44	35	29	24	22	20
80:20	52	45	38	32	28	26
90:10	84	77	73	68	63	61

decreases with ratios of greater than 80%. Extrapolating the lines in Figures 4.27 and 4.28, it appears that the most scale-forming ratio is between 60:40 and 70:30 for these standard formation and sea waters. The 10:90 ratio experiments were only carried out once because of the problems caused within the P.M.A.C. preheating coils, where the sea water was precipitating calcium carbonate within the coil and causing blockages which prevented the experiment being finished with any degree of accuracy. The ratio experiments for increasing the back pressure by 4 psi at 90°C also suffered from the same problems. The effect of temperature was as expected with the rate of deposition increasing at higher temperatures, which in turn increased the propensity to scale. These results confirm the effects found in changing the magnesium ion concentration (Sections 4.9.3 and 4.10.3), i.e. that the initial scale deposition accounted for the relatively long time for the layer of scale to deposit in the P.M.A.C. microbore tube.

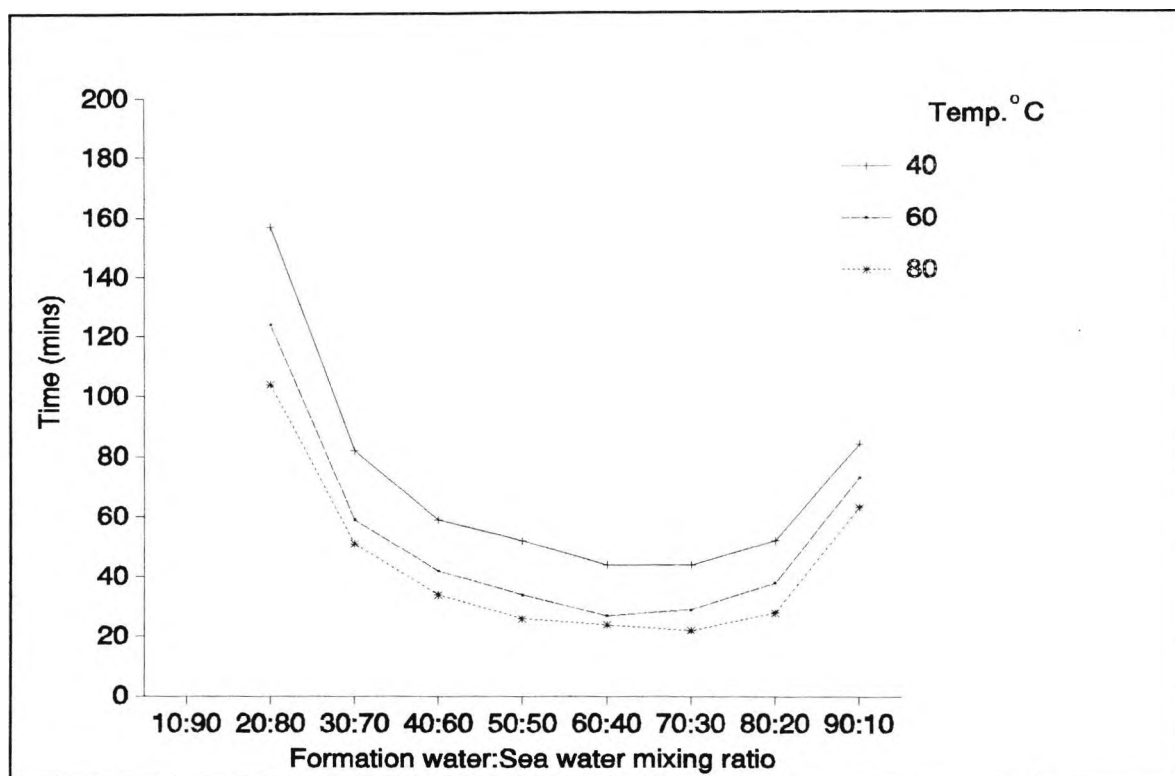


Figure 4.27 Effect of different ratios of mixing on the average scaling time for an increase in back pressure of 1 psi.

The cleaning of the microbore tube after each experiment did not follow the normal cleaning procedure. The ease of cleaning varied depending on which ratio experiment was being carried out. The easiest to clean were those of high sea water ratios, whereas the hardest to clean were those of high formation water ratios. These results have been confirmed by Thomas [29] at City University, who has carried out similar ratio of mixing studies with simulated formation and sea waters. His work was confined to the ratios 30:70 to 70:30, and showed the same trends as those found in the present work.

The results of varying the ratio of mixing of standard formation and sea waters confirm that there are statistically significant differences in the rate of scale formation and the types of scale formed in the propensity to scale experiments. Therefore precipitation studies were carried out to determine which

**Table 4.72 Effect of different ratios of mixing on an increase in back pressure of 4 psi: Average scaling times (mins).**

FW:SW	Temperature °C					
	40	50	60	70	80	90
10:90	>750	-	-	-	-	-
20:80	220	182	164	154	149	-
30:70	121	99	88	82	-	-
40:60	85	71	61	55	53	-
50:50	64	53	43	37	35	33
60:40	57	43	37	34	33	-
70:30	59	49	42	37	33	32
80:20	74	60	50	45	41	39
90:10	122	113	98	93	88	88

precipitates were forming at the following ratios: 10:90, 30:70, 50:50, 70:30 and 90:10. The experimental procedure for the precipitation tests is described in Section 4.7.2 and the results (mg scale/ kg mixed brines) are given in Tables 4.73 to 4.75 for each of the precipitates deposited.

The results of the precipitation tests given in Tables 4.73 to 4.75 explain the propensity to scale experiments. The tests show that the ratio of mixing greatly affects the quantities and types of scale formed. Calcium carbonate precipitation was found to be at its maximum for the ratio 10:90 because of the high hydrogen carbonate ion content (450 ppm) in sea water at this ratio.

As the sea water ratio was reduced to 50%, calcium carbonate precipitation decreased as the hydrogen carbonate ion concentration was reduced. Below 50% no calcium carbonate was precipitated as the solution was unsaturated with respect to calcium carbonate. The effect of temperature on calcium carbonate

precipitation was as expected, with the rate increasing at higher temperatures.

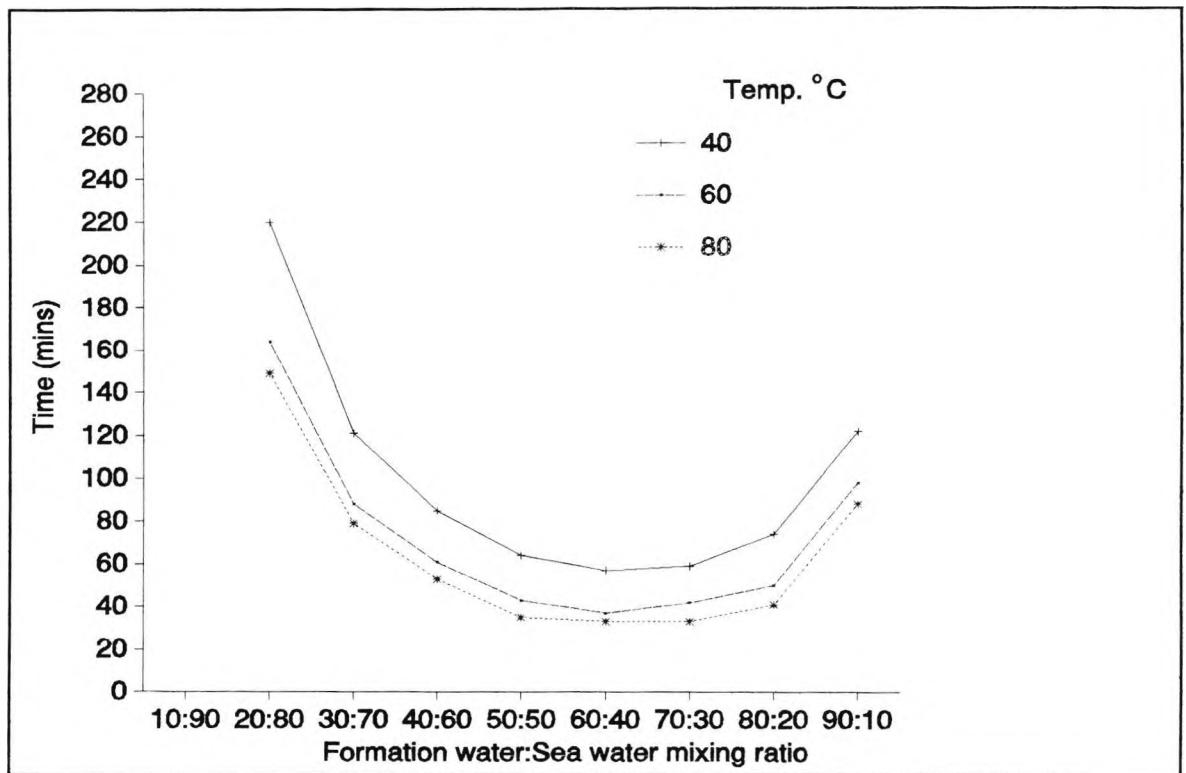


Figure 4.28 Effect of different ratios of mixing on increasing the back pressure by 4 psi.

Table 4.73 Weight (mg scale/ kg mixed brines) of calcium carbonate precipitate deposited.

Temp °C	Ratio of mixing FW:SW				
	10:90	30:70	50:50	70:30	90:10
40	144	114	39	0	0
50	180	159	89	0	0
60	207	177	126	0	0

Table 4.74 Weight (mg scale/ kg mixed brines) of strontium sulphate precipitate deposited.

Temp °C	Ratio of mixing FW:SW				
	10:90	30:70	50:50	70:30	90:10
40	24	65	108	77	0
60	24	70	137	107	0
80	24	85	154	134	0

Table 4.75 Weight (mg scale/ kg mixed brines) of barium sulphate precipitate deposited.

Temp °C	Ratio of mixing FW:SW				
	10:90	30:70	50:50	70:30	90:10
40	25	76	127	178	229
60	25	76	127	178	229
80	25	76	127	178	229

Strontium sulphate precipitation increased significantly as the formation water content rose to 60% (by extrapolation) after which it was reduced until at a ratio of 90:10 no strontium sulphate was formed. These effects are caused by the ratio of  $\text{Sr}^{2+}:\text{SO}_4^{2-}$  in the mixture. At a formation water content of greater than 70%, the lower sulphate ion concentration reduces the precipitation of strontium sulphate because barium sulphate precipitates in preference to strontium sulphate, which further reduces the sulphate ion concentration available. Strontium sulphate precipitation was increased at higher temperatures, as expected. Barium sulphate precipitation was increased as the formation water content was increased. At the 90:10 ratio the mixture contains the maximum concentration of barium ions used in these tests and the greatest weight of barium sulphate was precipitated. Temperature did not affect the quantity of barium sulphate precipitated. The results from Tables 4.73 to 4.75 are

shown graphically in Figure 4.29 at 80°C to illustrate the effect of ratio of mixing on the three precipitates formed.

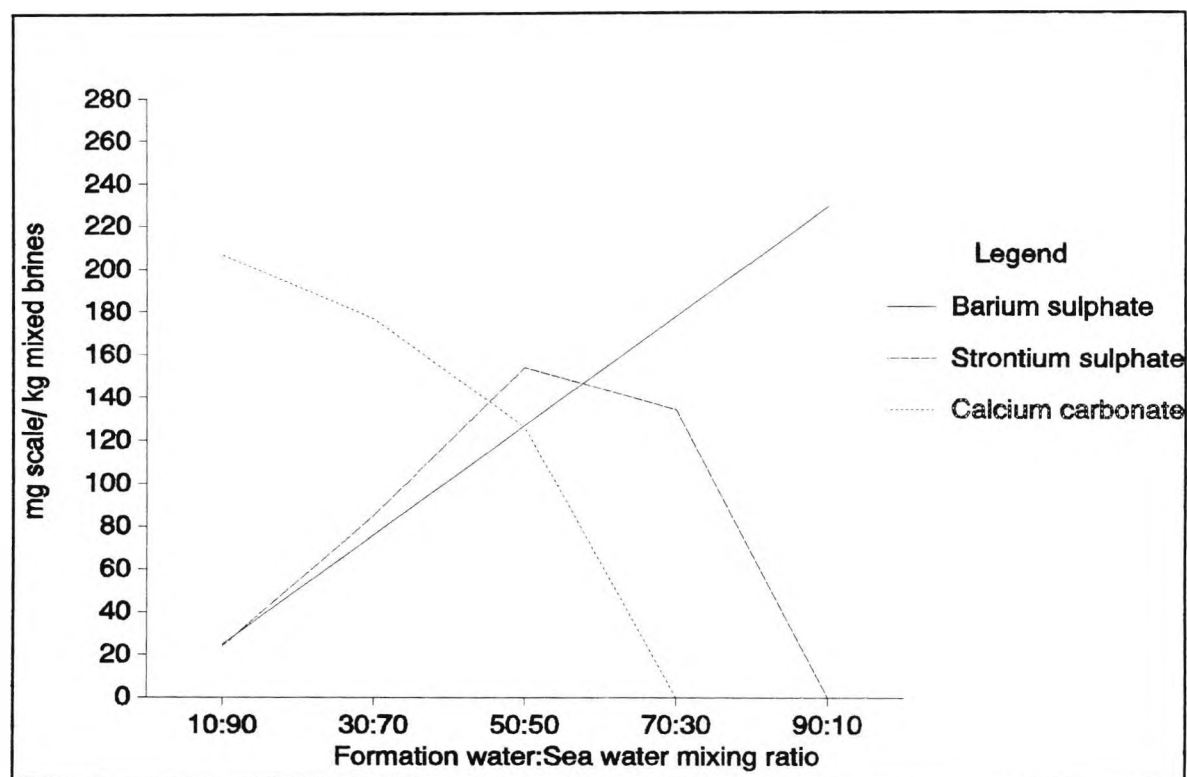


Figure 4.29 Weights (mg scale/ kg mixed brines) of each precipitate deposited at 80°C.

The formation of the three precipitates ( $\text{CaCO}_3$ ,  $\text{SrSO}_4$  and  $\text{BaSO}_4$ ) at different ratios of mixing explains why the ratio 10:90 is the least scale-forming ratio in the propensity to scale measurements. The scale at this ratio consists of calcium carbonate with little barium or strontium sulphate. As the formation water content rises to 60%, the precipitation of calcium carbonate is greatly reduced while that of strontium and barium sulphate is greatly increased. This results in an increase in the propensity to scale. As the formation water content is increased above 70%, barium sulphate becomes the predominant precipitate, until at a ratio of 90:10 it is the only precipitate formed, resulting in a significant reduction in the propensity to scale. The cleaning of the microbore tube after each experiment can now be explained. At the 10:90 ratio, calcium carbonate predominates and it is the easiest of the three

precipitates to remove (Section 4.4.3), whereas at 90:10 ratio barium sulphate is the only scale formed and it is very difficult to remove.

To confirm the differences found in the ratio of mixing experiments, the scaling prediction model [26] was applied to all the ratios in the propensity to scale experiments. The predictions (mg scale/ kg mixed brines) at 80°C are illustrated in Figure 4.30.

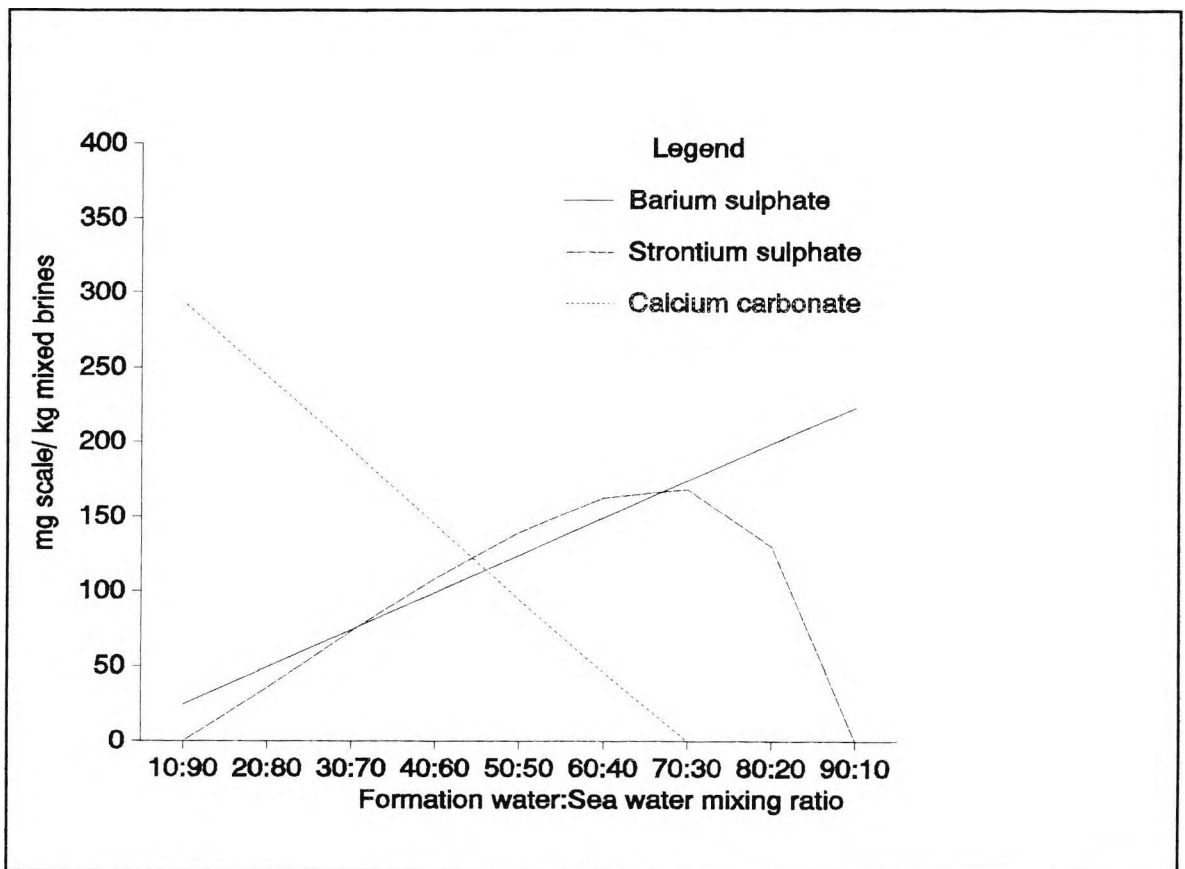


Figure 4.30 Predicted weight (mg scale/ kg mixed brines) of each precipitate deposited at 80°C.

The data in Figure 4.30 show the same trends as those found in the precipitation tests shown in Figure 4.29, in that as the sea water content is increased, calcium carbonate precipitation is enhanced and barium sulphate precipitation is reduced. Strontium sulphate precipitation reaches a maximum between the ratios of 60:40 and 70:30 as seen in the precipitation tests. Several

scaling prediction models [9,10,11] have been shown to give the same trends, as seen in the precipitation tests for different water compositions. However, these scaling predictions do not illustrate the relationship between precipitation of scale-forming compounds and their subsequent adherence to metal surfaces, indicated in the present work.

**4.13 THE EFFECT OF VARYING THE CONCENTRATIONS OF CONSTITUENT IONS IN SIMULATED FORMATION WATERS ON THE PROPENSITY TO SCALE FOR THE CaSO<sub>4</sub>-CaCO<sub>3</sub> SYSTEM**

The standard simulated formation and sea waters used in the propensity to scale experiments were made up by dissolving the quantities of salts shown in Tables 4.76 and 4.77 to give the significant ion concentrations listed.

**Table 4.76 Standard simulated formation water composition used in the propensity to scale experiments.**

Salt compound	wt. used g/l	sig. cation ppm
NaCl	20.0	7868
KCl	0.477	250
MgCl <sub>2</sub> .6H <sub>2</sub> O	1.297	155
CaCl <sub>2</sub> .2H <sub>2</sub> O	20.175	5500

The standard formation water was used as the base line against which waters of other concentrations were compared. It had a chloride concentration of 22540 ppm and a pH of 5.62. The aim of this set of experiments was to determine the effect of varying each significant ion concentration in the formation water separately, leaving the other concentrations unchanged. The propensity to scale of each formation water was then measured using the standard sea water as a precipitant (chloride concentration of 13752 ppm and a pH of 7.54). Five litres of each water were used in each set of propensity to scale measurements carried out over a range of temperatures.

The mixing flow rates for the experiments in this section were kept constant at 50:50, with Pump A, 42.6% and Pump B, 86.5%, each delivering 0.5 litres per hour of filtered formation or sea water into the P.M.A.C. microbore tube. The propensity to scale was measured for an increase of 3 psi above the distilled water base line, for each concentration investigated at temperatures of 55, 60, 65, 70, 75 and 80°C (except for the experiments described in Section 4.13.4, where measurements were made at 50°C). For each set of conditions, five experiments were carried out to ensure that statistically significant results were achieved. After each experiment the normal cleaning procedure was carried out as described in Section 4.7.1.

**Table 4.77 Standard simulated sea water composition used in the propensity to scale measurements.**

Salt compound	wt. used g/l	sig. ion ppm
NaCl	20.0	12504
KCl	1.506	790
MgCl <sub>2</sub> .6H <sub>2</sub> O	2.593	310
NaHCO <sub>3</sub>	0.138	100
Na <sub>2</sub> SO <sub>4</sub>	14.2	9597

#### 4.13.1 The Effect of Varying the Sodium Chloride Concentration in Simulated Formation Water on the Propensity to Scale

The sodium chloride concentrations used and the physical properties of the formation waters studied are given in Table 4.78. All the other ion concentrations in the formation waters were kept constant.

The results for the average scaling times for the sodium chloride concentration experiments are given in Table 4.79, and shown graphically in Figure 4.31. The details of replicate runs for each sodium chloride concentration experiment are given in Appendix Tables B.80 to B.83.

**Table 4.78 Changes in chemical composition on varying the sodium chloride concentration in formation water.**

Na <sup>+</sup> ppm	Cl <sup>-</sup> ppm	NaCl wt. g/l	pH
3934	16474	10	5.82
7868	22540	20	5.77
11802	28606	30	5.92
15736	34672	40	6.06

**Table 4.79 Effect of different sodium chloride concentrations on an increase in back pressure of 3 psi: Average scaling times (mins).**

Temp °C	NaCl 10 g/l	NaCl 20 g/l	NaCl 30 g/l	NaCl 40 g/l
55	22.2	27.4	32.6	35.0
60	15.4	20.6	21.2	25.4
65	13.0	16.6	17.8	22.0
70	11.2	13.2	14.8	18.0
75	9.8	11.0	12.2	15.4
80	7.8	9.0	11.0	13.2

The results show that varying the concentration of sodium chloride in formation waters significantly influences the rate of deposition of scale. The rate increases as the sodium chloride concentration is decreased. This trend was found at all the concentrations and temperatures studied. The formation water containing 40 g/l took 13 minutes longer than the formation water containing 10 g/l sodium chloride to form a scale at 55°C. However, at 80°C the time difference in the propensity to scale was 5.4 minutes between the two waters. The effect of temperature on the propensity to scale was also evident and, as expected,

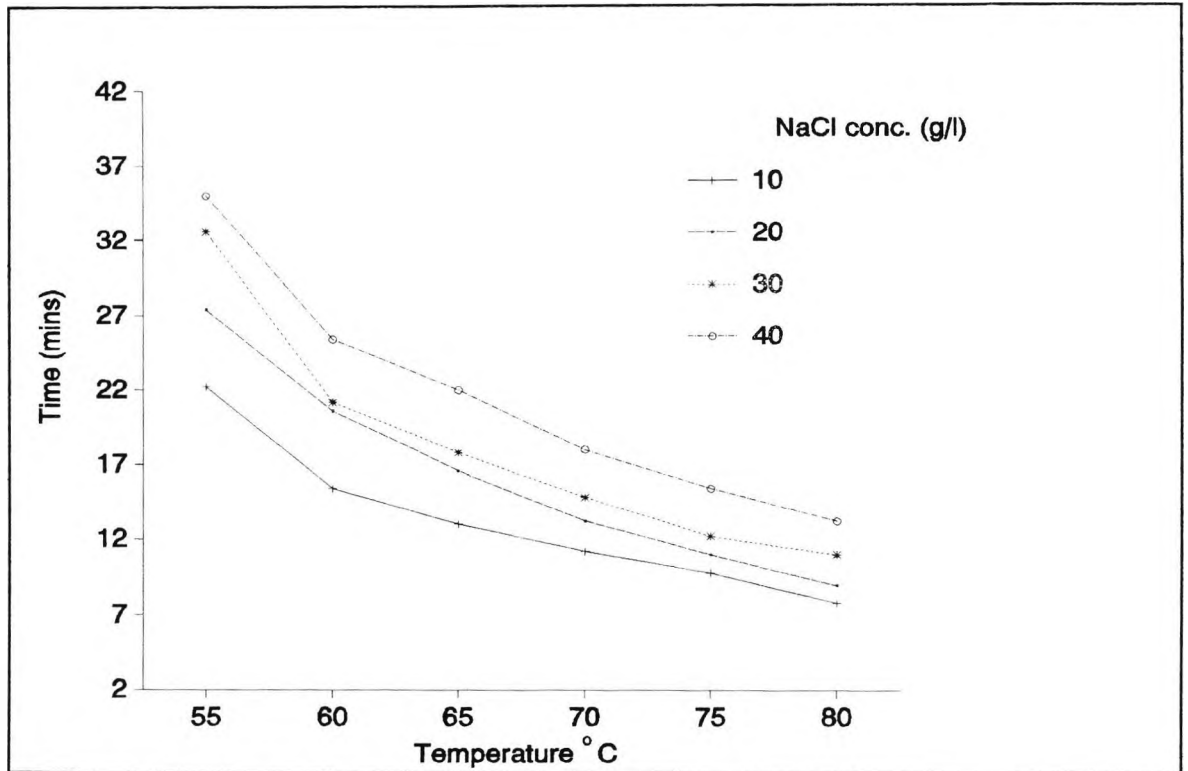


Figure 4.31 Effect of different sodium chloride concentrations on the average scaling times.

the rate of deposition of scale was shown to increase with temperature.

The reduction in propensity to scale at higher sodium chloride concentrations is a result of calcium sulphate being more soluble in waters containing higher salinity [8,10,19].

#### 4.13.2 The Effect of Varying the Potassium Ion Concentration in Simulated Formation Water on the Propensity to Scale

The potassium chloride concentrations used and the physical properties of the formation waters studied are given in Table 4.80. All the other ion concentrations in the formation water were kept constant.

The results for the average scaling times for the potassium ion concentration experiments are given in Table 4.81 and shown graphically in Figure 4.32. The details of replicate runs for

each potassium ion concentration experiment are given in Appendix Tables B.84 to B.87.

**Table 4.80 Changes in chemical composition on varying the potassium chloride concentration in formation water.**

K <sup>+</sup> ppm	Cl <sup>-</sup> ppm	KCl wt. g/l	pH
100	22404	0.191	5.73
500	22767	0.954	5.74
1000	23220	1.907	5.76
1500	23673	2.862	5.69

**Table 4.81 Effect of different potassium ion concentrations on an increase in back pressure of 3 psi: Average scaling times (mins).**

Temp °C	K <sup>+</sup> 100ppm	K <sup>+</sup> 500ppm	K <sup>+</sup> 1000ppm	K <sup>+</sup> 1500ppm
55	25.4	25.6	24.0	23.2
60	20.4	18.0	17.8	17.2
65	17.0	14.4	14.2	14.2
70	12.8	12.4	12.2	12.4
75	10.8	11.4	10.6	10.6
80	10.2	9.8	9.6	8.2

The results show that varying the concentration of potassium ion in formation water does not have any effect on the rate of deposition of scale. At all the temperatures studied, the average scaling time for an increase in back pressure of 3 psi varied by less than 3 minutes at all concentrations. The consistency of the measurements is shown in Figure 4.33, for five repeat runs of propensity to scale measurements for a potassium ion concentration of 100 ppm at temperatures of 55, 65 and 75°C, giving standard deviations of 0.55, 0.71 and 0.45, respectively. The effect of temperature on the propensity to scale was as

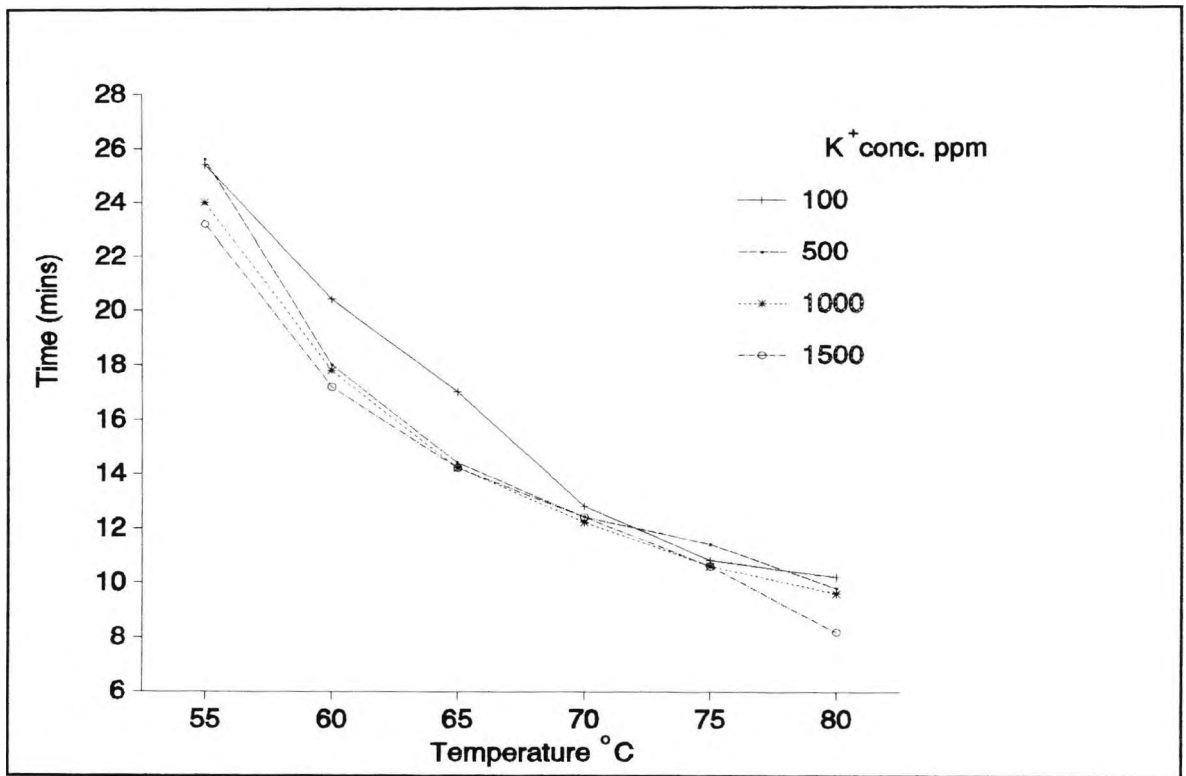


Figure 4.32 Effect of different potassium concentrations on the average scaling times.

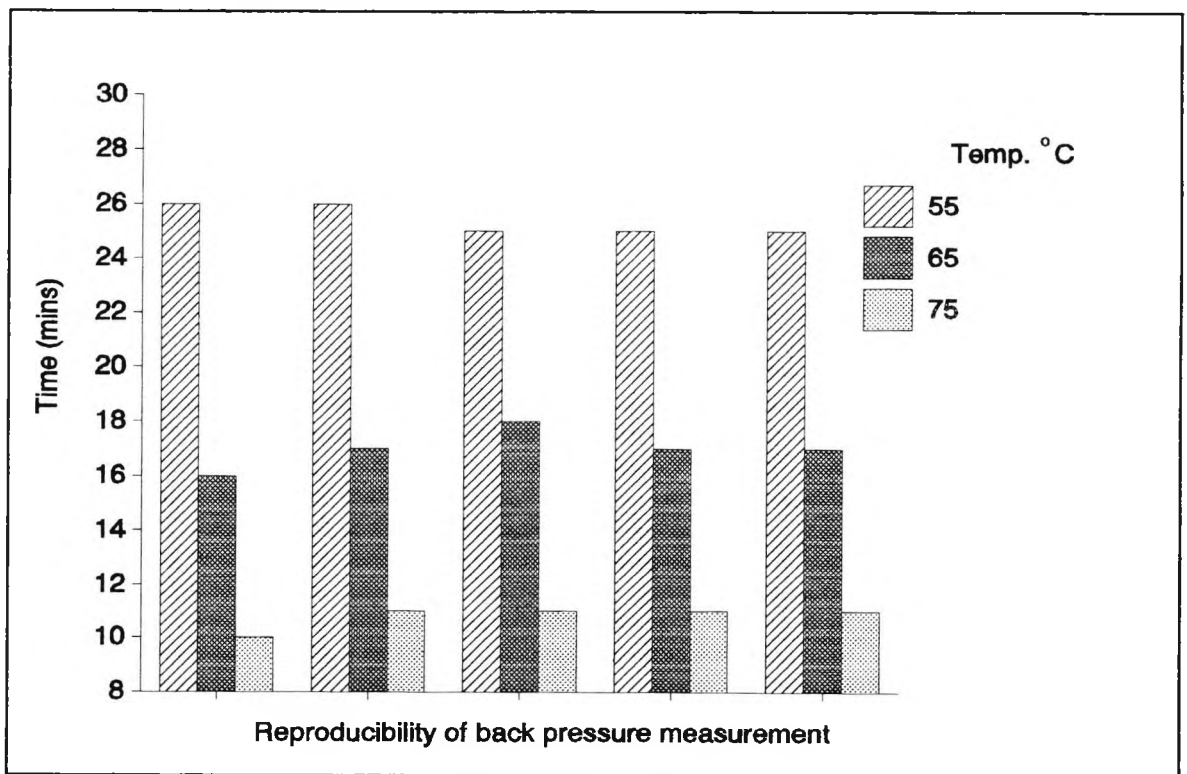


Figure 4.33 Reproducibility of back pressure measurements for the potassium ion concentration of 100 ppm in formation water.

expected, with the rate of deposition increasing at higher temperatures.

#### 4.13.3 The Effect of Varying the Magnesium Ion Concentration in Simulated Formation Water on the Propensity to Scale

The magnesium chloride concentrations used and the physical properties of the formation waters studied are given in Table 4.82. All the other ion concentrations in the formation water were unchanged.

**Table 4.82 Changes in chemical composition on varying the magnesium chloride concentration in formation water.**

Mg <sup>2+</sup> ppm	Cl <sup>-</sup> ppm	MgCl <sub>2</sub> .6H <sub>2</sub> O wt. g/l	pH
100	22380	0.837	5.88
500	23547	4.184	5.75
1000	25006	8.366	5.79
1500	26464	12.546	5.80

**Table 4.83 Effect of different magnesium ion concentrations on an increase in back pressure of 3 psi: Average scaling times (mins).**

Temp °C	Mg <sup>2+</sup> 100ppm	Mg <sup>2+</sup> 500ppm	Mg <sup>2+</sup> 1000ppm	Mg <sup>2+</sup> 1500ppm
55	29.2	28.0	31.6	39.0
60	21.8	21.8	23.6	28.8
65	17.4	18.6	19.0	22.6
70	13.4	15.0	16.6	19.0
75	11.4	12.2	14.2	15.6
80	9.4	11.2	11.8	13.6

The results for the average scaling times for the magnesium ion concentration experiments are given in Table 4.83 and are shown

graphically in Figure 4.34. The details of replicate runs for each magnesium ion concentration experiment are given in Appendix Tables B.88 to B.91.

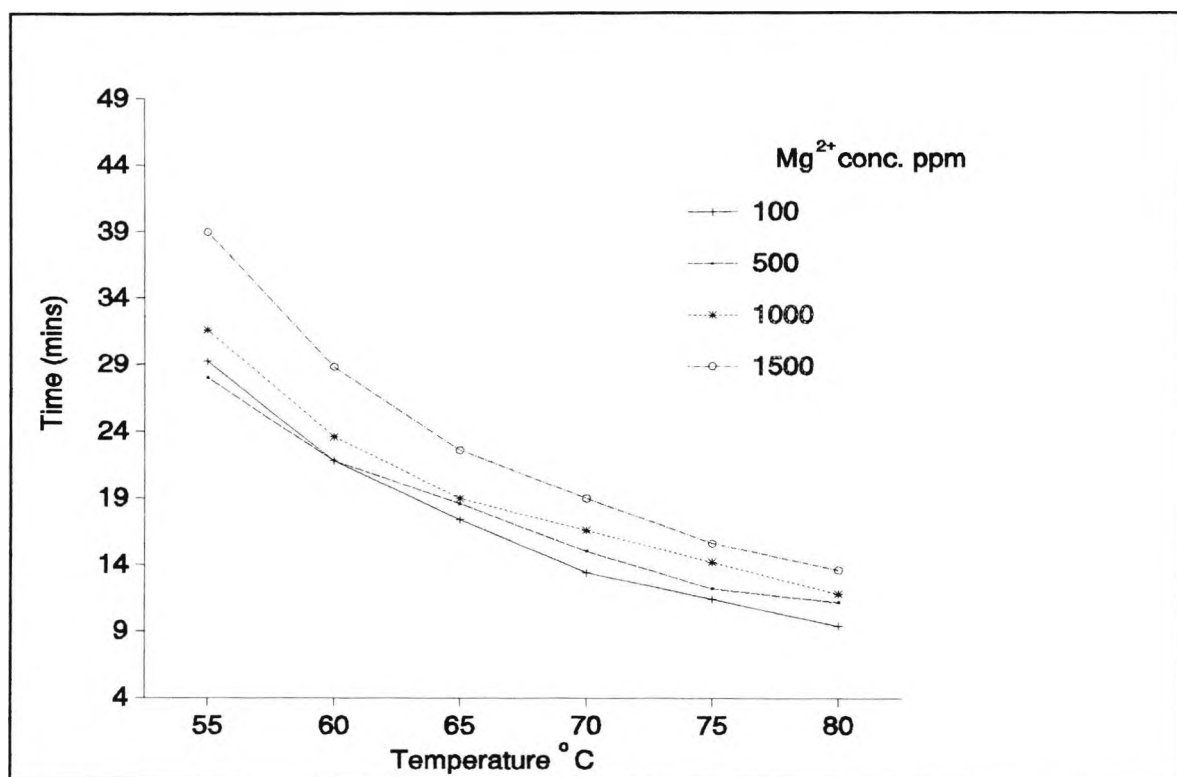


Figure 4.34 Effect of different magnesium ion concentrations on the average scaling times.

The results show that varying the concentration of magnesium ion in formation water significantly influences the rate of deposition of scale. The rate decreases as the magnesium ion concentration increases. At the two lowest concentrations, no apparent trend can be seen, but as the concentration is raised to 1000 ppm and above a clear trend can be seen. The formation water containing 1500 ppm of magnesium ion took 9.8 minutes longer than the formation water containing 100 ppm at 55°C to form a scale. However, at 80°C the time difference in the propensity to scale was 4.2 minutes between the two waters. The effect of temperature on the propensity to scale measurements was as expected, with the rate of deposition of scale increasing at higher temperatures.

The reduction in the propensity to scale as the magnesium ion concentration is increased has been linked to the formation of magnesium sulphate ion pairs [21,22] which would reduce the availability of sulphate ions to form calcium sulphate. Similar effects have been seen in the sea water solutions containing high magnesium ion levels (Section 4.14.3).

#### 4.13.4 The Effect of Varying the Calcium Ion Concentration in Simulated Formation Water on the Propensity to Scale

The calcium chloride concentrations used and the physical properties of the formation waters studied are given in Table 4.84. All the other ion concentrations in the formation water were unchanged.

**Table 4.84 Changes in chemical composition on varying the calcium chloride concentration in formation water.**

Ca <sup>2+</sup> ppm	Cl <sup>-</sup> ppm	CaCl <sub>2</sub> .2H <sub>2</sub> O wt. g/l	pH
5500	22540	20.175	5.62
6000	23425	22.009	5.85
7000	25193	25.677	5.82
8000	26991	29.404	5.74

The results for the average scaling times for the calcium ion concentration experiments are given in Table 4.85 and are shown graphically in Figure 4.35. The details of replicate runs for each calcium ion concentration experiment are given in Appendix Tables B.92 to B.95.

The results show that varying the calcium ion concentration in formation water significantly influences the rate of deposition of scale. The rate is increased as the calcium ion concentration is increased. This trend is found at all concentrations and temperatures studied. At 50°C, the formation water containing 5500 ppm of calcium ion took 33.4 minutes longer than the

**Table 4.85 Effect of different calcium ion concentrations on an increase in back pressure of 3 psi: Average scaling time (mins).**

Temp °C	Ca <sup>2+</sup>			
	5500ppm	6000ppm	7000ppm	8000ppm
50	65.2	52.2	38.2	31.8
55	41.0	34.0	27.6	21.2
60	30.0	24.4	19.8	15.2
65	25.2	17.6	12.6	10.6
70	20.6	14.4	9.8	8.2
75	17.4	12.8	7.6	5.8

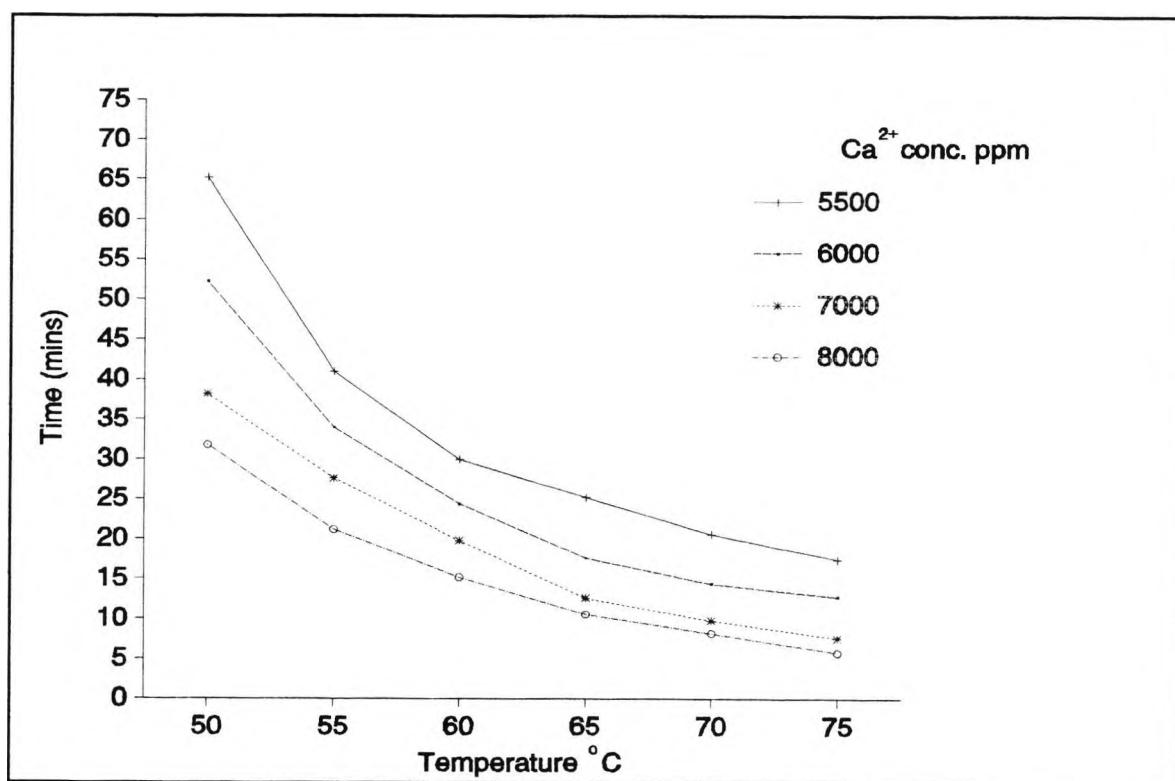


**Figure 4.35 Effect of different calcium ion concentrations on the average scaling times.**

formation water with 8000 ppm of calcium ion. However, at 75°C the time difference in the propensity to scale was 11.6 minutes between the two waters. The consistency of the measurements is

shown in Figure 4.36 for five repeat runs of propensity to scale measurements for a calcium ion concentration of 6000 ppm at temperatures of 55, 65 and 75°C, giving standard deviations of 1.22, 0.54 and 0.44, respectively. The effect of temperature was also evident and as expected, the rate of deposition of scale was shown to increase with temperature.

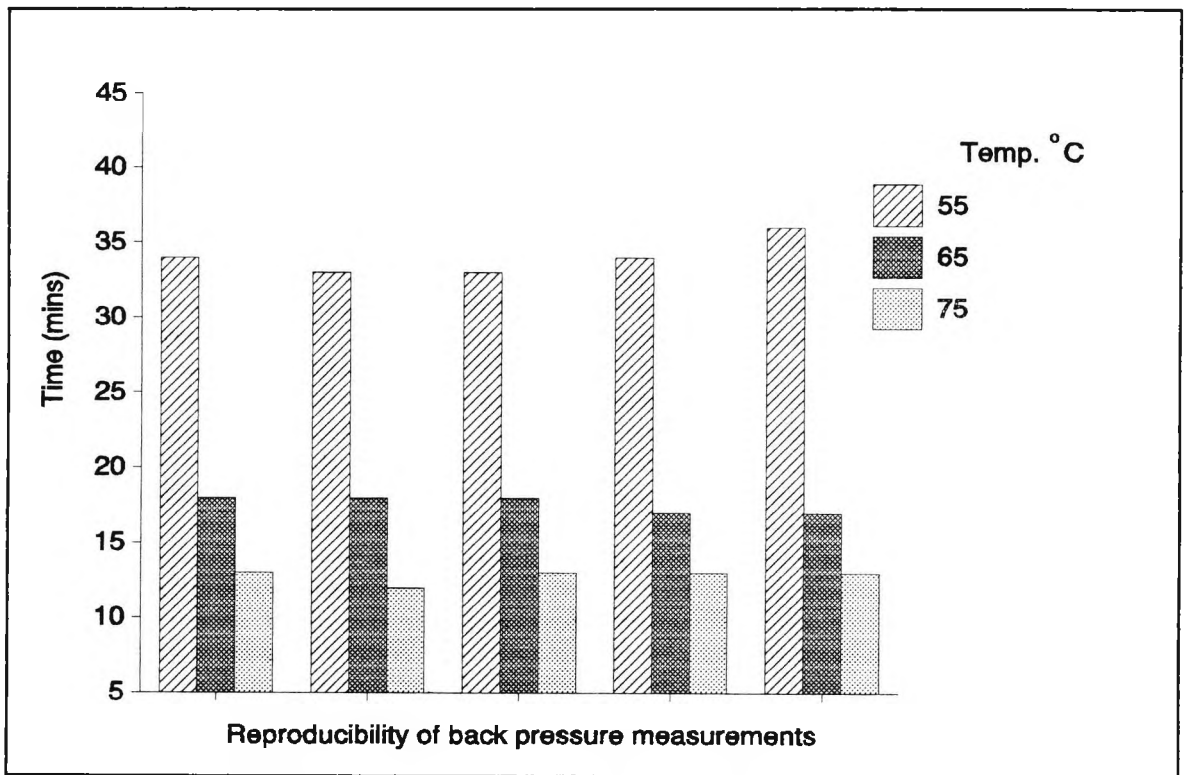


Figure 4.36 Reproducibility of back pressure measurements for the calcium ion concentration of 6000 ppm in formation water.

The increase in propensity to scale at higher calcium ion concentrations is a result of increased calcium sulphate deposition in the microbore tube.

#### 4.13.5 Summary of the Propensity to Scale Experiments

The effects of changing each significant ion concentration in simulated formation water separately, leaving the other concentrations unchanged, have yielded interesting results. Every significant ion changed has been shown to have a different effect on the propensity to scale as measured in the P.M.A.C. unit when

formation and sea waters are mixed. Table 4.86 summarises the general trends in the propensity to scale measurements by increasing each significant ion concentration.

**Table 4.86 Summary of the general trends in the propensity to scale.**

Ion	General trend in propensity to scale
Na <sup>+</sup>	Significant decrease
K <sup>+</sup>	No difference
Mg <sup>2+</sup>	Significant decrease at higher Mg <sup>2+</sup> concentrations
Ca <sup>2+</sup>	Significant increase

**4.14 THE EFFECT OF VARYING THE CONCENTRATIONS OF CONSTITUENT IONS IN SIMULATED SEA WATERS ON THE PROPENSITY TO SCALE FOR THE CaSO<sub>4</sub>-CaCO<sub>3</sub> SYSTEM**

The standard simulated formation and sea waters used in the propensity to scale experiments were made up by dissolving the quantities of salts shown in Tables 4.76 and 4.77 to give the significant ion concentrations listed. The standard sea water was used as the base line against which waters of other concentrations were compared. It had a chloride concentration of 13752 ppm and a pH of 7.54. The aim of this set of experiments was to determine the effect of varying each significant ion concentration in sea water separately leaving the other concentrations unchanged. The propensity to scale of each sea water was measured using the standard formation water as precipitant, having a chloride concentration of 22540 ppm and a pH of 5.62.

The mixing flow rates for the experiments in this section were kept constant at 50:50, with Pump A, 42.0% and Pump B, 86.5%, each delivering 0.5 litres per hour of filtered formation or sea water into the P.M.A.C. microbore tube. The propensity to scale

was measured for an increase in back pressure of 3 psi above the distilled water base line, for each concentration investigated at temperatures of 55, 60, 65, 70, 75 and 80°C. For each set of conditions five experiments were carried out to ensure that statistically significant results were achieved. After each experiment the normal cleaning procedure was carried out as described in Section 4.7.1.

#### 4.14.1 The Effect of Varying the Sodium Chloride Concentration in Simulated Sea Waters on the Propensity to Scale

The sodium chloride concentrations used and the physical properties of the sea waters studied are given in Table 4.87. All the other ion concentrations in the sea water were kept constant.

**Table 4.87 Changes in chemical composition on varying the sodium chloride concentration in sea water.**

Na <sup>+</sup> ppm	Cl <sup>-</sup> ppm	NaCl wt. g/l	pH
8570	7686	10	7.61
12504	13752	20	7.54
16438	19818	30	7.69
20372	25884	40	7.74

The results for the average scaling times for the sodium chloride concentration experiments are given in Table 4.88 and are shown graphically in Figure 4.37. The details of replicate runs for each sodium chloride concentration experiment are given in Appendix Tables B.96 to B.99.

The results show that varying the concentration of sodium chloride in sea waters significantly influences the rate of deposition of scale. The rate increases as the sodium chloride concentration is decreased. This trend was found at all concentrations and temperatures studied. The sea water containing 40 g/l sodium chloride took 15 minutes longer than the sea water

containing 10 g/l to form a scale at 55°C.

**Table 4.88 Effect of different sodium chloride concentrations on an increase in back pressure of 3 psi: Average scaling times (mins).**

Temp °C	NaCl 10 g/l	NaCl 20 g/l	NaCl 30 g/l	NaCl 40 g/l
55	25.8	28.2	32.4	40.8
60	18.0	19.8	26.2	31.8
65	14.6	16.4	21.2	27.4
70	12.2	13.6	16.8	19.2
75	10.2	10.8	14.0	16.6
80	9.0	9.2	12.0	14.8

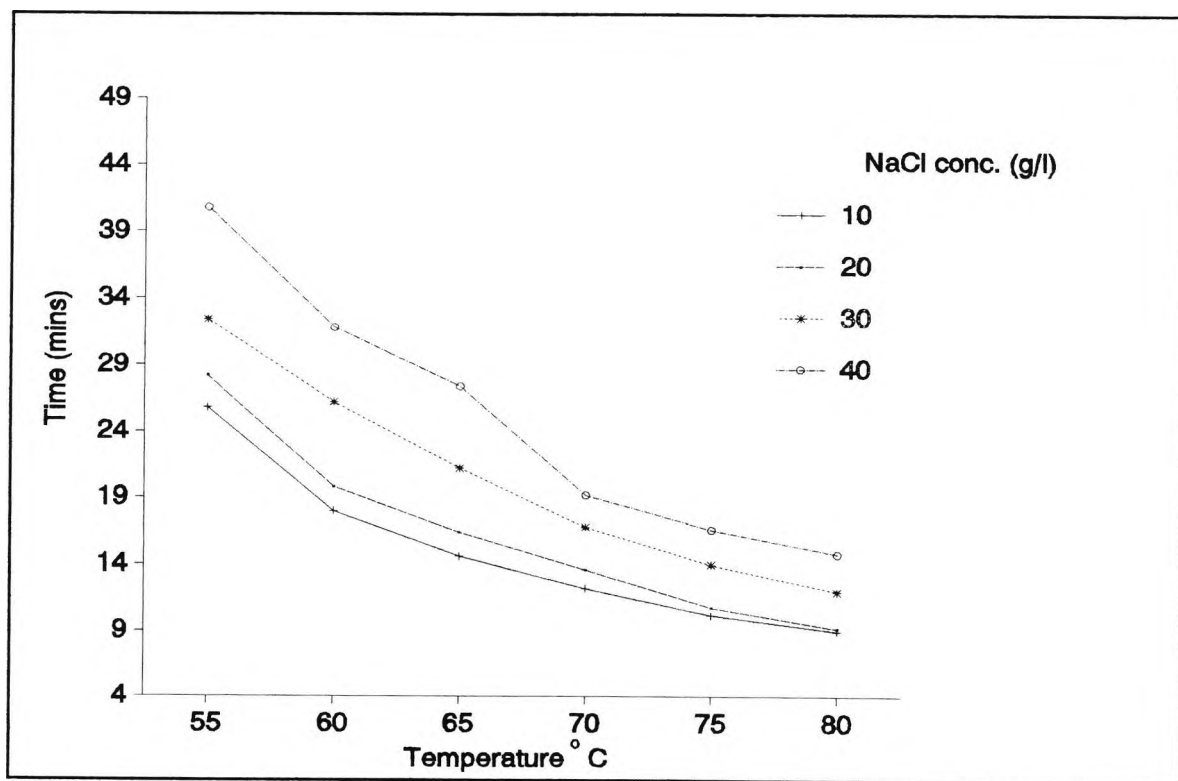


**Figure 4.37 Effect of different sodium chloride concentrations on the average scaling times.**

However, at 80°C the time difference in the propensity to scale was 5.8 minutes between the two waters. The effect of temperature on the propensity to scale was as expected, with the rate of deposition increasing at higher temperatures.

The reduction in propensity to scale at higher sodium chloride concentrations is a result of calcium sulphate being more soluble in waters containing higher salinity [8,10,19].

#### 4.14.2 The Effect of Varying the Potassium Ion Concentration in Simulated Sea Waters on the Propensity to Scale

The potassium chloride concentrations used and the physical properties of the sea waters studied are given in Table 4.89. All the other ion concentrations in the sea waters were kept constant.

**Table 4.89 Changes in chemical composition on varying the potassium chloride concentration in sea water.**

K <sup>+</sup> ppm	Cl <sup>-</sup> ppm	KCl wt. g/l	pH
250	13263	0.477	7.68
500	13490	0.954	7.65
1000	13943	1.907	7.71
1500	14397	2.862	7.64

The results for the average scaling times for the potassium ion concentration experiments are given in Table 4.90 and shown graphically in Figure 4.38. The details of replicate runs for each potassium ion concentration experiment are given in Appendix Tables B.100 to B.103.

The results show that varying the concentration of potassium ion in sea water does not affect the rate of deposition of scale. At all the temperatures studied, except 40°C, the average scaling time for an increase in back pressure of 3 psi varied by less

Table 4.90 Effect of different potassium ion concentrations on an increase in back pressure of 3 psi: Average scaling times (mins).

Temp °C	K <sup>+</sup> 250ppm	K <sup>+</sup> 500ppm	K <sup>+</sup> 1000ppm	K <sup>+</sup> 1500ppm
55	30.8	29.8	27.4	32.0
60	19.6	18.0	18.4	21.2
65	16.0	14.8	16.2	16.6
70	13.4	13.6	13.2	13.2
75	12.2	11.8	12.2	11.2
80	10.6	10.4	10.6	10.0

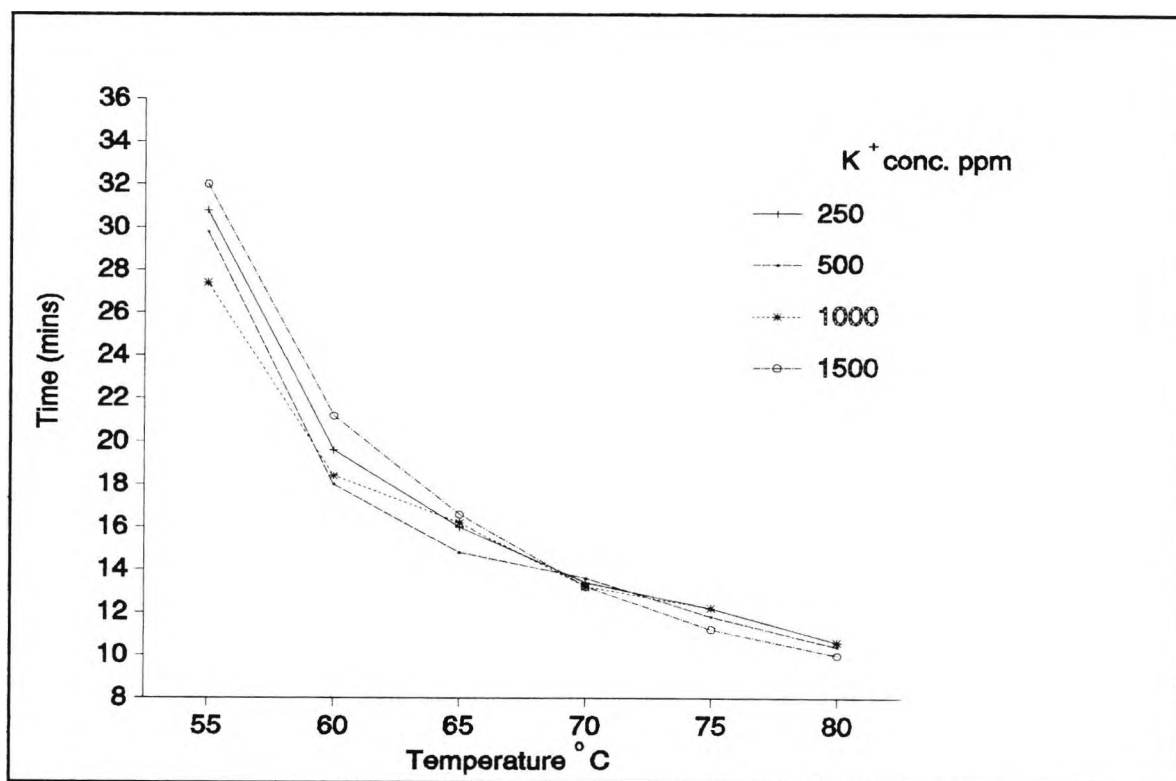
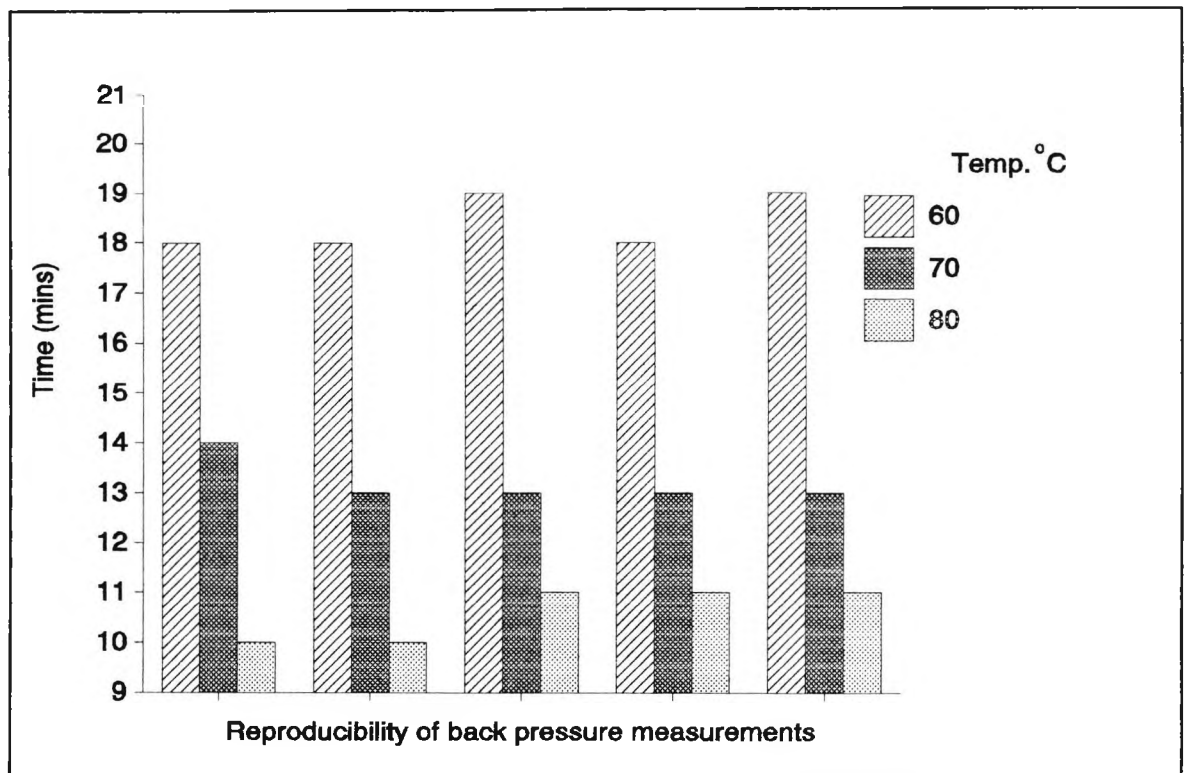


Figure 4.38 Effect of different potassium ion concentrations on the average scaling times.

than 3 minutes at all concentrations. The consistency of the measurements is shown in Figure 4.39, for five repeat runs of propensity to scale measurements for a potassium ion

concentration of 1000 ppm at temperatures of 60, 70 and 80°C, giving standard deviations of 0.55, 0.45 and 0.55, respectively.



**Figure 4.39 Reproducibility of back pressure measurements for the potassium ion concentration of 1000 ppm in sea water.**

The effect of temperature on the propensity to scale was as expected, with the rate of deposition increasing at higher temperatures.

#### **4.14.3 The Effect of Varying the Magnesium Ion Concentration in Simulated Sea Water on the Propensity to Scale**

The magnesium chloride concentrations used and the physical properties of the sea waters studied are given in Table 4.91. All the other ion concentrations in the sea water were kept constant.

The results for the average scaling times for the magnesium ion concentration experiments are given in Table 4.92 and shown graphically in Figure 4.40. The details of replicate runs for each magnesium ion concentration experiment are given in Appendix Tables B.104 to B.107.

**Table 4.91 Changes in chemical composition on varying the magnesium chloride concentration in sea water.**

Mg <sup>2+</sup> ppm	Cl <sup>-</sup> ppm	MgCl <sub>2</sub> .2H <sub>2</sub> O wt. g/l	pH
125	13213	1.046	7.56
250	13578	2.092	7.47
500	14307	4.184	7.42
1000	15766	8.367	7.38

**Table 4.92 Effect of different magnesium ion concentrations on an increase in back pressure of 3 psi: Average scaling times (mins).**

Temp °C	Mg <sup>2+</sup> 125ppm	Mg <sup>2+</sup> 250ppm	Mg <sup>2+</sup> 500ppm	Mg <sup>2+</sup> 1000ppm
55	30.8	25.8	28.2	34.8
60	22.0	18.2	20.0	23.2
65	18.8	16.2	17.2	19.6
70	16.0	14.0	15.6	17.8
75	14.2	11.8	13.6	15.6
80	12.0	10.6	11.0	13.6

The results show that varying the concentration of magnesium ion in sea waters significantly influences the rate of deposition of scale with two trends being seen. Below 250 ppm, the rate of deposition is increased, but as the concentration is raised to 500 ppm and above the rate of deposition decreases as the concentration increases. The sea water containing 1000 ppm of magnesium ion took 9 minutes longer than the sea water containing 250 ppm at 55°C to form a scale. However, at 80°C the time difference in the propensity to scale was 3 minutes between the two waters. The effect of temperature on the propensity to scale was as expected, with the rate of deposition of scale increasing

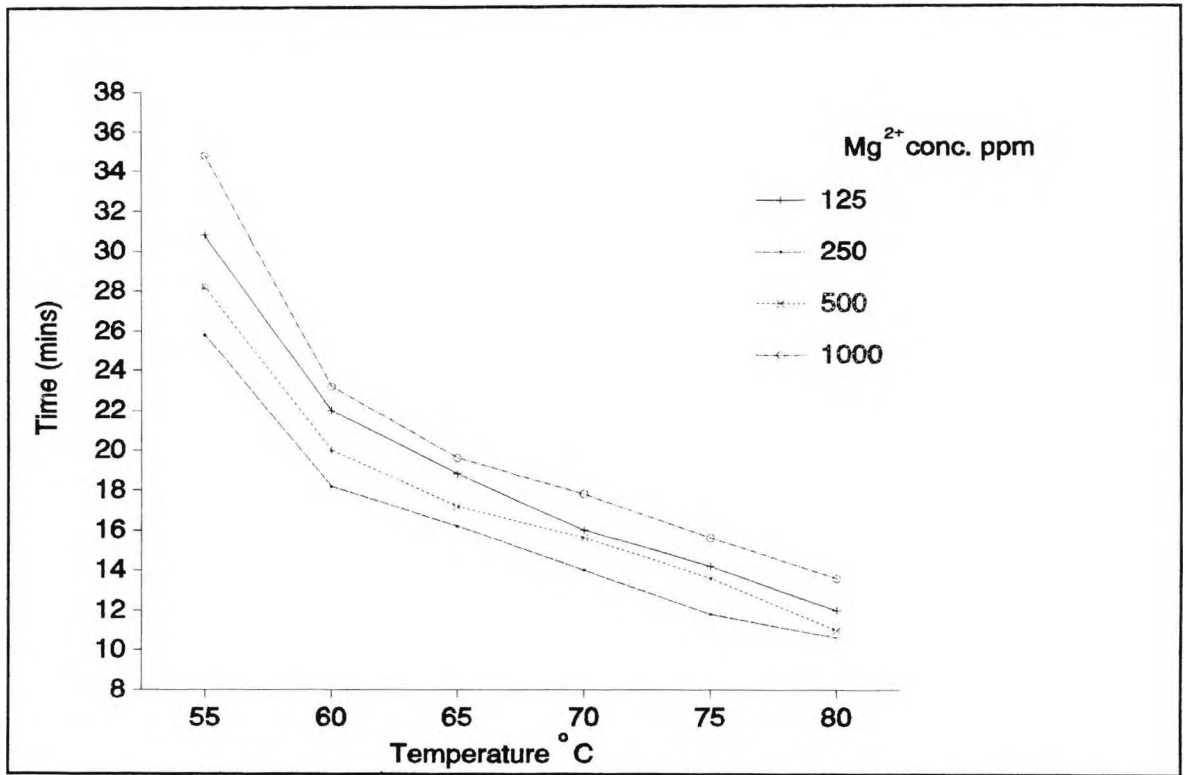


Figure 4.40 Effect of different magnesium ion concentrations on the average scaling times.

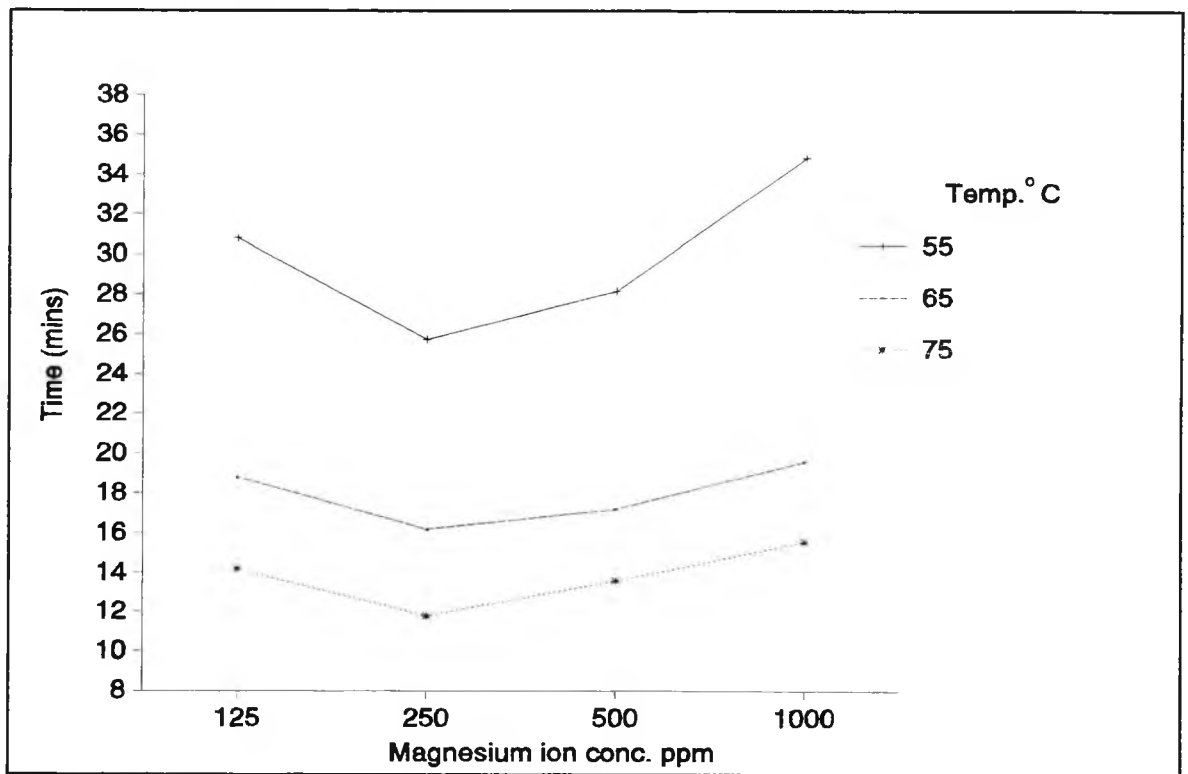


Figure 4.41 Effect of temperature on the average scaling times.

at higher temperatures. The significance of the results in Table 4.92 can be seen more clearly in Figure 4.41, when average scaling times are plotted against magnesium ion concentrations; the graph shows the increase in propensity to scale by raising the magnesium ion concentration to 250 ppm and the subsequent decrease for higher magnesium ion concentration levels.

The reduction in propensity to scale as the magnesium ion concentration is increased above 500 ppm has been linked to the formation of magnesium sulphate ion pairs [21,22], which reduces the availability of sulphate ions to form calcium sulphate. Similar effects have been seen in the formation water solutions containing high magnesium ion levels (Section 4.13.3). The increase in magnesium ion concentration before ion pairs are formed acts as a catalyst for the deposition of calcium sulphate, increasing the propensity to scale by reducing the time delay before calcium sulphate nuclei are formed.

#### 4.14.4 The Effect of Varying the Hydrogen Carbonate Ion Concentration in Simulated Sea Waters on the Propensity to Scale

The sodium hydrogen carbonate concentrations used and the physical properties of the sea waters studied are given in Table 4.93. All the other ion concentrations in the sea water were unchanged.

**Table 4.93 Changes in chemical composition on varying the sodium hydrogen carbonate concentration in sea water.**

Na <sup>+</sup> ppm	HCO <sub>3</sub> <sup>-</sup> ppm	NaHCO <sub>3</sub> wt. g/l	pH
12513	125	0.172	7.61
12560	250	0.344	7.77
12607	375	0.516	7.78
12654	500	0.688	7.95

The results for the average scaling times for the hydrogen carbonate ion concentration experiments are given in Table 4.94 and are shown graphically in Figure 4.42. The details of replicate runs for each hydrogen carbonate ion concentration experiment are given in Appendix Tables B.108 to B.111.

**Table 4.94 Effect of different hydrogen carbonate ion concentrations on an increase in back pressure of 3 psi: Average scaling times (mins).**

Temp °C	HCO <sub>3</sub> <sup>-</sup> 125ppm	HCO <sub>3</sub> <sup>-</sup> 250ppm	HCO <sub>3</sub> <sup>-</sup> 375ppm	HCO <sub>3</sub> <sup>-</sup> 500ppm
55	38.0	35.6	49.4	52.0
60	30.8	26.8	38.4	45.4
65	26.2	21.0	33.8	38.0
70	20.2	15.8	27.4	34.0
75	17.0	14.8	23.6	30.8
80	14.8	13.8	20.0	28.6

The results show that varying the concentration of hydrogen carbonate ion in sea water significantly influences the rate of deposition of scale with two trends being seen. Below 250 ppm the rate of deposition is increased as the hydrogen carbonate ion concentration is increased, but as the concentration is raised to 375 ppm and above the rate of deposition decreases as the hydrogen carbonate ion concentration increases. The sea water containing 500 ppm of hydrogen carbonate ion took 16.4 minutes longer than the sea water containing 250 ppm at 55°C to form a scale. However, at 80°C the time difference in the propensity to scale was 14.8 minutes between the two waters. The effect of temperature on the propensity to scale was as expected, with the rate of deposition of scale increasing at higher temperatures. The significance of the results in Table 4.94 can be seen more clearly in Figure 4.43, when average scaling times are plotted against hydrogen carbonate ion concentration; the graph shows the increase in propensity to scale by raising the hydrogen carbonate

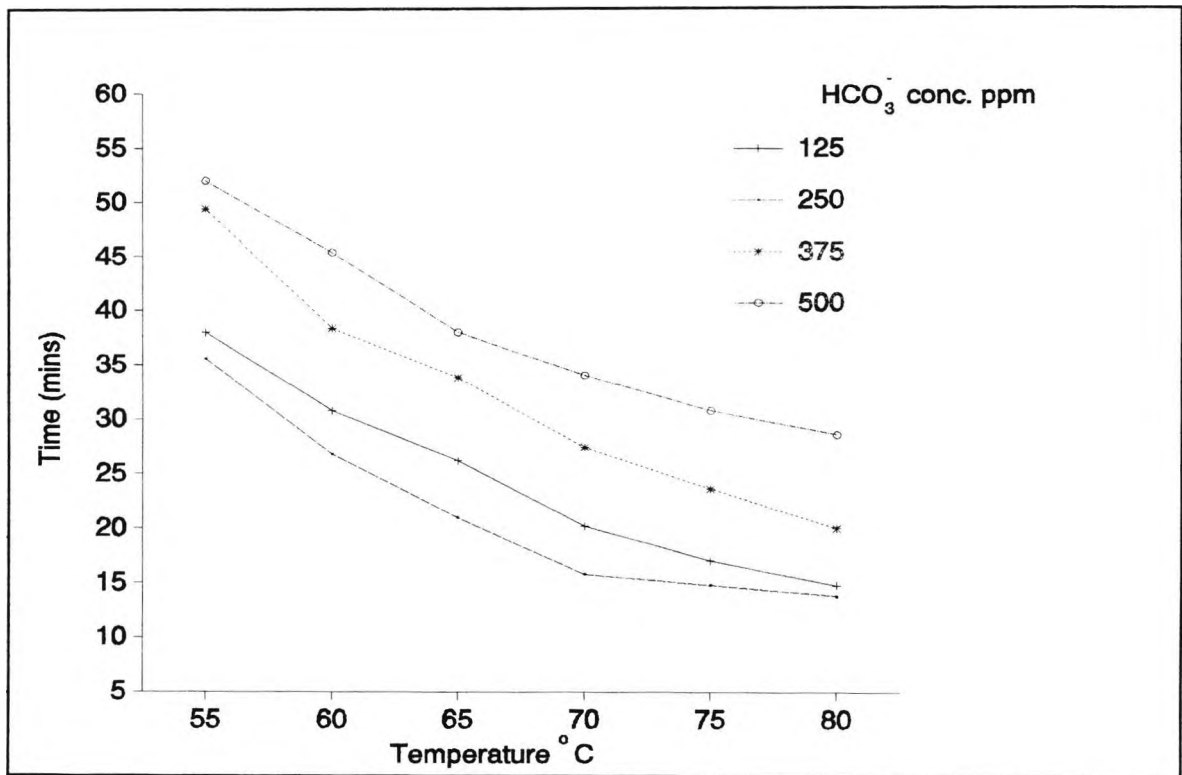


Figure 4.42 Effect of different hydrogen carbonate ion concentrations on the average scaling times.

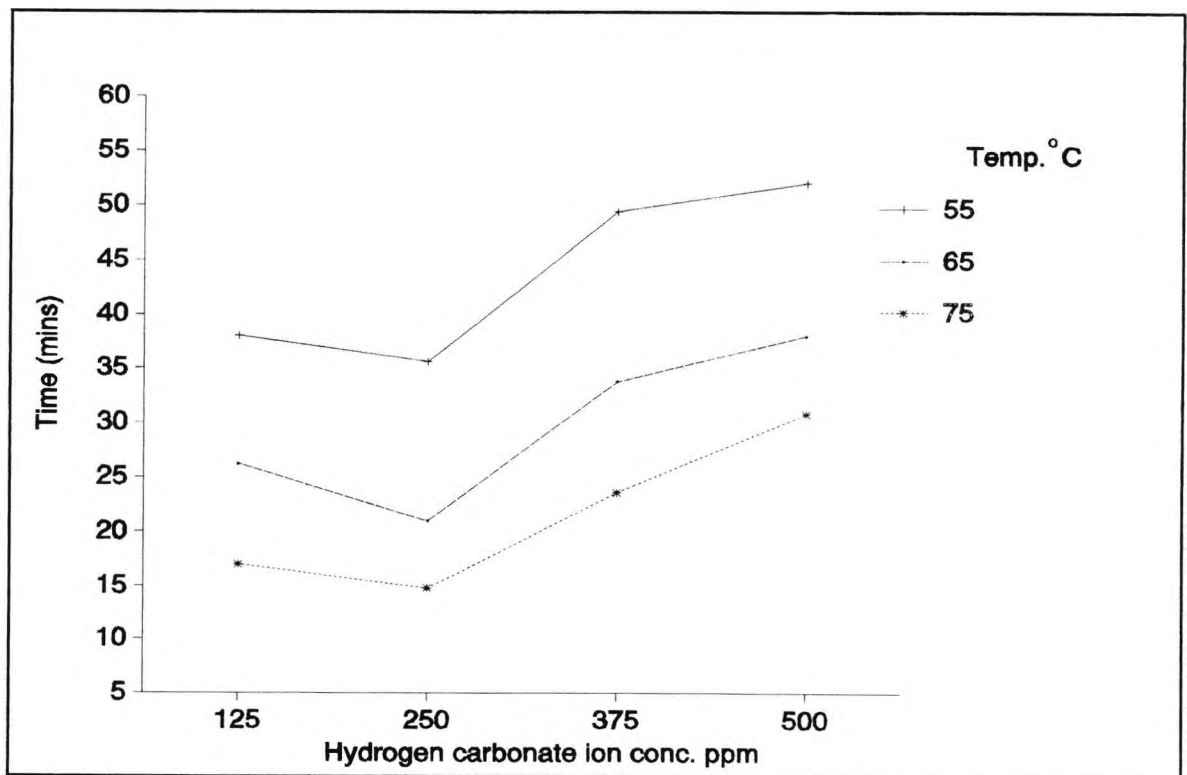


Figure 4.43 Effect of temperature on the average scaling times.

ion concentration to 250 ppm and the subsequent decrease for the higher hydrogen carbonate ion concentration levels.

The decrease in propensity to scale at higher hydrogen carbonate ion concentrations is a result of the formation of calcium carbonate in preference to calcium sulphate (which is much more soluble), which reduces the availability of calcium ions to form calcium sulphate. This is confirmed by the increased reduction in propensity to scale at 80°C as a result of increased decomposition of hydrogen carbonate ion to carbonate ion.

#### 4.14.5 The Effect of Varying the Sulphate Ion Concentration in Simulated Sea Water on the Propensity to Scale

The sodium sulphate concentrations used and the physical properties of the sea waters studied are given in Table 4.95. All the other ion concentrations were kept constant.

**Table 4.95 Changes in chemical composition on varying the sodium sulphate concentration in sea water.**

Na <sup>+</sup> ppm	SO <sub>4</sub> <sup>2-</sup> ppm	Na <sub>2</sub> SO <sub>4</sub> wt. g/l	pH
11739	8000	11.837	7.52
12219	9000	13.316	7.58
12698	10000	14.796	7.50
13177	11000	16.275	7.50

The results for the average scaling times for the sulphate ion concentration experiments are given in Table 4.96 and shown graphically in Figure 4.44. The details of replicate runs for each sulphate ion concentration experiment are given in Appendix Tables B.112 to B.115.

**Table 4.96 Effect of different sulphate ion concentrations on an increase in back pressure of 3 psi: Average scaling times (mins).**

Temp °C	SO <sub>4</sub> <sup>2-</sup> 8000ppm	SO <sub>4</sub> <sup>2-</sup> 9000ppm	SO <sub>4</sub> <sup>2-</sup> 10000ppm	SO <sub>4</sub> <sup>2-</sup> 11000ppm
55	56.0	43.2	30.8	27.4
60	41.6	32.6	22.6	16.8
65	29.6	25.4	19.4	11.6
70	22.2	20.8	16.0	9.8
75	20.0	16.8	14.0	8.6
80	17.2	13.8	11.8	7.2

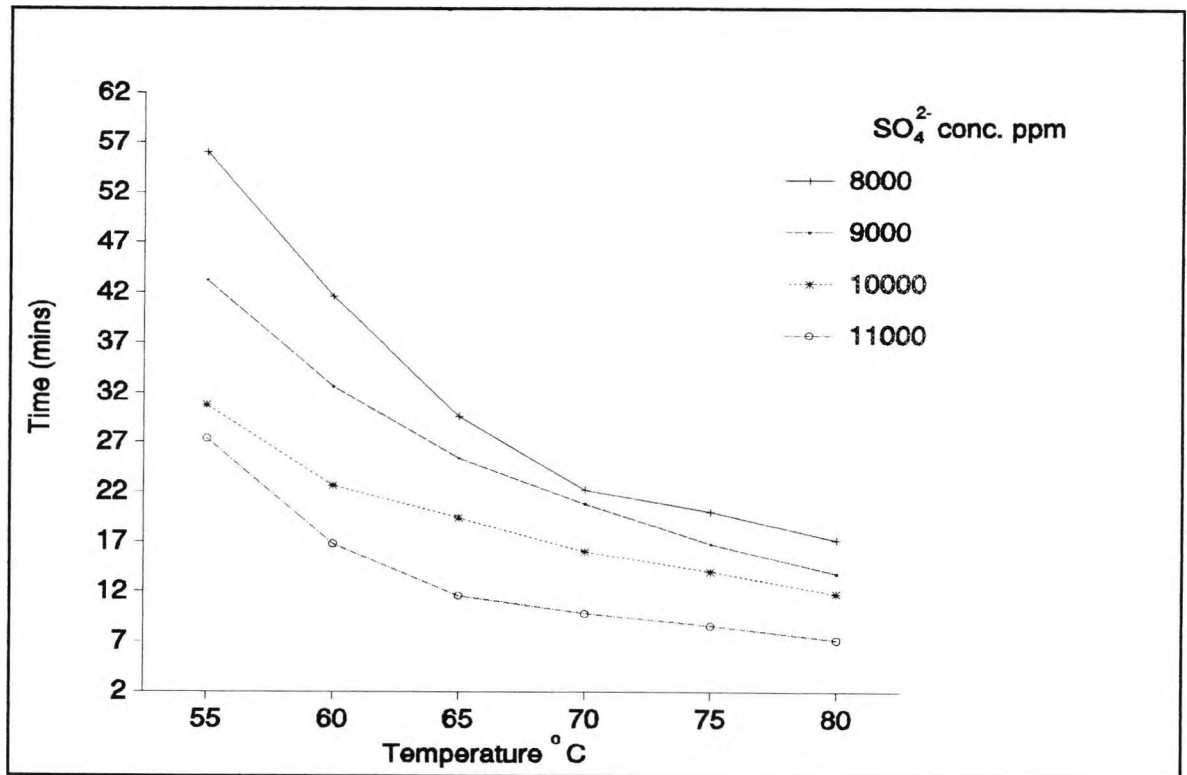


**Figure 4.44 Effect of different sulphate ion concentrations on the average scaling times.**

The results show that varying the sulphate ion concentration in sea waters significantly influences the rate of deposition of scale. The rate is increased as the sulphate ion concentration

is increased. This trend is found at all concentrations and temperatures studied. At 55°C the sea water containing 8000 ppm of sulphate ion took 28.6 minutes longer to scale than the sea water with 11000 ppm. However, at 80°C the time difference in the propensity to scale was 10 minutes between the two waters.

The consistency of the measurements is shown in Figure 4.45, for five repeat runs of propensity to scale measurements for a sulphate ion concentration of 10000 ppm at temperatures of 55, 65 and 75°C, giving standard deviations of 1.78, 0.55 and 0.71, respectively. The effect of temperature was also evident and, as expected, the rate of deposition of scale was shown to increase with temperature.

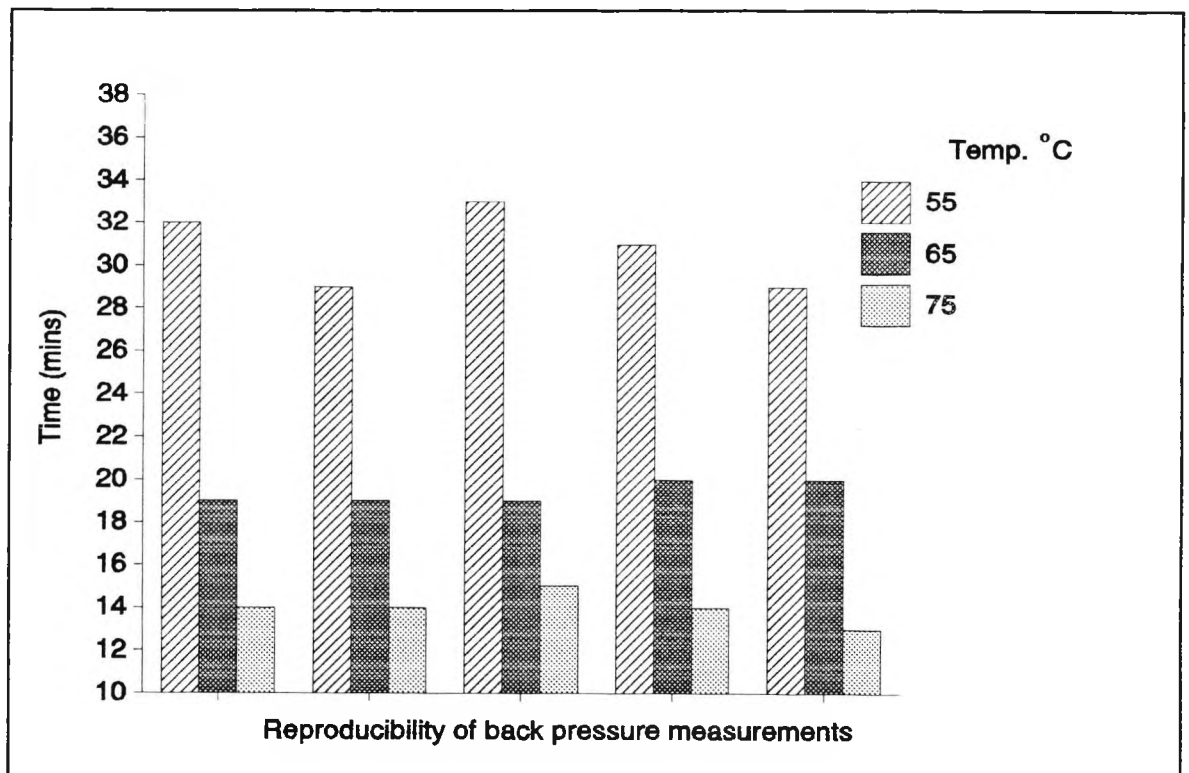


**Figure 4.45** Reproducibility of back pressure measurements for the sulphate ion concentration of 10000 ppm in sea water.

The increase in propensity to scale at higher sulphate ion concentrations is a result of increased calcium sulphate deposition in the microbore tube.

#### 4.14.6 Summary of the Propensity to Scale Measurements

The effects of changing each significant ion in simulated sea water separately, leaving the other ion concentrations unchanged, have yielded interesting results. Every significant ion changed has been shown to have a different effect on the propensity to scale as measured in the P.M.A.C. unit when formation and sea waters are mixed. Table 4.97 summarises the general trends found in the propensity to scale measurements by increasing each significant ion concentration.

Table 4.97 Summary of the general trends in the propensity to scale.

Ion	General trend in the propensity to scale
Na <sup>+</sup>	Significant decrease
K <sup>+</sup>	No difference
Mg <sup>2+</sup>	Significant decrease at higher Mg <sup>2+</sup> concentrations
HCO <sub>3</sub> <sup>-</sup>	Significant decrease at higher HCO <sub>3</sub> <sup>-</sup> concentrations
SO <sub>4</sub> <sup>2-</sup>	Significant increase

#### 4.15 CONCLUSIONS

The work described in this chapter provides information on the deposition of the BaSO<sub>4</sub>-SrSO<sub>4</sub>-CaCO<sub>3</sub> and CaSO<sub>4</sub>-CaCO<sub>3</sub> systems for solutions modelling off-shore oil well formation and sea waters. Particular attention is paid to the aggregation processes of these precipitates that lead to chemical scale formation in the pipework. Precipitation data and scale prediction model data have been used to provide information on the total amount of solid deposited in the BaSO<sub>4</sub>-SrSO<sub>4</sub>-CaCO<sub>3</sub> system only and propensity to scale data have been used to provide information on aggregation. In most cases the precipitation and scale prediction data were in agreement, while the propensity to scale data showed differences attributable to the effects of the concentrations of

ions present and their ratios on the aggregation process. While changes in propensity to scale occur in the presence of increasing amounts of ions present in formation or sea water they can also be related to solubility effects, ion-pair effects and kinetic effects.

## REFERENCES

1. Vetter, O.J., "Oilfield Scale- Can We Handle It?" J. Pet. Tech., 1976, (12), 1402-1408.
2. Mazzolini, E.I., Bertero, L. and Truefitt, C.S., SPEPE, (May 1992) 186-192.
3. Gates, G.L. and Caraway, W.H., Bureau of Mines, R16658, 1965.
4. El-Hattab, M.I., J. Pet. Tech., 1985, (9), 1640-1652.
5. Lindlof, J.C. and Stoffer, K.G., J. Pet. Tech., 1983, (7), 1256-1262.
6. Cowan, J.C. and Weintritt, D.J., "Water Formed Scale Deposits", Gulf Publishing Company, Houston, (1976).
7. Allen, T.O., et al. Production Operations Manual, Oil and Gas Consultants International, 1968.
8. Hausler, R.H., Oil & Gas J., (Sept. 18, 1979) 146-154.
9. Yuan, M.D. and Todd, A.C., SPEPE, (Feb. 1991) 63-72.
10. Haarberg, T., Seim, I., Granbakken, D.G., Østvold, T., Read, P. and Schmidt, T., SPEPE, (Feb. 1992) 75-84.
11. Vetter, O.J., Kandarpa, V. and Harouaka, A., J. Pet. Tech., 1982, (2), 273-284.
12. Weintritt, D.J. and Cowan, J.C. J. Pet. Tech., 1967, (10), 1381-1394.
13. Templeton, C.C., J. Chem. and Eng. Data, 1960, 5, (40), 514-516.
14. Uchameyshvili, N.Y., Malinin, S.D. and Khitarov, N.J., Geochem Intl., 1966, 3, 951-963.
15. Collins, G.A. and Zelinski, W.P., "The Solubilities of Barium and Strontium Sulphates in Oilfield Brines," Presented before the Division of Water, Air, and Waste Chemistry, American Chemical Society, Pittsburgh, Pa., March, 1966.
16. Davis, J.A. and Collins, G.A., Environ. Science and Tech., 1971, 5, (10), 1039-1043.
17. Morey, G.W. and Hesselgesser, J.M., Econ. Geol, 1951, 46, 821.

18. Hasson, D. and Zahavi, J., I & EC Fundamentals, 1970, 9, (1), 1-10.
19. Stiff, H.A., and Davis, L.E., Trans. AIME., 1952, 195, 25-28.
20. Vetter, O.J. and Phillips, R.C., J. Pet. Tech., 1970, (10), 1299-1308.
21. Johnson, K.S. and Pytkowicz, R.M., Mar. Chem., 1979, (8), 87-93.
22. Glater, J., Chan, M.C., Nicholls, R.J. and McCutchan, J.W., "Proceedings of the 7<sup>th</sup> International Symposium on Fresh Water from the Sea", 1980, 1, 381-388.
23. Todd, A.C. and Yuan, M., SPEPE, (Aug. 1990), 279-285.
24. Todd, A.C. and Yuan, M., SPEPE, (Feb. 1992), 85-92.
25. Prosser, J., Unpublished Manuscript.
26. S.B. Systems, Personal Communication.
27. Brower, E. and Renault, J., New Mex. State Bur. of Mines and Mineral Resources, Circular 116, Socorro, N.M., 1971.
28. Pytkowicz, R.M., J. Geol., 1965, 73, (1), 196-199.
29. Thomas, A.P.A., Ph.D. Thesis, City University, 1992.

## CHAPTER 5

### CONCLUSIONS

The nucleation, precipitation and aggregation processes when solid materials separate from their aqueous solutions can be affected by a number of factors. In these processes there will always be competition between growth of the solid material on suspended crystallites and on the walls of the container. When growth on the walls is favoured, deposition of chemical scale occurs. The work described in this thesis is concerned with some of the factors affecting nucleation, precipitation, aggregation and scale formation in systems of particular relevance to the offshore oil industry. The factors affecting the processes studied in this work are (1) the effects of applied electromagnetic fields on the deposition and scale-forming properties of calcium carbonate and (2) the effects of varying the significant ion concentrations and the ratios of mixing of solutions in the  $\text{BaSO}_4$ - $\text{SrSO}_4$ - $\text{CaCO}_3$  and  $\text{CaSO}_4$ - $\text{CaCO}_3$  systems. In all of the systems the main method used to study both the rate of precipitation and crystallisation was based on the deposition of solid material in a small bore tube such that the time taken to reach a cut-off back pressure provided a measurement of the rate of deposition and the propensity to form scale. The results show that this method of measurement gives reproducible results. In the rate of deposition and propensity to scale experiments sufficient measurements were made to ensure that the data obtained were both reproducible and statistically significant.

The effects of an applied electromagnetic field on deposition of calcium carbonate from aqueous solutions were studied using a Hydromag DN15 electromagnetic unit. This unit subjects the flow of water through it to an applied magnetic field of about 2500 Gauss in a system that involves a change in polarity for 5 seconds every minute. Experiments were carried out on (1) calcium carbonate deposited chemically by the addition of a solution of sodium hydrogen carbonate to a solution containing calcium ions

and (2) the deposition of calcium carbonate from hard waters in both laboratory experiments and industrially monitored trials. The results of propensity to scale measurements show that the magnetic treatment of calcium ion solutions significantly reduces the rate of deposition of calcium carbonate (when precipitated with sodium hydrogen carbonate solutions) compared to treatments in zero field conditions. This effect of applied fields was found to be significant over the range of flow rates tested for treating calcium ion solutions, with the Hydromag DN15 electromagnetic unit having an optimum flow rate of 6l/min. The magnitude of the effect was also shown to be dependent upon the sodium hydrogen carbonate concentration and the temperature at which the experiments were carried out. Replicate experiments show that the effects of applied fields on calcium ion solutions are reproducible in all the propensity to scale experiments. Heat exchanger experiments have also demonstrated that magnetic treatment significantly reduces the quantity of scale formed. Laboratory experiments show a significant difference in the crystal and aggregate sizes which affect the nature of the scale formed. In particular the crystallites obtained following magnetic treatment are distinct and show little tendency to aggregate to form scale. In the zero field experiments, the fundamental particles obtained are much smaller but they readily aggregate to form large conglomerates made up of these aggregated particles.

These effects on calcium carbonate precipitation can be explained in terms of the direct interaction of the applied magnetic field at the highly charged surfaces of calcium carbonate nuclei or prenuclear clusters. The results on the calcium carbonate scaling system, along with other data show unequivocally that the magnetic treatment of fluids (i.e. the interaction of charged species in fluids and applied fields) is a general phenomenon. The results can be explained in terms of the direct field-charge interaction between applied magnetic fields and the important charged species in the system.

The effects of coexisting ions on the precipitation of all possible solid phases in the systems  $\text{BaSO}_4$ - $\text{SrSO}_4$ - $\text{CaCO}_3$  and  $\text{CaSO}_4$ - $\text{CaCO}_3$  were studied in model systems for formation water and sea water mixing in offshore oil production.

Propensity to scale data for the  $\text{BaSO}_4$ - $\text{SrSO}_4$ - $\text{CaCO}_3$  system show that increasing each significant ion concentration in simulated formation and sea water separately, leaving the other ion concentrations unchanged, leads to different effects depending on the ion concentration increased. The ion concentrations which increase the rate of deposition of scale were those of the sulphate and barium ions. The rate of deposition of scale is decreased for increase in the concentration of sodium, magnesium and calcium ions, while increase in the potassium ion concentration did not affect the rate of deposition of scale. Increasing the strontium ion concentration in formation and sea water produced a significant decrease in the rate of deposition of scale below  $70^\circ\text{C}$ , but above  $70^\circ\text{C}$  a significant increase in scale deposition was found for high strontium ion concentrations in formation water. The results from mixing the most and least scale-forming formation and sea waters, as determined from the ion concentration experiments, vary depending on the combinations of each water used. The results for the ratio of mixing experiments showed that the most scale-forming ratio was between 60:40 and 70:30 for the standard formation and sea waters used. The least scale-forming ratio was found to be 10:90. Precipitation tests and scale prediction model data were used to provide information on the quantity of each material deposited. The precipitation of calcium carbonate was found to increase when the formation water to sea water ratio was small and reached a maximum at 10:90. The precipitation of strontium sulphate was found to be a maximum between the ratios of 50:50 and 70:30 in the precipitation tests compared with a maximum at 70:30 from the scale prediction model data. Barium sulphate precipitation increased as the formation water to sea water ratio increased and reached a maximum at 90:10.

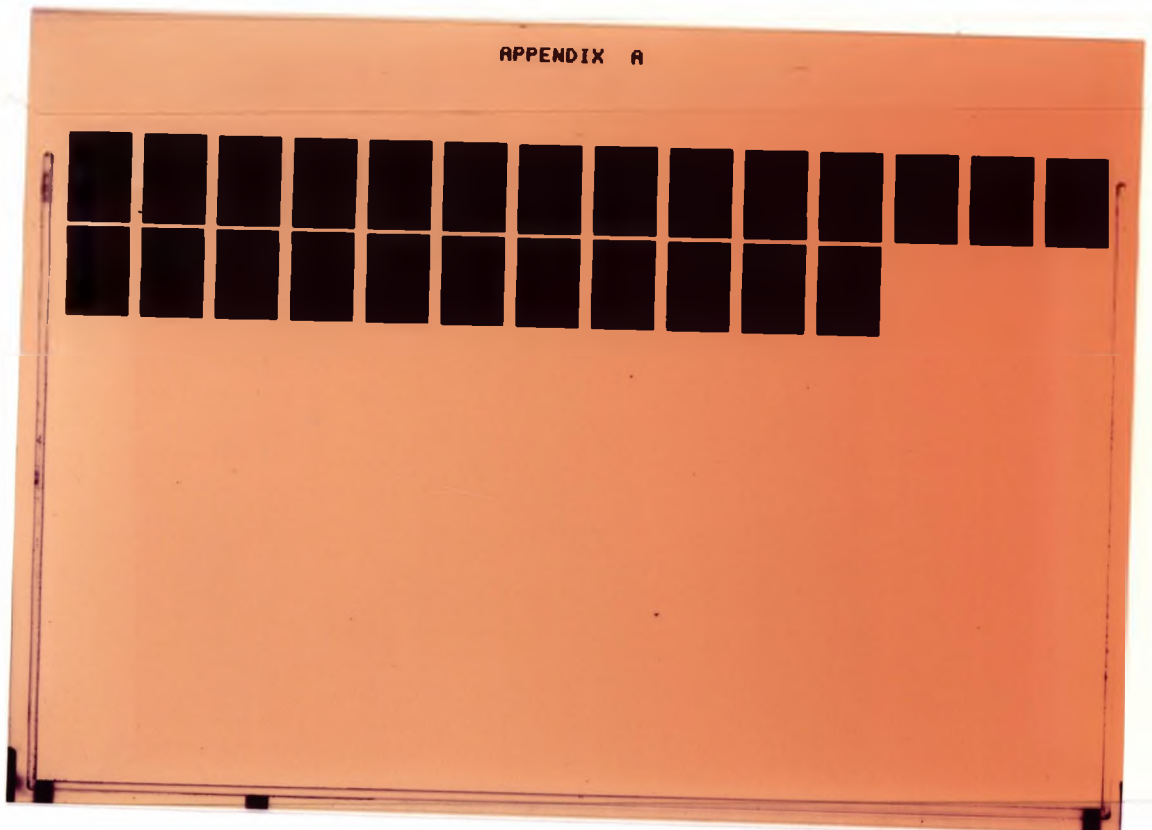
For the  $\text{CaSO}_4\text{-CaCO}_3$  system the effects of increasing each significant ion concentration in simulated formation and sea water separately, leaving the other ion concentrations unchanged, depend upon the particular ion increasing in concentration. The ion concentrations which increase the rate of deposition of scale are those of the calcium and sulphate ions, while increases in the sodium, magnesium and hydrogen carbonate ion levels decrease the rate of deposition of scale. Increase in the potassium ion concentration does not affect the rate of deposition of scale.

The data from this work on studies of the variation of the ion concentrations present in simulated formation and sea waters and the changes in the ratio of mixing of these waters results in changes in the rate of deposition of scale in the systems  $\text{BaSO}_4\text{-SrSO}_4\text{-CaCO}_3$  and  $\text{CaSO}_4\text{-CaCO}_3$ . The changes in the types and amount of scale-forming material deposited and in propensity to scale measurements are interpreted in terms of solubility effects, ion-pair effects and kinetic effects.

## APPENDIX A

### Index of Terms

- Time (mins) - Average scaling time for the experiments in minutes.
- S.D. - Standard Deviation from the experiments
- % -  $\frac{\text{Standard Deviation}}{\text{Average scaling time}} \times 100 = \%$
- Range (mins) - The time range of the experiments carried out in minutes.
- No. of Runs - The number of experiments carried out.



## APPENDIX B

### Index of terms

- Time (mins) - Average scaling time for the experiments in minutes.
- S.D. - Standard Deviation from the experiments.
- % -  $\frac{\text{Standard Deviation}}{\text{Average scaling time}} \times 100 = \%$
- Range (mins) - The time range of the experiments carried out in minutes.
- No. of Runs - The number of experiments carried out.

